



This project has received funding from the European Union's Horizon 2020 research and innovation programme under grant agreement No. 700748

LIQUEFACT
Deliverable 7.1

Manual for the assessment of liquefaction risk, defining the procedures to create the database, collect, define, symbolize and store information in the Georeferenced Information System and to perform and represent the risk analysis

LIQUEFACT

Assessment and mitigation of Liquefaction potential across Europe: a holistic approach to protect structures/infrastructure for improved resilience to earthquake-induced Liquefaction disasters.

H2020-DRA-2015

GA no. 700748



DELIVERABLE D7.1

Manual for the assessment of liquefaction risk, defining the procedures to create the database, collect, define, symbolize and store information in the Georeferenced Information System and to perform and represent the risk analysis

Authors:	Giuseppe Modoni, Rose Line Spacagna, Luca Paoletta, Alessandro Rasulo (UNICAS) Keith Jones, Maria Antonietta Morga (ARU) Carlo Lai, Francesca Bozzoni, Cludia Meisina (UNIPV) António Viana da Fonseca, Maxim Millen, Sara Rios, Cristiana Ferreira (UPORTO) Mirko Kosič, Matjaž Dolšek, Janko Logar (ULJ) Sadik Oztoprak, Ilknur Bozbey, Kubilay Kelesoglu, Ferhat Ozcep (INSTAN-UNI), Alessandro Flora, Emilio Bilotta (UNINA) Vincenzo Fioravante (ISMGEO) Abdelghani Meslem (NORSAR)
Responsible Partner:	Università degli Studi di Cassino e del Lazio Meridionale
Version:	1.0
Date:	30.04.2019
Distribution Level (CO, PU)	PU



This project has received funding from the European Union's Horizon 2020 research and innovation programme under grant agreement No. 700748

Manual for the assessment of liquefaction risk, defining the procedures to create the database, collect, define, symbolize and store information in the Georeferenced Information System and to perform and represent the risk analysis

DOCUMENT REVISION HISTORY

Date	Version	Editor	Comments	Status
28/02/2019	1	UNICAS: Giuseppe Modoni, Paolo Croce, Rose Line Spacagna, Alessandro Rasulo, Luca Paolella,	First Draft	Draft

LIST OF PARTNERS

Participant	Name	Country
UNICAS	Università degli Studi di Cassino e del Lazio Meridionale	Italy
ARU	Anglia Ruskin University	UK
UNIPV	University of Pavia	Italy
Uporto	University of Porto	Portugal
NORSAR	Stiftelsen Norsar	Norway
Istan-Uni	Istanbul Universitesi	Turkey
UNINA	Universita degli Studi di Napoli Federico II	Italy
ULJ	Univerza V Ljubljani	Slovenia
ISMGEO	Istituto Sperimentale Modelli Geotecnici	Italy



This project has received funding from the European Union's Horizon 2020 research and innovation programme under grant agreement No. 700748

Manual for the assessment of liquefaction risk, defining the procedures to create the database, collect, define, symbolize and store information in the Georeferenced Information System and to perform and represent the risk analysis

GLOSSARY

Acronym	Description
AC	Asbestos Cement
AGI	Associazione Geotecnica Italiana
AHEAD	Archive of Historical Earthquake Data
AHR	Average Head Ratio
ALARP	As Low As Reasonably Practicable
AEL	Annualized Earthquake Loss
AFE	Annual Frequency of Exceedance
ASTM	American Society for Testing and Materials International
BRT_i	Building Recovery Time (for the generic activity)
BTM	Building Typology Matrix
CAD	Computer-Aided Drafting
CALTRANS	California Department of Transportation
CAV	Cumulative Absolute Velocity
CCS	Consorcio de Compensación de Seguros
CEN	European Committee for Standardization
CEA	California Earthquake Authority
CES	Christchurch Earthquake Sequence
CGD	Canterbury Geotechnical Database
CLE	Limit Condition Emergency
CPT	Cone Penetration Test
CPTe	Electrical Cone Penetration Test
CPTm	Mechanical Cone Penetration Test



This project has received funding from the European Union's Horizon 2020 research and innovation programme under grant agreement No. 700748

Manual for the assessment of liquefaction risk, defining the procedures to create the database, collect, define, symbolize and store information in the Georeferenced Information System and to perform and represent the risk analysis

CPTu	Cone Penetration Test with Piezocone
CRR	Cyclic Resistance Ratio
CRS	Coordinate Reference System
CSR	Cyclic Stress Ratio
CT	Crust Thickness
CTL	Cumulative Thickness of Liquefiable Layers
Csv	Comma Separated Values
CTMS	Commissione Tecnica per la Microzonazione Sismica
DCI	Damage Consequence Index
DEM	Digital Elevation Model
DPC	Department of Civil Protection
DTM	Digital Terrain Model
EDP	Engineering Demand Parameter
EERI	Earthquake Engineering Research Institute
EILD	Earthquake Induced Liquefaction Disaster
EMEC	European-Mediterranean Earthquake Catalogue
EPV	Effective Peak Velocity
EQC	Earthquake Commission
ESHMs	European Seismic Hazard Maps
ESP	Equivalent Soil Profile
ESRI	Environmental Systems Research Institute
ETRS	European Terrestrial Reference System
EU	European Union
EWS	Early Warning Systems



This project has received funding from the European Union's Horizon 2020 research and innovation programme under grant agreement No. 700748

Manual for the assessment of liquefaction risk, defining the procedures to create the database, collect, define, symbolize and store information in the Georeferenced Information System and to perform and represent the risk analysis

FEMA	Federal Emergency Management Agency
FGDC	Federal Geographic Data Committee
F_L, FS_L	Factor of safety against Liquefaction
FLT	Functionality Loss Time
FORM	First Order Reliability Method
FOSM	First Order Second Moment
GDAL	Geospatial Data Abstraction Library
GEM	Global Earthquake Model
GeoTIFF	Georeferenced Tagged Image File Format
GIS	Geographical Information System
GMPE	Ground Motion Prediction Equation
GNU	General Public License
GRS	Geodetic Reference System
GSM	Guidelines for Seismic Microzonation
H_{crust}	Non-liquefiable crust thickness
HDPE	High Density Polyethylene
H_{liq}	Thickness of Liquefiable Layer
HR	Head Ratio
ICC	International Building Code
ICMS	Indirizzi e criteri per la microzonazione sismica
IM	Earthquake Intensity Measure
INGV	Istituto Nazionale Geofisica e Vulcanologia
INV_DAM_i	inventory losses for the business activity i
IR	Implementing Rules



This project has received funding from the European Union's Horizon 2020 research and innovation programme under grant agreement No. 700748

Manual for the assessment of liquefaction risk, defining the procedures to create the database, collect, define, symbolize and store information in the Georeferenced Information System and to perform and represent the risk analysis

ITRS	Internation Terrestrial Reference System
JER	Japanese Earthquake Reinsurance
JGS	Japan Geotechnical Society
KML	Keyhole Markup Language
LDI	Lateral Displacement Index
LDP	Liquefaction Demand Parameter
Li	Loss of Income
LPI	Liquefaction Potential Index
<i>LPI_{ISH}</i>	Ishihara-inspired Liquefaction Potential Index
LRFD	Load and Resistance Factors Design
LRG	Liquefaction Reference Guide
LSs	Limit State
LSN	Liquefaction Severity Number
MASW	Multichannel Analysis of Surface Waves
MBIE	Ministry of Business, Innovation and Employment (N. Z.)
MCEs	Maximum Credible Earthquakes
MCS	Macro Seismic Scale
MMI	Modified Mercalli Intensity
MPVC	Modified polyvinyl chloride
Mw	Moment Magnitude
NAICS	North American Industry Classification System
NCEER	National Center for Earthquake Engineering Research
NERA	Network of European Research Infrastructures for Earthquake Risk Assessment and Mitigation



This project has received funding from the European Union's Horizon 2020 research and innovation programme under grant agreement No. 700748

Manual for the assessment of liquefaction risk, defining the procedures to create the database, collect, define, symbolize and store information in the Georeferenced Information System and to perform and represent the risk analysis

NERIES	Network of Research Infrastructures for European Seismology
NEHRP	National Earthquake Hazard Reduction Program
NTC	Italian National Building Code
NZGS	New Zealand Geotechnical Society
OASIS	Organization for the Advancement of Structured Information Standards
OGC	Open Geospatial Consortium
OMG	Object Management Group
PBD	Performance Based Design
PEBA	Performance Based Earthquake Assessment
PEER	Pacific Earthquake Engineering Research
PESH	Potential Earth Science Hazards
PGA	Peak Ground Acceleration
PGD	Peak Ground Displacement
PGDf	Permanent Ground Deformation
PGV	Peak Ground Velocity
PL	Probability of Liquefaction
P_{LS}	probability of exceedance of designated limit states
PRR	Plans for Prevention of Risk
PSHA	Probabilistic Seismic Hazard Analysis
RAIF	Resilience Assessment and Improvement Framework
RC	Reinforced Concrete
R_c	Repair cost
RDBMS	Relational Data Base Management System
RER	Regione Emilia Romagna



This project has received funding from the European Union's Horizon 2020 research and innovation programme under grant agreement No. 700748

Manual for the assessment of liquefaction risk, defining the procedures to create the database, collect, define, symbolize and store information in the Georeferenced Information System and to perform and represent the risk analysis

RR	Repair Rate
RRI	Rapid Risk Identification
S	one-dimensional volumetric reconsolidation settlement
Sa	Spectral Acceleration
SBT	Soil Behavior Type
SCPT	Seismic Cone Penetration Test
SHEEC	SHARE European Earthquake Catalogue
SHM Map	Map of Seismically Homogenous Microzones
SLM_i	Service Interruption Multiplier (for the generic activity)
SLS	Serviceability Limit State
SM	Seismic Microzonation
SORM	Second Order Reliability Method
SPT	Standard Penetration Test
SQL	Structured Query Language
SSI	System Serviceability Index
TC4-ISSMGE 1999	Technical Committee for Earthquake Geotechnical Engineering of the International Society for Soil Mechanics and Geotechnical Engineering
TWG	Thematic Working Group
UBI	Uninhabitable Building Index
UBI_i	Upgrade Benefit Index
UL	Utility Loss
ULS	Ultimate Limit State
US	United States
UTM	Universal Transverse Mercator



This project has received funding from the European Union's Horizon 2020 research and innovation programme under grant agreement No. 700748

Manual for the assessment of liquefaction risk, defining the procedures to create the database, collect, define, symbolize and store information in the Georeferenced Information System and to perform and represent the risk analysis

V_s	Shear Wave Velocity
W3C	World Wide Web Consortium
WGS	World Geographic System
WCS	Web Coverage Service
WFS	Web Feature Service
WMS	Web Map Service
Z_AL_Q	Attention Zone
Z_RL_Q	Respect zone
Z_SL_Q	Susceptibility zone
a_{max}	maximum horizontal acceleration
a_{rms}	Root Mean Square Acceleration
CN	Overburden correction factor
D_w	Groundwater depth
D_r	Soil Relative Density
D_s	Shear-induced building settlement
F_c	Fine content
F_s	Sleeve friction
G	Shear modulus
I_c	Soil Behaviour Type Index
K_α	Corrected term for influence of static shear stress
K_σ	Corrected term for overburden pressure
MSF	Magnitude Scaling Factor
N₁₆₀	SPT number of blows.



This project has received funding from the European Union's Horizon 2020 research and innovation programme under grant agreement No. 700748

Manual for the assessment of liquefaction risk, defining the procedures to create the database, collect, define, symbolize and store information in the Georeferenced Information System and to perform and represent the risk analysis

$(N_{160})_{cs}$	Equivalent clean sand normalized number of blows
P_a	Atmospheric pressure
Q_c	Tip resistance in cone penetration test
$(q_{c1N})_{cs}$	Equivalent clean sand normalized cone tip resistance
R_d	depth-dependent shear stress reduction coefficient
R_u	Pore Pressure Ratio
S	Soil Factor
$S_a(T)$	Acceleration response spectrum
SSI	Soil Structure Interaction
T	Fundamental Period
U	Pore pressure
U_c	coefficient of uniformity
V_s	Shear wave velocity
V_{s1}	Normalized shear wave velocity
Z	Depth
β_k	Damage standard deviation value
Δu	Excess pore pressure
ϵ_v	Volumetric consolidation strains
ϵ_h	Horizontal strain
ϵ_{lim}	Limiting tensile strain
η	Damping correction factor
ξ_{sys}	Equivalent viscous damping



This project has received funding from the European Union's Horizon 2020 research and innovation programme under grant agreement No. 700748

Manual for the assessment of liquefaction risk, defining the procedures to create the database, collect, define, symbolize and store information in the Georeferenced Information System and to perform and represent the risk analysis

λ	Excitation wave length
σ_v	Total vertical stress
σ_v'	Effective vertical stress
σ	Normal stress
τ_{soil}	Shear stress of soil column mass
ϕ_{deg}	Equivalent degraded friction angle of the liquefiable layer
ψ	State parameter
γ	Shear strain
ρ	Mass density of the soil
ρ_{dyn}	Shaking-induced the settlement



This project has received funding from the European Union's Horizon 2020 research and innovation programme under grant agreement No. 700748

CONTENTS

SUMMARY	1
1. INTRODUCTION	2
1.1 SCOPE.....	2
1.2 END USERS OF RISK ASSESSMENT	7
1.2.1 Territory planning	8
1.2.2 Lifelines and critical infrastructures	11
1.2.3 Emergency planning	12
1.2.4 Owners of building assets/Investors.....	14
1.2.5 Insurance	16
1.2.6 Design of buildings and infrastructures	18
1.3 LIQUEFACTION ASSESSMENT IN THE INTERNATIONAL STANDARDS	18
1.4 BASIC CONCEPTS RELEVANT FOR LIQUEFACTION RISK ASSESSMENT	25
1.5 OVERVIEW OF THE GUIDELINES	27
2. LIQUEFACTION RISK ASSESSMENT.....	28
2.1 RISK AND UNCERTAINTY.....	28
2.2 QUALITATIVE VS QUANTITATIVE ASSESSMENT	30
2.3 RISK PERCEPTION AND ACCEPTANCE.....	31
2.4 SEISMIC RISK ASSESSMENT	32
2.5 DETERMINISTIC VS PROBABILISTIC ASSESSMENT.....	35
2.6 LIQUEFACTION RISK ASSESSMENT	37
2.7 SEISMIC INPUT.....	43
2.8 SUBSOIL RESPONSE.....	44
2.9 STRUCTURAL DAMAGE	48
2.10 HAZUS METHODOLOGY.....	50
2.11 LRG METHODOLOGY	54
3. GEOGRAPHICAL INFORMATION SYSTEMS	57
3.1 INTRODUCTION.....	57
3.2 GIS SOFTWARE	57
3.3 GIS STANDARDS	58
3.4 GIS STRUCTURE	65
3.5 COORDINATE SYSTEM.....	65
3.6 GEODATABASE.....	69
3.6.1 Data organization	69
3.6.2 Data formats and attribute information	69
3.6.2.1 Vector format	70
3.6.2.2 Raster format:.....	71



This project has received funding from the European Union's Horizon 2020 research and innovation programme under grant agreement No. 700748

Manual for the assessment of liquefaction risk, defining the procedures to create the database, collect, define, symbolize and store information in the Georeferenced Information System and to perform and represent the risk analysis

3.6.3	Geodatabase.....	72
3.6.4	Metadata	73
3.7	GEOPROCESSING.....	77
3.7.1	Tools for spatial analysis.....	77
3.7.2	Geostatistical analysis.....	79
3.7.2.1	Instrument for modelling the structure of data	79
3.7.2.2	Estimation.....	81
3.8	GEO-VISUALIZATION	86
4.	HAZARD	89
4.1	INTRODUCTION.....	89
4.2	SUSCEPTIBILITY	90
4.2.1	Geological Liquefaction Susceptibility	90
4.2.1.1	Macrozonation Scale	90
4.2.2	Liquefaction Susceptibility on the Microzonation Scale	92
4.2.2.1	Liquefaction susceptibility levels	96
4.2.2.2	Borehole – based method to assess the liquefaction susceptibility.....	97
4.2.2.3	CPT – Based method to assess the liquefaction Susceptibility.....	97
4.2.2.3.1	Possible corrections of CPT profiles	100
4.2.2.4	Example of liquefaction susceptibility assessment based on CPT.....	102
4.2.2.5	CRR_ESP METHOD	103
4.2.2.6	Granulometry of liquefiable soils.....	106
4.3	TRIGGERING	107
4.3.1	Ground motion definition.....	107
4.3.1.1	Basis for ground shaking.....	109
4.3.1.1.1	Scenario Earthquake Analysis	109
4.3.1.1.1.1	Seismic sources Database	110
4.3.1.1.1.2	Historical Earthquake Database	110
4.3.1.1.2	Probabilistic Seismic Hazard Maps.....	111
4.3.1.1.3	User-Supplied Seismic Hazard Maps	112
4.3.2	Intensity measures	112
4.3.3	Attenuation model	114
4.3.4	Code Design Response spectrum	115
4.3.4.1	Site-specific (scenario-based) elastic response spectrum	117
4.4	EARTHQUAKE INDUCED CYCLIC STRESS RATIO.....	118
4.5	CYCLIC RESISTANCE RATIO “CRR”	120
4.5.1	CPT-Based liquefaction triggering analysis	121
4.5.2	SPT-Based liquefaction triggering analysis.....	122
4.5.3	Vs-based liquefaction triggering analysis.....	124
4.6	LIQUEFACTION SEVERITY INDICATORS	126
4.6.1	Liquefaction Potential Index LPI (Iwasaki, 1978)	127



This project has received funding from the European Union's Horizon 2020 research and innovation programme under grant agreement No. 700748

Manual for the assessment of liquefaction risk, defining the procedures to create the database, collect, define, symbolize and store information in the Georeferenced Information System and to perform and represent the risk analysis

4.6.2	LPI Ishihara Inspired.....	128
4.6.3	Liquefaction-induced ground settlements.....	130
4.6.4	Liquefaction Severity Number (LSN) (van Ballegooy et al., 2014).....	132
4.6.5	Liquefaction Severity Number and Equivalent Soil Profile method	133
4.6.6	Zhang et al. (2004) procedure	134
4.6.7	Zhu et al. (2015) method	137
4.7	SUMMARY OF THE PROCEDURE FOR THE ASSESSMENT OF LIQUEFACTION HAZARD	138
5.	HAZARD AND RISK	144
5.1	INTRODUCTION.....	144
5.2	INVENTORY COLLECTION AND SCALE LEVEL DEFINITION	148
5.2.1	Scale level definition.....	148
5.2.2	Inventory of element at risk	149
5.3	DAMAGE MODELLING	150
5.3.1	Single building.....	152
5.3.2	General Building Stock – Buildings fragility curves	155
5.3.2.1	Liquefact Fragility Curves for RC buildings.....	159
5.3.2.2	Karamitros et al. formula (2013).....	160
5.3.2.3	Bray & Macedo (2017)	161
5.3.3	Transportation System	162
5.3.3.1	Liquefact Fragility Curves for Embankments.....	162
5.3.4	Lifeline System and Pipelines.....	165
5.3.4.1	Liquefact Empirical Fragility Curves for Pipelines	166
5.4	PHYSICAL DAMAGE	170
6.	LOSSES AND RELIABILITY OF INFRASTRUCTURES.....	172
6.1	CRITICAL INFRASTRUCTURES	172
6.2	ANNUALIZED LOSSES.....	173
6.3	BUILDINGS	176
6.3.1	Estimate of casualties	176
6.3.2	Economic losses.....	176
6.3.2.1	Direct economic losses	178
6.3.2.1.1	Repair/replacement cost	178
6.3.2.1.2	Building content and business inventory losses.....	181
6.3.2.2	Indirect economic losses.....	182
6.3.2.2.1	Interruption of function	182
6.3.2.2.2	Shelter needs	183
6.4	TRANSPORTATION NETWORKS	186
6.4.1	Direct economic losses	186
6.4.2	Indirect economic/social losses	188
6.5	LIFELINES.....	190



This project has received funding from the European Union's Horizon 2020 research and innovation programme under grant agreement No. 700748

Manual for the assessment of liquefaction risk, defining the procedures to create the database, collect, define, symbolize and store information in the Georeferenced Information System and to perform and represent the risk analysis

6.5.1	Direct economic losses	190
6.5.2	Indirect economic/social losses	192
7.	MITIGATION	196
7.1	INTRODUCTION	196
7.2	STRATEGIC MITIGATION	198
7.2.1	Resilience assessment and Improvement Framework (RAIF)	198
7.2.2	Urban planning	201
7.2.3	Management of lifelines	203
7.2.4	Insurance	203
7.3	TECHNICAL MITIGATION	205
7.3.1	Reduction of subsoil susceptibility by ground improvement	205
7.3.2	Reduction of structural vulnerability	209
8.	REFERENCES	212



This project has received funding from the European Union's Horizon 2020 research and innovation programme under grant agreement No. 700748

LIST OF FIGURES AND TABLE

FIGURES

Figure 1-1: Examples of flow failure induced by seismic liquefaction in (a) Alaska (1964) and (b) Indonesia (2018).....	3
Figure 1-2: Examples of damage induced by liquefaction on private buildings (a. Adazapari, Turkey, 1999), industrial building (b. Mirabello, Italy, 2012), bridge (c. Christchurch, New Zealand, 2011), embankment (d. Fukushima, Japan, 2011), harbour dock (e. Port au Prince, Haiti, 2010), pipeline (f. Christchurch, New Zealand, 2011), manholes (g. Tokachi Oki, Japan, 2003), sidewalk (g. Mirabello, Italy, 2012).....	4
Figure 1-3: Effects of liquefaction on buildings and infrastructures (adapted from Mian et al., 2013).....	5
Figure 1-4: Liquefaction evidences over Europe (extracted from the deliverable D2.4 of the present project).....	6
Figure 1-5: Levels of microzonation studies and their use for urban planning and building design (extracted by CTMS, 2017).....	9
Figure 1-6: Flow chart describing the methodology for the identification of the Liquefaction zones (Z_{LQ} , Z_{SLQ} , Z_{RLQ}) and example of map (extracted by CTMS, 2017).....	10
Figure 1-7: U.S. CI economic “use” interdependency. White &¼high-value inputs (\$100 billion to a maximum value of \$500 billion). Gray&¼medium value inputs (\$10–\$100 billion). Black &¼lower value of inputs (\$1 million to \$10 billion). Each sector block is proportional to the size of its total value of economic inputs consumed by the sector. Each square within each sector block indicates the proportional size of economic inputs in dollars. (Macaulay, 2009).....	12
Figure 1-8: Example of accessibility and connectivity to an emergency area and interference with buildings (CTMS, 2016).....	14
Figure 1-9: Map showing the change of liquefaction vulnerability severity classifications across the CES for 100 year return period levels of earthquake shaking (Tonkin & Taylor, 2016).....	15
Figure 1-10: Scheme of insurance in New Zealand (EQC, 2012).....	17
Figure 1-11: Overview of liquefaction vulnerability assessment (NZGS, 2016).	23
Figure 2-1: Precision and accuracy	29
Figure 2-2: Risk acceptance criteria (from Temfamariam & Goda, 2013).....	32
Figure 2-3: Components of risk assessment	33
Figure 2-4: Risk assessment methodology defined in HAZUS (FEMA, 2003).	34
Figure 2-5: Risk assessment methodology defined in SELINA (NORSAR, 2003).....	35
Figure 2-6: Probabilistic definition of risk assessment (Cornell and Krawinkler, 2000).	37
Figure 2-7: Factors determining seismic liquefaction	38
Figure 2-8: Coupled vs uncoupled computation of seismic response (Bradley, 2013).	39
Figure 2-9: Numerical analysis of seismic wave propagation through a multi-layered subsoil.	40
Figure 2-10: Numerical analysis of seismic wave propagation in a three-layer deposit subjected to the same seismic scenario (a. free field; b. with 10 m wide footing at the ground level carrying 50 kPa loading).	40
Figure 2-11: Definition of risk assessment for seismic liquefaction.....	43



This project has received funding from the European Union's Horizon 2020 research and innovation programme under grant agreement No. 700748

Manual for the assessment of liquefaction risk, defining the procedures to create the database, collect, define, symbolize and store information in the Georeferenced Information System and to perform and represent the risk analysis

Figure 2-12: Distribution of liquefaction damage caused by the 2012 earthquakes in Emilia Romagna (Italy).45

Figure 2-13: Liquefiable layer thickness over San Carlo Emilia drawn from all CPT tests (a) and after removing inconsistent data (b) (Contour lines represent the standard deviation of error).46

Figure 2-14: Three-dimensional subsoil model of San Carlo Emilia (green and brown surfaces represent respectively top and bottom surfaces of the liquefiable layer – the vertical scale is five times larger than horizontal one).48

Figure 2-15: Type and level of damage caused on buildings by liquefaction (van Ballegooy, 2014).49

Figure 2-16: Classification of damage from Poulos et al. (2001) (a), empirical relation between maximum absolute settlement and angular distortion (b) for shallow and piled foundations (Viggiani et al., 2012).49

Figure 2-17: Liquefaction Susceptibility of Sedimentary Deposits (from Youd and Perkins, 1978). 50

Figure 2-18: Conditional liquefaction probability for a given susceptibility category at a specified level of peak ground acceleration. 51

Figure 2-19: a. Moment Magnitude (Seed and Idriss, 1982) and b. groundwater depth Correction Factor for Liquefaction Probability Relationships. 52

Figure 2-20: Proportion of the map susceptible to liquefaction (Power et al., 1982). 52

Figure 2-21: Lateral spreading displacement relationship (after Youd & Perkins, 1978; Sadigh et al., 1986) and threshold ground acceleration (PGA_t) corresponding to zero probability of liquefaction. 53

Figure 2-22: Displacement correction factor, KD for Lateral spreading displacement relationship (after Seed & Idriss, 1982). 54

Figure 2-23: Ground settlements amplitudes for liquefaction susceptibility categories (after Tokimatsu & Seed, 1987). 54

Figure 2-24: Flowchart of the LRG procedure for risk assessment. 55

Figure 2-25: Flowchart of the general LRG procedure. To perform the analysis two options are available: the users can run the software as a standalone version or as an application of a Geographical Information System. 56

Figure 3-1: The structure of standardization process (Bartha and Kocsis, 2011). 59

Figure 3-2: GIS structure (ESRI,2001) 65

Figure 3-3: Reference system for Vertical Coordinate Systems 66

Figure 3-4: GIS thematic layers (Spacagna and Modoni, 2018) 69

Figure 3-5: Common vector feature representations (extract from ESRI, 2001) 70

Figure 3-6: Storage mechanisms of Raster (extract from ESRI, 2001) 72

Figure 3-7: Geodatabase structure 73

Figure 3-8: Example of geoprocessing procedure 77

Figure 3-9: Example of experimental variogram calculation. a) map of the location of the measuring points (the dimension of the point indicates the entity of the value of the variable); b) variogram cloud (cross), lag intervals (dashed lines) and experimental variogram (line) (Spacagna and Modoni, 2018) 79

Figure 3-10: Covariance C(h) and Variogram (h) (Spacagna and Modoni, 2018) 80

Figure 3-11: Main variogram model 81

Figure 3-12: Example of geostatistical interpolation a) Map of estimated variable, b) map of standard deviation error of the estimation. 83



This project has received funding from the European Union's Horizon 2020 research and innovation programme under grant agreement No. 700748

Manual for the assessment of liquefaction risk, defining the procedures to create the database, collect, define, symbolize and store information in the Georeferenced Information System and to perform and represent the risk analysis

Figure 3-13: Procedure for data filtering84

Figure 3-14: Example of cross validation result85

Figure 3-15: Box plot analysis85

Figure 3-16: Example of geostatistical interpolation after the application of the procedure of filtering data a) Map of estimated variable, b) map of standard deviation error of the estimation c) cross-validation of interpolation.86

Figure 3-17: Example of map with location of in situ test (points), roads (lines) and buildings (areas).....87

Figure 3-18: Example of 3 D representation of in situ test, soil stratification, ground elevation and buildings of selected area88

Figure 4-1: Strategy for liquefaction hazard assessment.....89

Figure 4-2: a) Stream network derived from Shuttle Radar Topography Mission Digital Elevation Model (SRTM DEM) of European area; b) Lithologies susceptible to liquefaction for the European territory are showed in the Map91

Figure 4-3: Distribution of liquefaction manifestations included in the catalogue across Europe. The colour of the circles is proportional to the event moment magnitude.....92

Figure 4-4: Illustrative diagram of instability zone types in SHM Maps and SM Maps. Data gathering and analyses permit a reduction in uncertainties from Level 1 to Level 3 (Technical Commission on Seismic Microzonation, Land Use Guidelines for Areas Affected by Liquefaction (LQ), version 1.0, Rome, 2018.). ...94

Figure 4-5: Scheme of the procedure to identify layers prone to liquefaction, as defined in WP2 (Task 2.6) 95

Figure 4-6: Example of main data source to define the geological and geotechnical model, according to the microzonation procedure (WP2); a,b) Superficial geological and surveys map of Mirabello district, c) a campaign of measures and the freatic level fluctuation analysis allowed to identify the position of water table in different seasons96

Figure 4-7: a) Example of instument to carry out a probing hole; b) the obtained carrots are stored in a box to define the stratigraphy. C) Common report of a borehole stratigraphy; depending on the groundwater level and the soil characteristics, the crust thickness and the cumuklative thickness of saturated sandy layer are indicated.97

Figure 4-8: Schematic flowchart to evaluate the Soil Behavior Type index (Robertson, 1998).98

Figure 4-9: Normalized CPT Soil Behavior Type (SBTn) chart, $Q_t - F$; (Robertson, 1990)99

Figure 4-10: Example of q_c , f_s/q_c (%) and pore pressure measures and soil behavior type characterization from CPT.....100

Figure 4-11: a) I_c values calculated from CPTm and CPTe data and best regression model adapted to mechanical CPT data; b) $q_{c1n,cs}$ values calculated from CPTm and CPTe data by following the procedure of Boulanger & Idriss (2014) and best regression models.101

Figure 4-12: Empirical calibration of I_c from CPTu vs I_c from borehole and data regression obtained for Cavezzo Municipality.....102

Figure 4-13: Example of geotechnical liquefaction susceptibility. The maps show the cumulative thickness of potentially liquefiable layer for Christchurch City (a) and Terre del Reno district (b).103

Figure 4-14: Scheme of the procedure to implement the CRR-fitted method and liquefact soil profile classification criteria.....105



This project has received funding from the European Union's Horizon 2020 research and innovation programme under grant agreement No. 700748

Manual for the assessment of liquefaction risk, defining the procedures to create the database, collect, define, symbolize and store information in the Georeferenced Information System and to perform and represent the risk analysis

Figure 4-15: Liquefact soil profile classes, as defined by WP3 (D3.3 of this Project). Threshold values for CRR, thickness and depth of liquefiable layer are highlighted in the left part of the Figure.....	106
Figure 4-16: Boundaries for potentially liquefiable soils if $U_c < 3.5$ (a) and $U_c > 3.5$ (b), from the Italian Standards (NTC 2018, 7.11).....	106
Figure 4-17: Information to characterize a seismic scenario.....	108
Figure 4-18: - Seismic hazard map depicts the 10% exceedance probability that a peak ground acceleration of a certain fraction of the gravitational acceleration g is observed within the next 50 year.....	111
Figure 4-19: Example of input file for user-defined seismic scenario.....	112
Figure 4-20: Geometric illustration of earthquake source and distance measures using a vertical cross-section through a fault rupture plane.....	115
Figure 4-21: Elastic design spectra of Type 1 and Type 2 for ground types A – E.....	117
Figure 4-22: To amplify the seismic action accounting for the stratigraphy, values of V_{s30} must be assigned to some profiles within the study area.....	118
Figure 4-23: Magnitude scaling factor (MSF) relationships.....	119
Figure 4-24: Shear stress reduction factor, r_d , relationships (Boulanger and Idriss, 2014).....	120
Figure 4-25: Flowchart of the Boulanger & Idriss (2014) CPT-based procedure.....	122
Figure 4-26: Example of input table for CPT-based liquefaction hazard evaluation. For each CPT, the tip resistance, sleeve friction and pore pressure must be provided in ASCII format.....	122
Figure 4-27: Flowchart of the Boulanger & Idriss (2014) SPT-based procedure for liquefaction triggering analysis.....	123
Figure 4-28: General input file for SPT-based liquefaction triggering analysis.....	123
Figure 4-29: Example of SPT input file for liquefaction triggering analysis.....	124
Figure 4-30: Flowchart of the Andrus & Stokoe (2000) procedure for liquefaction triggering evaluation ...	125
Figure 4-31: General input file for V_s -based liquefaction triggering analysis.....	126
Figure 4-32: Example of V_s Profile.....	126
Figure 4-33: Comparison of depth weighting functions used in the LPI and LPIISH procedures (Maurer et al., 2014).....	129
Figure 4-34: Example of CPT data for a site that showed no surficial manifestations of liquefaction during the 2010 Darfield earthquake (Maurer et al., 2015).....	130
Figure 4-35: Relationship between post-liquefaction volumetric densification strains, ϵ_v , and the normalized CPT tip resistance, qc_{1N} , for selected factors of safety, FS (Zhang et al., 2002).....	131
Figure 4-36: Liquefaction severity vs equivalent soil profile class for different levels of seismic hazard.	134
Figure 4-37: Relationship between maximum cyclic shear strain and factor of safety for different relative densities D_r for clean sands (Zhang et al., 2004).....	135
Figure 4-38: Comparison of measured lateral displacements less than 1 m and calculated lateral displacements for the available case histories for: a) gently sloping ground without a free face; b) level ground with a free face; and c) gently sloping ground with a free face (Zhang et al., 2004).....	137
Figure 4-39: Flowchart of the general methodology to evaluate the liquefaction potential on a given area, according to criteria defined for microzonation studies.....	139
Figure 4-40: Example of input data preparation.....	140
Figure 4-41: Example of liquefaction susceptibility analysis.....	141



This project has received funding from the European Union's Horizon 2020 research and innovation programme under grant agreement No. 700748

Manual for the assessment of liquefaction risk, defining the procedures to create the database, collect, define, symbolize and store information in the Georeferenced Information System and to perform and represent the risk analysis

Figure 4-42: Example of characterization of seismic scenarios. 142

Figure 4-43: Example of liquefaction hazard analysis..... 143

Figure 5-1: Qualitative example Fragility Curves for Slight, Moderate, Extensive and Complete Damage (FEMA, 1999)..... 146

Figure 5-2: Flowchart for the risk assessment 148

Figure 5-3: Different levels of the study area size can be selected. The extent of the study area affects the resolution and efforts to make. It is directly related to the needed resolution and level of detail of the end results (Lang, 2012). 149

Figure 5-4: Schematic procedure to evaluate liquefaction-induced physical damage for buildings, embankments and pipelines. 151

Figure 5-5: – Flowchart of the methodology outlined, among the WP7 activities, to evaluate the liquefaction-induced settlement on the single building scale 155

Figure 5-6: Sample fragility curves for designated limit states (left) and the liquefaction fragility curve (right) obtained based on the assumption of lognormal distribution of the fragility function (thin lines) and based on the empirical CDF (thick lines), as defined in D3.2 of this project. 159

Figure 5-7: Embankment geometry adopted by University of Ljubjana in the procedure to develop fragility curves 164

Figure 5-8: Example of fragility curves for road (a) and railway embankments (b). Damage states are defined according the SYNER-G (2013) criteria 165

Figure 5-9: General framework to develop the fragility model for pipelines, as defined by WP3 166

Figure 5-10: Examples of observed damage to the pipelines: a) Circumferential split on AC main, Rowan Avenue, b) AC main broken collar and longitudinal split (Cubrinovski et al., 2015); c) Longitudinal split on AC main, d) Broken CI main (Curbrinovski et al., 2014). 167

Figure 5-11: Samples of empirical fragility curves for pipelines, obtained for the Christchurch case study: (a) RR vs Settlement, (b) RR vs LSN, (c) RR vs LPIISH , (d) RR vs LPI..... 169

Figure 5-12: Simplified flowchart to evaluate the physical damage on a user-defined building portfolio, for a selected earthquake scenario. 171

Figure 6-1: Annual expenses for mitigation..... 174

Figure 6-2: Probabilistic loss curve (FEMA, 2003)..... 175

Figure 6-3: Flow chart describing the Hazus methodology to estimate casualties (FEMA, 2003)..... 177

Figure 6-4: Example of fragility curve for road embankment..... 190

Figure 7-1: Liquefaction risk model. 196

Figure 7-2: Strategies for liquefaction risk mitigation. 197

Figure 7-3: Situations where mitigation against liquefaction was effective during the big 2011 earthquake in Japan (JGS, 2011)..... 197

Figure 7-4: Schematic representation of the disaster resilience of place (DROP) model (Cutter et al., 2008). 199

Figure 7-5: Schematic representation of the disaster resilience of place (DROP) model (Cutter et al., 2008). 200

Figure 7-6: Scheme for the use of seismic microzonation studies in the municipal planning (from DPC, 2008). 202



This project has received funding from the European Union's Horizon 2020 research and innovation programme under grant agreement No. 700748

Manual for the assessment of liquefaction risk, defining the procedures to create the database, collect, define, symbolize and store information in the Georeferenced Information System and to perform and represent the risk analysis

Figure 7-7: Example of technical chart describing the ground improvement technique.	208
Figure 7-8: Flow chart describing mitigation analysis for risk assessment.	209
Figure 7-9: Proposed TC3 foundation types (MBIE, 2012).....	210
Figure 7-10: Summary of foundation types proposed for TC3 structures (MBIE, 2012).....	211
Figure 7-11: Schematic plots of the different foundation types (MBIE, 2012).	211



This project has received funding from the European Union's Horizon 2020 research and innovation programme under grant agreement No. 700748

Manual for the assessment of liquefaction risk, defining the procedures to create the database, collect, define, symbolize and store information in the Georeferenced Information System and to perform and represent the risk analysis

TABLES

Table 1-1: End users of risk assessment8

Table 1-2: Levels, maps and corresponding types of liquefaction zones9

Table 1-3: Remedial Measures against Soil Liquefaction (JGS, 1998)19

Table 1-4: Strategy for liquefaction assessment on bridges foundation and estimate of cost increase (Caltrans, 2008).20

Table 1-5: General performance of liquefied deposits (NZGS, 2016).24

Table 2-1: Severity liquefaction indicators proposed in the literature47

Table 3-1: Example of open source GIS software58

Table 3-2: Series of ISO Standard for Geographical Information60

Table 3-3: INSPIRE Data Specification - Technical Guidelines – Annexes I.....63

Table 3-4: INSPIRE Data Specification - Technical Guidelines – Annexes II.....63

Table 3-5: INSPIRE Data Specification - Technical Guidelines – Annexes III.....64

Table 3-6: Metadata elements for Identification (INSPIRE Technical Guideline)74

Table 3-7: Metadata elements for Geographic location (INSPIRE Technical Guideline)75

Table 3-8: Metadata elements for Classification of spatial data and services (INSPIRE Technical Guideline) 75

Table 3-9: Metadata elements for Temporal reference (INSPIRE Technical Guideline)75

Table 3-10: Metadata elements for Conformity (INSPIRE Technical Guideline)76

Table 3-11: Metadata elements for Responsible organisation (INSPIRE Technical Guideline)76

Table 3-12: Metadata elements for Quality and validity (INSPIRE Technical Guideline)76

Table 3-13: Metadata elements for Constraints related to access and use (INSPIRE Technical Guideline)77

Table 3-14: Metadata elements for Metadata on metadata (INSPIRE Technical Guideline)77

Table 3-15: Common geoprocessing tools78

Table 3-16: Patterns for visualization87

Table 4-1: Liquefaction susceptibility of sedimentary deposits (from Youd and Perkins, 1978)91

Table 4-2: Punctual level of liquefaction susceptibility (“CMS”- University of Ferrara, 2014).97

Table 4-3: Soil behaviour type index ranges and inferred soil types (Robertson & Wride 1998).99

Table 4-4: List of the available geognostic tests from the Emilia-Romagna Region database (<https://geo.regione.emilia-romagna.it/geocatalogo/>).....104

Table 4-5: Example of general input file for seismic scenarios characterization. By default, the strike and dip of the fault are set equal to 0.110

Table 4-6: Definition of a subset of the principal Intensity Measures present in literature.114

Table 4-7: Definition of a subset of the principal ground motion Cumulative Measure114

Table 4-8: Ground types provided by Eurocode 8116

Table 4-9: Values of the parameters describing Eurocode 8 – Type 1 spectra117

Table 4-10: Values of the parameters describing Eurocode 8 – Type 2 spectra117

Table 4-11: Topographic amplification factors according to Eurocode 8 (EN 1998-5:2003, CEN 2004b).118

Table 4-12: The most widespread indicators, except the LDI which was defined for lateral spreading, quantify the damage to the ground by integrating the estimated effects of liquefaction in the first 20 m depth127



This project has received funding from the European Union's Horizon 2020 research and innovation programme under grant agreement No. 700748

Manual for the assessment of liquefaction risk, defining the procedures to create the database, collect, define, symbolize and store information in the Georeferenced Information System and to perform and represent the risk analysis

Table 4-13: Iwasaki observed that LPI values can range from 0 to 100, with the following indicators of liquefaction induced damage.128

Table 4-14: The following additional constraints are applied to the volumetric densification calculations using the equations given in Appendix A of Zhang et al. (2002)132

Table 4-15: LSN Ranges and observed land effects.133

Table 4-16: Liquefaction severity classes for ESP classification from macro-zonation (D3.2 of this project).134

Table 5-1: RISK-UE Building Typology Matrix.157

Table 5-2: Damage states for traffic embankments (SYNER-G, 2013).164

Table 5-3: Table showing (a) Lengths of different pipe types (b) Repairs conducted after each event of CES (c) Lengths of different Pipe Materials.168

Table 6-1: Example of USGS hazard data (FEMA, 2003).175

Table 6-2: Building occupancy classes (FEMA, 2003).....178

Table 6-3: Cost ratios for structural, non-structural (acceleration and drift sensitive) repairs expressed as percentage of replacement costs (FEMA, 2003).....180

Table 6-4: Business inventory as percentage of annual gross sales (FEMA, 2003).181

Table 6-5: Recovery time (in days) for different categories of building (a) and time interruption multipliers (b) for different activities (FEMA, 2003).182

Table 6-6: Default values for damage state probabilities (FEMA, 2003).....184

Table 6-7: Shelter category weights (FEMA, 2003).....185

Table 6-8: Shelter relative modification factors (FEMA, 2003).....185

Table 6-9: Replacement costs and damage ratios for highway and railway systems (FEMA, 2003).187

Table 6-10: Main attributes/properties of the road Transportation network class (Syner G, 2013).188

Table 6-11: Damage states for road and railway embankments (SYNER-G, 2013).190

Table 6-12: Replacement costs and damage ratios for utility lifelines (FEMA, 2003).191

Table 6-13: Main attributes/properties of the potable water supply system class (Syner G, 2013).....192

Table 6-14: Methodology for the assessment of risk in potable water supply systems defined in SYNER-G (2013).....194

Table 7-1: Factors affecting vulnerability, adaptive capacity and resilience of urban communities (from D.1.3).200

Table 7-2: Classification of ground improvement methods for soil liquefaction countermeasure (JGS, 2011).206



This project has received funding from the European Union's Horizon 2020 research and innovation programme under grant agreement No. 700748

Manual for the assessment of liquefaction risk, defining the procedures to create the database, collect, define, symbolize and store information in the Georeferenced Information System and to perform and represent the risk analysis

SUMMARY

Although liquefaction is not dramatic and shocking like other effects of earthquake such as collapse of structures, landslides and tsunamis, it is similarly harmful for the communities in terms of economic and social impact. Liquefaction is usually considered a secondary hazard in the context of earthquake-induced losses, but this condition absolutely does not diminish its importance. The extensive physical damage produced on buildings and lifelines is just a part of the impact as injuries are aggravated by the prolonged reduced serviceability of the critical infrastructures, i.e. systems and organizations that deliver goods and services fundamental for the life of the society and for the economy of the productive asset (Macaulay et al., 2009). The experience of real events has shown that damage usually occurs not only on the buildings, but also the facilities connected directly or indirectly to the productive systems (roads, waterways, electric and communication lines), in this way undermining for long time the whole social organization and the recovery capacity of the communities.

The above concerns raise the need for improving the resilience and for involving all stakeholders (governmental and regulatory boards, suppliers of services, citizens) in an unified process aimed at increasing security, preparedness and survivability. Being resilient for a community means to assume a proactive behaviour, being ready to survive disasters and maintain economic competitiveness or, in other words, move beyond a just protective posture to an attitude that withstand crisis and deflect attacks. This behaviour implies for the community to be aware of risks, vulnerabilities and of the current capabilities to deal with them, in order to promptly make informed tactical and strategic decisions. A comprehensive assessment of risks that correctly estimate losses addressing the distribution over the territory of hazard, vulnerability and exposure becomes fundamental. It assists the decision-making of the stakeholders (city planners, governmental institutions, emergency agencies, insurance companies, private investors and citizens) who need to control their 'portfolio' of properties, undertake appropriate mitigation actions and optimize the budget allocation.

The holistic assessment of liquefaction risk at different scales, from single structures to aggregates, and the improvement of community resilience is the goal of Liquefact. Thanks to the spread of geoinformatics, rich spatial databases can be nowadays created, empirical connections, mechanical based schemes or artificial intelligence tools can be adopted to connect information and map the results of complex analyses. Applying them to the assessment of liquefaction risk means to assemble into a unique geographical information system seismic hazard, geotechnical properties of the subsoil, structural and functional characteristics of buildings and infrastructures.

This deliverable illustrates how the above scope can be pursued on different systems, like urban aggregates, industrial districts infrastructural networks. Difficulties and uncertainties that affect the assessment are highlighted inspired from case studies where liquefaction has pervasively affected territory and community.



This project has received funding from the European Union's Horizon 2020 research and innovation programme under grant agreement No. 700748

1. INTRODUCTION

1.1 Scope

In the general scope of the project, aimed at defining an operative strategy to quantify and mitigate the liquefaction risk on critical infrastructures, the Work Package WP7 has the role of validating the defined procedures with the retrospective analysis of past events and of summarizing the outcomes into guidelines that enable operators to implement methodologies for risk assessment and the EU Commissions to produce technical standards. Bearing this goal in mind, the action has been focused on two complementary targets, i.e. evaluate the liquefaction risk of a generic system and standardize the use of remediation technologies.

With specific reference to the first target, the assessment requires the characterization in terms of risk of the system to be analysed, being it a community at different geographical scale (national, regional, municipal ...), a subsystem like an industrial or sanitary district, or an infrastructural network. In all cases, the impact on the resilience of the system must be evaluated identifying the fundamental nodes of the system (critical infrastructures), quantifying hazard, vulnerability and loss of functionality due to liquefaction and finally evaluating the impact of the considered seismic event on the whole system. Considering that this analysis is normally performed on entities of variable territorial extension, the present deliverable defines the procedures to set up the database in the appropriate Georeferenced Information System, to collect, symbolize and store information, to overlap them for the computation of risk and to represent outcomes. A GIS structure must be thus customized to the specific target including all factors necessary to quantify liquefaction risk (seismic hazard, geological setting, geotechnical properties of the subsoil, groundwater conditions, structural, economic and strategic characteristics of buildings and infrastructures etc.). In this framework, a methodology is necessary to collect and store data, transform qualitative into quantitative information and adopt a unified system of symbols for a harmonized representation.

Objective of this document is to frame the experience of the participants at the project and outcomes of the different tasks into recommendation guidelines useful for the revision task groups of EU building standards to produce technical standards that address liquefaction in the most complete and up-to-date form. Considering this goal, the present document starts introducing the general principles of risk assessment and with a preliminary recognition of the current procedures for Liquefaction assessment in the European Standards or in other national/international codes. Aims and limitations of the liquefaction risk assessment are then addressed, identifying the stakeholders interested to the process and specifying their different scale and outcomes of interest. The risk assessment methodology is then developed introducing concepts, tools, terminology and symbolization and describing the algorithms introduced in the toolbox software for the different levels of analysis.

Liquefaction rarely produces the dramatic and shocking number of casualties typical of other earthquake effects like building collapse, landslides and tsunamis. Only in few cases liquefaction affects massively the territory, like in the flow failure examples occurred in 1964 in Alaska, that caused 32 casualties, or in the more recent 2018 earthquake occurred in Indonesia (Figure 1-1). Flow failure occurs when the static shear stresses on sloping ground exceed the frictional shear strength of the soil deteriorated by the pore pressure



This project has received funding from the European Union's Horizon 2020 research and innovation programme under grant agreement No. 700748

build-up. Displacements in this case can be very large, in the order of tens of metres or even more, and may disrupt buildings and infrastructure over wide areas.



(a)



(b)

Figure 1-1: Examples of flow failure induced by seismic liquefaction in (a) Alaska (1964) and (b) Indonesia (2018).

However, even when such massive disruption does not occur, the effects of liquefaction are harmful as well for the communities in terms of economic losses and social consequences. The fact that liquefaction is considered just as a secondary hazard in the context of earthquake-induced losses by no means diminishes its importance as it threatens all the fundamental assets of the community. Typical examples of damage produced worldwide by liquefaction are reported in Figure 1-2 for dwelling buildings (Figure 1-2.a), industrial buildings (Figure 1-2.b), bridge abutments (Figure 1-2.c), embankments (Figure 1-2.d), harbour docks (Figure 1-2.e), pipelines (Figure 1-2.f) and manholes (Figure 1-2.g).

The extensive physical damage produced on buildings and lifelines is only a part of the impact of liquefaction, as injuries are aggravated by the prolonged reduced serviceability of the critical infrastructures (Figure 1-3), i.e. those systems and organizations that deliver goods and services fundamental for the functioning of society and economy (Macaulay et al., 2009).



This project has received funding from the European Union's Horizon 2020 research and innovation programme under grant agreement No. 700748

Manual for the assessment of liquefaction risk, defining the procedures to create the database, collect, define, symbolize and store information in the Georeferenced Information System and to perform and represent the risk analysis



(a)



(b)



(c)



(d)



(e)



(f)



(g)



(h)

Figure 1-2: Examples of damage induced by liquefaction on private buildings (a. Adazapari, Turkey, 1999), industrial building (b. Mirabello, Italy, 2012), bridge (c. Christchurch, New Zealand, 2011), embankment (d. Fukushima, Japan, 2011), harbour dock (e. Port au Prince, Haiti, 2010), pipeline (f. Christchurch, New Zealand, 2011), manholes (g. Tokachi Oki, Japan, 2003), sidewalk (g. Mirabello, Italy, 2012)



This project has received funding from the European Union's Horizon 2020 research and innovation programme under grant agreement No. 700748

Manual for the assessment of liquefaction risk, defining the procedures to create the database, collect, define, symbolize and store information in the Georeferenced Information System and to perform and represent the risk analysis

Population, structures, utilities and socio-economic activities form together an integrated system of interdependent entities. Therefore, damages affecting the building asset or the facilities (roads, waterways, electric and communication lines) impact, directly or indirectly, onto the whole systems, undermine its productive capacity and the whole social organization in a way that quality of life is jeopardized. The long time necessary to restore original conditions plays the final negative role at a point that population may be discouraged to undertake reclamation and persuaded to abandon the place.

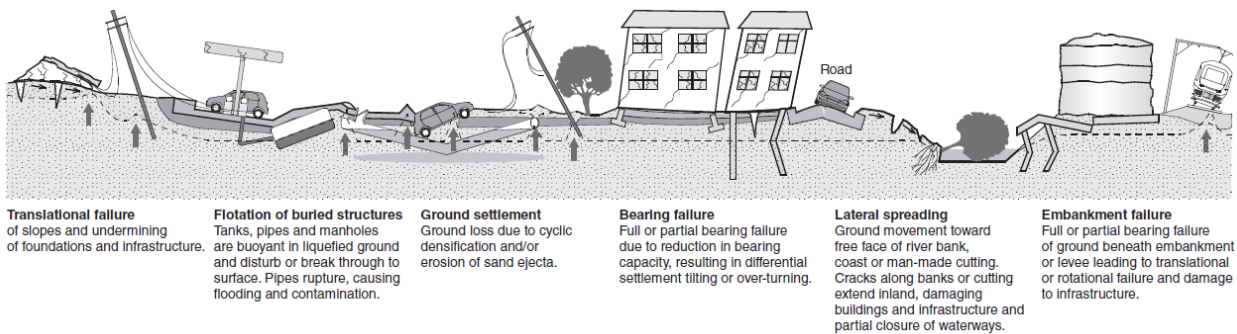


Figure 1-3: Effects of liquefaction on buildings and infrastructures (adapted from Mian et al., 2013)

The above concerns raise the need for improving the recovery capacity and resilience of the community, involving stakeholders (boards, governments, regulators, suppliers of services) in a unified strategy aimed at increasing security, preparedness and survivability. The international community has become progressively aware that resilience is the key to describe earthquake engineering performance and that technological units and social systems cannot be decoupled (e.g. Bruneau et al., 2003). The focus on technological aspects applied to critical infrastructure must be broadened to include the interplay of multiple systems – human, environmental, and others – which together add up to ensure the functioning of a society.

Being resilient for a community means to assume a proactive behavior, ready to survive disasters and maintain economic competitiveness. In other words, the question is to move beyond a just protective posture to an attitude that withstand crisis and deflect attacks. This behavior implies for the community to be aware of risks, vulnerabilities and of the current capabilities to deal with them, in order to promptly make informed tactical and strategic decisions. A comprehensive assessment of risks that correctly estimate losses addressing the distribution over the territory of hazard, vulnerability and exposure becomes fundamental. It assists the decision-making of the stakeholders (city planners, governmental institutions, emergency agencies, insurance companies, private investors and citizens) who need to control their 'portfolio' of properties, undertake appropriate mitigation actions and optimize the budget allocation.

The relevance of liquefaction over Europe is evident from the study carried out within the Work Package 2 (Deliverable D2.4 of Liquefact Project) that counts 920 recorded cases of liquefaction induced by 196 earthquakes. Figure 1-4 reporting the GIS-based catalogue of historical occurrences shows that liquefaction is spread all over the seismic portion of the European territory practically with no exceptions. Fourteen countries are involved in total, with an obviously greater frequency for the most seismic regions, primarily Italy, Greece and Turkey, but with examples recorded also in the other countries. The phenomenon is related

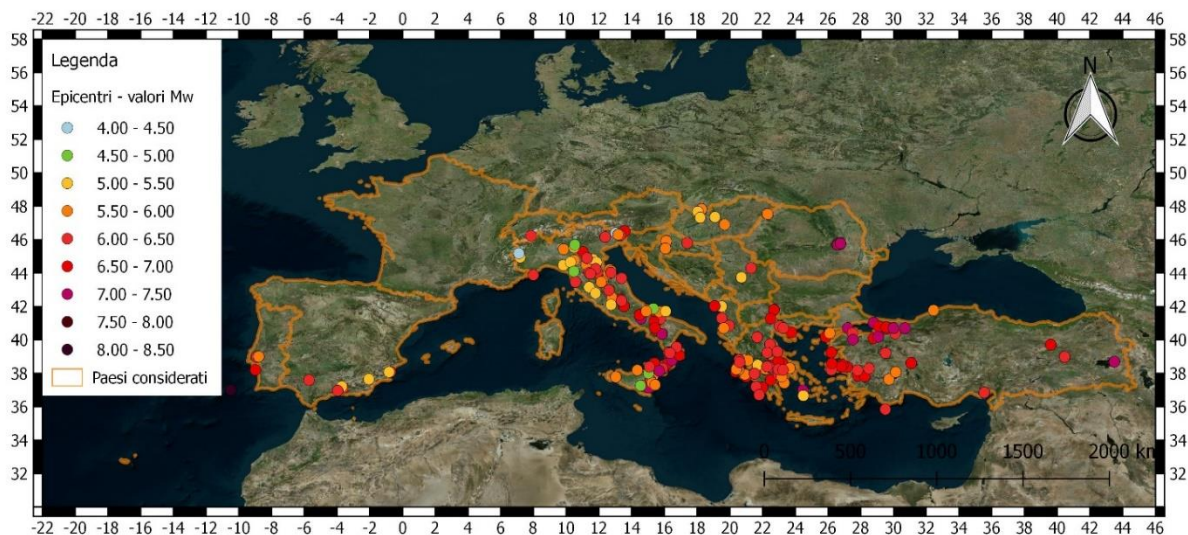


This project has received funding from the European Union's Horizon 2020 research and innovation programme under grant agreement No. 700748

Manual for the assessment of liquefaction risk, defining the procedures to create the database, collect, define, symbolize and store information in the Georeferenced Information System and to perform and represent the risk analysis

not only to the shaking intensity, as the highest frequency of liquefaction events has been noticed for 6÷6.5 magnitudes but depends fundamentally on the combination of the latter with the susceptibility of the subsoil both affected by a significant spatial variability.

The challenge for risk assessment comes from the need to investigate different concurrent factors, seismicity affecting the territory in the radius of dozens of kilometres from the epicentre and susceptibility of the subsoil, i.e. the set of geological conditions by which recent deposits of saturated granular soils tend to compact and develop excess pore pressures upon cyclic shearing, variable in the scale of dozens of meters. A combination of different studies must thus be conceived conjugating information at largely different geographical scales: seismic hazard dictated by macrophenomena producing effects at the regional scale; lithological, stratigraphic, geotechnical and hydrogeological conditions.



COUNTRY	LIQUEFACTION
Albania	12
Bulgaria	4
Croatia	13
France	2 ?
FYROM	13
Greece	183
Hungary	26
Italy	393
Montenegro	15
Portugal	76
Romania	39
Serbia	4
Spain	33
Turkey	107

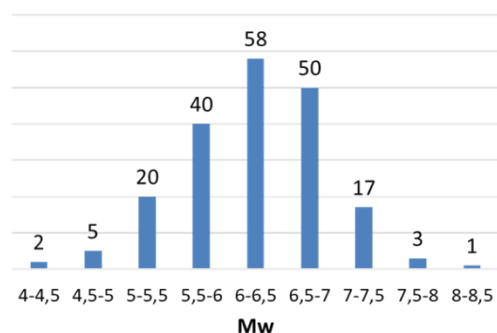


Figure 1-4: Liquefaction evidences over Europe (extracted from the deliverable D2.4 of the present project)



This project has received funding from the European Union's Horizon 2020 research and innovation programme under grant agreement No. 700748

Manual for the assessment of liquefaction risk, defining the procedures to create the database, collect, define, symbolize and store information in the Georeferenced Information System and to perform and represent the risk analysis

The question becomes more complex when considering that risk assessment involves buildings and infrastructures whose vulnerability must be assessed firstly at the physical level, considering their structural characteristics, then at the operability level implying to estimate their weight on the life of the community.

Proven that the most sophisticated tools are nowadays able to reproduce phenomena with good accuracy, but also ascertained that results depend very much on the quality of the available information used as input, primarily the geometrical and mechanical properties of soil and structures, the efficacy of risk assessment is a matter of how precisely the predictive model is built. This need imposes to seek the maximum precision in conjunction with the coverage of the studied area optimizing the investigation strategy. Investigation should be thus preferably performed where risk exposure is not negligible and information should be interpreted altogether, taking advantage of their spatial distribution.

Methodologies and approaches for the assessment of liquefaction potential are the subject of significant and ongoing research, and this document tries to summarize part of the extensive body of technical literature in this area to define a methodology for risk assessment. Considering the variability of possible situations, given by different scopes of the analysis (e.g. loss estimates, urban planning, emergency management, etc.), different typology of the system exposed (building assets, horizontal infrastructures etc.), different extension (region, municipality, district or even single building) the methodology has been purposely defined in the general terms, leaving a variety of options.

1.2 End users of risk assessment

Earthquake is a multi-facet problem that involves several actors (stakeholders), each with a different requirement. The main categories of subjects interested in liquefaction risk assessment are listed below:

- Urban and territory planners
- Owner/manager of lifelines /services
- Emergency planners
- Investors/Owners of building assets
- Insurance Companies
- Designers

Each category has a different specific interest, summarized by the question reported in Table 1-1. Very often interests are interconnected and answers to multiple questions can be found in risk assessment.



This project has received funding from the European Union's Horizon 2020 research and innovation programme under grant agreement No. 700748

Manual for the assessment of liquefaction risk, defining the procedures to create the database, collect, define, symbolize and store information in the Georeferenced Information System and to perform and represent the risk analysis

Table 1-1: End users of risk assessment

Stakeholder	Question
Urban and territory planners	Quantify hazard over the territory to plan the define land use, plan urban/industrial development, ultimately motivating people to abandon risky area
Owner/manager of lifelines/services	Estimate economic losses and increase the reliability of lifelines
Emergency planners	Increase awareness of risk among the population. Identify safe areas and verify their connectivity with the outer communication lines under catastrophic events
Investors/Owners of building assets	Determine seismic performance of their portfolio of buildings
Insurance Companies: estimate losses	Estimate losses to fix the premium of the insurance
Designers	Assess safety and serviceability of buildings or infrastructures and design remediation

1.2.1 Territory planning

Urban planning is an important component of earthquake risk mitigation. Engineering and scientific/technical knowledge can overcome all difficult natural environment but this may imply important costs in design and construction and be always a less equilibrated solution. Urban planning should define better uses of the territory in view of all possible threats, setting limits to the types of construction, layouts and size or defining more detailed seismic action for that environment, envisaging the possibility of excluding high level hazard zones. Urban planning may establish the degree of intervention in an existing block of buildings, the need for reinforcing, etc. But a great deal of application comes from integration into urban planning of land use restrictions related to other effects beyond the direct ground motion, such as the influence of known active faults, the induced phenomena of liquefaction and landslides, but also the tsunami flooding, flooding from dam failure, etc.

An example of an important development of rules related to municipal urban planning has been carried out in France by the Plans for Prevention of Risk (PPR), whose strategy is published in Commissariat General du Plan (1997). An important number of municipalities have developed their own local Plan during the last few years.

Therefore, Identifying the presence of areas possibly affected by liquefaction and evaluating risk is fundamental to regulate land uses and urban transformation. The relationship between seismic hazard and



This project has received funding from the European Union's Horizon 2020 research and innovation programme under grant agreement No. 700748

Manual for the assessment of liquefaction risk, defining the procedures to create the database, collect, define, symbolize and store information in the Georeferenced Information System and to perform and represent the risk analysis

the different settlement contexts must be considered for this purpose. A tool for urban planning in the Italian territory is provided by the CTMS (2017) that specifies the Microzonation Studies previously defined by the ICMS (2008). The latter document suggests proceeding with a three levels of in depth investigation defining hazard at a progressively higher detail (Figure 1-5).

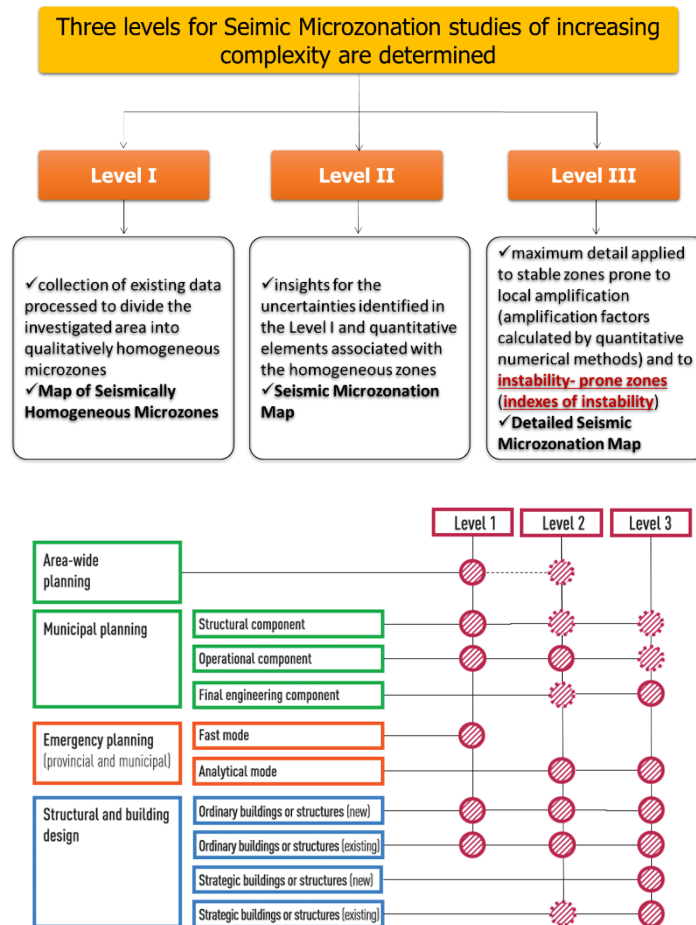


Figure 1-5: Levels of microzonation studies and their use for urban planning and building design (extracted by CTMS, 2017)

In the guidelines for liquefaction, the same three levels of in-depth strategy is defined for the identification of the areas potentially affected by liquefaction (Figure 1-6). In particular, three zones recalled in Table 1-2 as Attention ($Z_{A_{LQ}}$), Susceptibility ($Z_{S_{LQ}}$) and Respect Zone ($Z_{R_{LQ}}$) are defined each affected by an increasing hazard.

Table 1-2: Levels, maps and corresponding types of liquefaction zones

Livello di MS	Carta	Zone di liquefazione	Elementi informativi	Metodi
1	MOPS	Zone di Attenzione ($Z_{A_{LQ}}$)	Minimi	-
3	MS	Zone di Suscettibilità ($Z_{S_{LQ}}$)	Specifici	Semplificati (<i>sensu</i> AGI, 2005)
3	MS	Zone di Rispetto ($Z_{R_{LQ}}$)	Specifici	Avanzati (<i>sensu</i> AGI, 2005)



This project has received funding from the European Union's Horizon 2020 research and innovation programme under grant agreement No. 700748

Manual for the assessment of liquefaction risk, defining the procedures to create the database, collect, define, symbolize and store information in the Georeferenced Information System and to perform and represent the risk analysis

Then, depending on the zone, strategies are defined for each of the following urban categories and for infrastructures:

- Built-up areas (recent or consolidated)
- Non-developed areas (with foreseen transformation)
- Non-urbanized areas (where limited transformability is foreseen)

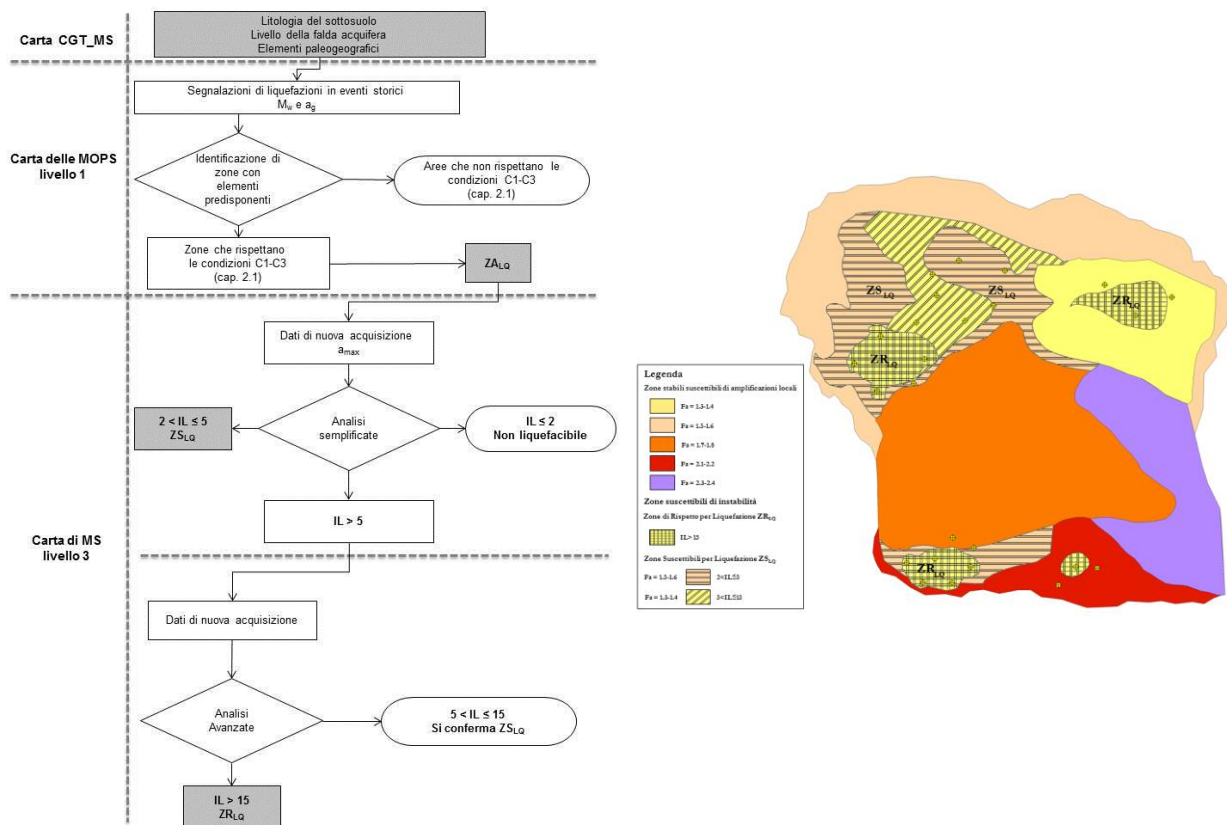


Figure 1-6: Flow chart describing the methodology for the identification of the Liquefaction zones (ZA_{LQ} , ZS_{LQ} , ZR_{LQ}) and example of map (extracted by CTMS, 2017).

In view of this subdivision, the discipline of land use and transformation forecasts in the liquefaction zones is divided into: urban planning indications, which define possible regulations from the urban planning instrument also in terms of intervention categories, destination and methods of implementation; building indications referred to the anti-seismic technical regulation, that define possible categories of intervention and classes of use for existing and new buildings.

According to the previous definitions, the management of risk is coordinated with a hierarchy of roles among the different institutions, namely State, Regional Governments and municipal authorities with the former dictating the general criteria, Regions developing specific regulation and municipalities taking the responsibility for carrying out the assessment.



This project has received funding from the European Union's Horizon 2020 research and innovation programme under grant agreement No. 700748

Manual for the assessment of liquefaction risk, defining the procedures to create the database, collect, define, symbolize and store information in the Georeferenced Information System and to perform and represent the risk analysis

1.2.2 Lifelines and critical infrastructures

Societal functions in the developed countries are highly dependent on networked systems. Even the most basic day-to-day functions involve interaction with a variety of critical infrastructure systems. “Critical Infrastructures are the organizations delivering goods and services in an economy that is fundamental to the functioning of society and the economy” (Macaulay, 2009). For example, millions of people around the world use transportation infrastructure to get to work, school, or to run everyday activities. Telecommunication infrastructure is used for a large variety of purposes going from financial transactions, exchange of non-physical goods, social communication. Energy infrastructure is used to heat homes, power industries and deliver fuel for transportation.

Any loss of functionality of a critical Infrastructure impacts somehow on the goods and services that people use on a constant basis. The critical lifelines for a community can be categorized in the following sectors:

- Energy
- Communication
- Finance
- Health
- Food
- Water
- Transportation
- Safety
- Manufacturing

With regard to seismic risk and, more particularly to liquefaction, the interest of the owners stems from the need to estimate the potential losses and consequent repair caused by damage to the physical support of the service (roads, pipelines, electric or communication cables etc.). Basically, the required output from risk assessment is an estimate of the economic losses that should be faced in comparison with the expenditure for mitigation.

Managers are interested in maintaining the operability of the system as continuously as possible at a sufficient level without interruptions. They refer to the concept of “reliability of the infrastructure” as the probability that a given element in a critical infrastructure system is functional at any given time” (Murray & Grubestic, 2007). In other words, reliability of an element or system is a probabilistic measure of the ability of the subject to resist or keep functioning, given a series of established benchmarks or performance guidelines. For this purpose, damage on systems can be thus estimated with economic losses (e.g. missed income), or with reductions of the performance (time delay, reduced number of served customer etc.).

In both cases, evaluation of risk on critical infrastructures means to determine the geographical distribution of hazard over the served area, the physical fragility of exposed elements and the vulnerability of the operative conditions. Steps may be largely different from case to case, but ultimately operators should be able to assess reliability of their service and plan improving strategies.



This project has received funding from the European Union's Horizon 2020 research and innovation programme under grant agreement No. 700748

Manual for the assessment of liquefaction risk, defining the procedures to create the database, collect, define, symbolize and store information in the Georeferenced Information System and to perform and represent the risk analysis

The question becomes somehow more intricate when considering that systems are mutually interconnected in a way that failure or malfunctioning of an infrastructure impacts on the others rendering them partly inoperable. Figure 1-7 shows the relative importance and interconnection for US among the different sectors cited above.



Figure 1-7: U.S. CI economic “use” interdependency. White & ¼ high-value inputs (\$100 billion to a maximum value of \$500 billion). Gray & ¼ medium value inputs (\$10–\$100 billion). Black & ¼ lower value of inputs (\$1 million to \$10 billion). Each sector block is proportional to the size of its total value of economic inputs consumed by the sector. Each square within each sector block indicates the proportional size of economic inputs in dollars. (Macaulay, 2009)

1.2.3 Emergency planning

Very often earthquakes have struck densely urbanised areas with severe consequences for the population. This situation has clearly shown the importance of being prepared for a community by implementing adequate emergency plans to face the post-earthquake scenarios. The main purpose of emergency is to reduce the number of casualties, provide reasonable life conditions to the affected population and speed up the recovery to normality. It is clearly demonstrated that speed, volume and quality of critical humanitarian assistance increase when the following goals are pursued:

- Reach a common understanding of earthquake risk to ensure early action;
- Establish a minimum level of earthquake preparedness across clusters:
- Build the basis for a joint response strategy to meet the needs of affected people in the short and medium period;
- Define considerations for detailed contingency planning on the basis of the worst-case scenario, especially around access and logistics;



This project has received funding from the European Union's Horizon 2020 research and innovation programme under grant agreement No. 700748

Manual for the assessment of liquefaction risk, defining the procedures to create the database, collect, define, symbolize and store information in the Georeferenced Information System and to perform and represent the risk analysis

- Minimize the consequences of secondary disasters after earthquake

For the above purposes, a primary advantage of risk assessment is that population are informed of the risk that may incur during earthquakes, connected directly or indirectly to liquefaction. Awareness may prompt to behave correctly in case of seismic events as well as to undertake remediation policies to reduce risk.

Civil Protection bodies are the agencies of larger public impact and visibility, responsible for the actions of earthquake risk mitigation. Emergency preparedness is the direct consequence of a good definition of hazard, vulnerability and risk assessment. Planning rescue operations, including transportation of injured, managing homeless problems, providing basic services, etc., and managing post-events in all their ramifications is of utmost importance for reducing the pain of the affected populations and in returning life to a normal standard. Planning requires a prior definition of the seismic scenario or collection of seismic scenarios. For each one, the effect of the simulated motion is treated and transformed into variables to be used in the planning of all operations. Planning should consider the zones more prone to different occurrences, and prepare logistic and field exercises to simulate situations that may happen in the case of a real earthquake. Concerning this issue, a correct behaviour at the community scale is the establishment of emergency strategies. For instance, the Italian Department of Civil Protection has recently promoted a manual for the assessment of Limit Condition Emergency, also named CLE (CTMS, 2016). This procedure analyses the response of an urban settlement in the limit condition that it is damaged at a level that any function, including the residential one, is interrupted. Strategic emergency functions must be thus preventively planned, defining safe areas for their installation, verifying accessibility of these areas and the connection with the territorial context and with the outer transportation system (Figure 1-8.a).

This question implies to analyse risk over the territory and define suitable areas, i.e. safe in case of earthquakes and to check the reliability of the road network in order to guarantee mobility of the emergency vehicles after earthquakes, identifying a number of candidate emergency paths and checking the possible interference with buildings (Figure 1-8.b). Travel time methodologies are currently implemented to assess the reliability of transportation networks, in some cases quantifying the probability that a given destination can be reached at all, in other cases evaluating the probability that a given destination can be reached within an acceptable time interval.

Modern technological developments can provide Civil Protection and other managing and security bodies with new forms of mitigation such as the seismic Early Warning systems (EWS). These systems are essentially of two types. The most widely accepted EWS takes advantage of real time modern seismology and deals with the lead time one can gain after the onset of an event by identifying from the first seconds of the P-wave the size of the S-wave which will arrive at a later stage. If the distance that the waves travel to a site is sufficiently large, one can gain tens of seconds and be able to send information prior to the arrival of the large S-amplitudes.

Depending on the gained time, this technique will allow launching of important actions, such as shutdown of industries, closing networks, stopping dangerous activities, or preparing for active control of constructions. These new ideas are already being practiced in several locations as test cases, the most known one being the



This project has received funding from the European Union's Horizon 2020 research and innovation programme under grant agreement No. 700748

Manual for the assessment of liquefaction risk, defining the procedures to create the database, collect, define, symbolize and store information in the Georeferenced Information System and to perform and represent the risk analysis

system for stopping the Shinkansen train in Japan. Knowing the distribution of seismic, and particularly of liquefaction enables to optimize strategies.

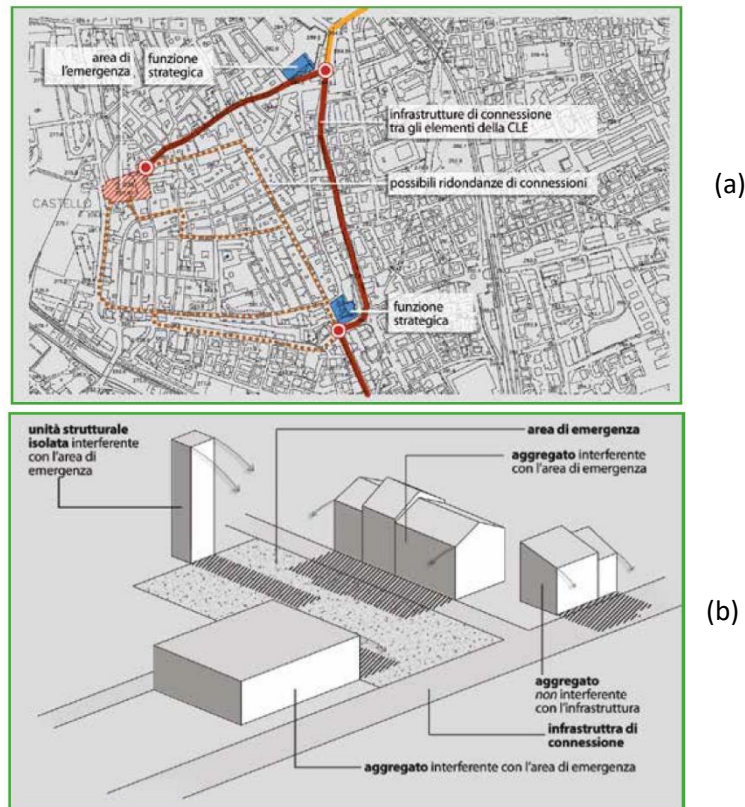


Figure 1-8: Example of accessibility and connectivity to an emergency area and interference with buildings (CTMS, 2016).

1.2.4 Owners of building assets/Investors

Liquefaction risk assessment finally attributes a level of hazard to the different areas within the urban context in some way ruling the market of construction. Discrepancies arise for the owners of portfolios of properties that may end in solutions consequences depending on the relative viewpoint. Low liquefaction hazard on some area may motivate people to move to that places and generate a surplus for the demand of houses with consequent increase of cost. On the other hand, the owners of buildings in highly hazardous areas might be subjected to very restrictive regulations that impose technical improvement or modification of structures and foundations. Figure 1-9 shows the example of Christchurch (New Zealand) where, after the Earthquake Sequence of 2010-2011.

The landscape of the city was profoundly modified by the liquefaction induced by earthquakes and a part of the city (red zone) was definitely abandoned. Estimate of the phenomenon severity over the territory led to a reclassification that produced significant changes in the construction requirements.

In some cases, the large vulnerability of buildings may require mitigation actions, like the adoption of a stiffer foundation system, reinforcement with piles, ground improvement that may increase the cost of new houses



This project has received funding from the European Union's Horizon 2020 research and innovation programme under grant agreement No. 700748

LIQUEFACT Deliverable 7.1

Manual for the assessment of liquefaction risk, defining the procedures to create the database, collect, define, symbolize and store information in the Georeferenced Information System and to perform and represent the risk analysis

or the rehabilitation of old ones. On one side, this occurrence leads to an increased quality, safety and serviceability of the buildings and as such money spent on mitigation turn into a higher value to the property. One possible advantage could be the reduced premium to be paid for insuring the property. On the other side, the increase of costs may reach a point that the house becomes out of market and this may motivate people to prefer other less expensive areas for living. Owners are in the position to evaluate the economical convenience of undertaking mitigation action or to downgrade their property. Provided that decision is dictated by a combination of factors, including commercial issues not strictly related with seismic risk, liquefaction risk assessment noticeably contribute to the definition of the property value.

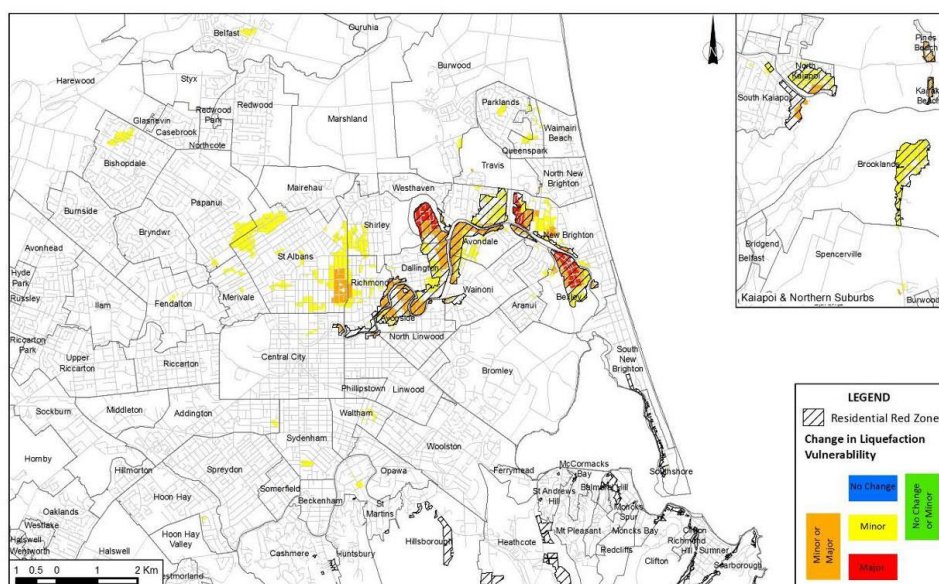


Figure 1-9: Map showing the change of liquefaction vulnerability severity classifications across the CES for 100 year return period levels of earthquake shaking (Tonkin & Taylor, 2016)



This project has received funding from the European Union's Horizon 2020 research and innovation programme under grant agreement No. 700748

Manual for the assessment of liquefaction risk, defining the procedures to create the database, collect, define, symbolize and store information in the Georeferenced Information System and to perform and represent the risk analysis

1.2.5 Insurance

In earthquake risk management, besides enhancing seismic provisions for new construction and retrofitting existing structures and infrastructure (i.e. hard measures for seismic risk mitigation), insurance serves as a valuable vehicle to mitigate financial risk (i.e. soft measure for seismic risk mitigation).

Insurance is a risk transfer instrument for economic/financial consequences and smoothes out fluctuation/variability of a stakeholder's asset caused by contingencies. A stakeholder pays premium to an insurer and receives compensation, according to a pre-agreed contract, upon the occurrence of specific loss events. In the context of earthquake insurance, the occurrence of seismic damage cost, exceeding a specified deductible, triggers the pay-out from an insurer. A typical pay-out function includes deductible, cap, and co-insurance factor. The earthquake insurance premium consists of pure premium, which is equivalent to the expected damage cost, and risk premium (plus transaction cost). The risk premium is an overcharge requested by an insurer for undertaking low-probability and high consequence events, and can be much greater than pure premium. The appreciation of benefit from purchasing earthquake insurance coverage varies significantly, depending on risk attitudes, financial status, personal experience, and many other factors (Palm, 1995). Therefore, even when the overall premium is reasonably priced, not so many stakeholders voluntarily purchase earthquake risk coverage.

Insurance companies are interested to know the potential impact of earthquakes, including possible liquefaction phenomena, to decide if the insurance coverage may lead to profits, to fix rates of the policies in relation with the location and probability of earthquake losses. Rates may be cheaper for less hazardous zones and for less vulnerable properties. In the past, earthquake loss was assessed using a collection of mass inventory data and was based mostly on experts' opinions. Today it is estimated using a Damage Ratio (DR), a ratio of the earthquake damage money amount to the total value of a building (EERI, 2000). Another method is the use of HAZUS (FEMA, 2003), a procedure for seismic risk assessment and loss estimation.

From a general viewpoint, insurance against earthquakes can be seen as a non-technical measure to face losses, but policies differ largely from country to country, being insurance strongly promoted or even compulsory in some countries, poorly adopted in some others.

A critical point for insurance companies when facing large scale disasters like earthquakes, flooding, hurricane etc., is the fact that events will simultaneously affect many buildings in the same area and this may lead to financial collapse of the company in case of catastrophic event. California residents purchase more earthquake insurance than in any other state in the U.S. For this reason, a quasi-public (privately funded, publicly managed) agency called the CEA California Earthquake Authority was created to comply the law that forces companies to include earthquake coverage in home insurance with the resistance of insurers to undertake the above described financial risk. Companies may voluntarily become members of CEA, transferring earthquake premiums to the authority that covers claims from homeowners with a CEA policy from member insurers.

The government of Japan created a similar authority named "Japanese Earthquake Reinsurance" in 1966. Homeowners may buy earthquake insurance from a company as an optional rider to a fire



This project has received funding from the European Union's Horizon 2020 research and innovation programme under grant agreement No. 700748

Manual for the assessment of liquefaction risk, defining the procedures to create the database, collect, define, symbolize and store information in the Georeferenced Information System and to perform and represent the risk analysis

insurance policy. Insurers enrolled in the JER scheme who have to pay earthquake claims to homeowners share the risk among themselves and also the government, through the JER. The government pays a much larger proportion of the claims if a single earthquake causes aggregate damage of over about 1 trillion yen (about US \$8.75 billion). The maximum payout in a single year to all JER insurance claim filers is 5.5 trillion yen (about US \$39.4 billion); if claims exceed this amount, then the claims are pro-rated among all claimants.

In 1945 New Zealand has created the Earthquake Commission (EQC), a government-owned crown entity which provides primary natural disaster insurance to the owners of residential properties. In addition to its insurance role, EQC also undertakes research and provides training and information on disaster recovery. Figure 1-10 reports a scheme of insurance for New Zealand developed by EQC, showing for a dwelling what is included and what is not in the insurance contract.

In all cases, risk assessment helps to manage these situation making stakeholders aware of the financial risks.

Insurances (public and private), differentiating the premium, may contribute to control the quality of design and construction. Several models for the application of insurance are available and practiced throughout the world. Essentially, one can have centralized bodies as practiced in Spain by the Consorcio de Compensación de Seguros (CCS, 2008), or a moderate centralized scheme such as the Solidarity Fund created in the EU in the aftermath of the large Central Europe floods of summer 2002. But the most practiced case is the existence of individual national or international companies with pools through international re-insurance.

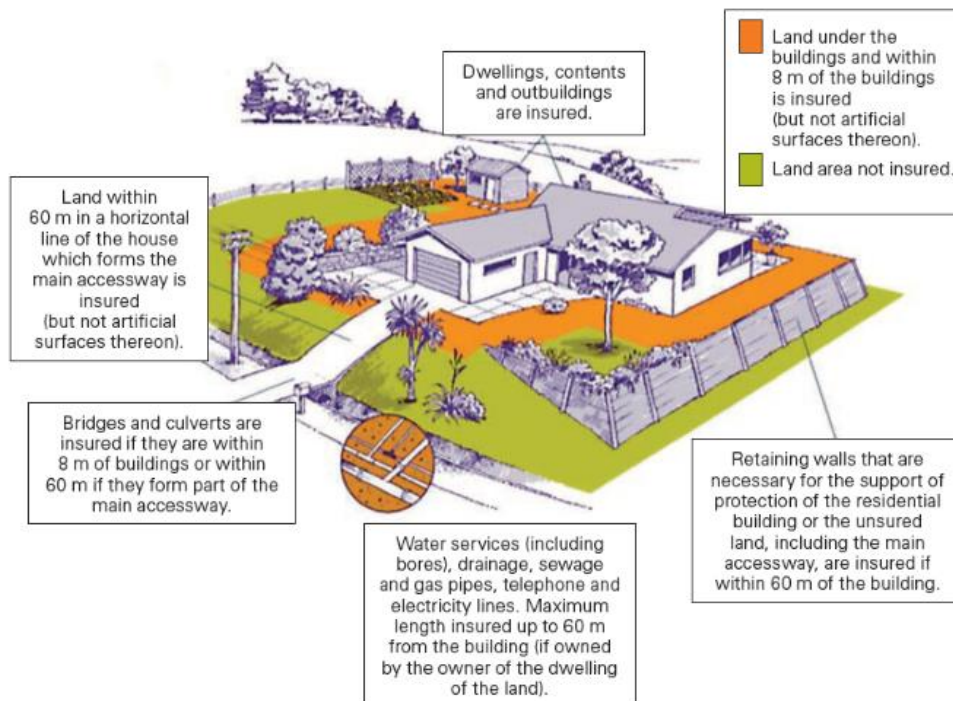


Figure 1-10: Scheme of insurance in New Zealand (EQC, 2012).



This project has received funding from the European Union's Horizon 2020 research and innovation programme under grant agreement No. 700748

Manual for the assessment of liquefaction risk, defining the procedures to create the database, collect, define, symbolize and store information in the Georeferenced Information System and to perform and represent the risk analysis

1.2.6 Design of buildings and infrastructures

Risk assessment of liquefaction usually refers to large portions of the territory and thus cannot directly used for the design of structures, as the latter regards a much smaller scale that deserves more specific studies. However, notwithstanding the different scales and level of precision of the two analyses, the fundamental questions posed by design and risk assessment are similar as both concern safety and serviceability of the structures. Despite it is never recommendable to use results of risk assessment for design, that should be on the contrary based on specific investigations and analyses, considerable advantage may derive from knowing risk on the area hosting their structure to anticipate issues related with liquefaction. An overview of the design methodologies adopted worldwide is made in the next section to examine the applicability of different possible approaches to risk assessment.

1.3 Liquefaction assessment in the international standards

Many international codes adopt principles and methodologies to assess liquefaction potential on structures similar to those currently used for risk assessment. It is thus worth to overview the design practice in the international standards to learn methodologies that can be borrowed to increase efficacy of the risk assessment.

The assessment of liquefaction is part of several design codes although with meaningful differences from case to case. In Japan the subject is not dealt by a unified code, but specific standards are developed by the Authorities responsible for the different structures or infrastructures (harbour, road railway etc.) (Table 1-3). In all cases, the assessment of liquefaction triggering below the structure is prescribed with deterministic calculation where safety factors are computed combining the seismic action and the soil properties derived from in situ tests (SPT tests or, more rarely, laboratory tests on undisturbed samples). Mitigation actions are consequently prescribed in case the above assessment highlight safety factors lower than 1.



This project has received funding from the European Union's Horizon 2020 research and innovation programme under grant agreement No. 700748

Manual for the assessment of liquefaction risk, defining the procedures to create the database, collect, define, symbolize and store information in the Georeferenced Information System and to perform and represent the risk analysis

Table 1-3: Remedial Measures against Soil Liquefaction (JGS, 1998)

Design codes and standards		Year
Title	Organization	
1. Design standards for port andharbour facilities	The Japan Port and Harbour Association	1970
2. Technical standards for port andharbour facilities in Japan	ditto	1990
3. Seismic design manual for highway bridges	Japan Road Association	1970
4. Specifications for highway bridges, part 5 seismic design	ditto	1990
5. Design standard for railway structures, foundation and retaining wall	Japan National Railway	1970
6. Design standard for national railway structures (foundation and retaining wall)	Japan Society for Civil Engineers	1986
7. Design criteria of building foundation structures and commentaries	Architectural Institute of Japan	1970
8. Recommendations for design of building foundations	ditto	1983
9. Notification specifying particulars of technical standards concerning control of hazardous materials	Ministry of Home Affairs, Fire Defense Agency	1978
10. Recommended practice for LNG in-ground storage	The Japan Gas Association	1979
11. Guidelines for remedial measures of water works facilities against earthquakes	Japan Water Works Association	1979
12. Specifications of construction of tailings dams and commentary	Japan Mining Industry Association, Ministry of International Trade and Industry	1979
13. Guidelines for remedial measures of sewage works facilities against earthquakes	Japan Sewage Works Association	1982
14. Design manual for common utility ducts	Japan Road Association	1981
15. Highway earthwork series, manual for soft ground remediation	ditto	1986
16. Technical guidelines for aseismic design of nuclear power plants	Japan Electric Association	1987

□ Liquefaction assessment was introduced in standards.
 △ Standard was revised, but liquefaction assessment was not corrected.
 ○ Standard was revised (corrected).

The International Building Code (ICC, 2009), adopted in several U.S. States and Municipalities (Alabama, Florida, Idaho, Iowa, Maine, Massachusetts, Michigan, Montana, Las Vegas Nevada, New Hampshire,

New Jersey, New Mexico, North Carolina, North Dakota, Ohio, Oklahoma, Oregon, Pennsylvania, Rhode Island, Utah, West Virginia, Wisconsin) specifies that liquefaction assessment is needed on buildings classified as D, E or F in the seismic categorization given by ASCE taking into account the Occupancy Category of the building (I, II, III, IV), the Mapped Acceleration Parameters (S_s and S₁) and Site Class (A-F). In this case, specific investigation is required to assess the potential for liquefaction and soil strength loss for site peak ground acceleration, magnitude and source characteristics consistent with the design earthquake ground motions and to estimate differential settlements, lateral movements and lateral loads on foundations.

A similar approach is adopted by the California Dept of Transportation (Caltrans, 2008). It requires a three-steps analysis to evaluate the effects of liquefaction on bridge foundations: identify potentially liquefiable soils, assess triggering under design earthquake motion, quantify permanent ground deformations. The results of this analysis serve to evaluate the magnitude of forces acting on the bridge foundations due to permanent ground displacement and finally to foresee an increase of costs (Table 1-4).



This project has received funding from the European Union's Horizon 2020 research and innovation programme under grant agreement No. 700748

Manual for the assessment of liquefaction risk, defining the procedures to create the database, collect, define, symbolize and store information in the Georeferenced Information System and to perform and represent the risk analysis

Table 1-4: Strategy for liquefaction assessment on bridges foundation and estimate of cost increase (Caltrans, 2008).

TABLE 1 LIQUEFACTION SEVERITY LEVELS			
Liquefaction Severity	Example of Subsurface Conditions	Possible Effects on Bridge Foundation	Mitigating Alternatives
Negligible	<ul style="list-style-type: none"> Subsurface materials are not prone to liquefy. 	N/A	N/A
Liquefaction without Lateral Spreading	<ul style="list-style-type: none"> Acceleration levels high enough to cause liquefaction. Surface and subsurface conditions not favorable for the development of permanent lateral ground displacements 	<ul style="list-style-type: none"> Reduction in shear strength of liquefiable soils affects axial and lateral capacity of bridge foundations; foundation performance may be affected. Permanent horizontal displacements unlikely to develop. Post-liquefaction settlements will likely develop. Depending on the subsurface stratification, down drag forces may develop. 	<ul style="list-style-type: none"> Strengthening of existing pile foundations likely to be required. New piles may need to extend deeper to compensate for reduced axial and lateral load-carrying capacity. Countermeasures against reduced axial and lateral capacity, as well as potential down drag forces include larger pile size, CISS piles or CIDH piles.
Liquefaction with Lateral Spreading	<ul style="list-style-type: none"> Acceleration levels high enough to cause liquefaction. Continuous liquefiable material across site. Surface and subsurface conditions favorable for the development of permanent lateral ground displacement such as: <ul style="list-style-type: none"> Gently sloping ground surface, or level ground adjacent to a free face. Sloping base of liquefiable deposit. Approach embankments built over liquefiable material. 	<ul style="list-style-type: none"> Reduction in shear strength of liquefiable soils severely affects lateral and axial capacity of bridge foundations; foundation performance is considerably affected. Permanent horizontal displacements will develop and adversely affect pile foundations, pile caps and abutments. High soil pressure on foundations systems expected if a stiff, non-liquefiable deposit overlies liquefied material. Post-liquefaction settlements may be significant. Down drag forces will affect axial load carrying capacity of pile foundations under service loading conditions. 	<ul style="list-style-type: none"> Foundation strengthening required. Countermeasures against reduced axial capacity, down drag forces and lateral pressure include CISS piles or large diameter CIDH piles. Ground improvement may be considered in conjunction with foundation strengthening. Bridge system may need to be modified to allow larger permanent ground displacements without collapse. Increase ductility of foundation to absorb estimated permanent lateral displacement. Bridge relocation to an alternate non-liquefiable site should be considered.

TABLE 3 LIQUEFACTION SEVERITY vs ESTIMATED COST INCREASE (FOR PLANNING PURPOSES)	
Liquefaction Severity	Estimated Bridge Foundations Cost Increase at Impacted Locations (%)
Negligible Liquefaction	0
Liquefaction without Lateral Spreading	0 to 300
Liquefaction with Lateral Spreading	200 to 500



This project has received funding from the European Union's Horizon 2020 research and innovation programme under grant agreement No. 700748

Manual for the assessment of liquefaction risk, defining the procedures to create the database, collect, define, symbolize and store information in the Georeferenced Information System and to perform and represent the risk analysis

Eurocodes 8 part 5 (EN1998-5: Foundations, retaining structures and geotechnical aspects) in its present form prescribes the assessment of liquefaction for siting and foundations. Liquefaction susceptibility must be evaluated for soils including extended layers or thick lenses of loose sand, with or without silt/clay fines, beneath the water table level, and when the water table level is close to the ground surface. This evaluation shall be performed for the free-field site conditions (ground surface elevation, water table elevation) prevailing during the lifetime of the structure. The assessment is carried out in two steps: firstly, there is the assessment of susceptibility based on earthquake magnitude, soil composition and groundwater table position; then triggering is estimated computing a safety factor where seismic action (Cyclic Stress Ratio) is compared with the resistance derived from in situ tests (e.g. SPT) (Boulanger & Idriss, 2014). Minimum safety factors are given for different situations (1.25 for foundation, 2 for earth retaining structures). This analysis preludes to undertake mitigation actions consisting of ground improvement or piling in case of negative outcomes. Currently, Eurocodes are undergoing a complete revision process whose end is foreseen in 2020 and the liquefaction assessment will be updated.

In recent years, the New Zealand Geotechnical Society (NZGS, 2016) has issued a set of guidelines to “promote consistency of approach to everyday practice and improve geotechnical-earthquake aspects of the performance of the built environment” (NZGS, 2016). Guidelines aim to support rational design approaches on the following issues:

- Geotechnical investigation for earthquake engineering
- Identification, assessment, and mitigation of liquefaction hazards
- Earthquake resistant foundation design
- Ground improvement including Specification for residential properties in the Canterbury region
- Retaining walls

In particular, the strategy defined in Module 3 (Identification, assessment, and mitigation of liquefaction hazards) is articulated in a sequence of steps defined by the flow chart depicted in Figure 1-11. Within this methodology the criteria reported in Table 1.5 are proposed to estimate severity of liquefaction. With regard to this table, the authors provide the following series of warning that somehow limit the generality of the criterion:

- *Liquefaction of relatively thin layers of near-surface soils could be very damaging and may produce effects equivalent to Performance Levels L3 and L4.*
- *A relatively thin liquefied layer with low residual strength could be responsible for lateral spreading and consequent very severe effects (Performance Level L5).*
- *LPI (Iwasaki et al., 1978) and LSN (van Ballegooy et al., 2014) are damage indices that quantify liquefaction-induced damage by combining the effects of the severity of liquefaction (value of FL or FS), thickness of liquefied soils and their location within the soil profile. The threshold values for these indices shown in relation to the performance levels are only indicative values.*
- *these thresholds may vary and do not cover all liquefaction cases (scenarios and ground conditions). These indices are typically applied for area-based screening, and in such applications have reasonable predictive capacity, but may mis predict damage/performance for about 20 percent to 30 percent of*



This project has received funding from the European Union's Horizon 2020 research and innovation programme under grant agreement No. 700748

Manual for the assessment of liquefaction risk, defining the procedures to create the database, collect, define, symbolize and store information in the Georeferenced Information System and to perform and represent the risk analysis

- the cases. Maurer et al. (2015) and van Ballegooy et al. (2014) provide significant insights on liquefaction-induced land damage and its interpretation through land damage indices LPI and LSN.*
- *All being equal (i.e. FL, thickness and location of liquefied layer), liquefaction consequences and magnitude of liquefaction-induced ground deformation strongly depend on the density of the soil. LSN quantifies this effect in a simplified manner. Severity of liquefaction effects decreases with increasing density of the soils, and importantly the mechanism of ground deformation also changes as the density of the soil increases (eg flow liquefaction, zero-effective stress liquefaction, and nearly zero-effective stress transient liquefaction with cyclic mobility are characteristic types of behaviour associated with very loose, loose to medium dense, and dense sands respectively).*
 - *The LPI and LSN should be considered in the context of particular ground conditions and structure of interest. The ranges provided in the table are based on triggering calculations using Boulanger and Idriss (2014) method, and analyses and interpretation of liquefaction effects in the 2010-2011 Canterbury earthquakes.*



This project has received funding from the European Union's Horizon 2020 research and innovation programme under grant agreement No. 700748

Manual for the assessment of liquefaction risk, defining the procedures to create the database, collect, define, symbolize and store information in the Georeferenced Information System and to perform and represent the risk analysis

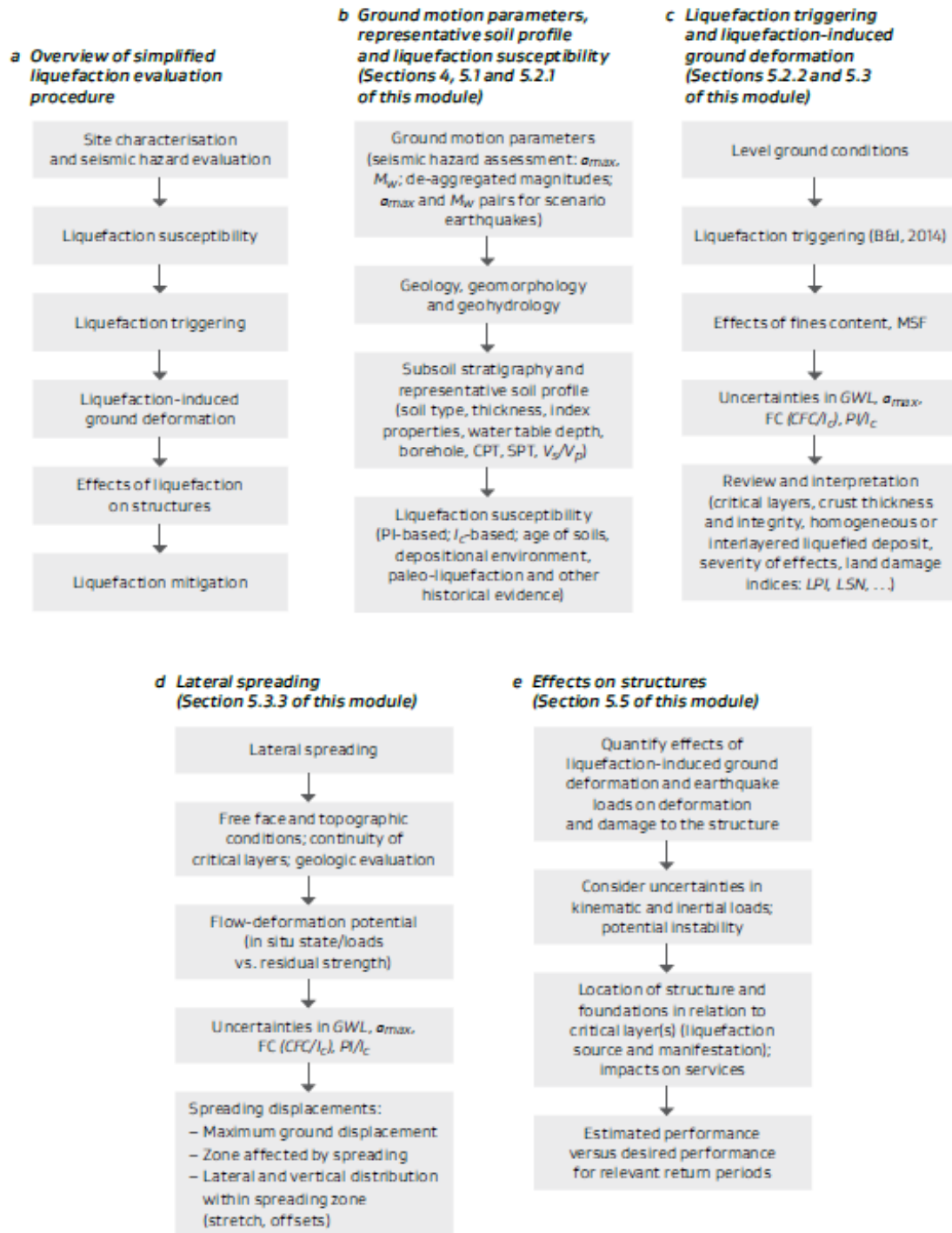


Figure 1-11: Overview of liquefaction vulnerability assessment (NZGS, 2016).



This project has received funding from the European Union's Horizon 2020 research and innovation programme under grant agreement No. 700748

Manual for the assessment of liquefaction risk, defining the procedures to create the database, collect, define, symbolize and store information in the Georeferenced Information System and to perform and represent the risk analysis

Table 1-5: General performance of liquefied deposits (NZGS, 2016).

PERFORMANCE LEVEL	EFFECTS FROM EXCESS PORE WATER PRESSURE AND LIQUEFACTION	CHARACTERISTICS OF LIQUEFACTION AND ITS CONSEQUENCES	CHARACTERISTIC F_L , LPI
L0	Insignificant	No significant excess pore water pressures (no liquefaction).	$F_L > 1.4$ LPI=0 LSN <10
L1	Mild	Limited excess pore water pressures; negligible deformation of the ground and small settlements.	$F_L > 1.2$ LPI = 0 LSN = 5 – 15
L2	Moderate	Liquefaction occurs in layers of limited thickness (small proportion of the deposit, say 10 percent or less) and lateral extent; ground deformation results relatively small in differential settlements.	$F_L = 1.0$ LPI < 5 LSN 10 – 25
L3	High	Liquefaction occurs in significant portion of the deposit (say 30 percent to 50 percent) resulting in transient lateral displacements, moderate differential movements, and settlement of the ground in the order of 100mm to 200mm.	$F_L < 1.0$ LPI = 5 – 15 LSN = 15 – 35
L4	Severe	Complete liquefaction develops in most of the deposit resulting in large lateral displacements of the ground, excessive differential settlements and total settlement of over 200mm.	$F_L \ll 1.0$ LPI > 15 LSN > 30
L5	Very severe	Liquefaction resulting in lateral spreading (flow), large permanent lateral ground displacements and/or significant ground distortion (lateral strains/stretch, vertical offsets and angular distortion).	

The above defined procedures for the assessment of liquefaction are based on a load-strength approach as they rely on the computation of safety factor (CRR/CSR) along with the subsoil depth. This calculation can be incorporated in the Load and Resistance Factors Design (LRFD) methodology adding different factors to account for the uncertainties in seismic actions, soil properties etc.. On the other side, limiting deformation is the most relevant requirements for building foundations or other structures. In normal practice, where gravity loads are basically considered, settlements are checked at the Serviceability Limit State SLS assuming that a footing meeting SLS and ULS criteria would prevent the instability of the superstructure. Extending this practice to seismic assessment, and particularly to liquefaction, is not straightforward as deformation is dictated by several factors (consolidation due to dissipation of excess pore water pressure, sedimentation and re-solidification of soil, volume loss due to sand ejecta, lateral spreading) not fully predictable. Additional complexity is given by the presence of the structure whose weight alters the initial stress level and trigger further deformation.

Performance based design PBD is a different strategy that aims at optimizing the trade-off between construction costs and building performance (NASEM 2016). It aims at a more comprehensive appraisal of the building performance under various loading scenarios with a sophisticated modelling of the building dynamic response (effects of non-linearity, quantification of damage etc.) that accounts for the uncertainties related with earthquake loading, foundation performance and soil response. Analyses should incorporate all possible earthquake ground motions (intensity and magnitude) together with their probable frequency of occurrence and account for the variability of parameters necessary to characterize site and buildings.



This project has received funding from the European Union's Horizon 2020 research and innovation programme under grant agreement No. 700748

Manual for the assessment of liquefaction risk, defining the procedures to create the database, collect, define, symbolize and store information in the Georeferenced Information System and to perform and represent the risk analysis

The uncertainties involved in the assessment of earthquake ground motions, system response, physical damage, and losses make probabilistic methods for liquefaction consequence assessment central to PBD. Fully probabilistic procedures considering the contributions from all potential levels of ground motion have proven to produce more complete and logical estimates of liquefaction hazards in different seismic environments compared with deterministic methods.

Procedures developed for liquefaction triggering have been recently extended to consequences such as lateral spreading and post-earthquake free-field settlement and to test reliability of current procedures used to estimate liquefaction hazards.

Advances in performance-based procedures for liquefaction problems requires improvement in the understanding of the vulnerability of structures and facilities for given liquefaction-induced ground deformation and improved understanding of the costs and time requirements to repair liquefaction-associated damage.

Apart from the above difficulties, the requirement of computing capacity sufficient to perform the voluminous calculations involved in probabilistic performance-based frameworks represents another limitation for the spreading of this more rational approach.

For the above reasons, the adoption of a performance-based assessment for liquefaction risk is desirable although additional difficulties are given with the larger uncertainty connected with the lower density of information.

1.4 Basic concepts relevant for liquefaction risk assessment

Ground motion – movement of the Earth surface determined by the combination of source mechanism, characteristics of the crossed medium and geotechnical properties of the soil at the studied site.

Hazard assessment – the probability that a certain ground motion parameter (MMI, PGA, Spectra) will be attained or passed within a lifetime period.

Site effects – Modification of ground motion in amplitude, frequency content and duration determined by the local condition.

Liquefaction effects - flow sliding lateral spreading settlement caused by the shear waves on susceptible soils.

Susceptibility - proneness of a soil to undergo liquefaction

Site-city interaction – Interaction between buildings of a city and its subsoil.

Vulnerability – Degree (level) of performance of a system (engineering structure, network, social group, etc.) under a certain level of seismic action.

Fragility – Similar to vulnerability but where the performance is viewed in a statistical way.



This project has received funding from the European Union's Horizon 2020 research and innovation programme under grant agreement No. 700748

Manual for the assessment of liquefaction risk, defining the procedures to create the database, collect, define, symbolize and store information in the Georeferenced Information System and to perform and represent the risk analysis

Damage (victims, casualties) – “physical damage”: deaths, injures (severe, light, etc.), homeless, damage to buildings, economic impact; “indirect damage”: social impact; “immaterial damage”: psychological impact, etc.

Damage scenario – Geographical distribution of damage for a given earthquake event or a set of events.

Risk – The convolution of hazard with vulnerability for a group of structures, a region, etc.

Zonation. Microzonation – Identification of geographical areas having homogeneous similar behaviour under seismic action. Depending on the scale of work, we may consider only the regional differences derived from seismic sources and path, as the case of a gross scale, or consider site effects if working at a detail scale. Microzoning may include also other effects beyond the traditional seismic action parameters, such as landslide, liquefaction, etc.

Networks (lifelines) – Systems of transportation (car traffic, water, gas, electricity, communications, etc.) spread in a region, subjected to different levels of ground motion during a given event.

Critical infrastructures – Installations or equipment whose performance during an earthquake is decisive under various different functions: to serve in the emergency operation, to avoid leakage of dangerous products, or due to have a large concentration of population. These facilities, due to their importance should be kept functional under severe or extreme conditions, depending on the expected consequences of failure.

Urban system analysis – An integrated system subsuming all possible consequences of the earthquake impact in an urban center.

Direct, indirect, economic, commercial, business, social, etc., consequences of the earthquake are weighted for a global index value.

Performance – The form a system responds to a given earthquake action in terms of measurement of the functions assigned to that system.

Mitigation – Policies for reduction of consequences of earthquake activity within a lifetime period.

Codes – The most practical and efficient form of designing a structure to withstand seismic action, by defining the minimum requirements (compulsory in some societies and recommendations in others) as far as structural performance.

Structural reinforcement – The form of mitigation which considers that vulnerable constructions should undergo reinforcement of their structural system in order to decrease that vulnerability. Recent technological advances have enlarged the spectrum of action for better performance, by using base-isolation techniques, damping devices or dynamic control of structures.

Emergency – Set of actions to be launched when the earthquake occurs. These should optimize the time of intervention (rescue, hospital treatment, etc.) in the most efficient way to minimize the suffering of the populations. Emergency to be fully effective at the needed time requires a great deal of preparation in a great variety of fields of human activity.

Preparedness - preparation for the intervention.



This project has received funding from the European Union's Horizon 2020 research and innovation programme under grant agreement No. 700748

Manual for the assessment of liquefaction risk, defining the procedures to create the database, collect, define, symbolize and store information in the Georeferenced Information System and to perform and represent the risk analysis

Alert – Possibility of expecting a certain level of impact in a region hit by an earthquake, preparing the emergency system for action.

1.5 Overview of the guidelines

According to the above defined scope, the present guidelines provides a set of rules for implementing the assessment of liquefaction risk.

In the second chapter the strategies for liquefaction risk assessment is introduced, giving an appropriate terminology and particularizing it to different possible situations. Scope and limitations of the assessment are a primary condition and the most typical are thus highlighted.

The third chapter defines the rules for creating a Geographical Information System in accordance with the most recent standards. Procedures to create the database, symbolize and store information are defined together with a number of possible ways to represent results of the risk analysis.

In the fourth chapter the criteria to assess liquefaction hazard are defined. Methods taken from previous studies or specifically defined in the project are reported to quantify susceptibility, firstly at the geological then at the geotechnical scale, to analyze triggering conditions and to quantify surface manifestation. Synthetic schemes are provided at the end of the chapter summarizing the methodology for creating databases.

The fifth chapter is dedicated to the methodology for the liquefaction risk assessment. The first part deals with the characterization of the systems at risk, making explicit references to buildings, road and water infrastructures. The criteria defined in the project to define fragility on each of these elements are described, defining them as the probability that prescribed limit states are exceeded, and characterizing physical damage consistently with the type of required function and with the loss of serviceability for each system.

The sixth chapter is dedicated to define a methodology to quantify losses and reliability of infrastructures. Starting from the physical damage, methodologies to quantify direct and indirect financial are given for buildings, road networks and water distribution systems.

The seventh and last chapter outlines the strategy for mitigation and for improving the system resilience. The entire risk assessment process is reviewed to identify methodologies that operates at different level to reduce the impact of liquefaction on the society.



This project has received funding from the European Union's Horizon 2020 research and innovation programme under grant agreement No. 700748

2. LIQUEFACTION RISK ASSESSMENT

2.1 Risk and uncertainty

The primary goal of seismic risk assessment is to facilitate a sound and efficient decision making in the facing of earthquake (Tefamariam & Goda, 2013). In general terms, risk is defined as the possibility of losing something valuable. Determining the risks due to natural events implies to calculate the probability of occurrence and potential consequences of hazardous scenarios. Risk may be thus evaluated as the probability that a specified loss will exceed some quantifiable value during a given exposure time.

Currently the framework for seismic risk analysis addresses:

- multiple earthquake-induced hazards (strong ground shaking, surface ruptures, liquefaction, landslides, and tsunamis)
- vulnerability of structural/non-structural components, and infrastructure systems (i.e. occurrence of damage given hazard),
- consequences of damage (i.e. casualty and economic loss, including both direct and indirect costs).

In the last decade, remarkable progress has been made to develop frameworks that support decision making for earthquake risk mitigation, prioritization of available options, pursue of reliability and economy (e.g. Ellingwood 2001; Wen 2001; FEMA/NIBS 2003; Crowley et al. 2005; Baker and Cornell 2008; Goda and Hong 2008).

The knowledge of seismic phenomena unavoidably involves several uncertainties that make the assessment less reliable. The determination of ground motion and its occurrence probability, the role of subsoil, the fragility of building and infrastructure and the quantification of values (e.g. Crowley et al. 2005; Kwona and Elnashai 2006; Goda and Hong 2008) all incorporate a noticeable degree of indeterminacy deriving from the quality, or even validity, scarcity and variability of the underlying data (Walley 1991) and from the simplification necessarily introduced with models. The above uncertainty factors can be broadly categorized into:

- Aleatory, also defined as statistical, representative of unknowns that differ each time an experiment is run. Uncertainty come out from the impossibility of precisely knowing all inputs of a phenomenon that are thus dealt statistically.
- Epistemic, also defined as systematic, due to things one could in principle know but doesn't in practice. This may arise from inaccuracy of measurement, approximation of models that neglect certain effects, or because some data have been deliberately neglected.

The two categories can be visualized with the concept of precision and accuracy in experimental measurement; even with an ideally perfect simulation of the phenomenology, randomness (aleatory uncertainty) of the input data due to imprecise knowledge leads to imprecise predictions; the most precise knowledge of input information may lead to inaccurate prediction due to approximate modelling (Figure 2-1).



This project has received funding from the European Union's Horizon 2020 research and innovation programme under grant agreement No. 700748

Manual for the assessment of liquefaction risk, defining the procedures to create the database, collect, define, symbolize and store information in the Georeferenced Information System and to perform and represent the risk analysis

One of the major challenges for seismic risk analysts is the estimate of uncertainty associated with earthquakes. Here the two above categories of uncertainty are combined. The current prediction of earthquake magnitude in a specific site is based on the statistical inference of historical data. Randomness is thus implicit in this prediction, being typically managed with the adoption of probabilistic models. However, one should admit that human experience is insufficient to predict all possible seismic scenarios and surprises, beyond the expected range of situation, must unavoidably be admitted. Although occurring in acknowledged seismic regions, the earthquakes of February 22nd, 2011 in Christchurch (New Zealand), March 11th 2011 in Tohoku Oki (Japan) and May 21st 2012 in Emilia Romagna (Italy) had some level of unpredictability. This highlights the limitation of our current methodologies based on inference of statistical data and the necessity of introducing extrapolation functions or relaxing axioms of classical probability (e.g. total sum of the event probabilities equals one).

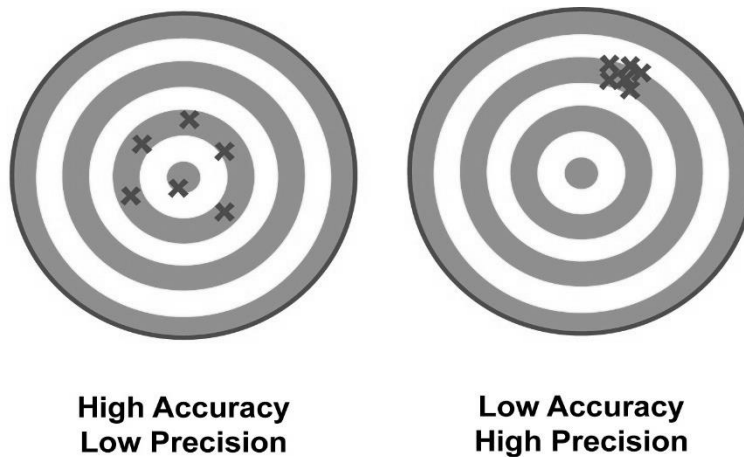


Figure 2-1: Precision and accuracy

Aleatory and epistemic uncertainties also affect the subsoil characterization, where noticeable effort must be produced to balance completeness and accuracy with relatively limited amount of information. The usually low number of investigations implies that geotechnical models, i.e. stratigraphic conditions and constitutive models, are built introducing simplistic and generally conservative assumptions. In addition, engineers are perfectly aware that, even with a great amount of information, the scattering of experimental results coming from laboratory or site tests is much larger for soils than for artificial construction materials.

Owing to unavoidable uncertainties and complexities of seismic risk, assessment is also influenced by non-physical factors, beyond characteristics of engineering materials and systems, like risk perception (e.g. expert versus public), criteria (individual versus societal, or voluntary versus involuntary), political process, and risk communication (Tsfamariam & Goda, 2013). Depending on history of past events and public concern/reaction, objective risk assessment results may be disputed and on occasion overruled.

Evaluating the role of uncertainty in the assessment of risk is a special case of error propagation. The basic idea is that uncertainties in the values of parameters propagate through the rest of the calculation and affect the result. For example, an engineer might estimate a factor or a property (a seismic intensity measure, the



This project has received funding from the European Union's Horizon 2020 research and innovation programme under grant agreement No. 700748

Manual for the assessment of liquefaction risk, defining the procedures to create the database, collect, define, symbolize and store information in the Georeferenced Information System and to perform and represent the risk analysis

parameters of a soil model etc.) use these in some cascade calculation process and use results to compute risk. Each of these steps involves errors on its own, and uncertainties in the original estimate will affect the numbers calculated at each subsequent step. The study of error propagation is aimed at dealing rationally with this problem (e.g. Baecher & Christian, 2003). In cascade phenomena like earthquakes, uncertainty arisen at a certain level propagates at the upper levels and methodologies are needed to evaluate effects (e.g. Kaplan 1981; Paté-Cornell 1994; Bradley et al. 2009; Ching et al. 2009). Well-established reliability methods, such as FOSM, FORM/SORM and Monte Carlo simulation, provide useful techniques for quantifying the propagation of uncertainty at the upper level (Nadim, 2007) and reveal which parameters contribute most to the uncertainty and probability of failure.

Notwithstanding the above situation, it is important to develop quantitative decision support tools for earthquake risk mitigation. Such tools are useful to quantify/compare seismic risks for different options and to facilitate informed decision making. Reducing uncertainties within tolerable levels and evaluating reliability of conclusions is of paramount importance for a successful risk assessment and must be thus continuously considered as the reference goal along the whole process.

2.2 Qualitative vs quantitative assessment

Risk assessment can be performed with quantitative or qualitative analyses depending on the problems under concern and on the available knowledge. In fact, the choice of a quantitative or qualitative method depends on the availability of a metric for evaluating hazard and the level of analysis needed to make a confident decision.

Qualitative assessment is based on judgment and expert opinion to estimate proxies of risk and consequences. '*. . . a man cannot, in general, tell what will happen, but his conception of nature of things, the nature of the men and their institutions and affairs, and of the non-human world enable him to form a judgment as to whether any suggested thing can happen*' (Zadeh, 1965). Qualitative methods offer analyses without detailed information, are carried out with intuitive and subjective processes and may result in different outcomes/conclusions depending on those who use them. Albeit suspected of leading to subjective conclusions, they offer the possibility of considering factors hardly quantifiable, like those connected with the human behaviour, and sometimes lead to adequate assessment of risk. An overview of the theories to transform qualitative into quantitative assessment (e.g. imprecise interval probability, possibility and evidence theories) is provided by Tesfamariam & Goda (2013).

By contrast, quantitative analyses rely on probabilistic/statistical methods and databases that quantify probability and consequent values. Quantitative analyses generally provide a more objective and unanimously acknowledged understanding but their efficacy relies fundamentally on the quality of available information, i.e. numerosity and accuracy of data, representativeness of the variety of possible situations.

When possible, a quantitative approach must be preferred being more objective and examining the system in greater detail, but an integration with qualitative analyses should be considered as well. A combination is



This project has received funding from the European Union's Horizon 2020 research and innovation programme under grant agreement No. 700748

Manual for the assessment of liquefaction risk, defining the procedures to create the database, collect, define, symbolize and store information in the Georeferenced Information System and to perform and represent the risk analysis

appropriate to sum the advantage of both approaches, becomes fundamental when not all factors can be parametrized.

2.3 Risk perception and acceptance

Unavoidably any decision based on risk assessment must end with tolerating some risk. Perception of the consequences is thus fundamental, and sometimes critical, for decision making and risk management. This “feeling” determines the satisfaction that is gained from a decision. If it deviates from an objective and fair assessment of the true risk (whether it exists in reality or not), the perceived benefit of alternative options may vary significantly. Performance Based Design offers a way to quantitatively estimate the consequences of risk acceptance, balancing the costs of construction and repair during the lifecycle, and thus leading to an optimal choice.

More frequently, risk perception is rooted in cognitive limitation of human beings that is not easy to eliminate or even to alleviate. It entails consideration of health, safety, and welfare of citizens (Paté-Cornell 1994; Hayes 1998; Hall and Wiggins 2000; May 2004a,b). A consequence of this is that the public may fail to receive the correct message from risk analysis and may make suboptimal choices. Abundant evidence of suboptimal decisions is remarked by Kunreuther (1996) in natural disaster insurance. Politicians, city planners, and experts should be well aware of the public’s risk perception, as failure to meet the public demand might result in political turmoil.

A widely used method for defining what risk connected with earthquake is acceptable is given by the F-N curve (Temfamariam & Goda, 2013) plotting for earthquakes their probability of exceedance (F) against the number of caused deaths (N). The F-N curve identify acceptable, as low as reasonably practicable (ALARP), and unacceptable regions (Melchers 2001) (see Figure 2-2). As previously pointed out, the number of fatalities connected with liquefaction is generally very low than for other earthquake related phenomena and thus the adoption of the F-N curves would lead to consider acceptable a high probability of exceedance that could end in huge economic losses. However, the principle expressed by the curves holds true if the number of fatalities is replaced by some indicator of the economic and social losses.



This project has received funding from the European Union's Horizon 2020 research and innovation programme under grant agreement No. 700748

Manual for the assessment of liquefaction risk, defining the procedures to create the database, collect, define, symbolize and store information in the Georeferenced Information System and to perform and represent the risk analysis

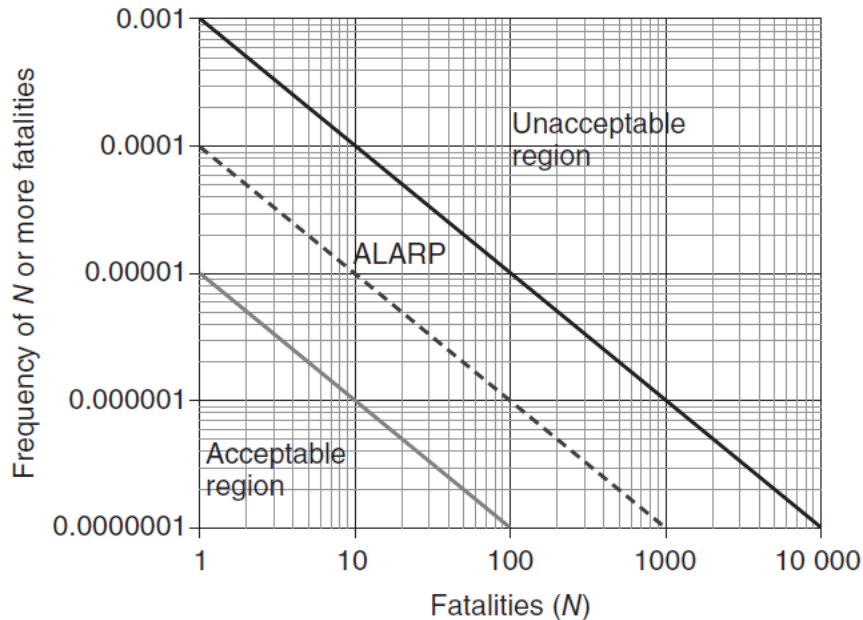


Figure 2-2: Risk acceptance criteria (from Temfamariam & Goda, 2013).

The above questions are tightly connected with risk communication, i.e. those activities aiming at increasing the public's knowledge and awareness. Participation of the public (stakeholders) in the management of risk and policy-making process is fundamental to promote holistic strategies as decisions cannot be made by technical experts and public officials only. Risk communication implies a continuous interaction among parties – risk experts, policy makers, and stakeholders (see Chapter 1). This is particularly true for highly uncertain events like earthquakes determining potentially catastrophic loss for the society. In this field, scientific/technical assessments among the experts vary significantly and public risk perception can be considerably far from the estimates of experts. Significance of risk communication in the context of earthquake risk management should not be overlooked.

2.4 Seismic risk assessment

While the more scientific field of earthquake engineering deals with the physical mechanisms induced by earthquakes, i.e. spectral-dependent ground motion, local site amplification, structural response, the more recent field of seismic risk assessment addresses which consequences this respective seismic ground motion may cause to a particular site, both for what concerns the built environment, building and infrastructure assets, or human factors related with the community. In this respect, seismic hazard establishes one key component of any assessment. In order to estimate the risk to a certain region, in terms of expected damages and losses, three integral components must be quantified (Figure 2-3):

- hazard providing information on the seismic ground motion level and, in case of a probabilistic risk assessment, the ground motion's probability of occurrence
- vulnerability (damageability) of buildings, infrastructure facilities and population



This project has received funding from the European Union's Horizon 2020 research and innovation programme under grant agreement No. 700748

Manual for the assessment of liquefaction risk, defining the procedures to create the database, collect, define, symbolize and store information in the Georeferenced Information System and to perform and represent the risk analysis

- exposure of these assets in terms of their inventory and spatial distribution over the respective study area.

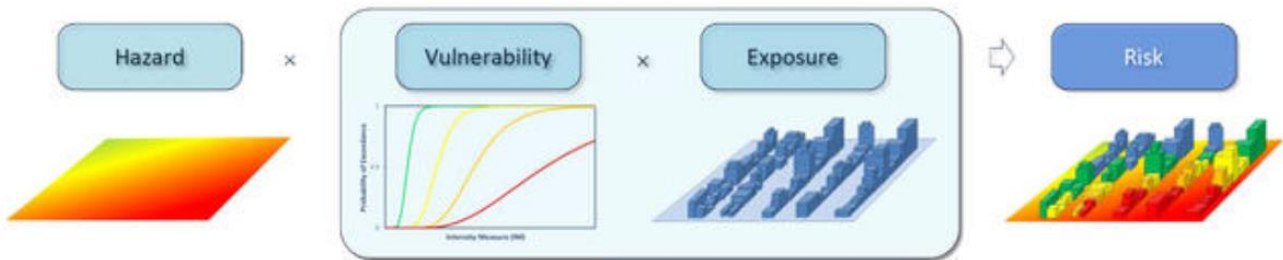


Figure 2-3: Components of risk assessment

Software packages exist, some of which are publicly available, that enable a complete assessment of the seismic risk based on a modular structure. The components of earthquake loss estimation adopted by HAZUS (FEMA, 2003) are depicted in the flow chart of Figure 2-4.

From the operative viewpoint, the methodology implemented in HAZUS is articulated as follows:

- Selection of scenario earthquakes and PESH inputs
- Selection of appropriate methods (modules) to meet different user needs
- Collection of required inventory data, i.e., how to obtain necessary information
- Costs associated with inventory collection and methodology implementation
- Presentation of results including appropriate terminology, etc.
- Interpretation of results including consideration of model/data uncertainty.

Authors point out that one of the main differences in the types of risk assessment procedures consists in the time, effort and level of expertise needed to carry out analyses, that obviously turn out in a different detail and reliability of the analysis. Considering this issue, the software permits to run analyses with different levels of complexity:

- Default Data Analysis requiring minimum effort by the user, input obtained by government agencies or published information, providing crude output as initial loss estimates to determine where more detailed analyses are warranted.
- User-Supplied Data Analysis that requires more extensive inventory data and effort and expertise by the user aimed at providing the best estimates of earthquake damage/loss with standardized methods of analysis.
- Advanced Data and Models Analysis incorporating results from engineering and economic studies carried out with external methods and software, requiring a high level of expertise with an extensive participation by local utilities and owners of special facilities.



This project has received funding from the European Union's Horizon 2020 research and innovation programme under grant agreement No. 700748

Manual for the assessment of liquefaction risk, defining the procedures to create the database, collect, define, symbolize and store information in the Georeferenced Information System and to perform and represent the risk analysis

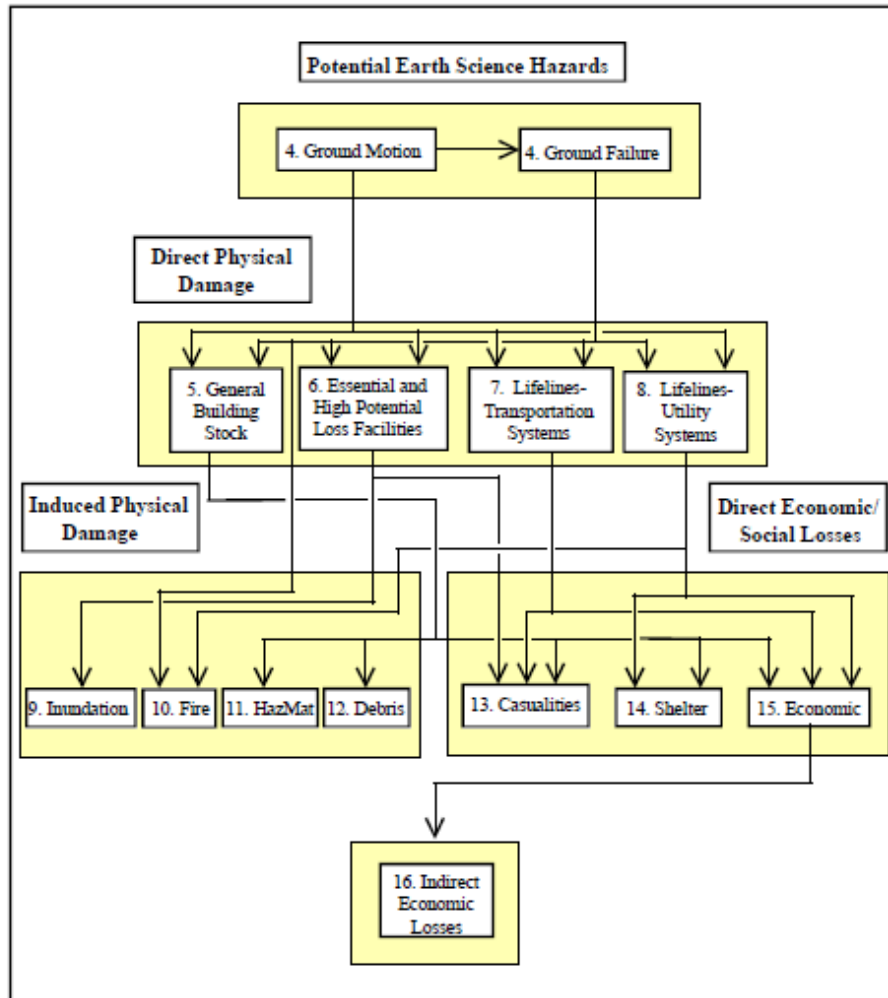


Figure 2-4: Risk assessment methodology defined in HAZUS (FEMA, 2003).

A similar approach is defined in SELINA, a software for SEismic Loss Estimation using a logic tree Approach, produced by NORSAR. The structure of this software is depicted in Figure 2-5. SELINA allows for three analysis types which differ in the way the seismic impact is described: (1) deterministic analysis; (2) probabilistic analysis; and (3) real-time ground motion data.

In general, spectral ordinates of seismic ground motion at different reference periods have to be provided for each geographical unit (i.e., census tract), in order to allow the construction of a design spectra following a selectable seismic code provision.

Once the seismic ground motion in each geographic unit is defined, the computation of physical damage to the building stock is computed by the application one of the selectable Capacity Spectrum-based methods. Based upon the damage estimates, total economic losses related to these damages and the number of casualties, i.e., the number of injured people and fatalities is conducted. Additional loss outputs are shelter demands (temporary housing) as well as debris estimates. Damage results are given in terms of cumulative



This project has received funding from the European Union's Horizon 2020 research and innovation programme under grant agreement No. 700748

Manual for the assessment of liquefaction risk, defining the procedures to create the database, collect, define, symbolize and store information in the Georeferenced Information System and to perform and represent the risk analysis

probabilities of being in or exceeding one particular state following the classification scheme given by HAZUS-MH into none, Slight, Moderate, Extensive and Complete damage.

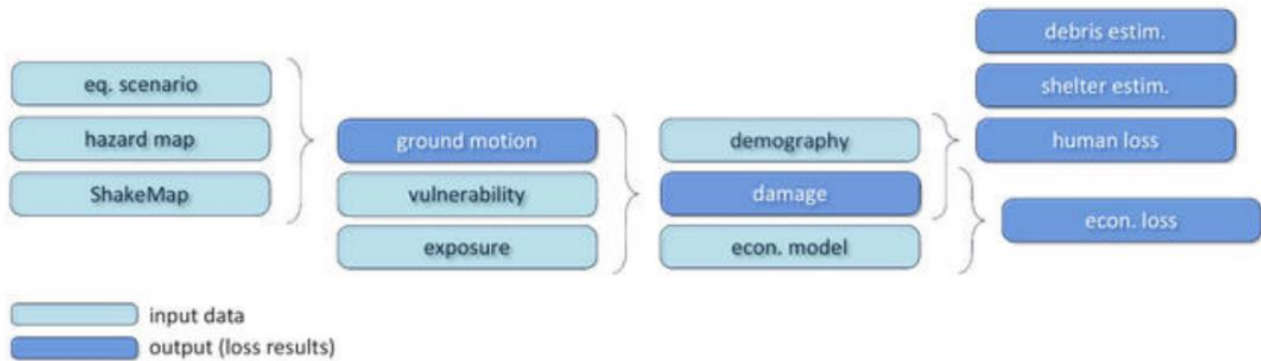


Figure 2-5: Risk assessment methodology defined in SELENA (NORSAR, 2003).

2.5 Deterministic vs Probabilistic Assessment

A common method of estimating the seismic performance of a system is to perform deterministic analyses. In this approach, strong ground motion involves assigning a Maximum Credible Earthquake to a specific fault. Once location (e.g. epicenter) and magnitude of the scenario earthquake are defined, an appropriate scenario earthquake location can be defined for instance from a database of seismic sources (faults) or specifying an event based on a database of historical earthquake epicentres. Then a specific attenuation relationship is assumed to determine the PGA at the project site based on the geographic location of the study region and on the type of fault. For example, Hazus code (FEMA, 2003) assumes (1) strike-slip (SS) faults, (2) reverse-slip (R) faults, (3) normal (N) faults (4) Interface (IF) events and (5) Interslab (IS) events.

Amplification of ground shaking to account for local site conditions is usually based on site classes and soil amplification factors. The 1997 NEHRP Provisions (FEMA, 1992) define a standardized site geology classification scheme and specify soil amplification factors for most site classes based, in part, on the average shear wave velocity of the upper 30 meters of the local site geology.

This procedure can be carried out for all seismic sources that contribute significantly to the ground motions at a site. Uncertainty in the resulting ground motion estimates can be assessed by incorporating the standard deviations in both seismicity rates and attenuation relationships. The advantage of this approach is that both the intensity of ground shaking (PGA) and the duration of the motions, as related to the earthquake magnitude, are known. The primary disadvantages of this approach include; (1) the PGA values do not necessarily reflect the cumulative, or aggregate, hazard in the region, and (2) assessing the influence of uncertainties in factors such as earthquake magnitude or source-to-site distance on the resulting PGA are accounted for by performing additional parametric studies of each variable.

In this way only the largest reasonably possible earthquake associated with a source is accounted for. The recurrence interval of this Maximum Credible Earthquake and the temporal aspect of the seismic hazard are



This project has received funding from the European Union's Horizon 2020 research and innovation programme under grant agreement No. 700748

Manual for the assessment of liquefaction risk, defining the procedures to create the database, collect, define, symbolize and store information in the Georeferenced Information System and to perform and represent the risk analysis

not specified (Dickenson, 2005). Deterministic analyses can accommodate seismicity rates associated with individual sources by incorporating the exposure interval of interest (e.g 500 or 1000 years) and estimating the magnitude of the event having this return period. This method of seismic hazard analysis was common up through the 1970's and many practitioners continue to regard deterministic PGA analyses as independent of exposure interval. In contemporary practice, deterministic analyses are rarely performed without at least an indirect accounting for the exposure time of interest.

An alternative method to estimate PGA is based on the probabilistic approach that combines the contributions of all sources in a cumulative estimate of the ground motion parameter of interest. Probability distributions of key variables such as rupture location along a fault, location of random sources, seismicity rates, and ground motion estimates from attenuation relationships can be incorporated into one seismic hazard analysis. Other uncertainties such as the likelihood of activity along mapped faults, direction of fault rupture propagation and predominant style of faulting can be incorporated into the evaluation (e.g., Kramer 1996, Vick 2002, McGuire 2004). A primary advantage of probabilistic seismic hazard analysis is that by assigning locations and seismicity rates to all sources the ground motion parameter of interest expected at a specific site can be determined along with its probability distribution, which is useful for illustrating uncertainty in the ground motion variable. Repeating the analysis for multiple locations, specified as grid points, throughout a region allows for the creation of contour maps of the ground motion parameters for specified exposure intervals. These maps have been referred to as "uniform" or "aggregate" hazard maps as the contributions of all sources have been incorporated into a single ground motion value.

Once the Probabilistic Seismic Hazard Analysis (PSHA) has been completed, ground motion maps can be obtained for any specified exposure interval. This information forms the input of risk assessment. For a generic system with its lifecycle, risks of any nature can be computed writing the following integral that convolutes the probability of demand $p(D)$ (Hazard) and the consequent losses connected to the demand $P(L|D)$ (Vulnerability):

$$P(L) = \int_D P(L|D) * p(D)$$

Equation 2-1

The application of Equation 2-1 to the assessment of liquefaction risk should separately disclose and quantify the uncertainties on:

- potentially critical scenarios
- models describing the response of the system
- quantification of relevant parameters
- risk evaluation

For seismic risk, Equation 2-1 can be expressed applying the performance-based earthquake assessment (PEBA) cascade methodology defined by the Pacific Earthquake Engineering Research (PEER) Center (Cornell and Krawinkler, 2000) and depicted in Figure 2-6.



This project has received funding from the European Union's Horizon 2020 research and innovation programme under grant agreement No. 700748

Manual for the assessment of liquefaction risk, defining the procedures to create the database, collect, define, symbolize and store information in the Georeferenced Information System and to perform and represent the risk analysis

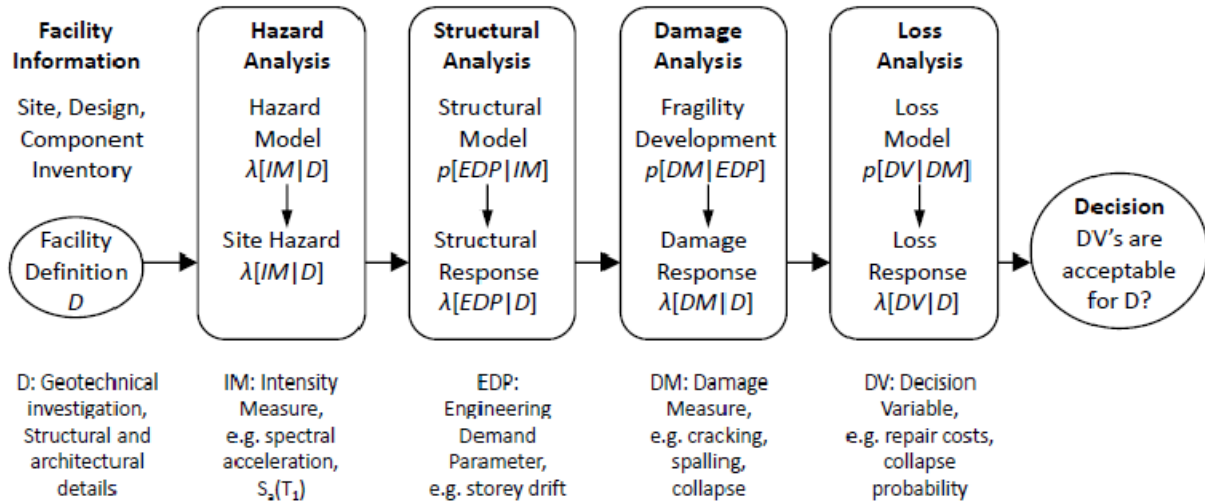


Figure 2-6: Probabilistic definition of risk assessment (Cornell and Krawinkler, 2000).

Equation 2-1 is transformed as follows where the function $p(D)$ is exploded considering the different factors defining the cascade phenomenon:

$$P(L) = \int_{IM} \int_{EDP} \int_{DM} P(VD|DM) * p(DM|EDP) * p(EDP|IM) * p(IM) \quad \text{Equation 2-2}$$

$p(IM)$ is the probability that a seismic event of intensity measure IM occurs during the lifecycles of the system, $p(EDP|IM)$ is the density probability of the engineering demand parameter (EDP) for the given IM , $p(DM|EDP)$ is the probability that a physical damage occurs on the structural component of the system for a given EDP and $P(VD|DM)$ is an cumulative probability of the assumed evaluator of the system performance for a given damage DM (Lee and Mosalam 2006; Moehle 2003; Porter 2003; Comerio 2005; Krawinkler 2005; Mitrani-Reiser et al. 2006).

2.6 Liquefaction risk assessment

Liquefaction is a seismic phenomenon and as such involves different factors in a cascade process (Figure 2-7) that starts with the release of energy associated with rapid movement on active faults, the propagation of waves through media of different properties, the coupling of the shaking with the soil-water system, the physical impact on structures. Then the impact moves from a physical level (structural damage) to the losses for the community that involve serviceability consideration. Assessment may thus proceed stepwise, considering the response of each element of the chain separately from the others or grouping two or more altogether in a coupled analysis.



This project has received funding from the European Union's Horizon 2020 research and innovation programme under grant agreement No. 700748

Manual for the assessment of liquefaction risk, defining the procedures to create the database, collect, define, symbolize and store information in the Georeferenced Information System and to perform and represent the risk analysis

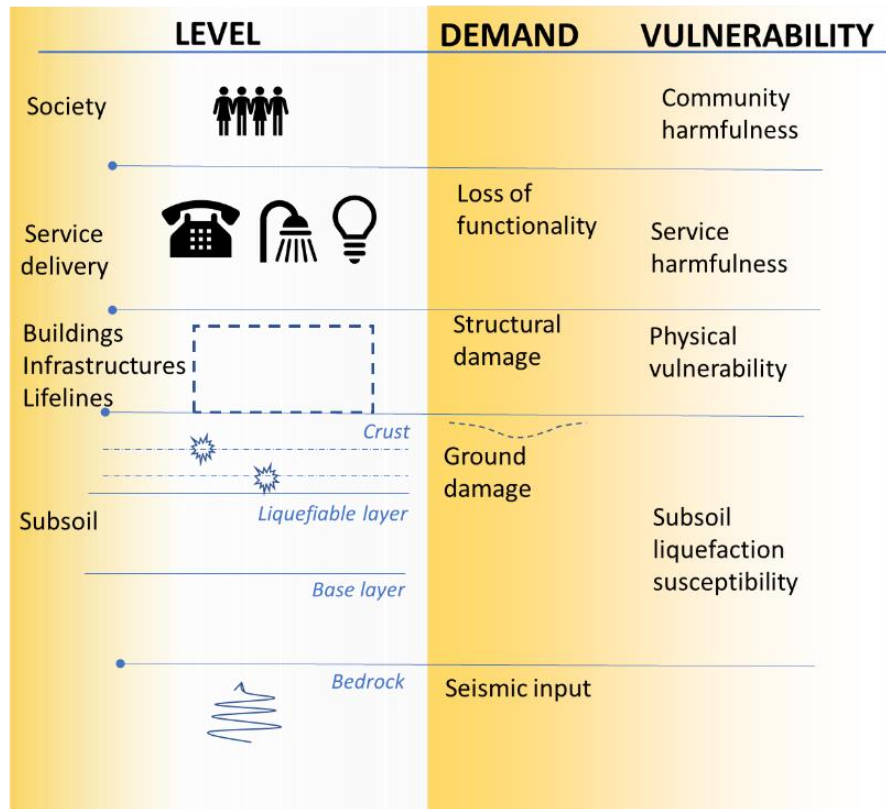


Figure 2-7: Factors determining seismic liquefaction

A similar example for ground motion selection is provided by Bradley (2013). Here two broad approaches are available to compute the seismic performance of a structure located at a particular site, as shown in Figure 2-8. In the first approach (Figure 2-8.a), seismic rupture, wave propagation, local site and structural response are considered in a coupled fashion, and the seismic response (denoted by EDP) is computed. The second uncoupled approach (Figure 2-8.b) treats the same problem in two (or possibly more) parts by introducing a conceptual boundary between the domains of (i) earthquake rupture and wave propagation; and (ii) engineering response of the local soil and structure. The uncoupled approaches have numerous benefits, the most important of which is the ability to use different methodologies for each task.



This project has received funding from the European Union's Horizon 2020 research and innovation programme under grant agreement No. 700748

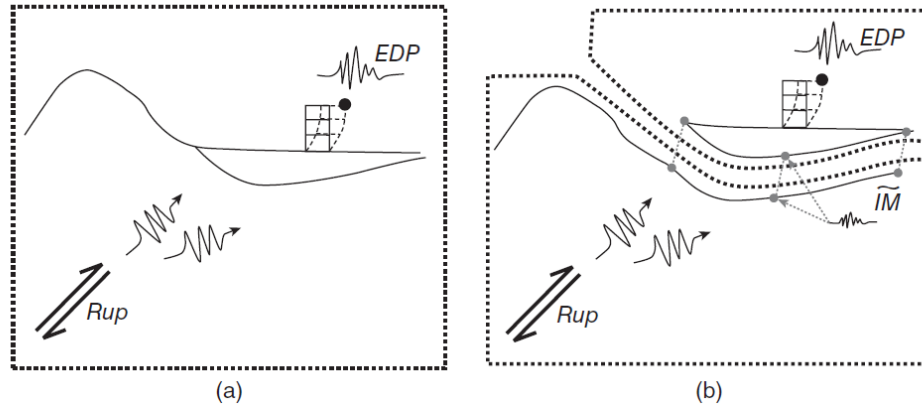


Figure 2-8: Coupled vs uncoupled computation of seismic response (Bradley, 2013).

In particular, it may be impractical to perform simulations that involve earthquake rupture and wave propagation simulations for the problem under consideration due to a lack of expertise, input information (i.e. fault rupture details as well as seismic velocity structure of the propagation medium), and the perceived limitations of such models (often, the adequate simulation of high-frequency ground motion). Consequently, (simple) empirical ground motion prediction equations (GMPEs) are often used to provide the distribution of various ground motion intensity measures (represented by a intensity measure vector, IM) at the site of interest (e.g. peak ground acceleration). Most importantly, however, such GMPEs provide only the distribution of ground motion intensity measures, but not ground motion time histories. Hence, in such cases the problem becomes how to select ground motion time histories based on the obtained distributions of ground motion intensity measures.

Coupled approaches have the indubitable advantage of being more realistic as they account for the backward influence of each factor. The question can be seen from Figure 2-9 that shows a coupled hydro-mechanical analysis carried with the Finite Difference Code FLAC 2D (Itasca 2016) simulating the response of sand with a non-linear model (PM4Sand by Boulanger & Ziotopoulou, 2012) that accounts for the strain accumulation due to repetitive loading. The simulation inspired by a stratigraphy of San Carlo reveals that the onset of liquefaction in the lower sandy layer ($r_u = \Delta u / \sigma'_{vo} \approx 1$) modifies the acceleration time history in the upper layers, generating a reduction of the short period spectral acceleration and preventing the further increase of pore pressure.



This project has received funding from the European Union's Horizon 2020 research and innovation programme under grant agreement No. 700748

Manual for the assessment of liquefaction risk, defining the procedures to create the database, collect, define, symbolize and store information in the Georeferenced Information System and to perform and represent the risk analysis

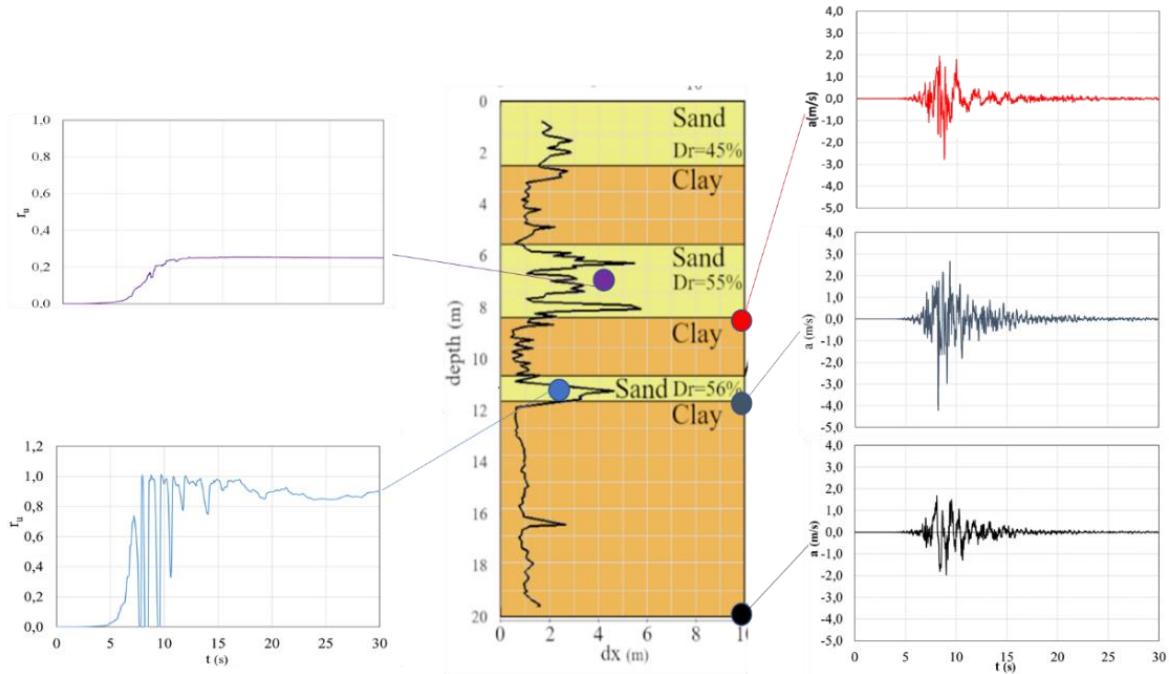
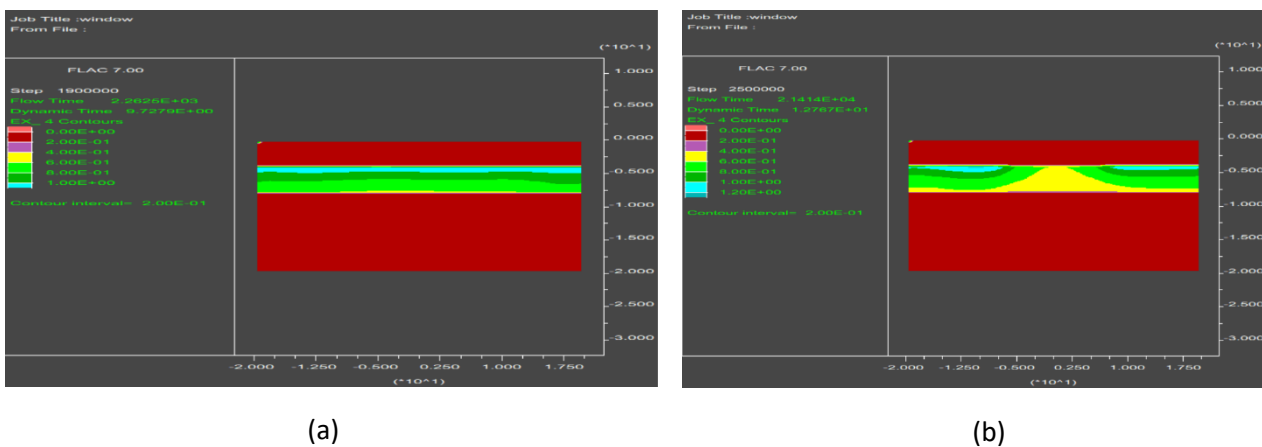


Figure 2-9: Numerical analysis of seismic wave propagation through a multi-layered subsoil.

Additionally, the presence of buildings at the ground level determines an initial shear stress distribution that influences the deformation and pore pressure generation in the soil. The case reported in Figure 2-10 shows a numerical analysis similar carried out with the same code used above, applied to a three-layer deposit, with two clayey layers at the top and bottom and an intermediate layer of sand. Two case are examined subjected to the same seismic scenario. Figure 2-10.a reports the case of free field condition, with no load at the ground level, while Figure 2-10.b reports the case of building at the ground level, schematized with a 10 m wide strip foundation (the analysis is carried out in plane strain conditions) carrying 50 kPa loading. As clearly seen, the presence of buildings forces liquefaction to occur on the two side of the building.



(a)

(b)

Figure 2-10: Numerical analysis of seismic wave propagation in a three-layer deposit subjected to the same seismic scenario (a. free field; b. with 10 m wide footing at the ground level carrying 50 kPa loading).



This project has received funding from the European Union's Horizon 2020 research and innovation programme under grant agreement No. 700748

Manual for the assessment of liquefaction risk, defining the procedures to create the database, collect, define, symbolize and store information in the Georeferenced Information System and to perform and represent the risk analysis

More frequently assessment of liquefaction hazard is carried out with the uncoupled approach, i.e. assigning seismic input at the ground level, computing the response of soil separately from the building. Despite lacking accuracy (epistemic uncertainty), this approach has the advantage of being faster and simpler and thus more easily applicable to extensive assessment like those performed at the urban scale.

Each element of the liquefaction chain includes uncertainties that unavoidably affect the outcomes of risk assessment. The uncertainties affecting liquefaction risk assessment concern Intensity and duration of the ground motion, in-situ properties of the soil (composition, density, fabric, aging), groundwater levels. For sites covering large distances, the degree of uncertainty associated with all these quantities may be meaningful and a simple binary conclusion e.g. 'liquefaction/no liquefaction' represents an over-simplification. However, the majority of methodologies present in the literature, whether based on empirical evidence or numerical modelling, assess the liquefaction potential with such a deterministic approach. Assessment consists in estimating the triggering of liquefaction at some depth. Then severity is quantified by different proxies, e.g. Iwasaki et al. (1978), Zhang et al., (2002), van Ballegooy et al. (2014). In spite of simplicity and speed of calculation, this approach ends with the conclusion that mitigation becomes compulsory beyond certain values of the outcomes. It does not offer any possibility to assess the economical convenience of mitigation.

Probabilistic approaches quantifying probability based on the randomness of the empirical data are becoming more and more popular (e.g. Juang et al., 2005; Cetin et al., 2004; Moss et al., 2006). They provide a very useful framework for taking into consideration the uncertainty in input parameters and presenting the results in the form of a probability of liquefaction (PL). These methods express the probability of liquefaction as a function of both loading terms (peak ground acceleration and moment magnitude M_w) and resistance terms (e.g. SPT blow counts, fines content and vertical effective stress). However, these reliability-based probabilistic methods are not fully probabilistic methods as the ground motion hazard is not considered in a probabilistic manner. Since in most cases ground motion hazard is assessed and defined probabilistically using probabilistic seismic hazard analysis (PSHA), this leads to some inconsistency and confusion.

As design procedures move towards a performance-based approach (Kramer & Mayfield, 2007), it may be appropriate to determine the probability of liquefaction at a given site subjected to ground motions at a range of hazard levels, and to understand facility performance if these levels are exceeded. There are several methods that combine probabilistic ground motions with conventional liquefaction potential procedures (Mayfield, 2007; Juang et al., 2013). In these approaches the standard liquefaction assessment follows a PSHA in which the joint probability distribution of the two key input parameters of the conventional liquefaction assessment, PGA and earthquake moment magnitude for earthquake scenarios, is determined. Fully probabilistic methods for liquefaction potential evaluation should take into account uncertainties in both ground motion (i.e. earthquake occurrence and ground-motion intensity) and soil resistance (i.e. material properties, ground profile, etc.). These methods also employ outcomes of a PSHA, in the form of a seismic hazard curve and associated disaggregation results, to account for the joint probability distribution of ground motion parameters and moment magnitude of earthquake scenarios. The joint probability distribution is then integrated with reliability-based liquefaction evaluation procedures. The outcome of such a fully probabilistic analysis is a direct estimate of the return period of liquefaction, rather than a factor of safety or



This project has received funding from the European Union's Horizon 2020 research and innovation programme under grant agreement No. 700748

Manual for the assessment of liquefaction risk, defining the procedures to create the database, collect, define, symbolize and store information in the Georeferenced Information System and to perform and represent the risk analysis

probability of liquefaction conditional upon ground shaking for a specific return period. Whether probabilistic or deterministic approaches are used, there is always a need for engineers to rigorously manage the uncertainties in their calculations. Within a deterministic framework, engineering judgement can be used to assign qualitative ratings to the probability of liquefaction. For example, the simultaneous occurrence of several low-probability scenarios that would give rise to liquefaction, would have a very low probability of occurrence (Idriss & Boulanger, 2008). On major infrastructure projects, it is often considered appropriate to use probabilistic approaches in conjunction with deterministic 'sense check'.

Considering the sequence of subsystems involved in seismic liquefaction (see Figure 2-11), the PEBA methodology can be expressed quantifying the uncertainties on earthquake intensity, ground motion, structural response, physical damage, and economic or human losses. The scheme of Figure 2-11 shows that the above formula can be applied to the whole system or to subsystems composed of one or more elements, provided demand and vulnerability are properly defined. Changing the position of the lines bordering the vulnerable system (on the right column of the Figure 2-11), different definitions of hazard and risk are obtained. In particular, the earthquake can be considered as the primary hazard factor and liquefaction occurs if the soil has specific characteristics, namely a grain size distribution composed of sand with limited fine content, sufficiently low density and saturation. Therefore, the combination of earthquake and subsoil response determines the demand for the structure positioned at the ground level. However, physical damage for the latter can be computed considering the subsoil-structures as a unique coupled system or evaluating the response of the two components separately. In the first case the earthquake intensity measure IM becomes also the engineering demand parameter EDP and the vulnerability function $p(DM|EDP)$ quantifies the response of the subsoil-structure system for the given seismic input. In the second case, the soil response provides the demand function $p(EDP|IM)$ for the structure and physical vulnerability is computed considering the $p(DM|EDP)$ function for the sole structure. HAZUS code (FEMA 1998) adopts this second approach considering soil liquefaction in a group of secondary hazards called ground failures affecting building assets and infrastructure networks.

Following the sequence depicted by Figure 2-11, physical damage represents the demand for the delivery capability of the system whose vulnerability is defined by a function that relates the loss of serviceability to the different levels of damage. Finally, the latest level of risk assessment concerns the community: it is harmed by the loss of safety and serviceability and risk can be assessed in terms of deaths, injuries, loss of incomes, damage to cultural and environmental heritage.



This project has received funding from the European Union's Horizon 2020 research and innovation programme under grant agreement No. 700748

Manual for the assessment of liquefaction risk, defining the procedures to create the database, collect, define, symbolize and store information in the Georeferenced Information System and to perform and represent the risk analysis

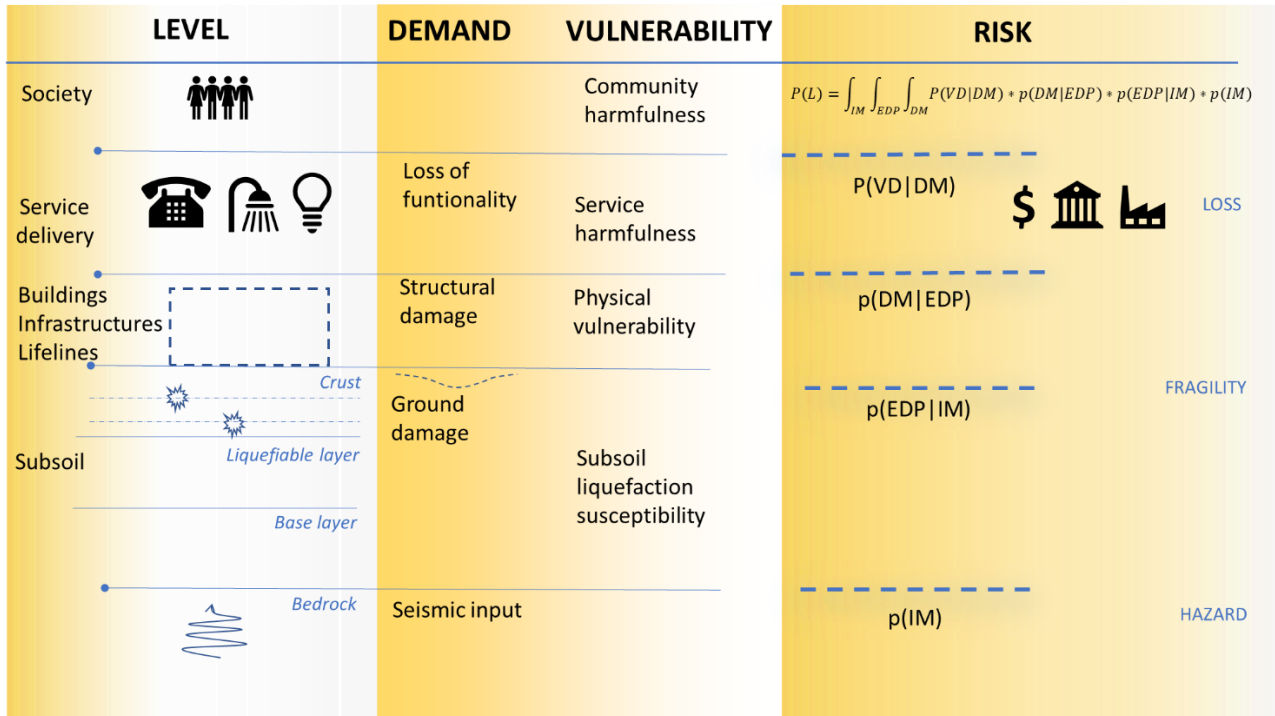


Figure 2-11: Definition of risk assessment for seismic liquefaction.

The terms of Equation 2-2 can be quantified in different manners, sometimes with probabilistic inference of statistical observations, sometimes applying theoretical models with stochastically variable inputs, sometimes with less objective procedures. For instance, it is customary to express severity of damage in terms of financial losses based on expert judgement, qualitative estimates or even rules of thumb that make the process unavoidably subjective.

2.7 Seismic input

One main question arises on the Intensity Measure relevant for liquefaction. Studying the performance of different IMs on liquefaction versus advanced numerical calculations, Karimi and Dashti (2017) observed that the evolutionary settlements of structures depend on intensity, duration and frequency content of the ground motion and concluded that cumulative energy is a more appropriate to represent intensity measure, more than peak variables. They propose the cumulative absolute velocity (Campbell & Bozorgnia, 2012) as a potential candidate as also recently assumed by Bray and Macedo (2017) and Karamitros et al., (2013). Other authors (e.g. Youd et al., 2002; Youd & Perkins, Bardet et al., 2002; Rauch & Martin, 2000) combine magnitude, distance from the rupture and peak ground acceleration. Tokimatsu & Seed (1987) adopt the cyclic stress ratio CSR introduced by Seed & Idriss (1971) corrected (e.g. Idriss & Boulanger, 2010) for magnitude values.

As for any other seismic assessment, the characteristic seismic input at the rigid base can be retrieved on hazard zonation maps (e.g. www.share-eu.org) that generally provide seismic spectra for different return periods T_r . Therefore, given a lifecycle of the considered structure, the probability associated to each event



This project has received funding from the European Union's Horizon 2020 research and innovation programme under grant agreement No. 700748

Manual for the assessment of liquefaction risk, defining the procedures to create the database, collect, define, symbolize and store information in the Georeferenced Information System and to perform and represent the risk analysis

can be computed as function of T_r . Possible amplifications must then be considered for the specific site, referring to the subsoil types defined in the standards (e.g. Fardis et al., 2005) and considering maps giving information on the subsoil (e.g. <https://earthquake.usgs.gov/data/vs30/>) or, preferably, adopting seismic microzonation studies. Alternatively, a seismic response analysis can be performed on the site to be studied. Lately, the scenario earthquakes can be obtained in terms of response spectra, artificial, recorded or simulated accelerograms quantifying IM for each of them. The choice essentially depends on the quality of available data for subsoil characterization, connected with the extent of the studied area.

2.8 Subsoil response

The quantification of subsoil response moves along three subsequent steps (e.g. Bird et al., 2006): determine susceptibility to liquefaction based on qualitative criteria; evaluate the conditions for liquefaction triggering by the scenario earthquake; predict the expected demand for the structure (ground deformations or other proxies of damage).

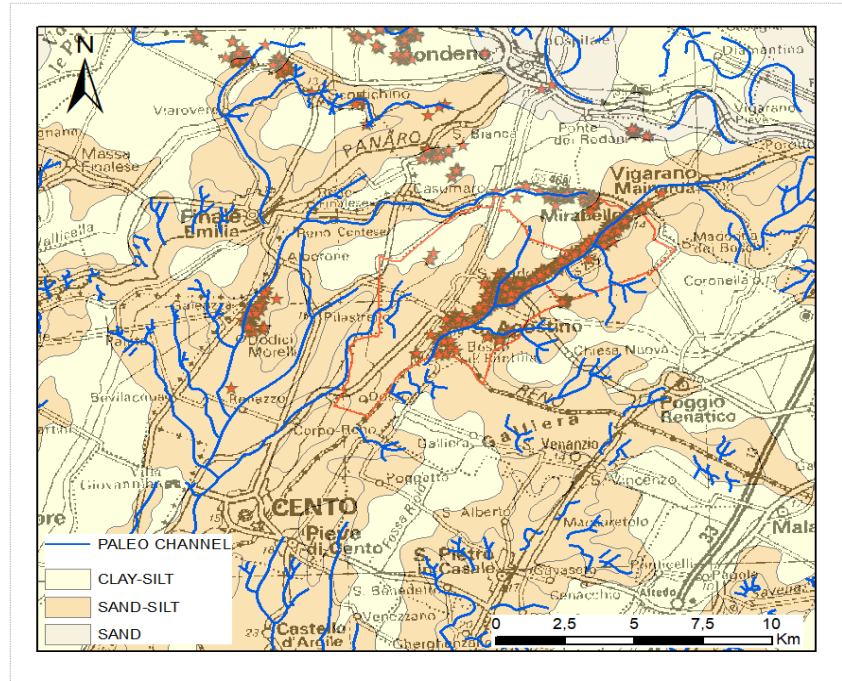
The first step is normally accomplished at the geological level, involving larger portions of the territory and considering broad subsoil classifications like the one proposed by Youd & Perkins (1978). This criterion emphasizes the depositional environment and age of the deposit observing that liquefaction susceptibility is rather high for Holocene or more recent (e.g. artificial) deposits, low or very low for Pleistocene or older ones. A remarkable example is the strong correlation noticed in Figure 2-12 between the distributions of paleo-rivers and liquefaction manifestation during the 2012 seismic sequence in Emilia Romagna. The overlapping is particularly evident between the municipalities of Sant'Agostino and Mirabello. Historical documents report that the Reno river was crossing this zone for a period of three hundred years, from the half of fifteenth to the half of eighteen century, releasing sediments with very high rates (10÷30cm/year).

Once the above conditions are ascertained, the co-existence of paramount factors, i.e. grain size distribution and water level must be determined at a smaller scale with a more refined investigation. To estimate triggering, many standards worldwide (e.g. NZGS, 2016; Yasuda e Ishihawa, 2018; DPC, 2017) adopt relations between in situ soil density and cyclic shear stress induced by ground shaking. For a given soil profile, the triggering of liquefaction at different depths is evaluated computing a safety factor (FSL) given by the ratio of the cyclic stress ratio τ/σ'_v producing liquefaction (CRR) and the one induced by the earthquake (CSR). Robertson & Wride (1998), Idriss & Boulanger (2010) and Boulanger and Idriss (2015), provide empirical formulations of the Cyclic Resistance Ratio based on the survey of liquefaction and the results of common geotechnical in-situ tests (CPT, SPT, V_s profile).



This project has received funding from the European Union's Horizon 2020 research and innovation programme under grant agreement No. 700748

Manual for the assessment of liquefaction risk, defining the procedures to create the database, collect, define, symbolize and store information in the Georeferenced Information System and to perform and represent the risk analysis



★ Liquefaction manifestation

Figure 2-12: Distribution of liquefaction damage caused by the 2012 earthquakes in Emilia Romagna (Italy).

The above relationships are derived deterministically as medians of case history databases. As such, they are affected by uncertainties arising from the definition of CSR (model uncertainty on the triggering relationship) and from the quality and interpretation of investigation (measurement or parameter uncertainty) (Toprak et al., 1999; Cetin et al., 2004). Analysing a database of 230 cases, Idriss & Boulanger (2010) derive the following relation to estimate the conditional probability of liquefaction for known values of $CSR_M=7.5$, $\sigma'_v=1atm$ and the standard penetration resistance corrected for the presence of finer soil $N_{1,60cs}$:

$$P_L((N_1)_{60cs}, CSR_M=7.5, \sigma'_v=1atm) = \Phi \left[-\frac{\frac{(N_1)_{60cs}}{14.1} + \left(\frac{(N_1)_{60cs}}{126}\right)^2 - \left(\frac{(N_1)_{60cs}}{23.6}\right)^3 + \left(\frac{(N_1)_{60cs}}{25.4}\right)^4 - 2.67 - \ln(CSR_M=7.5, \sigma'_v=1atm)}{\sigma_{ln(R)}} \right] \quad \text{Equation 2-3}$$

The authors find that a standard deviation $\sigma_{ln(R)}$ equal to 0.13 correctly represents variability.

Even considering with probabilistic models the uncertainty associated with the ground-motion estimation and the likelihood of liquefaction triggering, the above procedures are affected by other uncertainties related with measurement biases of in situ data (Baecher & Christian, 2003). In spite of a tendency to discipline the execution and interpretation of subsoil investigation for improving consistency, quality and reliability (e.g. NZGS, 2016), the major part of data presently available for risk assessment have been obtained in previous times with out of date standards. An attempt to fill this gap is proposed by Madiari et al., 2016 who performed an experimental study to convert the results of mechanical CPT into equivalent electrical CPT data.

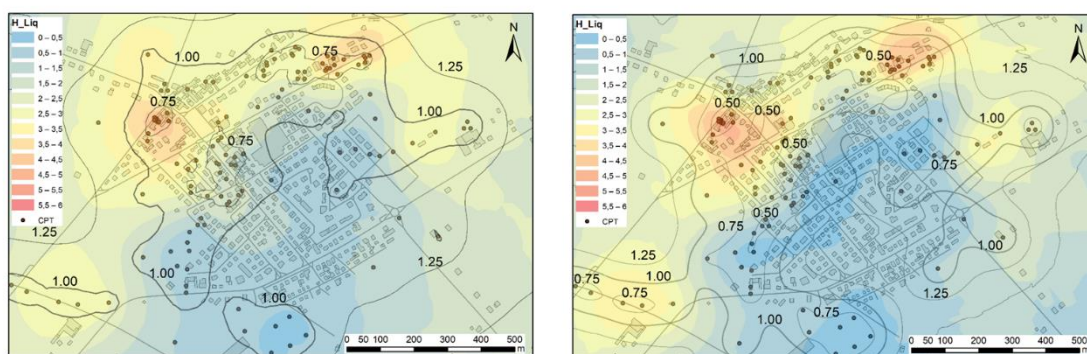


This project has received funding from the European Union's Horizon 2020 research and innovation programme under grant agreement No. 700748

Manual for the assessment of liquefaction risk, defining the procedures to create the database, collect, define, symbolize and store information in the Georeferenced Information System and to perform and represent the risk analysis

Inconsistency of investigation is one of the major causes of error in interpolating information over the areas. Tests performed at mutual distance of few meters may give markedly different estimates of important parameters. Geostatistical tests (Chilès and Delfiner, 2012) are very helpful to identify singularities, e.g. where experimental results differ too much from the spatial trend inferred from contiguous investigations, and to quantify uncertainty of the estimate in each position. From the viewpoint of the probabilistic risk assessment, this result quantifies the reliability of the estimate and the uncertainty associated with the subsoil characterization and provides a criterion to plan optimal campaigns to integrate information.

As an example, Figure 2-13 shows the map of liquefiable layer thickness over San Carlo Emilia (Italy), a village struck by severe liquefaction during the 2012 earthquake. The Figure 2-13.a reports the map built with all available CPT tests, the Figure 2-13.b shows the same map obtained after removing some inconsistent tests (CPT positions are marked with dots). The estimate of liquefiable layer is affected by the water table position, that was here taken from a study of (RER, 2012). The exam to evaluate consistency/inconsistency is based on the difference between variables estimated directly from the test and from interpolation of contiguous data. CPT logs for which this difference exceed 5% and 95% fractile of the error distribution were removed. This operation slightly modifies the map, but the contour lines that quantify the estimate error show an improved quality of the information. The remaining error is mainly connected with the density of information (in the present case, CPTs were mostly performed close to damaged buildings), and thus a criterion is obtained to select areas where investigation is more needed.



a)

b)

Figure 2-13: Liquefiable layer thickness over San Carlo Emilia drawn from all CPT tests (a) and after removing inconsistent data (b) (Contour lines represent the standard deviation of error).

The effects at ground level are normally predicted (e.g. NZGS, 2016; DPC, 2017) with indicators of severity that empirically synthesize the paramount factors dictating liquefaction in free field conditions. They are computed as integral over fixed depths of a function of the safety factor $f(FSL)$ weighted with a function of depth from the ground level $w(z)$.



This project has received funding from the European Union's Horizon 2020 research and innovation programme under grant agreement No. 700748

Manual for the assessment of liquefaction risk, defining the procedures to create the database, collect, define, symbolize and store information in the Georeferenced Information System and to perform and represent the risk analysis

$$INDEX = \int_{z_{max}} f(FSL) * w(z) dz$$

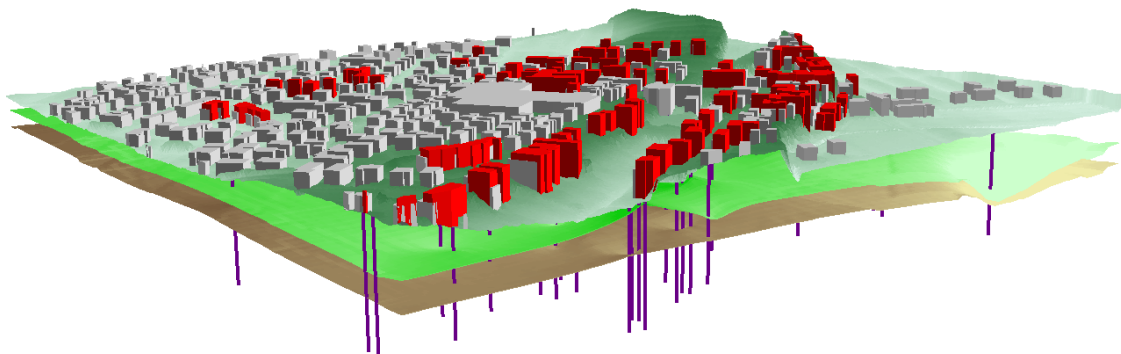
Equation 2-4

Table 2-1 shows a list of the most common indexes. In spite of simplicity that makes these indicators appealing for an extensive assessment, they suffer the implicit limitation of quantifying the subsoil response with a sum of contributions from all susceptible layers ($FSL < 1$) located at different depths, ignoring in this way any possible mechanical and hydraulic cross-interaction between susceptible layers located at different depths (Cubrinovski, 2017) (see Figure 2-9).

This phenomenon affects the reliability of assessment with simplified methods in the case of multilayered systems and thus a preliminary check is necessary to verify if the schematization with three layers (base, liquefiable layer and crust) is applicable to the studied case and if more sophisticated models must be adopted. Millen (2019) propose a test based on CRR to verify the equivalence of soil profiles derived from CPTU tests with three layers models described by the combination of depth (H_{crust}), thickness (H_{liq}) and mean CRR of the liquefiable layer. This test gives positive results for all CPT performed in San Carlo Emilia, basically because the liquefiable layer in this case is induced by a continuous depositional event occurred over a limited time period. Figure 2-14 shows a view of the three-dimensional model of San Carlo.

Table 2-1: Severity liquefaction indicators proposed in the literature

INDEX	REFERENCE	f1(FSL)	w(z)	Z
LPI	Iwasaki, 1978	$\begin{cases} 1 - FSL & \text{if } FSL < 1 \\ 0 & \text{if } FSL \geq 1 \end{cases}$	$10 - 0.5z$	$\begin{cases} Z_{min} = 0 \\ Z_{max} = 20m \end{cases}$
LPlish	Maurer, 2014	$\begin{cases} 1 - FSL & \text{if } FSL \leq 1 \cap H1 \cdot m(FSL) \leq 3 \\ 0 & \text{otherwise} \end{cases}$	$\frac{25.56}{z}$	$\begin{cases} Z_{min} = H1 \\ Z_{max} = 20m \end{cases}$
W	Zhang et al., 2002	$\varepsilon_v = \varepsilon_v(FSL, qc1N_{cs})$	-	$\begin{cases} Z_{min} = 0 \\ Z_{max} = \text{max depth} \end{cases}$
LDI	Zhang et al., 2004	$\gamma_{max} = \gamma_{max}(FSL, qc1N)$	-	$\begin{cases} Z_{min} = 0 \\ Z_{max} < 23m \end{cases}$
LSN	van Ballegooy, 2014	$\varepsilon_v = \varepsilon_v(FSL, qc1N_{cs})$	$\frac{1000}{z}$	$\begin{cases} Z_{min} = 0 \\ Z_{max} = 20m \end{cases}$





This project has received funding from the European Union's Horizon 2020 research and innovation programme under grant agreement No. 700748

Manual for the assessment of liquefaction risk, defining the procedures to create the database, collect, define, symbolize and store information in the Georeferenced Information System and to perform and represent the risk analysis

Figure 2-14: Three-dimensional subsoil model of San Carlo Emilia (green and brown surfaces represent respectively top and bottom surfaces of the liquefiable layer – the vertical scale is five times larger than horizontal one).

2.9 Structural damage

For a given hazard, the physical damage induced by liquefaction on structures and infrastructures depends on their typology, planimetric extension and capability to adsorb absolute and differential movements. The estimate of losses is by far more complex than the assessment of liquefaction occurrence in the subsoil (Bird et al., 2006). Uncertainties basically stem from the following reasons:

- Coupling of liquefaction and ground shaking
- Identify damage mechanisms and define a demand for liquefaction
- Classify damage into levels
- Categorize structure response into homogenous groups

The above concerns become even more relevant and problematic for buildings due to the larger variety of structural typologies and construction materials adopted worldwide.

The issue of combined ground shaking and liquefaction has been largely debated. More often buildings that have undergone liquefaction do not exhibit ground shaking damage, giving the idea that a base isolation could be induced by the liquefied soil on the building. However, evidences of buildings damaged by both shaking and liquefaction suggest that severe ground shaking might take place before the groundwater pressure builds up. Bird et al. (2005) claim that the differential settlement induced by liquefaction on framed buildings causes a drift of columns additional to that produced by shaking and thus structures previously affected by shaking are more vulnerable to liquefaction. Following this idea, these authors propose a cumulative analytical methodology considering permanent shaking deformation as a reduction of the building capacity against liquefaction. The connection between the two mechanisms is even more evident for masonry structures.

Focusing solely on the effects of liquefaction, a list of possible building damages is provided by van Ballegooy (2014) together with the threshold movements defining the level of damage. Differential settlements or horizontal movements dictated by inhomogeneous load distributions and stratigraphic conditions (e.g. inherent variability of homogeneous subsoil and, moreover, boundary between liquefied and non-liquefied soils) are recognised among the most critical causes of damage. Rigid body movements like uniform settlement, tilting and horizontal sliding may add, increasingly affecting aesthetic, serviceability and, ultimately, stability of buildings. The relative weight among mechanisms is mainly dictated by the stiffness of the structural system with a paramount role of its foundation, whether made of isolated footings, continuous beams or pads, pile reinforcement. A classification of severity levels cumulatively including shaking and liquefaction has been proposed by Bird et al. (2006). They define four classes of damage, namely slight, moderate, extensive and complete based on reparability of the building. However, as pointed out by the same authors, a general applicability of this criterion is affected by the strong dependency of the fixed limits on the type of structure, on the suitability of buildings and foundation to sustain repair works, plus several other factors dictated by the local practice. van Ballegooy et al. (2014) (Figure 2-7) distinguishes damage



This project has received funding from the European Union's Horizon 2020 research and innovation programme under grant agreement No. 700748

Manual for the assessment of liquefaction risk, defining the procedures to create the database, collect, define, symbolize and store information in the Georeferenced Information System and to perform and represent the risk analysis

according to the deformation mechanisms activated on the building and on the extent of settlement. A more general classification of damage on buildings of different typology, not just referred to liquefaction, is provided by Poulos et al. (2001) where a distinction is made among the type of structure (framed, masonry, bridges) and level of damage. In all cases, predicting the overall kinematics of buildings is not easy, moreover for large-scale assessment where geotechnical and structural information are largely incomplete. Following a methodology adopted for the serviceability limit state analysis of foundations under static loads (Grant et al., 1974), differential settlements quantified by the relative rotation θ have been related to the absolute settlements of the building.

Once the equivalence between absolute settlement and distortion is established, it is readily seen that the classification criteria defined by van Ballegooy (Figure 2-15) and Poulos (Figure 2-16) lead to similar limit values of settlements. In both cases, damage is triggered for absolute settlements in the range 10-100 mm, being severity dependent on the building type. Absolute settlements may thus be considered as Engineering Demand Parameters for the estimate of damage.

Dwelling Foundation Damage Categories							
Type of Damage	Minor	Moderate	Major	Type of Damage	Minor	Moderate	Major
Stretching 	0 to 5mm	5 to 30mm	>30mm	Tilting 	0 to 20mm	20 to 50mm	>50mm
Hogging 	0 to 20mm	20 to 50mm	>50mm	Abrupt Differential Movement 	0 to 10mm	10 to 20mm	>20mm
Dishing 	0 to 20mm	20 to 50mm	>50mm	Global Settlement 	0 to 50mm	50 to 100mm	>100mm
Racking/Twisting 	0 to 10mm	10 to 30mm	>30mm				

Figure 2-15: Type and level of damage caused on buildings by liquefaction (van Ballegooy, 2014).

Type of structure	Type of damage/concern	Quantity to be considered	Limiting value
Framed building and reinforced load bearing walls	Structural damage	Angular distortion	1/150-1/250
	Cracking in walls and partitions	Angular distortion	1/500 (1/100-1/1400 for end bays)
	Visual appearance	Tilt	1/300
	Connection to services	Total settlement	50-75 mm (sand) 75-135 mm (clay)
Tall buildings	Operation of lifts and elevators	Tilt after lift installation	1/1200-1/2000
Structures with unreinforced load bearing walls	Cracking by sagging	Deflection ratio	1/2500 (L/H=1) 1/1250 (L/H=5)
	Cracking by hogging	Deflection ratio	1/5000 (L/H=1) 1/2500 (L/H=5)
Bridges - general	Ride quality	Total settlement	100 mm
	Structural distress	Total settlement	63 mm
	Function	Horizontal movement	38 mm
Bridges - multiple span	Structural damage	Angular distortion	1/250
Bridges - single span	Structural damage	Angular distortion	1/200

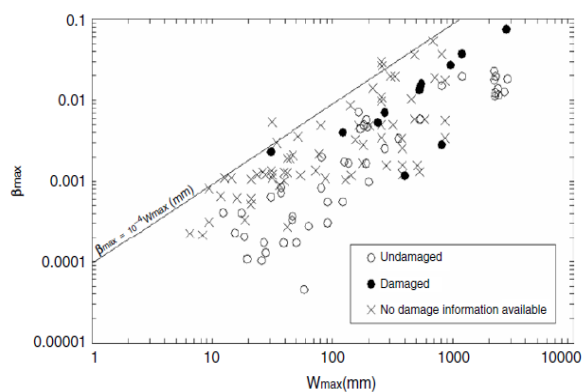


Figure 2-16: Classification of damage from Poulos et al. (2001) (a), empirical relation between maximum absolute settlement and angular distortion (b) for shallow and piled foundations (Viggiani et al., 2012).



This project has received funding from the European Union's Horizon 2020 research and innovation programme under grant agreement No. 700748

Manual for the assessment of liquefaction risk, defining the procedures to create the database, collect, define, symbolize and store information in the Georeferenced Information System and to perform and represent the risk analysis

2.10 HAZUS methodology

In Hazus, a procedure is proposed to estimate liquefaction hazard based on geological data concerning the depositional environment and age of the subsoil. The procedure is accomplished with the following steps:

- Estimate susceptibility with a qualitative rating based upon general depositional environment and geologic age of the deposit is given following Youd and Perkins (1978) (Figure 2-17)

Type of deposit (1)	General distribution of cohesionless sediments in deposits (2)	Likelihood that Cohesionless Sediments, When Saturated, Would Be Susceptible to Liquefaction (by Age of Deposit)			
		<500 yr (3)	Holocene (4)	Pleis-tocene (5)	Pre-pleis-tocene (6)
(a) Continental Deposits					
River channel	Locally variable	Very high	High	Low	Very low
Flood plain	Locally variable	High	Moderate	Low	Very low
Alluvial fan and plain	Widespread	Moderate	Low	Low	Very low
Marine terraces and plains	Widespread	—	Low	Very low	Very low
Delta and fan-delta	Widespread	High	Moderate	Low	Very low
Lacustrine and playa	Variable	High	Moderate	Low	Very low
Colluvium	Variable	High	Moderate	Low	Very low
Talus	Widespread	Low	Low	Very low	Very low
Dunes	Widespread	High	Moderate	Low	Very low
Loess	Variable	High	High	High	Unknown
Glacial till	Variable	Low	Low	Very low	Very low
Tuff	Rare	Low	Low	Very low	Very low
Tephra	Widespread	High	High	?	?
Residual soils	Rare	Low	Low	Very low	Very low
Sebka	Locally variable	High	Moderate	Low	Very low

Type of deposit (1)	General distribution of cohesionless sediments in deposits (2)	Likelihood that Cohesionless Sediments, When Saturated, Would Be Susceptible to Liquefaction (by Age of Deposit)			
		<500 yr (3)	Holocene (4)	Pleis-tocene (5)	Pre-pleis-tocene (6)
(b) Coastal Zone					
Delta	Widespread	Very high	High	Low	Very low
Estuarine	Locally variable	High	Moderate	Low	Very low
Beach	High wave energy	Widespread	Moderate	Low	Very low
	Low wave energy	Widespread	High	Moderate	Low
Lagoonal	Locally variable	High	Moderate	Low	Very low
Fore shore	Locally variable	High	Moderate	Low	Very low
(c) Artificial					
Uncompacted fill	Variable	Very high	—	—	—
Compacted fill	Variable	Low	—	—	—

Figure 2-17: Liquefaction Susceptibility of Sedimentary Deposits (from Youd and Perkins, 1978).

- Estimate the probability of liquefaction combining susceptibility of the soil, amplitude and duration of ground shaking and depth of groundwater with the following formula:

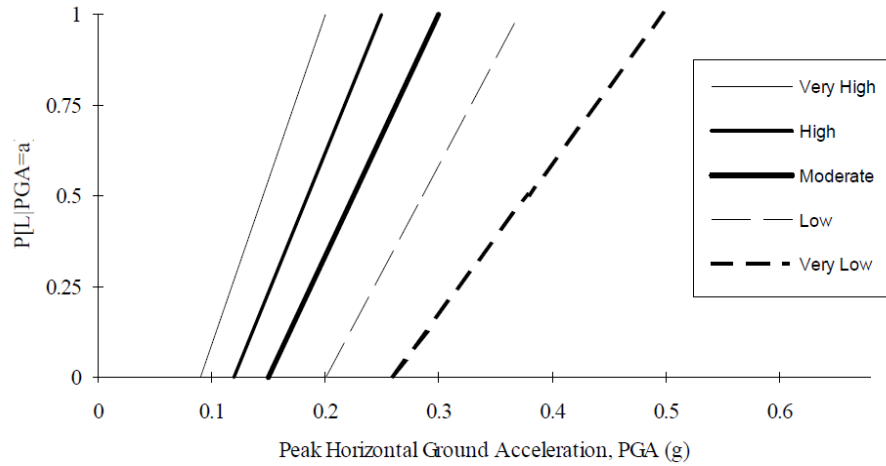
$$P[\text{Liquefaction}_{sc}] = \frac{P[\text{Liquefaction}_{sc} | \text{PGA} = a]}{K_M \cdot K_W} \cdot P_{ml} \quad \text{Equation 2-5}$$

where the conditional liquefaction probability $P[\text{Liquefaction}_{sc} | \text{PGA} = a]$ is expressed for the above given susceptibility categories based on the state-of-practice empirical procedures, as well as the statistical modelling of the empirical liquefaction catalogue presented by Liao et. al. (1986) for a $M = 7.5$ earthquake and for an assumed groundwater depth of five feet (Figure 2-18).



This project has received funding from the European Union's Horizon 2020 research and innovation programme under grant agreement No. 700748

Manual for the assessment of liquefaction risk, defining the procedures to create the database, collect, define, symbolize and store information in the Georeferenced Information System and to perform and represent the risk analysis



Susceptibility Category	P [Liquefaction PGA = a]
Very High	$0 \leq 9.09 a - 0.82 \leq 1.0$
High	$0 \leq 7.67a - 0.92 \leq 1.0$
Moderate	$0 \leq 6.67a - 1.0 \leq 1.0$
Low	$0 \leq 5.57a - 1.18 \leq 1.0$
Very Low	$0 \leq 4.16a - 1.08 \leq 1.0$
None	0.0

Figure 2-18: Conditional liquefaction probability for a given susceptibility category at a specified level of peak ground acceleration.

Correction factors to account in Equation 2-5 for moment magnitudes (M) and groundwater depths (d_w) different than respectively 7.5 and 5 feet, are given by Equations 2.4 and 2.5 (Seed and Idriss, 1982; Seed, et. al., 1985; National Research Council, 1985) and represented graphically in Figure 2-19.a and Figure 2-19.b:

$$K_M = 0.0027M^3 - 0.0267M^2 - 0.25M + 2.9188 \quad \text{Equation 2-6}$$

$$K_W = 0.022d_w + 0.93 \quad \text{Equation 2-7}$$



This project has received funding from the European Union's Horizon 2020 research and innovation programme under grant agreement No. 700748

Manual for the assessment of liquefaction risk, defining the procedures to create the database, collect, define, symbolize and store information in the Georeferenced Information System and to perform and represent the risk analysis

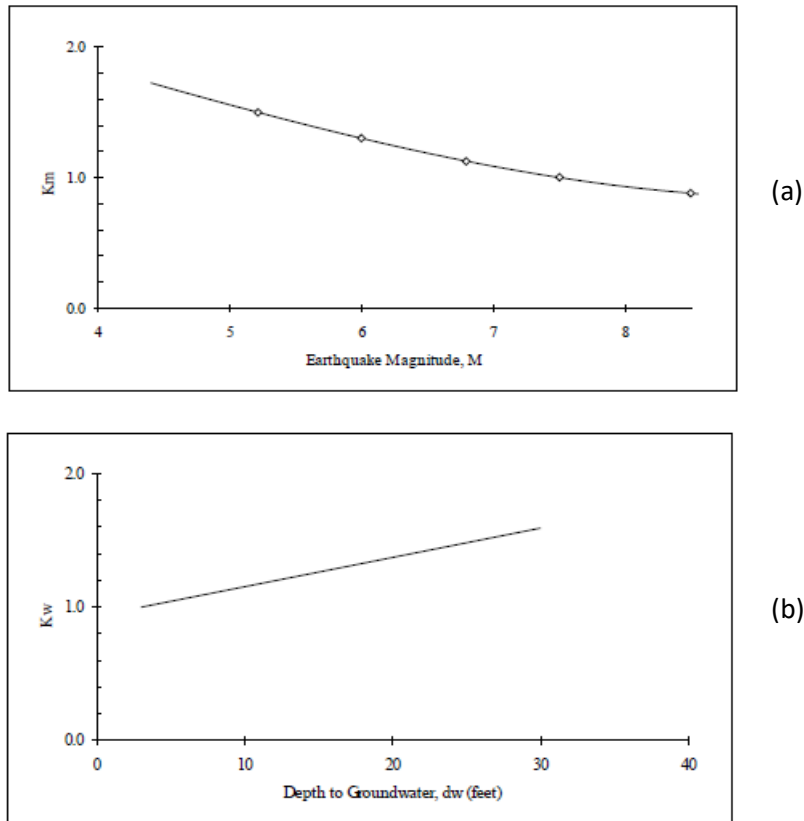


Figure 2-19: a. Moment Magnitude (Seed and Idriss, 1982) and b. groundwater depth Correction Factor for Liquefaction Probability Relationships.

For a given subsoil category, liquefaction is unlikely to occur over the whole portion of the geologic map, and this should be considered in assessing the probability of liquefaction at any given location. Considering that non-susceptible portions are expected to be smaller for higher susceptibilities a probability factor that quantifies the proportion of a geologic map unit deemed susceptible to liquefaction (i.e., the likelihood of susceptible conditions existing at any given location within the unit) is inserted. For the various susceptibility categories, default values are provided in Figure 2-20.

Mapped Relative Susceptibility	Proportion of Map Unit
Very High	0.25
High	0.20
Moderate	0.10
Low	0.05
Very Low	0.02
None	0.00

Figure 2-20: Proportion of the map susceptible to liquefaction (Power et al., 1982).



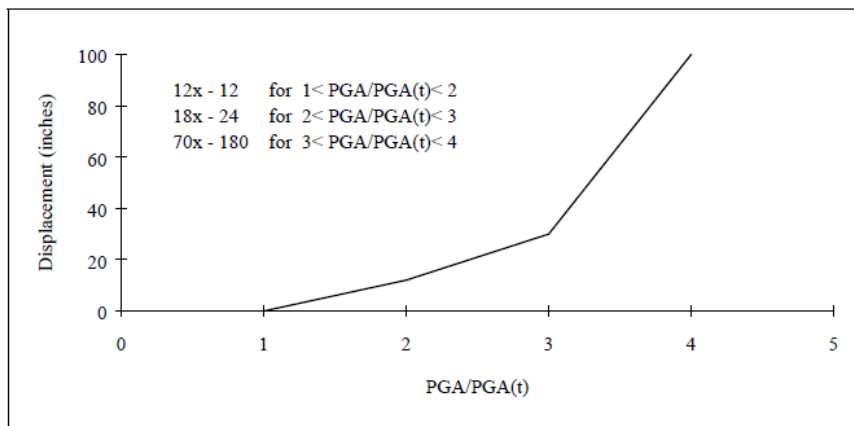
This project has received funding from the European Union's Horizon 2020 research and innovation programme under grant agreement No. 700748

Manual for the assessment of liquefaction risk, defining the procedures to create the database, collect, define, symbolize and store information in the Georeferenced Information System and to perform and represent the risk analysis

The HAZUS procedure allows to estimate the Lateral Spreading Permanent Ground Displacements with the following relationship (provided by Youd and Perkins, 1987) with the ground motion attenuation relationship developed by Sadigh, et. al. (1986) as presented in Joyner and Boore (1988):

$$E[PGD_{SC}] = K_{\Delta} \cdot E[PGD|(PGA/PL_{SC}) = a] \quad \text{Equation 2-8}$$

where $E[PGD|(PGA/PL_{SC}) = a]$ is the expected ground displacement for a given susceptibility category under a specified level of normalized ground shaking ($PGA/PGA(t)$) (shown in Figure 2-21), $PGA(t)$ is the threshold ground acceleration necessary to induce liquefaction (Figure 2-21).



Susceptibility Category	PGA(t)
Very High	0.09g
High	0.12g
Moderate	0.15g
Low	0.21g
Very Low	0.26g
None	N/A

Figure 2-21: Lateral spreading displacement relationship (after Youd & Perkins, 1978; Sadigh et al., 1986) and threshold ground acceleration ($PGA(t)$) corresponding to zero probability of liquefaction.

K_D is the displacement correction factor introduced to account for Moment magnitudes different than 7.5 (Seed & Idriss, 1982), expressed by Equation 2-9 and plotted in Figure 2-22.

$$K_M = 0.0086M^3 - 0.0914M^2 + 0.4698M - 0.9835 \quad \text{Equation 2-9}$$

HAZUS also report a simple methodology to estimate ground settlement associated with liquefaction. The latter is assumed to be related to the susceptibility category assigned to an area according to Tokimatsu and Seed (1987) that indicate strong correlations between volumetric strain (settlement) and soil relative density (a measure of susceptibility). Considering that experience has shown that deposits of higher susceptibility tend to have increased thicknesses of potentially liquefiable soils, the ground settlement is computed



This project has received funding from the European Union's Horizon 2020 research and innovation programme under grant agreement No. 700748

Manual for the assessment of liquefaction risk, defining the procedures to create the database, collect, define, symbolize and store information in the Georeferenced Information System and to perform and represent the risk analysis

multiplying a characteristic settlement amplitude appropriate to the susceptibility category (Figure 2-23) with the probability of liquefaction computed with Equation 2-3 for a given ground motion level.

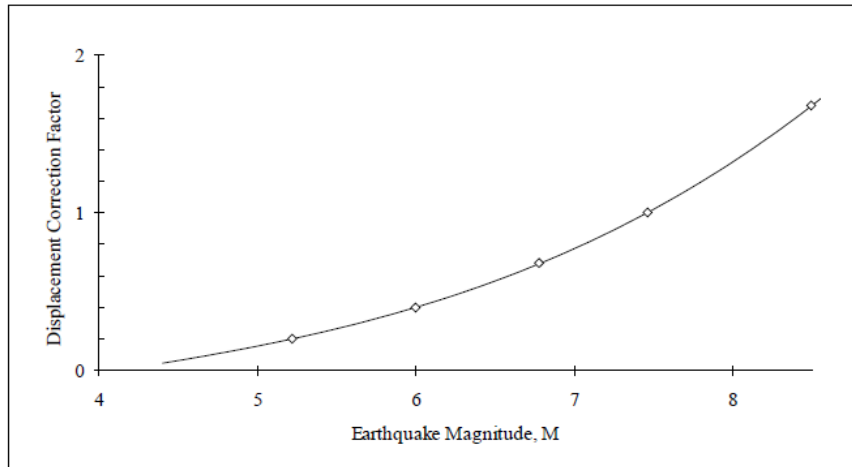


Figure 2-22: Displacement correction factor, KD for Lateral spreading displacement relationship (after Seed & Idriss, 1982).

Relative Susceptibility	Settlement (inches)
Very High	12
High	6
Moderate	2
Low	1
Very Low	0
None	0

Figure 2-23: Ground settlements amplitudes for liquefaction susceptibility categories (after Tokimatsu & Seed, 1987).

The above described procedure enables to estimate probability and, with a relatively high uncertainty, the effects of liquefaction, but at a very large geographical scale. Considering that subsoil characterisation is based on geological information (environment and age of the deposit), the results do not allow to distinguish the situation at the scale of buildings or even on aggregates. The challenge for the user is to translate regional/local data, experience and judgment into site specific relationships. HAZUS provides just a series of comments related with this issue in order to drive user defined risk assessment procedures (called Expert-Generated Ground Failure Estimation) based on the collection of geotechnical data.

2.11 LRG methodology

Liquefaction Reference Guide is a software toolbox developed in Liquefact project. It implies a stepwise analysis, summarised in the flowchart of Figure 2-24. The analysis can be carried out in three subsequent steps:



This project has received funding from the European Union's Horizon 2020 research and innovation programme under grant agreement No. 700748

Manual for the assessment of liquefaction risk, defining the procedures to create the database, collect, define, symbolize and store information in the Georeferenced Information System and to perform and represent the risk analysis

- Hazard assessment
- Risk assessment
- Risk assessment and mitigation framework

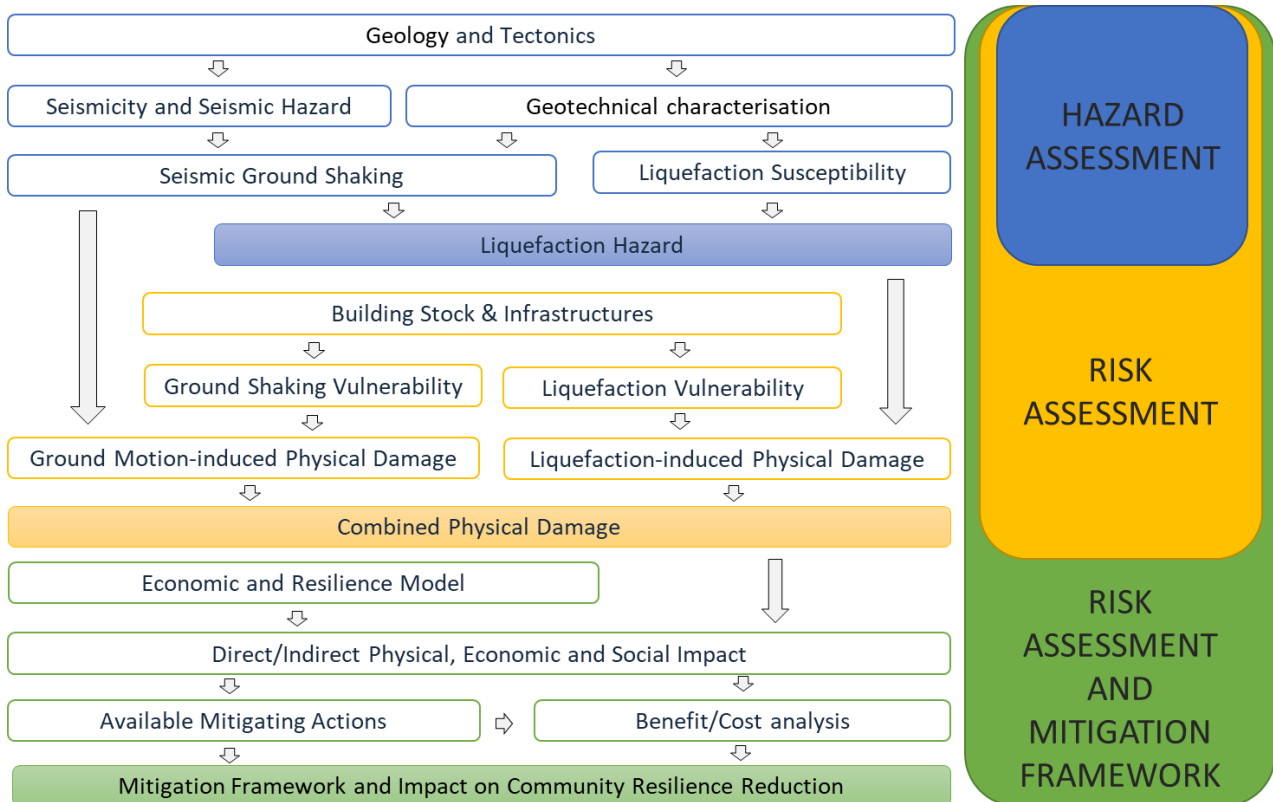


Figure 2-24: Flowchart of the LRG procedure for risk assessment.

Liquefaction geological susceptibility should be preliminary evaluated (over a regional scale) in order to address further more detailed studies. Then, accounting for the geotechnical features of the study area (i. e. a region, city, aggregate or individual structure), the liquefaction susceptibility level can be defined considering the thicknesses of the non-liquefiable crust and of the potentially liquefiable layer.

In the following steps, geotechnical tests (CPT, SPT and Vs profile) need to be combined with the specific seismicity of the area to estimate the liquefaction hazard. This is commonly assessed through liquefaction severity indicators, evaluated by applying several simplified stress-based approaches. The output of liquefaction hazard assessment is represented by maps of liquefaction severity indicators, obtained from geostatistical interpolation of the punctual results.

Liquefaction hazard can be defined for a generic structure as the probability that a given value of the liquefaction severity indicator (demand) will be produced during the lifetime of the structure. The practice of characterizing liquefaction hazard through these indicators is applied in many countries to quantify risk on structures and infrastructures present in a given territory (e.g. DPC 2017, MBIE 2016, Yasuda and Ishikawa, 2018).



This project has received funding from the European Union's Horizon 2020 research and innovation programme under grant agreement No. 700748

Manual for the assessment of liquefaction risk, defining the procedures to create the database, collect, define, symbolize and store information in the Georeferenced Information System and to perform and represent the risk analysis

Moreover, liquefaction severity indicators can be seen as proxies of the permanent ground deformation (PGDf) (Bird et al.,2006) or, more generally, of damage and as the “liquefaction demand” for the assessment of the response of the overlying structures and infrastructures, characterized by their own vulnerability.

By combining seismic and liquefaction demand with the specific vulnerability of the structures, the physical expected damage can be estimated for a given scenario. To do this, structures and infrastructures present in the study area must be grouped and characterised with appropriate fragility models. Fragility functions are defined as log-normal probability distributions, representing the conditional probability of reaching or exceeding a damage level for a given value of the demand. Depending on the goal of the analysis, three types of vulnerability models can be defined. In the first two, ground shaking and liquefaction vulnerability are separately considered, while the third one considers a model accounting for both ground shaking and liquefaction. Seismic and liquefaction-induced physical damage on buildings and lifelines are then combined. Such combined physical damage is then converted into earthquake (direct/indirect) economic and social impact after the introduction of adequate economic and resilience models. This step is required since the physical damage is only a part of the impact of liquefaction on a community.

Finally, the mitigation framework and impact on community resilience reduction is obtained after the evaluation of the performance (in reducing such total impact and improving the community resilience) of the available mitigating action. This goal is achieved by applying benefit-cost analysis criteria. The obtained results are shown with maps that show the spatial distribution of the estimated damage levels for the selected scenario. These maps can be either produced by the user in any GIS environment or directly by the software (standalone version) (Figure 2-25).

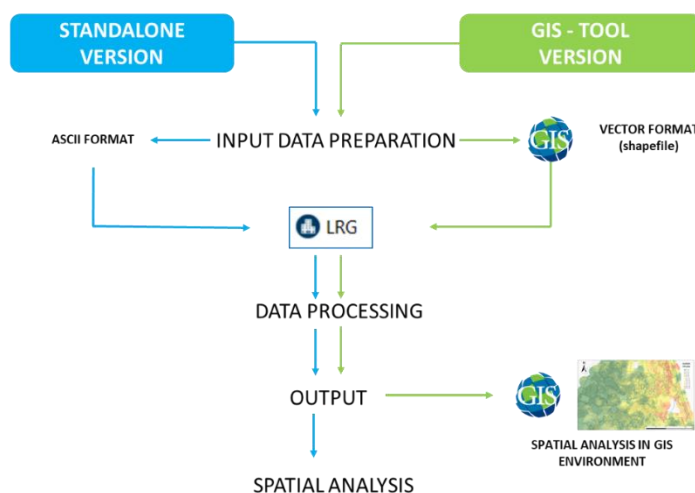


Figure 2-25: Flowchart of the general LRG procedure. To perform the analysis two options are available: the users can run the software as a standalone version or as an application of a Geographical Information System.



This project has received funding from the European Union's Horizon 2020 research and innovation programme under grant agreement No. 700748

3. GEOGRAPHICAL INFORMATION SYSTEMS

3.1 Introduction

The current models for decision-making against risk rely on tools capable to handle analyses characterized by a spatial multiscale approach. In addition to the description and location over the territory, the information required for this analysis must consider the spatial relationship between territory elements and phenomena involving human activities. The Geographical Information Systems (GIS) provide an efficient solution for public authorities and private companies, firstly to collect, define and store information, then to perform and represent the output of risk assessment.

Advanced software and hardware platforms nowadays allow to analyse geographical information at any resolution level, combining different types of data (raster, vectors, tables, ...) and providing a dynamic and interactive representation of the results. This flexibility enables also to integrate different disciplines (geology, geotechnical, structure, economic, ...) to interpret complex problems and to extend the analysis to wider fields of application.

The creation of GIS project for the management of spatial data is ruled by several standards defined at international and national levels. According to them, spatial data and geographical information should be preserved and updated in standardised formats. In this case, data are analysed and represented in a common framework, information can be shared in order to speed up the performance of analyses and to support authorities for the management of risk and the implementation of mitigation strategies.

3.2 GIS software

The currently available GIS software has rapidly evolved in recent years, improving its own functionality and reaching an excellent level of maturity, also for the open-source versions. This category of software is now able to fulfil many needs from different institutions and companies that face the necessity to handle geospatial data. The most common free and open Source Software¹ and those licensed under the GNU General Public License² are listed in Table 3-1.

1 Free and open-source software (FOSS) is software that can be classified as both free software and open-source software. That means that anyone is freely licensed to use, copy, study, and change the software in any way, and the source code is openly shared so that people are encouraged to voluntarily improve the design of the software. This is in contrast to proprietary software, where the software is under restrictive copyright licensing and the source code is usually hidden from the users.






2 The GNU General Public License is a free, copyleft license for software and other kinds of works. The GNU General Public License is intended to guarantee your freedom to share and change all versions of a program to make sure it remains free software for all its users. The Free Software Foundation, use the GNU General Public License for most of our software; it applies also to any other work released this way by its authors. The General Public Licenses are designed to ensure to distribute copies of free software, and source code, to change the software or use pieces of it in new free programs. The GNU GPL protect the rights with two steps: assert copyright on the software, and giving legal permission to copy, distribute and/or modify it. The precise terms and conditions for copying, distribution and modification define by Copyright © 2007 Free Software Foundation, Inc. <https://fsf.org/>.



This project has received funding from the European Union's Horizon 2020 research and innovation programme under grant agreement No. 700748

Manual for the assessment of liquefaction risk, defining the procedures to create the database, collect, define, symbolize and store information in the Georeferenced Information System and to perform and represent the risk analysis

Table 3-1: Example of open source GIS software

 <p>GRASS GIS</p>  <p>https://grass.osgeo.org/</p>	<p>Geographic Resources Analysis Support System (GRASS) is originally developed by the US Government in 1984. Is written in C, C++, Python, Tcl.</p>
 <p>https://qgis.org/</p>	<p>Quantum Geographical Information System (QGIS) is written in C++, Python, Qt, developed by the QGIS Development Team (from 2002).</p>
 <p>http://www.saga-gis.org/</p>	<p>System for Automated Geoscientific Analyses (SAGA) is written in C++, developed by the Department of Physical Geography, University of Göttingen, Germany, SAGA User Group Association (from 2005).</p>
 <p>http://www.gvsig.com/</p>	<p>gvSIG is an interoperable GIS software written in Java, developed by GvSIG association in October 2004.</p>

Together with the above there are also commercial software, like the ArcGIS developed by Environmental Systems Research Institute (ESRI) in 1999 (<https://www.esri.com>).

The choice of GIS software is quite independent on the approach, the problems to be solved and the workflows described in the following. Obviously, procedures and operational commands change from case to case. This document illustrates the main objectives and methodologies to be implemented for liquefaction risk assessment in a generic GIS platform.

3.3 GIS Standards

Together with the dissemination of open data, nowadays available in an astonishing abundance, the development of tool for geographical information software and analysis of spatial data have required to strengthen the technologies able to manage such large amount of data.

The use of standards in GIS technology is recommended to facilitate the development, sharing and use of data, software and services, for the management and the analysis of geographical information and spatial data. Rules are defined in technical documents and guidelines that include requirements and recommendations for products, systems, processes or services. Standard allows to reduce misunderstandings, harmonize technical specifications for developers, business partners and users and improve quality.



This project has received funding from the European Union's Horizon 2020 research and innovation programme under grant agreement No. 700748

Manual for the assessment of liquefaction risk, defining the procedures to create the database, collect, define, symbolize and store information in the Georeferenced Information System and to perform and represent the risk analysis

There are several organisations in charge of developing new standards and updating existing ones. Two of them, the Federal Geographic Data Committee (FGDC) and Open Geospatial Consortium (OGC) have produced copyrighted but free of charge standards.

Standards are normally established at the international level, e.g. European level, then are implemented at the national level. The standardization process in EU Member State includes three different levels (Figure 3-1).

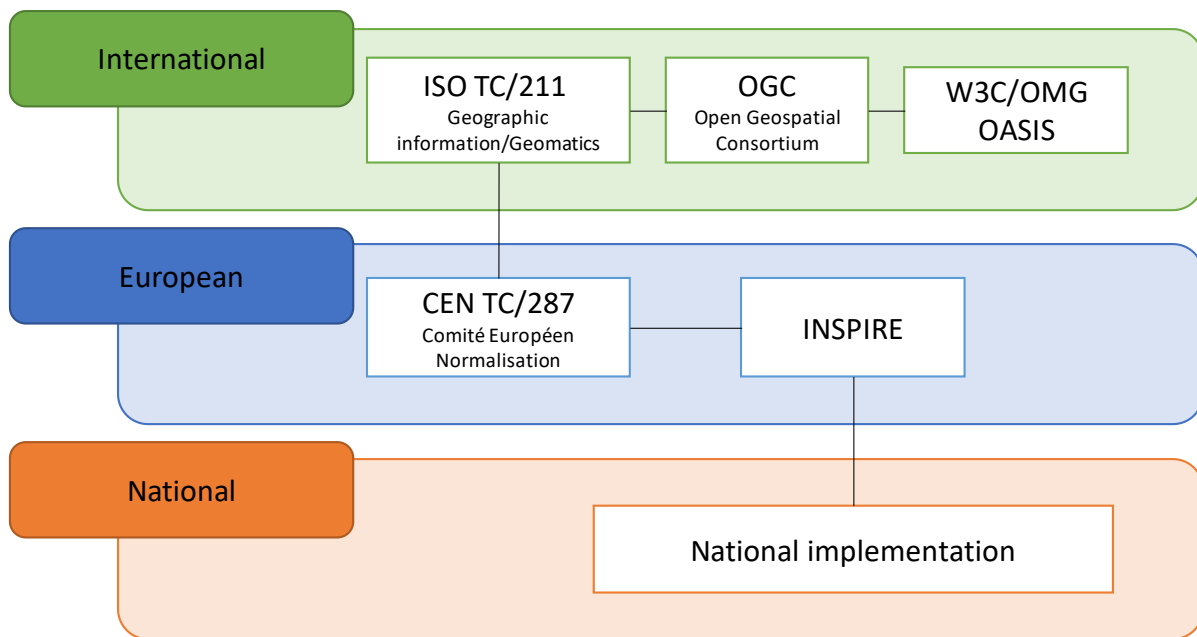


Figure 3-1: The structure of standardization process (Bartha and Kocsis, 2011)

The standard for geographical information has been elaborated by ISO Technical Committee (TC) 211 as Geographic information/Geomatics standard based on the proposals of Open Geospatial Consortium (OGC), World Wide Web Consortium (W3C), Object Management Group (OMG), Organization for the Advancement of Structured Information Standards (OASIS) (ISO/TC 211 Advisory Group on Outreach, 2009). The ISO 19100 series (Table 3-2) was selected as international standard for the technical base for INSPIRE by the European standardization organization *Comité Européen Normalisation* - CEN TC/211.

The INSPIRE Directive (Infrastructure for Spatial Information in the European Community) sets the minimum conditions for interoperable sharing and exchange of spatial data across Europe as part of a larger European Interoperability Framework and the e-Government Action Plan that contributes to the Digital Single Market Agenda. The INSPIRE proposal (<https://inspire.ec.europa.eu/>) was adopted as Directive 2007/2/EC of the European Parliament and of the Council, the Directive was published in the official Journal on the 25th April 2007. The complete implementation of the INSPIRE project is foreseen by 2019.



This project has received funding from the European Union's Horizon 2020 research and innovation programme under grant agreement No. 700748

Manual for the assessment of liquefaction risk, defining the procedures to create the database, collect, define, symbolize and store information in the Georeferenced Information System and to perform and represent the risk analysis

Table 3-2: Series of ISO Standard for Geographical Information

ISO Standard	Title
6709	Standard representation of latitude, longitude and altitude for geographic point locations
19101	Reference model
19101-2 -	Reference model - Part 2: Imagery
19103	Conceptual schema language
19104	Terminology Introduction
19105	Conformance and testing
19106	Profiles
19107	Spatial schema
19108	Temporal schema
19109	Rules for application schema
19110	Methodology for feature cataloguing
19111	Spatial referencing by coordinates
19112	Spatial referencing by geographic identifiers
19113	Quality principles
19114	Quality evaluation procedures
19115	Metadata
19115-2	Metadata - Part 2: Extensions for imagery and gridded data
19116	Positioning services
19117	Portrayal
19118	Encoding
19119	Services
19120	Functional standards
19121	Imagery and gridded data
19122	Qualifications and Certification of personnel
19123	Schema for coverage geometry and functions
19124	Imagery and gridded data components
19125-1	Simple feature access - Part 1: Common architecture
19125-2	Simple feature access - Part 2: SQL option
19126	Profile - FACC Data Dictionary
19127	Geodetic codes and parameters
19128	Web Map server interface
19129	Imagery, gridded and coverage data framework
19130	Sensor and data models for imagery and gridded data
19131	Data product specifications
19132	Location based services possible standards
19133	Location based services tracking and navigation
19134	Multimodal location-based services for routing and navigation
19135	Procedures for registration of geographical information items
19136	Geography Markup Language
19137	Generally used profiles of the spatial schema and of similar important other schemas
19138	Data quality measures
19139	Metadata - Implementation specification
19140	Technical amendment to the ISO 191**Geographic information series of standards for harmonization and enhancements



This project has received funding from the European Union's Horizon 2020 research and innovation programme under grant agreement No. 700748

Manual for the assessment of liquefaction risk, defining the procedures to create the database, collect, define, symbolize and store information in the Georeferenced Information System and to perform and represent the risk analysis

To ensure that the spatial data infrastructures of the Member States are compatible, the INSPIRE Directive requires common Implementing Rules (IR) to be adopted in different specific areas:

- Metadata
- Data Specifications
- Network Services
- Data and Service Sharing
- Spatial Data Services

With regard to Monitoring and Reporting for Data Specifications, the Technical Guidelines specify common data models, code lists, map layers and additional metadata on the interoperability to be used when exchanging spatial datasets. These documents describe detailed implementation aspects and relations with existing standards, technologies, and practices. Their implementation included 34 themes subdivided into three groups and included into the INSPIRE directive in three annexes (Table 3-3, Table 3-4 and



This project has received funding from the European Union's Horizon 2020 research and innovation programme under grant agreement No. 700748

LIQUEFACT
Deliverable 7.1

Manual for the assessment of liquefaction risk, defining the procedures to create the database, collect, define, symbolize and store information in the Georeferenced Information System and to perform and represent the risk analysis

Table 3-5). For each theme, Technical Guidelines have been developed by the Thematic Working Group (TWG). This document provides guidelines for the implementation of the provisions laid down in the Implementing Rule for spatial data sets and services of the INSPIRE Directive. It also includes additional requirements and recommendations that, although not included in the Implementing Rule, are relevant to guarantee or to increase data interoperability.



This project has received funding from the European Union's Horizon 2020 research and innovation programme under grant agreement No. 700748

Manual for the assessment of liquefaction risk, defining the procedures to create the database, collect, define, symbolize and store information in the Georeferenced Information System and to perform and represent the risk analysis

Table 3-3: INSPIRE Data Specification - Technical Guidelines – Annexes I










	INSPIRE Data Specification on Addresses – Technical Guidelines
	INSPIRE Data Specification on Administrative Units – Technical Guidelines
	INSPIRE Data Specification on Cadastral Parcels – Technical Guidelines
	INSPIRE Data Specification on Coordinate Reference Systems – Technical Guidelines
	INSPIRE Data Specification on Geographical Grid Systems – Technical Guidelines
	INSPIRE Data Specification on Geographical Names – Technical Guidelines
	INSPIRE Data Specification on Hydrography – Technical Guidelines
	INSPIRE Data Specification on Protected Sites – Technical Guidelines
	INSPIRE Data Specification on Transport Networks – Technical Guidelines

Table 3-4: INSPIRE Data Specification - Technical Guidelines – Annexes II





















	INSPIRE Data Specification on Land Cover – Technical Guidelines
	INSPIRE Data Specification on Orthoimagery – Technical Guidelines
	INSPIRE Data Specification on Elevation – Technical Guidelines
	INSPIRE Data Specification on Geology – Technical Guidelines



This project has received funding from the European Union's Horizon 2020 research and innovation programme under grant agreement No. 700748

Manual for the assessment of liquefaction risk, defining the procedures to create the database, collect, define, symbolize and store information in the Georeferenced Information System and to perform and represent the risk analysis

Table 3-5: INSPIRE Data Specification - Technical Guidelines – Annexes III

	INSPIRE Data Specification on Utility and Government Services – Technical Guidelines
	INSPIRE Data Specification on Agricultural and Aquaculture Facilities – Technical Guidelines
	INSPIRE Data Specification on Area Management/Restriction/ Regulation Zones and Reporting Units – Technical Guidelines
	INSPIRE Data Specification on Atmospheric Conditions and Meteorological Geographical Features – Technical Guidelines
	INSPIRE Data Specification on Bio-geographical Regions– Technical Guidelines
	INSPIRE Data Specification on Buildings – Technical Guidelines
	INSPIRE Data Specification on Energy resources – Technical Guidelines
	INSPIRE Data Specification on Environmental Monitoring Facilities – Technical Guidelines
	INSPIRE Data Specification on Habitats and Biotopes – Technical Guidelines
	INSPIRE Data Specification on Human Health and Safety – Technical Guidelines
	INSPIRE Data Specification on Land Use – Technical Guidelines
	INSPIRE Data Specification on Mineral Resources – Technical Guidelines
	INSPIRE Data Specification on Natural Risk Zones – Technical Guidelines
	INSPIRE Data Specification on Oceanographic geographical features – Technical Guidelines
	INSPIRE Data Specification on Population Distribution – Technical Guidelines
	INSPIRE Data Specification on Production and Industrial facilities – Technical Guidelines
	INSPIRE Data Specification on Sea Regions – Technical Guidelines
	INSPIRE Data Specification on soil – Technical Guidelines
	INSPIRE Data Specification on Species Distribution – Technical Guidelines
	INSPIRE Data Specification on Statistical Units– Technical Guidelines



This project has received funding from the European Union's Horizon 2020 research and innovation programme under grant agreement No. 700748

Manual for the assessment of liquefaction risk, defining the procedures to create the database, collect, define, symbolize and store information in the Georeferenced Information System and to perform and represent the risk analysis

3.4 GIS structure

The structure of GIS platform is characterized by three elements: geodatabase, geoprocessing and geo-visualization (Figure 3-2). The *geodatabase* represents the spatial database, where the geographical information model and data information are organized with thematic layers. This represent the fundamental aspect of the GIS project as it provides an organization of data, useful for understanding complex scenarios (e.g. risk connected damage of structure or infrastructures). The *geoprocessing* contains a set of tools used for the analysis and processing of geospatial data, able to generate derived datasets. The *geo-visualization* allows to create geographical representations whose purpose is not only to distinguish the elements on the territory, but also to highlight their spatial relationships. This feature includes the possibility to express queries in interactive maps, three-dimensional scenes and to analyse network relationships.

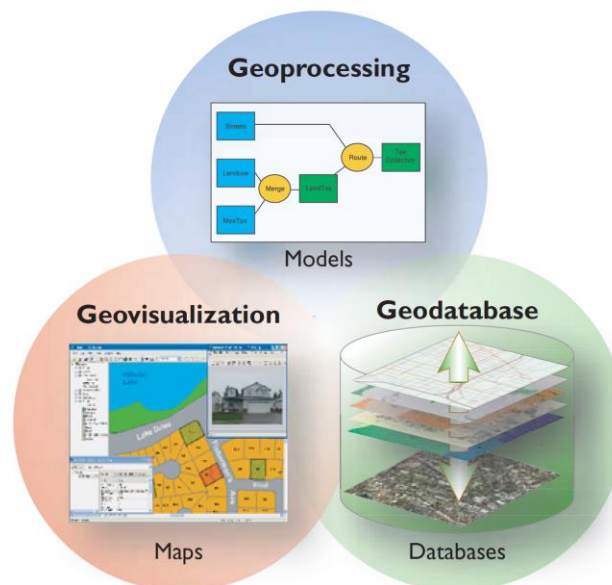


Figure 3-2: GIS structure (ESRI,2001)

3.5 Coordinate system

The creation of the dataset is a critical step and is closely related to the ability in georeferencing data. It primarily consists in the need to know the original position of the data, in terms of coordinates (longitude, latitude, altitude or by other geocode systems). The coordinate systems create a common coordinate framework aimed at performing various integrated process such as overlaying of data layers from different sources.

A coordinate system is a reference system used to represent the location of geographic features, imagery, and observation with a common geographic framework, defined by:

- the type of framework: geographic (spherical coordinates are measured from the earth's center) or planimetric (the earth's coordinates are projected onto a two-dimensional planar surface);



This project has received funding from the European Union's Horizon 2020 research and innovation programme under grant agreement No. 700748

Manual for the assessment of liquefaction risk, defining the procedures to create the database, collect, define, symbolize and store information in the Georeferenced Information System and to perform and represent the risk analysis

- the unit system: typically, decimal degrees for latitude-longitude, feet or meters for projected coordinate systems;
- and other descriptive information as projection system for projected coordinate systems, spheroid of reference, a datum, standard parallels, a central meridian, and possible shifts in the x- and y-directions.

The common coordinate systems used in GIS platform are:

- global or spherical coordinate systems, such as latitude-longitude, define as geographic coordinate systems (such as WGS84);
- projected coordinate systems, such as universal transverse Mercator (UTM), which provide various models to project maps of the earth's spherical surface in a two-dimensional Cartesian coordinate plane. Projected coordinate systems are referred to as map projections.

The vertical coordinate systems define the reference system for the elevation and the depth values (z-values). The unit of the measure is linear and define by the international standard (feet or meters). The z-axis direction is positive “up” for elevation and positive “down” for depth.

The two vertical coordinate systems are illustrated in the Figure 3-3. The mean sea level is used as the zero level for elevation values and the mean low water is a depth-based vertical coordinate system.

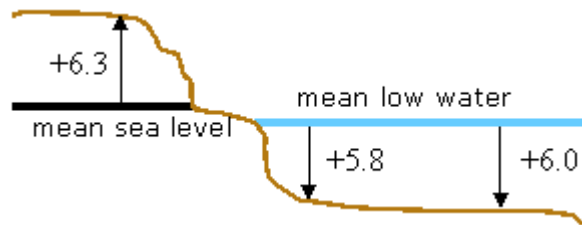


Figure 3-3: Reference system for Vertical Coordinate Systems

The vertical coordinate system on a dataset can be define without a corresponding geographic or projected coordinate system.

The [INSPIRE Data Specification on Coordinate Reference Systems – Technical Guidelines](#) provides a harmonised data specification for the spatial data theme Coordinate Reference Systems. This specification establishes:

- The geodetic datums and coordinate reference systems to be used, unless otherwise required for data of a specific theme.



This project has received funding from the European Union's Horizon 2020 research and innovation programme under grant agreement No. 700748

Manual for the assessment of liquefaction risk, defining the procedures to create the database, collect, define, symbolize and store information in the Georeferenced Information System and to perform and represent the risk analysis

IR Requirement

Annex II, Section 1.2

Datum for three-dimensional and two-dimensional coordinate reference systems

For the three-dimensional and two-dimensional coordinate reference systems and the horizontal component of compound coordinate reference systems used for making spatial data sets available, the datum shall be the datum of the European Terrestrial Reference System 1989 (ETRS89) in areas within its geographical scope, or the datum of the International Terrestrial Reference System (ITRS) or other geodetic coordinate reference systems compliant with ITRS in areas that are outside the geographical scope of ETRS89. Compliant with the ITRS means that the system definition is based on the definition of the ITRS and there is a well documented relationship between both systems, according to EN ISO 19111:2007.

The WGS84 system designates a full set of geodetic standards, in which successive realisations of a unique TRS has been provided. The most recent WGS84 realisations are in agreement with the ITRF at the level of a few centimetres. In consequence, the WGS84 products (as concerning TRS issues) are considered as realisations of the ITRS. The WGS84 is linked to the ITRS.

- Three-dimensional CRS are used to express both, the horizontal and the vertical components of geographical locations. This may be performed by means of:
 - Cartesian CRS, where X, Y, and Z coordinates are used to define the location, or;
 - Three-dimensional geodetic CRS, where latitude, longitude and ellipsoidal height define the location.

IR Requirement

Annex II, Section 1.3

Coordinate Reference Systems

Spatial data sets shall be made available using at least one of the coordinate reference systems specified in sections 1.3.1, 1.3.2 and 1.3.3, unless one of the conditions specified in section 1.3.4 holds.

1.3.1. Three-dimensional Coordinate Reference Systems

- Three-dimensional Cartesian coordinates based on a datum specified in 1.2 and using the parameters of the Geodetic Reference System 1980 (GRS80) ellipsoid.
- Three-dimensional geodetic coordinates (latitude, longitude and ellipsoidal height) based on a datum specified in 1.2 and using the parameters of the GRS80 ellipsoid.

(...)

- Two-dimensional CRS are used to express the horizontal component. This may be performed by means of:
 - Two-dimensional geodetic CRS, where latitude and longitude on a reference ellipsoid are used to define the horizontal location;

or



This project has received funding from the European Union's Horizon 2020 research and innovation programme under grant agreement No. 700748

Manual for the assessment of liquefaction risk, defining the procedures to create the database, collect, define, symbolize and store information in the Georeferenced Information System and to perform and represent the risk analysis

- Plane CRS (suitable map projections), where a pair of coordinates - either (N, E) or (Y, X) - defines the horizontal location through the projection

IR Requirement
Annex II, Section 1.3
Coordinate Reference Systems

Spatial data sets shall be made available using at least one of the coordinate reference systems specified in sections 1.3.1, 1.3.2 and 1.3.3, unless one of the conditions specified in section 1.3.4 holds.

(...)

1.3.2. Two-dimensional Coordinate Reference Systems

- Two-dimensional geodetic coordinates (latitude and longitude) based on a datum specified in 1.2 and using the parameters of the GRS80 ellipsoid.
- Plane coordinates using the ETRS89 Lambert Azimuthal Equal Area coordinate reference system.
- Plane coordinates using the ETRS89 Lambert Conformal Conic coordinate reference system.
- Plane coordinates using the ETRS89 Transverse Mercator coordinate reference system.

(...)

- Plane coordinates reference systems (map projections) adopted and recommended for different purposes. Map projections are used for geo-referencing spatial information in plane coordinates

Recommendation 1 For pan-European spatial analysis and reporting, where true area representation is required, the ETRS89-LAEA is recommended

Recommendation 2 For conformal pan-European mapping at scales smaller than or equal to 1:500,000, the ETRS89-LCC is recommended

Recommendation 3 For conformal pan-European mapping at scales larger than 1:500,000, the Transverse Mercator ETRS89-TMzn is recommended

Recommendation 4 It is recommended that the projections referred in section 1.3.2 of Annex II of Commission Regulation (EU) No 1089/2010) are available in INSPIRE transformation services.

For regions outside continental Europe, for example overseas MS territories, the MS shall define a map projection they consider most suitable for the application. The ETRS89-LAEA projection in INSPIRE is recommended for spatial analysis and reporting.

The Transverse Mercator (ETRS89-TMzn) is identical to the Universal Transverse Mercator (UTM) grid system for the Northern hemisphere when applied to the ETRS89 geodetic datum and the GRS80 ellipsoid. The UTM system was developed for worldwide application between 80° S and 84° N.



This project has received funding from the European Union's Horizon 2020 research and innovation programme under grant agreement No. 700748

Manual for the assessment of liquefaction risk, defining the procedures to create the database, collect, define, symbolize and store information in the Georeferenced Information System and to perform and represent the risk analysis

3.6 Geodatabase

3.6.1 Data organization

The data organization is based on the logical model inherited from the Computer-Aided Drafting software (CAD) which divides the information into overlapping layers (Figure 3-4). These Layers can be compared to each other using the overlapping technique because they are georeferenced with respect to a coordinate system. This technique allows to manage and query geographic information simultaneously on various levels and extract information based on their position.

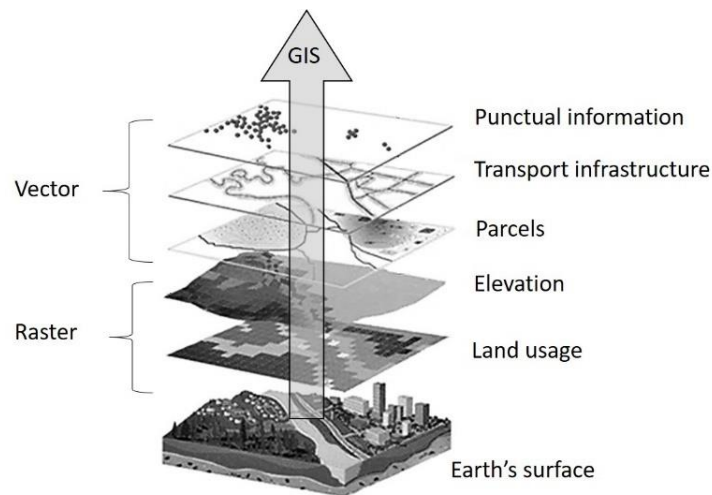


Figure 3-4: GIS thematic layers (Spacagna and Modoni, 2018)

3.6.2 Data formats and attribute information

In the GIS platform, the geographical information is shared in two major categories of format: raster and vector. Data reading and writing operations are managed by libraries, released by the Open Source Geospatial Foundation³. For the raster format is used the GDAL Library⁴ and for vector format is used the OGR Simple Features Library, which is part of the GDAL source tree.

The geographical information can be store in three main way:

- file: the geodata is stored on disk in a file with a user-defined path;
- folder: the geodata are represented by a specific folder, with a well-defined file structure;
- database: the geodata are store in relational database (RDBMS) with spatial functionality to which the GIS software can connect.

³ The Open Source Geospatial Foundation (OSGeo), is a non-profit non-governmental organization whose mission is to support and promote the collaborative development of open geospatial technologies and data (www.osgeo.org).

⁴ Geospatial Data Abstraction Library (GDAL) (www.gdal.org).



This project has received funding from the European Union's Horizon 2020 research and innovation programme under grant agreement No. 700748

Manual for the assessment of liquefaction risk, defining the procedures to create the database, collect, define, symbolize and store information in the Georeferenced Information System and to perform and represent the risk analysis

In addition to this storage mode, GIS services are used to transfer spatial data in remote access stored on a web server, define by the OGC. They allow users to interact with data, usually through browser web, in rapid way and in real time. This contains visualization maps, access and querying of data, running analysis and download of spatial data. Supported services are for example:

- WMS: Web Map Service for sharing maps in image format such as PNG, GIF or JPEG
- WFS: Web Feature Service for sharing feature of vector data.
- WCS: Web Coverage Service for sharing raster vector.

3.6.2.1 Vector format

The vector feature is frequently used for the representation of geographic objects, well suited for representing features with discrete boundaries such as wells, streets, rivers, states and parcels. The vectors features are objects for which the location is stored as one of the properties. These features are spatially represented essentially as points, lines or polygons (Figure 3-5) and are organized into classes with a common spatial representation and set of attributes. For example, the point feature class is used for wells and the line feature class is used for rivers.

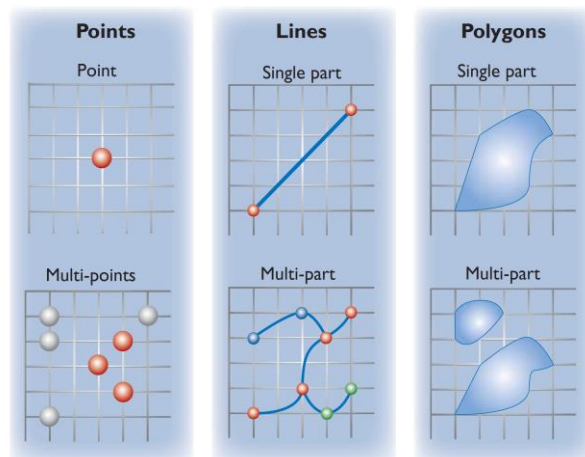


Figure 3-5: Common vector feature representations (extract from ESRI, 2001)

Several geographical features are adequately expressed by a precise range of geometric elements: points (dimensionless elements used for the simple location within an aerial representation); lines and polylines (one-dimensional elements used for the localization of linear elements); polygons (two-dimensional elements used for the representation of geographic elements having characteristics such as to cover a particular area of the soil surface).

The most common vector format is:

1. **ESRI Shapefile:** The shapefile format is an open digital vector format for storing geometric location and associated attribute information. It is the most popular geospatial vector data format for GIS software. It is developed and regulated by the Environmental Systems Research Institute (ESRI).



This project has received funding from the European Union's Horizon 2020 research and innovation programme under grant agreement No. 700748

Manual for the assessment of liquefaction risk, defining the procedures to create the database, collect, define, symbolize and store information in the Georeferenced Information System and to perform and represent the risk analysis

A shapefile represents one single vector layer in the legend of the GIS software and it is characterised by a unique feature (point, line or polygon). A shapefile actually consists of several files. The following three are required:

- .shp file containing the feature geometries
- .dbf file containing the attributes in dBase format
- .shx index file

Shapefiles also can include .prj file, which contains the projection. Although this file is not mandatory, it is essential to have information about coordinate system and projection system used.

For each shapefile layer is available a specific table of database, call attribute table, in which each record (row) corresponds to a specific geographic object contained in the layer.

2. Keyhole Markup Language (KML): Express geographic data, labels, and symbology in 2D and 3D for web map and globes. This GIS format is XML-based and is primarily used for Google Earth, developed by Keyhole Inc and later acquired by Google. KMZ (KML-Zipped), compressed version, replace KML as being the default Google Earth geospatial. KML/KMZ became an international standard of the Open Geospatial Consortium in 2008.
3. Comma-separated values (CSV) is a text format containing the coordinate X and Y of the georeferenced feature, easily imported into the GIS software.

3.6.2.2 Raster format:

The raster is used to represent continuous layers, such as elevation, vegetation, ecc. The raster consists on a matrix of cells (or pixels) to which the value of the represented quantity is associated. Rasters are most commonly used for the storage of digital or scan maps, satellite imageries, digital aerial photographs (Figure 3-6).

The raster format most common are:

1. GeoTIFF, Georeferenced Tagged Image File Format, is an open file format, based on the standard of the TIFF format and incorporate geographical references. It can include projections, ellipsoids, datums, coordinates, and all that is needed to establish the exact spatial reference for the file. GeoTIFF is in wide use in NASA Earth science data systems. The GeoTIFF Standards are developed by Working Group at the Open Geospatial Consortium (OGC).



This project has received funding from the European Union's Horizon 2020 research and innovation programme under grant agreement No. 700748

Manual for the assessment of liquefaction risk, defining the procedures to create the database, collect, define, symbolize and store information in the Georeferenced Information System and to perform and represent the risk analysis

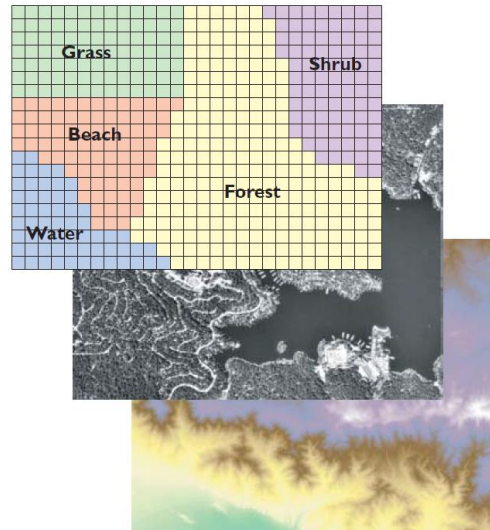


Figure 3-6: Storage mechanisms of Raster (extract from ESRI, 2001)

2. GeoJPEG 2000 is an open format derived from the format developed by the Joint Photographic Experts Group committee (JPEG). This format is a wavelet-based image compression standard (ISO specification (ISO/IEC 15444), particularly efficient for remote sensing images. Although the standard JPEG 2000 format does not include geocoding, this format supports metadata in XMK format which includes geographic metadata such as projection used or geographic coverage of data in GML format. So GeoJPEG2000 or GeoJP2 is an improved JPEG2000 file with additional geocoding information.

3.6.3 Geodatabase

The term database refers to Relational Data Base Management System (RDBMS). This system allows to manage data based on the relational model. Basically, the database is structured in tables, each subdivided into fields and records that describe the geographical objects. In GIS, each vector information layer corresponds to a table for storing attributes. The information contained in the attribute tables can be of various types: string (for example the name of geological lithology), number (for example the deep of the borehole), logical or Boolean (true/false), or date. The information of the attribute table can be interrogated (query) based on the SQL database language (Structured Query Language). The query allows to extract from the database in a reduced set of elements that can be consulted both within the geographical area and in the table.

Geodatabases have a comprehensive information model for representing and managing geographic information. This comprehensive information model is implemented as a series of tables holding feature classes, raster datasets, and attributes. In addition, advanced GIS data objects add GIS behavior; rules for managing spatial integrity; and tools for working with numerous spatial relationships of the core features, raster, and attributes (Figure 3-7).



This project has received funding from the European Union's Horizon 2020 research and innovation programme under grant agreement No. 700748

Manual for the assessment of liquefaction risk, defining the procedures to create the database, collect, define, symbolize and store information in the Georeferenced Information System and to perform and represent the risk analysis

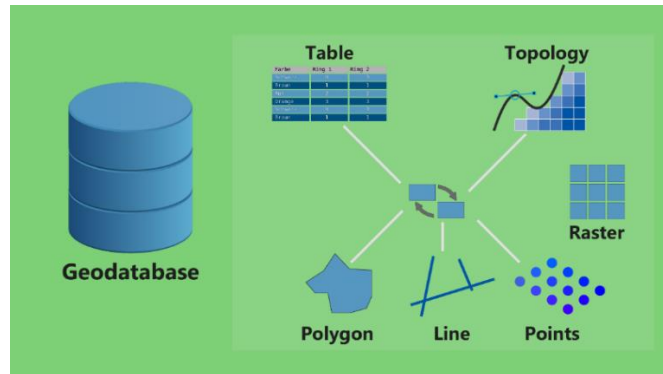


Figure 3-7: Geodatabase structure

The most common geodatabase are:

- PostGIS, the spatial extension of PostgreSQL, is OGC standard format able to manage vector data and raster data;
- MySQL spatial, the spatial extension of widespread database MySQL;
- Oracle spatial, the geographical component of the well-known relational database Oracle;
- SpatiaLite, is OGC standard extension of SQLite.
- Geopackage, an OGC standard, is an recent (2014) extended SQLite 3 database file (*.gpkg) containing data and metadata tables with specified definitions, integrity assertions, format limitations and content constraints.

3.6.4 Metadata

Metadata are data that provides information about other data. The geographic metadata standards are:

- ISO 19115-1:2014: Geographic information -- Metadata -- Part 1: Fundamentals
- ISO 19115-2:2019: Geographic information -- Metadata -- Part 2: Extensions for acquisition and processing

Standards give the structure for creating and organizing metadata in a consistent terminology for catalogs and global search. They define how to describe geographical information and associated services, including contents, spatial-temporal purchases, data quality, access and rights to use. It is preserved by the ISO/TC 211 committee.

The INSPIRE Implementing Rules on Metadata (IRs) specify the needs to be considered at a generic level, while the non-binding Technical Guidelines specify how legal obligations could be implemented. In particular, the [INSPIRE Metadata Implementing Rules: Technical Guidelines based on EN ISO 19115 and EN ISO 19119](#).

The information required for metadata implementation concerns:

- Identification (Table 3-6),
- Geographic location (Table 3-7),



This project has received funding from the European Union's Horizon 2020 research and innovation programme under grant agreement No. 700748

Manual for the assessment of liquefaction risk, defining the procedures to create the database, collect, define, symbolize and store information in the Georeferenced Information System and to perform and represent the risk analysis

- Classification of spatial data and services (Table 3-8),
- Temporal reference (Table 3-9),
- Conformity (Table 3-10),
- Responsible organisation (Table 3-11),
- Quality and validity (Table 3-12),
- Constraints related to access and use (Table 3-13),
- Metadata on metadata (Table 3-14).

The tables indicate a summary description of the metadata elements. The detailed description is given in the INSPIRE Technical Guideline.

Table 3-6: Metadata elements for Identification (INSPIRE Technical Guideline)

Metadata element name	Description
Resource title	Characteristic, and often unique, name by which the resource is known. The title is the most informative element of a metadata record and usually the highest priority as search engines go to this element.
Resource abstract	Brief narrative summary of the content of the resource. The abstract provides a clear and concise statement that enables the reader to understand the content of the data or service.
Resource Type	This is the type of resource being described by the metadata and it is filled in with a value from a classification of the resource based on its scope. The choice of Resource Type will be probably the first decision made by the user and it will define the metadata elements that should be filled.
Resource Locator for data sets and dataset series	The Resource Locator is the 'navigation section' of a metadata record which point users to the location (URL) where the data can be downloaded, or to where additional information about the resource may be provided. Setting up the correct resource locators is important for the connection between the data and the services that provide access to them or for providing additional information concerning the resource.
Resource Locator for Services	The Resource Locator for Services, if available, provides the access point of the service, that is an Internet address containing a detailed description of a spatial data service, including a list of endpoints to allow an automatic execution
Unique resource identifier	This element is a value uniquely identifying the resource. Value uniquely identifying an object within a namespace
Coupled resource	If the resource is a spatial data service, this metadata element refers to, where relevant, the target spatial data set(s) of the service. It is implemented by reference, i.e. through a URL that points to the metadata record of the data on which the service operates. It helps therefore linking services to the relevant datasets.
Resource language	It refers to the language(s) used within the resource (dataset, series, or service if relevant).



This project has received funding from the European Union's Horizon 2020 research and innovation programme under grant agreement No. 700748

Manual for the assessment of liquefaction risk, defining the procedures to create the database, collect, define, symbolize and store information in the Georeferenced Information System and to perform and represent the risk analysis

Table 3-7: Metadata elements for Geographic location (INSPIRE Technical Guideline)

Metadata element name	Description
Geographic bounding box	This is the extent of the resource in the geographic space, given as a bounding box. Defining the coordinates of a rectangle representing the resource area on a map allows the discovery by geographical area

Table 3-8: Metadata elements for Classification of spatial data and services (INSPIRE Technical Guideline)

Metadata element name	Description
Topic category	Main theme(s) of the dataset. The topic category is a high-level classification scheme to assist in the grouping and topic-based search of available spatial data resources. A correct categorization is very important to help users to search and find the resources they are looking for.
Spatial data service type	A service type name from a registry of services. This is a classification to assist in the search of available spatial data services. The list of language-neutral values as in Part D3 of the INSPIRE Metadata Regulation 1205/2008/EC includes: discovery, view, download, transformation, invoke and other.
Keyword value	The keyword value is a commonly used word, formalised word or phrase used to describe the subject
Originating controlled vocabulary	Name of the formally registered thesaurus or a similar authoritative source of keywords

Table 3-9: Metadata elements for Temporal reference (INSPIRE Technical Guideline)

Metadata element name	Description
Temporal extent	The temporal extent defines the time period covered by the content of the resource. This time period may be expressed as: an individual date, an interval of dates (starting date and ending date), a mix of individual dates and intervals of dates
Date of publication	This is the date of publication of the resource when available, or the date of entry into force.
Date of last revision	This date describes when the resource was last revised, if the resource has been revised.
Date of creation	This date describes when the resource was created.



This project has received funding from the European Union's Horizon 2020 research and innovation programme under grant agreement No. 700748

Manual for the assessment of liquefaction risk, defining the procedures to create the database, collect, define, symbolize and store information in the Georeferenced Information System and to perform and represent the risk analysis

Table 3-10: Metadata elements for Conformity (INSPIRE Technical Guideline)

Metadata element name	Description
Degree	Indication of the conformance result (true, false, or null)
Specification	Citation of the product specification or user requirement against which data is being evaluated

Table 3-11: Metadata elements for Responsible organisation (INSPIRE Technical Guideline)

Metadata element name	Description
Responsible party	Identification of, and means of communication with, person(s) and organization(s) associated with the resource(s)
Responsible party role	This is the role of the responsible organisation

Table 3-12: Metadata elements for Quality and validity (INSPIRE Technical Guideline)

Metadata element name	Description
Lineage	<p>According to the Implementing Rules for Metadata, Lineage is “a statement on process history and/or overall quality of the spatial data set. Where appropriate it may include a statement whether the data set has been validated or quality assured, whether it is the official version (if multiple versions exist), and whether it has legal validity. The value domain of this element is free text.”</p> <p>The process history may be described by information on the source data used and the main transformation steps that took place in creating the current data set (series)</p>
Spatial resolution	<p>Spatial resolution refers to the level of detail of the data set. It shall be expressed as a set of zero to many resolution distances (typically for gridded data and imagery-derived products) or equivalent scales (typically for maps or map-derived products).</p> <p>An equivalent scale is generally expressed as an integer value expressing the scale denominator. A resolution distance shall be expressed as a numerical value associated with a unit of length</p>



This project has received funding from the European Union's Horizon 2020 research and innovation programme under grant agreement No. 700748

Table 3-13: Metadata elements for Constraints related to access and use (INSPIRE Technical Guideline)

Metadata element name	Description
Limitations on public access (access constraints)	Access constraints applied to assure the protection of privacy or intellectual property, and any special restrictions or limitations on obtaining the resource
Limitations on public access (other constraints)	Other restrictions and legal prerequisites for accessing and using the resource or metadata
Limitations on public access (classification)	Name of the handling restrictions on the resource
Conditions applying to access and use	Restrictions on the access and use of a resource or metadata

Table 3-14: Metadata elements for Metadata on metadata (INSPIRE Technical Guideline)

Metadata element name	Description
Metadata point of contact	The date which specifies when the metadata record was created or updated
Metadata date	This is the role of the responsible organisation
Metadata language	This is the language in which the metadata elements are expressed

3.7 Geoprocessing

3.7.1 Tools for spatial analysis

Geoprocessing is a GIS operation implemented to manipulate spatial data. A typical geoprocessing operation considers an input dataset, performs an operation on that dataset, and returns an output dataset (Figure 3-8).

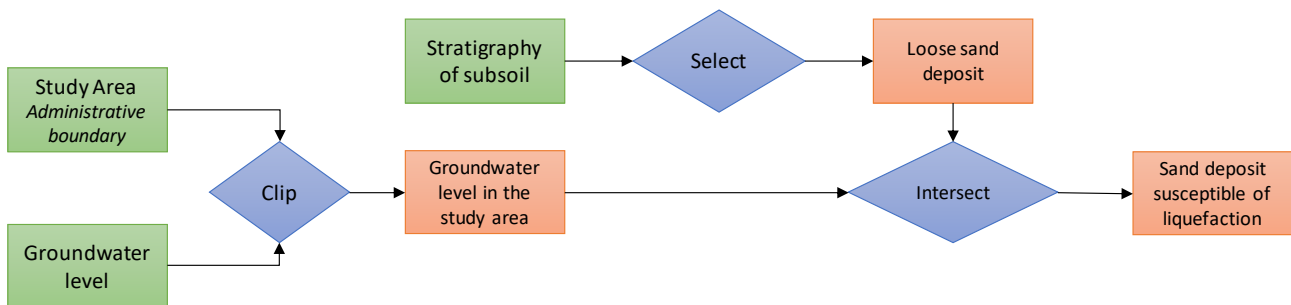


Figure 3-8: Example of geoprocessing procedure

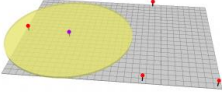
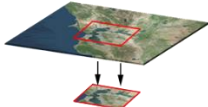
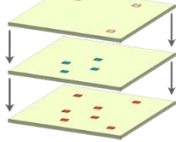
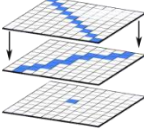
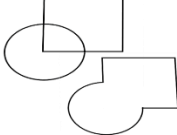
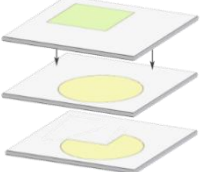


This project has received funding from the European Union's Horizon 2020 research and innovation programme under grant agreement No. 700748

Manual for the assessment of liquefaction risk, defining the procedures to create the database, collect, define, symbolize and store information in the Georeferenced Information System and to perform and represent the risk analysis

Common geoprocessing operations include geographic feature overlay, feature selection and analysis, topology processing, raster processing, and data conversion. The most used processing tools are reported and illustrated in the Table 3-15 (<https://gisgeography.com/geoprocessing-tools/>).

Table 3-15: Common geoprocessing tools

Tool	Description
 <p data-bbox="288 752 359 781">Buffer</p>	<p data-bbox="507 636 1430 741">Buffers are proximity functions. It creates a polygon or collection of cells that within a specified proximity of a set of features. Buffers can have fixed and variable distances.</p>
 <p data-bbox="300 913 343 952">Clip</p>	<p data-bbox="507 788 1430 893">The clip tool is an overlay function that cuts out an input layer with the extent of a defined feature boundary. The result of this tool is a new clipped output layer.</p>
 <p data-bbox="284 1115 359 1144">Merge</p>	<p data-bbox="507 958 1430 1064">The merge geoprocessing tool combines data sets that are the same data type (points, lines or polygons). When you run the merge tool, the resulting data will be merged into one.</p>
 <p data-bbox="268 1294 375 1328">Intersect</p>	<p data-bbox="507 1151 1430 1256">The Intersect Tool is very similar to the clip tool. The Intersect Tool performs a geometric overlap. All features that overlap in all layers will be part of the output feature class – attributes preserved.</p>
 <p data-bbox="288 1485 359 1516">Union</p>	<p data-bbox="507 1335 1430 1440">The Union Tool maintains all input features boundaries and attributes in the output feature class. The Union tool spatially combines two data layers. It preserves features from both layers at the same extents.</p>
 <p data-bbox="264 1709 384 1738">Difference</p>	<p data-bbox="507 1523 1430 1664">The Erase Tool removes features that overlap the erase features. This geoprocessing tool maintains portions of input features falling outside the erase features extent. The result is a new feature with the erase feature extent removed.</p>

Moreover, thanks to the remarkable potential of the GIS tool, spatial analyses can be performed through the adoption of specific statistical and modelling methods, developed in external applications.



This project has received funding from the European Union's Horizon 2020 research and innovation programme under grant agreement No. 700748

3.7.2 Geostatistical analysis

From sampling data, it is possible to describe and represent a phenomenon over the whole area interpolating information using the structure of the data distribution. Natural phenomenon, as the stratigraphy of subsoil is, in fact, characterized by a structural character, which depends on the genesis of the phenomenon itself. The discipline known under the name of geostatistics has been developed since the early sixties to define the dimension and extension of mineral deposits. The theory behind this discipline takes into account the spatial dependence between the variables of interest, and is called the "theory of regionalized variables" (Matheron, 1962). The structural characteristics of the phenomenon are sought on the measured data, sometimes also counting on additional qualitative information in order to improve the knowledge of the phenomenon. The variables are called "regionalized variables", because they are related to their location in the field.

3.7.2.1 Instrument for modelling the structure of data

The value assumes by the regionalized variable in a point dependent of the value measured in another location. In particular, values measured in neighbouring points are more related than values measured at distant points. This spatial correlation constitutes the structure of the regionalized phenomenon and is analysed by means of the variogram. The inference of the variogram is performed from a series of experimental data. The regionalized variable $z(x)$ is considered as a realization of the random function $Z(x)$. The variogram is written as follows:

$$\hat{\gamma}(h) = \frac{1}{2|N(h)|} \sum_{N(h)} [z(x_\alpha) - z(x_\beta)]^2$$

Equation 3-1

where $N(h) = \{(\alpha, \beta): x_\alpha - x_\beta = h\}$ and $|N(h)|$ number of pair.

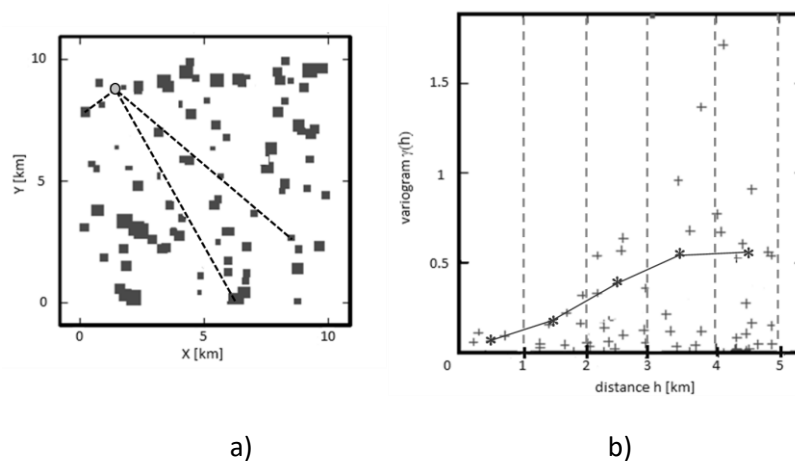


Figure 3-9: Example of experimental variogram calculation. a) map of the location of the measuring points (the dimension of the point indicates the entity of the value of the variable); b) variogram cloud (cross), lag intervals (dashed lines) and experimental variogram (line) (Spacagna and Modoni, 2018)



This project has received funding from the European Union's Horizon 2020 research and innovation programme under grant agreement No. 700748

The calculation of the experimental variogram is based on considering the differences of the regionalized variable values in two different locations, separated by a distance h (Figure 3-9.a). A procedure needs to be implemented as follows:

- plot the squared increments between each couple of measured data as function of the distances (h) between the sampling points (Figure 3.b); the obtained graph is called variogram cloud.
- define a number of intervals with an amplitude (lags, number of lags)
- compute the average values falling within the intervals, defining in this way the experimental variogram (Figure 3-9.b).

In this way, the expected value for a couple of points with a distance each other equal to h can be expressed by the following arithmetic expression:

$$\gamma(h) = \frac{1}{2} E\{[Z(x+h) - Z(x)]^2\} \quad \text{Equation 3-2}$$

The experimental variogram is a discrete series of points, it is not defined for all distances h , and cannot be used directly. Therefore, it becomes necessary to infer a theoretical variogram, as similar as possible to the experimental variogram. This theoretical variogram brings in all the structural features of the regionalised variables describing the phenomenon. This modelling is called structural analysis or variographical analysis, fundamental stage in geostatistics. A bad modelling can produce bad results.

The main characteristic of the variogram are:

- the behaviour at the origin indicates the degree of regularity of regionalization;
- the presence or absence of the sill, remembering that the presence of the sill is symptom of second order stationarity. In this case, the covariance function is deduced from the variogram by the following relationship:

$$\gamma(h) = C(0) - C(h) \quad \text{Equation 3-3}$$

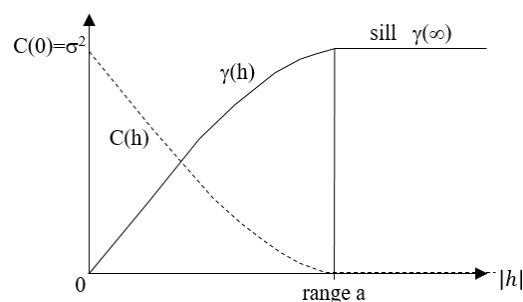


Figure 3-10: Covariance $C(h)$ and Variogram $\gamma(h)$ (Spacagna and Modoni, 2018)



This project has received funding from the European Union's Horizon 2020 research and innovation programme under grant agreement No. 700748

The variogram $\gamma(h)$ describes the link between two values of the variable measured at a distance equal to h . In general, the difference grows with h , indicating that the variability increases with distance, until reaching at a certain distance to a limit value $\gamma(\infty)$ called "sill" C . In this case the random function is stationary of order 2, and the sill C and the variance are equal. The distance within which the equal sign occurs is called "range" a (Figure 3-10). Two values $Z(x)$ and $Z(x+h)$ are related if the length of the vector h is less than the distance a . The range translates the notion of "area of influence" of a value. Beyond to a , the variogram assumes a constant value equal to the sill C , and the variables $Z(x)$ and $Z(x+h)$ are no more related (independent).

In the literature, there are several variogram models (Chilès and Delfiner, 1999). Figure 3-11 shows the most common models for regionalized variables studied.

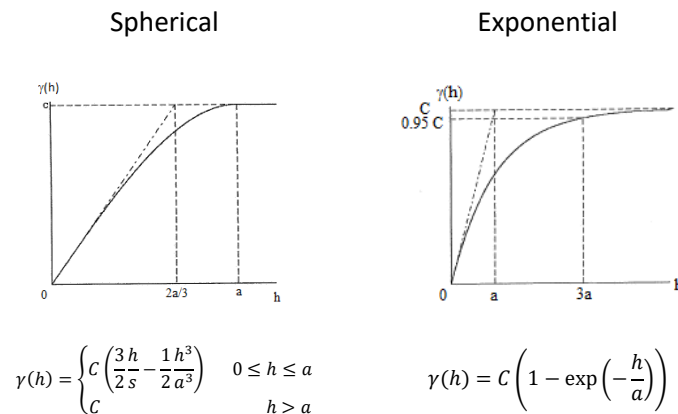


Figure 3-11: Main variogram model

The spherical model is the most common model. The polygonal expression increases to a certain distance after which the value stabilizes. The tangent at the origin intersect the sill C abscissa $2a/3$.

As for the spherical model, the exponential model has a linear behavior for small values of h . The exponential model only asymptotically reaches the sill C . At constant sill, it is observed that the exponential model, compared to the spherical model, growing faster initially but then increase more slowly until you get the same value of C . They are however very similar models. The difference lies in understanding how, how fast it degrades the value within the range of influence.

The nugget effect represents changes in small-scale and / or measurement errors. This discontinuity at the origin derives from the experience in mineralogy (mines gold) and has been proposed by G. Matheron (Matheron, 1965). The nugget effect model translates a phenomenon of absence of correlation between the values of variables even next to each other.

3.7.2.2 Estimation

The Geostatistics method allows to estimate the values from a limited number of points (sampling points), and to quantify the reliability of the estimation. The global estimation covers the entire area where is



This project has received funding from the European Union's Horizon 2020 research and innovation programme under grant agreement No. 700748

Manual for the assessment of liquefaction risk, defining the procedures to create the database, collect, define, symbolize and store information in the Georeferenced Information System and to perform and represent the risk analysis

necessary to characterize the variable, which describe the phenomenon. The value in a non-sampled point is evaluate using a weighted linear combination of the measured values of the sampled points. The weights should take into account the spatial dependence of the data such as the correlations between values of different sites, bases on the variogram model previously defined. The directional analysis of the spatial structure of the data allows to find any anisotropy, highlighting a characteristic of the phenomenon under study.

The linear interpolator use in Geostatistical analysis is called Kriging. This interpolator offers several advantages compared to conventional interpolation techniques. In fact, the kriging consent to:

- estimate without distortion the value of the variable, taking into account the geometrical nature of the data (number and configuration of data) and structural information contained in the variogram;
- appreciate quantitatively the accuracy of the estimation by mean of the estimation variance.

The punctual kriging estimates the value of the variable in each nodes of regular grid. The estimation of the variable Z at the point x_0 is given by the following equation (Chilès and Delfiner, 1999):

$$Z^*(x_0) = \sum_{\alpha=1}^n \lambda_{\alpha} Z(x_{\alpha}) \quad \text{Equation 3-4}$$

The expected value of the error estimation is written:

$$E[Z^*(x_0) - Z(x_0)] = \sum_{\alpha=1}^n \lambda_{\alpha} E[Z^*(x_0)] - E[Z(x_0)] = m \left(\sum_{\alpha=1}^n \lambda_{\alpha} - 1 \right) \quad \text{Equation 3-5}$$

In the case of the punctual ordinary kriging, where m is unknown, to ensure the absence of error distortion is to impose the following condition, called universality condition:

$$\sum_{\alpha=1}^n \lambda_{\alpha} = 1 \quad \text{Equation 3-6}$$

The variance of estimation-error $Var[Z^*(x_0) - Z(x_0)]$ is minimized under the condition of the absence of distortion.

The weights λ_{α} of kriging are evaluated considering:

- the distances between the points to be estimated and observed points;
- the geometric configuration of the observed points;
- the spatial structure of the regionalization described by the variogram γ .



This project has received funding from the European Union's Horizon 2020 research and innovation programme under grant agreement No. 700748

Manual for the assessment of liquefaction risk, defining the procedures to create the database, collect, define, symbolize and store information in the Georeferenced Information System and to perform and represent the risk analysis

The weight and variance estimation do not depend on the values of the data but only on the kriging layout and on the model of the variogram. Therefore, the accuracy of the estimation can be evaluated knowing the configuration of the measuring points, and the variogram model.

The map of the estimated values of generic variable (Figure 3-12 a) should be associated to the map of the standard deviation of the error of the estimation (Figure 3-12 b). In that case it is possible to assess the quality of the estimation, setting a threshold of the standard deviation error of the estimation, for which the estimate no longer has a good quality. The error of the estimation is higher both in areas with a reduced number of sampling data and where nearby points have very different values (outliers).

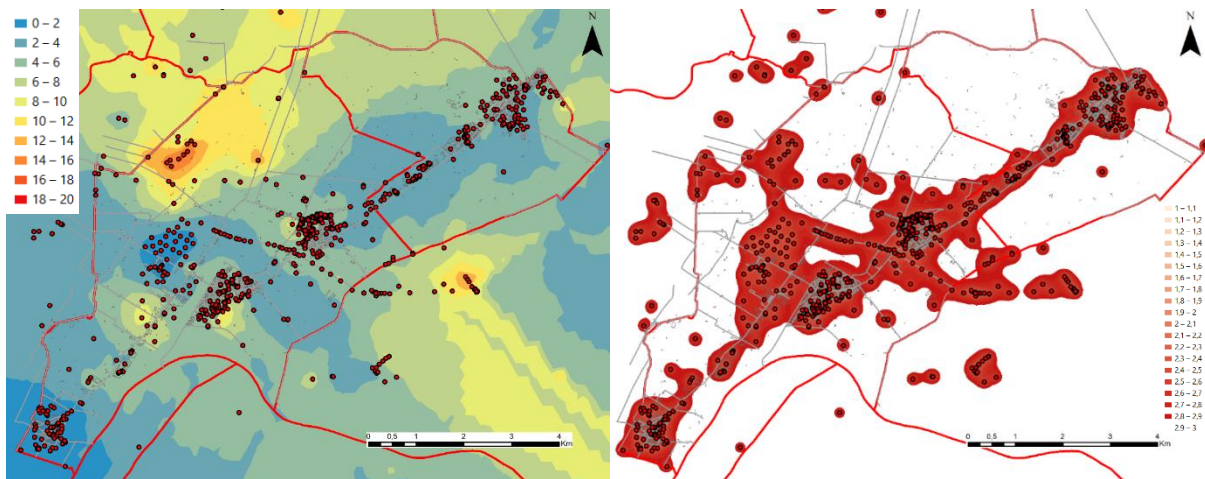


Figure 3-12: Example of geostatistical interpolation a) Map of estimated variable, b) map of standard deviation error of the estimation.

Statistical methods and geostatistical tools allow to identify the presence of outliers in order to improve the structure of the spatial data, the model of the variogram and consequently the quality of the estimation, following the procedure of the Figure 3-13.



This project has received funding from the European Union's Horizon 2020 research and innovation programme under grant agreement No. 700748

Manual for the assessment of liquefaction risk, defining the procedures to create the database, collect, define, symbolize and store information in the Georeferenced Information System and to perform and represent the risk analysis

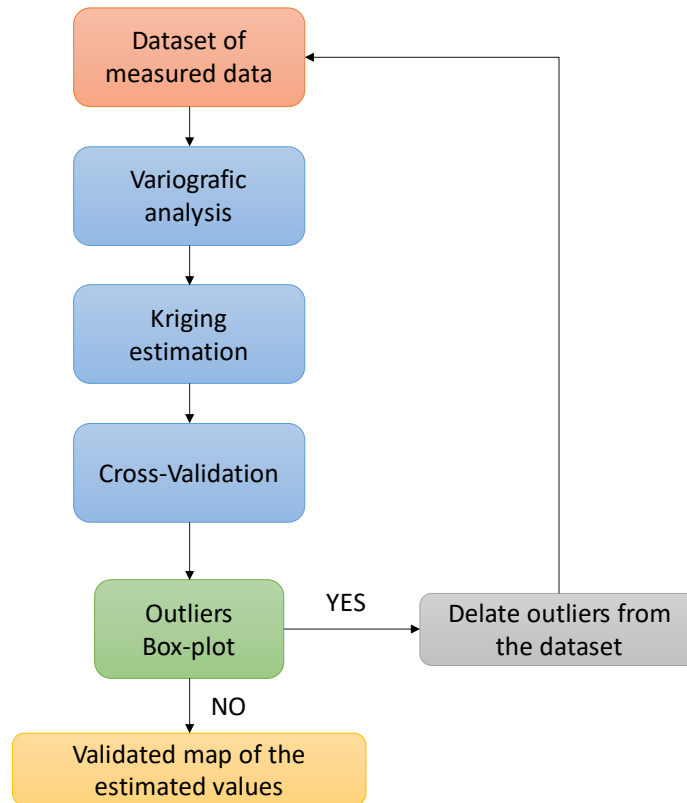


Figure 3-13: Procedure for data filtering

The cross-validation analysis compares the predicted value and the measured value at the same location (Figure 3-14). The error of the estimation is evaluated by mean of the difference between the predicted value and the measured value. Thanks to the box-plot statistical tool (Figure 3-15), it is possible to identify the sampled point with high error of estimation. The Figure 3-14 shows an example of the results of the cross-validation of the estimation performed in the Figure 3-12. The outliers are indicated with red dot. These sampled points are then removed from the dataset and the procedure is repeated, in order to obtain a validated map to the estimated values.



This project has received funding from the European Union's Horizon 2020 research and innovation programme under grant agreement No. 700748

Manual for the assessment of liquefaction risk, defining the procedures to create the database, collect, define, symbolize and store information in the Georeferenced Information System and to perform and represent the risk analysis

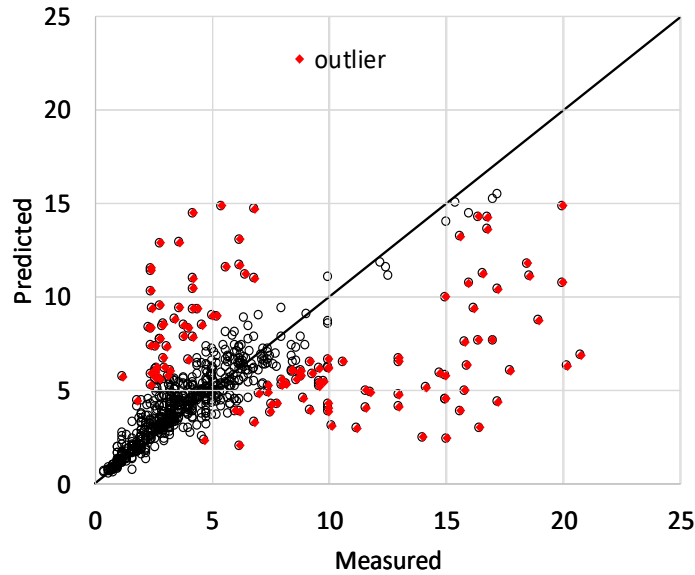


Figure 3-14: Example of cross validation result

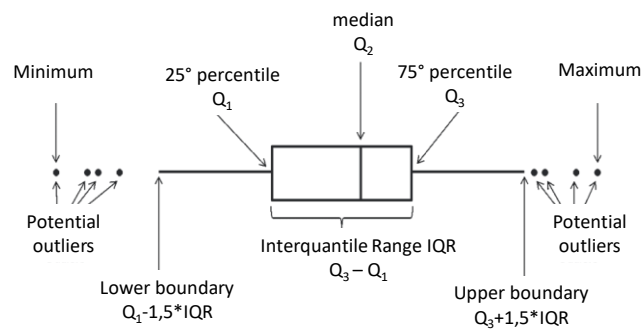


Figure 3-15: Box plot analysis

The Figure 3-16 shows the result of the application of the procedure of data filtering applied on the dataset used to performed the estimation illustrated in Figure 3-12. Setting the same threshold, the map of standard deviation of the error of estimation (Figure 3-16 a) presents lower values. The quality of the estimation is clearly improved according to the results of the cross-validation (Figure 3-16 c).



This project has received funding from the European Union's Horizon 2020 research and innovation programme under grant agreement No. 700748

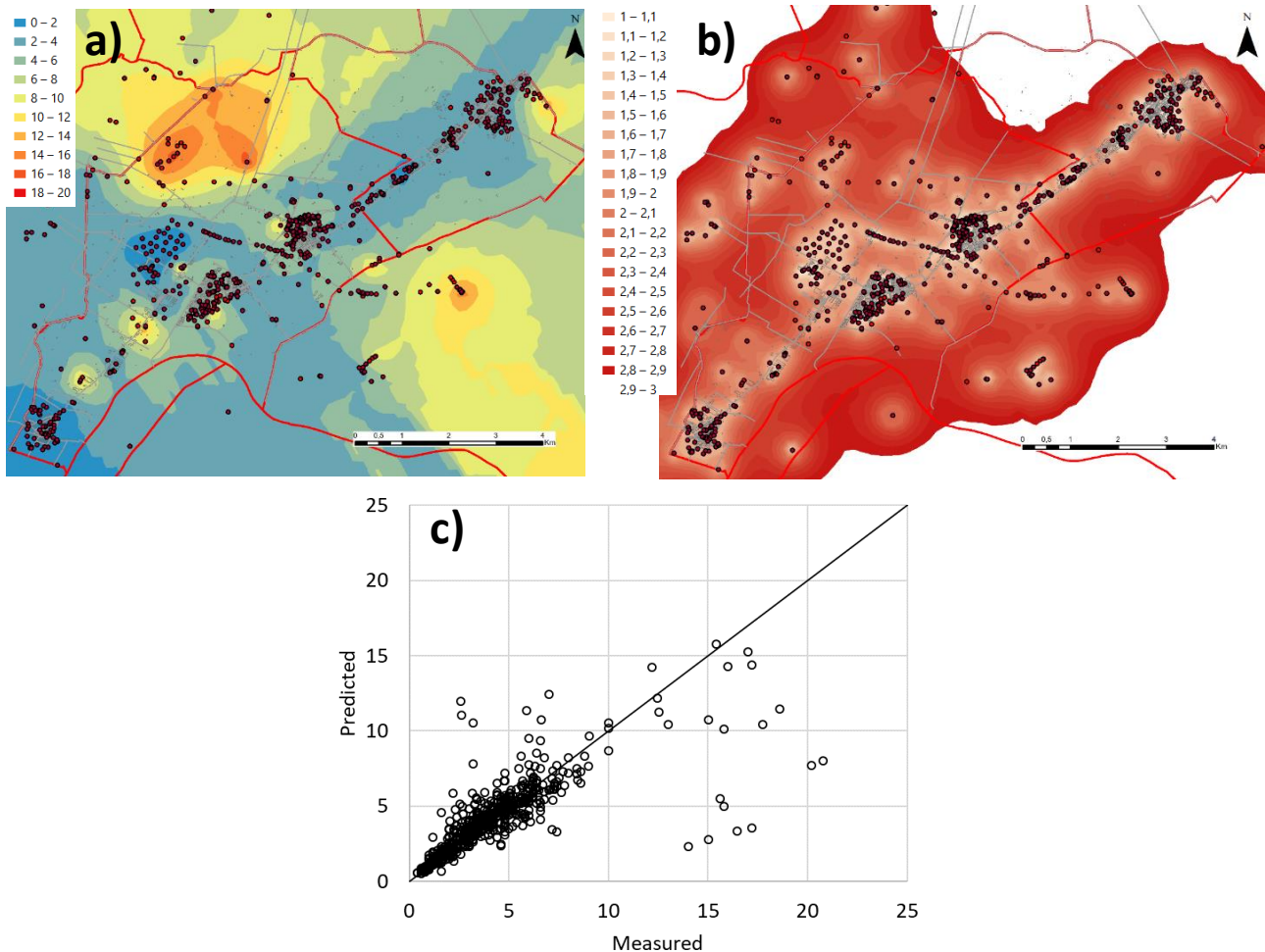


Figure 3-16: Example of geostatistical interpolation after the application of the procedure of filtering data a) Map of estimated variable, b) map of standard deviation error of the estimation c) cross-validation of interpolation.

3.8 Geo-visualization

Geo-visualization refers to a set of tools and techniques supporting the analysis of geospatial data through the use of interactive visualization. In particular, maps represent an efficient tool for communication, analysis, synthesis, and exploration, of geographic data and information (Lawson et al, 2001).

The traditional visualization are static maps with limited exploratory capability. GIS and geo-visualization allow to access to more interactive maps, including the ability to explore different layers of the map, to zoom in or out, and to change the visual appearance of the map, usually on a computer display.

The GIS visualization techniques focus on the presentation of points, lines and polygons (Table 3-16) in static maps, such as, paper-based maps (Figure 3-17).



This project has received funding from the European Union's Horizon 2020 research and innovation programme under grant agreement No. 700748

Manual for the assessment of liquefaction risk, defining the procedures to create the database, collect, define, symbolize and store information in the Georeferenced Information System and to perform and represent the risk analysis

Table 3-16: Patterns for visualization

Pattern	Description
Point	Display the data point, such as the location of in situ test. The shape, the dimension and color of the point give information on the represented element.
Line	Display vectors or lines such as roads, lifelines. The type, the width and the color of the lines give information on the represented element.
Area	Display a polygon such as the administrative boundary or dimension of building. The filling, the color give information on the represented element.

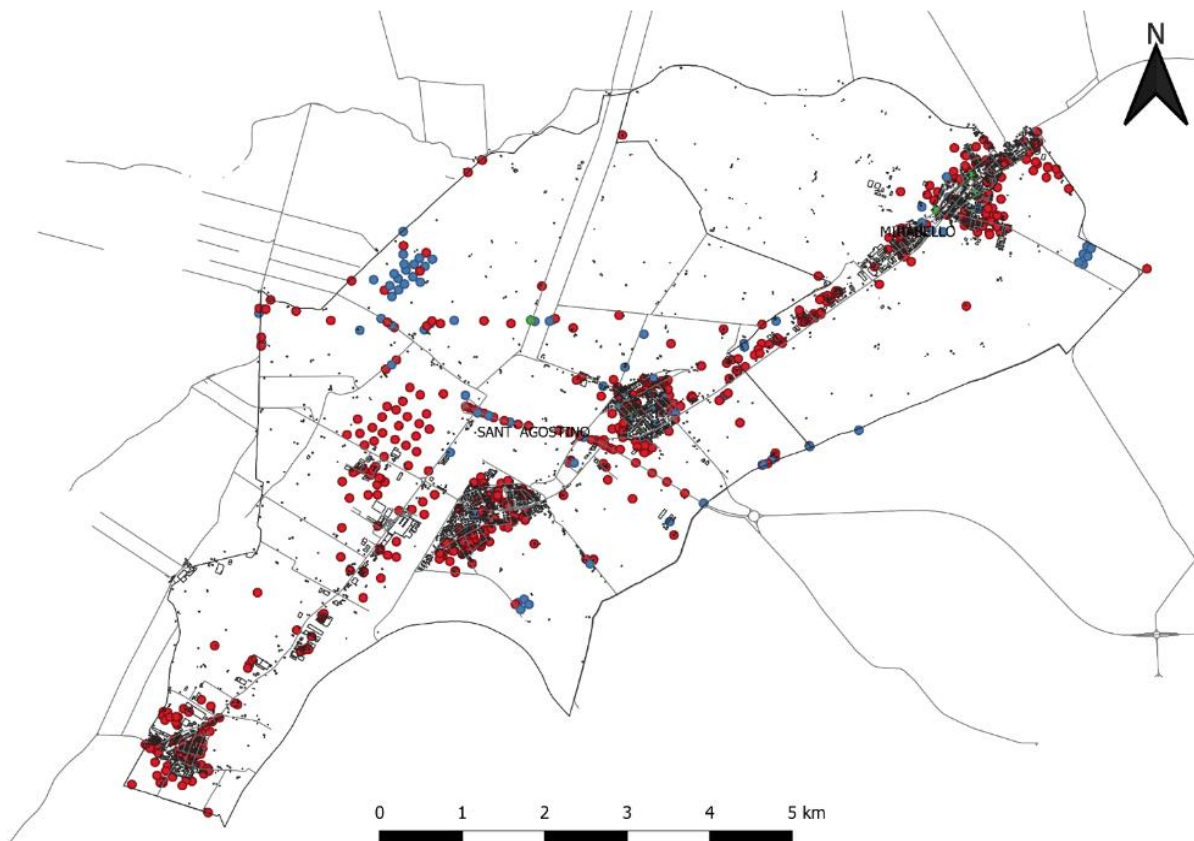


Figure 3-17: Example of map with location of in situ test (points), roads (lines) and buildings (areas).

The choose of the pattern, the color, the size and the class intervals is fundamental aspects for the map presentation. Those aspect have a very impact on the interpretation of the information presented on the map (Yasobant et al., 2015). The INSPIRE Technical Guidelines provide a common implementation for improve the interoperability of spatial datasets, based on existing standards, technologies, and practices.

Moreover, the Geovisualization tools allows to combine different information in three dimensions (Figure 3-18), providing a useful representation for the analysis of complex phenomena, such as risk assessment of natural disaster, considering the strong interaction between the various elements.



This project has received funding from the European Union's Horizon 2020 research and innovation programme under grant agreement No. 700748

Manual for the assessment of liquefaction risk, defining the procedures to create the database, collect, define, symbolize and store information in the Georeferenced Information System and to perform and represent the risk analysis

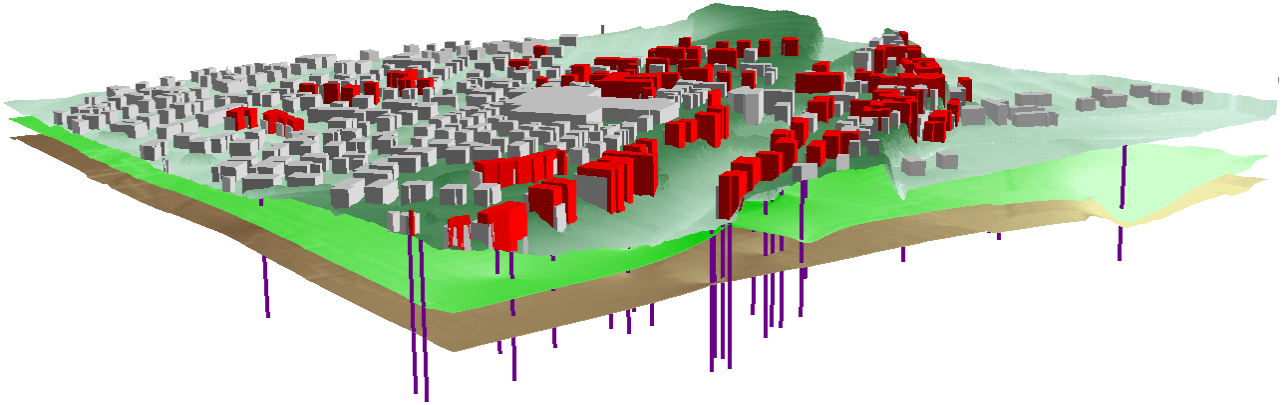


Figure 3-18: Example of 3 D representation of in situ test, soil stratification, ground elevation and buildings of selected area



This project has received funding from the European Union's Horizon 2020 research and innovation programme under grant agreement No. 700748

Manual for the assessment of liquefaction risk, defining the procedures to create the database, collect, define, symbolize and store information in the Georeferenced Information System and to perform and represent the risk analysis

4. HAZARD

4.1 Introduction

The proposed strategy for assessing liquefaction hazard, outlined in the scheme of Figure 4-1, implies a number of analyses to be carried out in a sequence. The first step is to estimate susceptibility of subsoil to liquefaction and this analysis is carried out firstly at the large scale based on geological studies, estimating the tendency of geological formation to undergo liquefaction, then at the local level with geotechnical analyses where the detailed stratigraphy is analyzed. The further step is to estimate the tendency of developing liquefaction under a given seismic input (triggering).

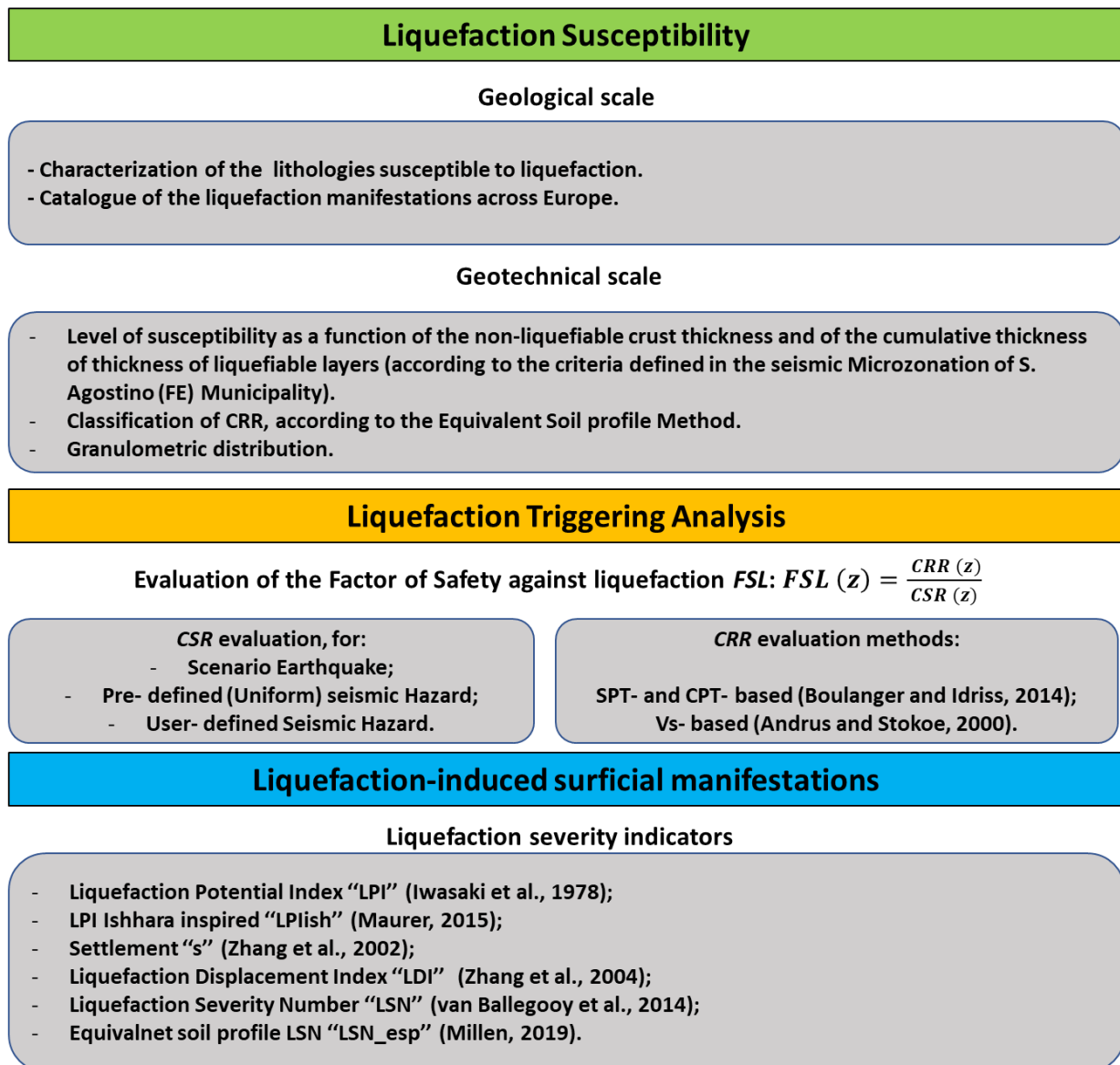


Figure 4-1: Strategy for liquefaction hazard assessment



This project has received funding from the European Union's Horizon 2020 research and innovation programme under grant agreement No. 700748

Manual for the assessment of liquefaction risk, defining the procedures to create the database, collect, define, symbolize and store information in the Georeferenced Information System and to perform and represent the risk analysis

This analysis can be performed with different methods, simplified when based on empirical or sound theoretical relations, or analytical if based on the reproduction of the mechanical phenomena taking place in saturated soil under seismic excitation (e.g numerical).

The last step implies to evaluate the effects at the ground level. At this stage analyses are conducted in free field conditions, neglecting the presence of buildings or infrastructures and their possible interaction with the subsoil, and thus indicators are adopted to broadly quantify the severity of liquefaction.

A possible methodology is described in this chapter showing the different possibilities proposed in the literature or developed in the present project.

4.2 Susceptibility

The initial step of the liquefaction hazard evaluation is to characterize the liquefaction susceptibility based on the soil/geologic conditions of a region or subregion. No specific information on the earthquake is required at this level.

Past studies (Youd & Perkins, 1978; Galli & Meloni, 1993) and ground observations after recent seismic events, as the M_w 6.1 Emilia – Romagna (Italy) 2012, Christchurch (New Zealand) 2010-11 and 2017, M_w 9.0 Tohoku (Japan) 2011 Earthquakes, have shown that liquefaction-induced phenomena are not randomly localized, but are tightly related to the geology of the territory. For this reason, geologic maps and direct survey provide an useful basis for depicting the liquefaction susceptibility. A distinction must be done between methods operating at the continental or regional scale. Such tools are usually employed as guidance for more detailed studies.

4.2.1 Geological Liquefaction Susceptibility

4.2.1.1 Macrozonation Scale

For a considered subsoil type, the distribution of saturated cohesionless sediments in the deposit and the likelihood to liquefy is related to the age of the deposit by Youd and Perkins (1978). These authors rated the the liquefaction susceptibility of geologic units, from very low to very high, as shown in Table 4-1. These criteria can be used to further develop qualitative maps of liquefaction potential referred to entire regions.

Soils susceptible to liquefaction consist substantially of saturated uniform grain size distributions deposited in loose states, having nil to low plasticity and low to moderate permeability. Under a strong enough seismic shaking, these soils can be prone to liquefy. On the other hand, liquefaction resistance increases with the soil aging (Schmertman, 1991).

Available data to assess liquefaction susceptibility at the continental scale include: Quaternary Geology, Hydrogeological Maps and Digital Elevation Model (DEM) of the selected area. This study of liquefaction susceptibility, even if often accomplished in a qualitative way, is sometimes used as a preliminary risk response in catastrophe models.



This project has received funding from the European Union's Horizon 2020 research and innovation programme under grant agreement No. 700748

Manual for the assessment of liquefaction risk, defining the procedures to create the database, collect, define, symbolize and store information in the Georeferenced Information System and to perform and represent the risk analysis

Table 4-1: Liquefaction susceptibility of sedimentary deposits (from Youd and Perkins, 1978)

Type of deposit	General distribution of cohesionless sediments in deposits	Likelihood that cohesionless sediments when saturated would be susceptible to liquefaction (by age of deposit)			
		< 500 yr Modern	Holocene < 11 ka	Pleistocene 11 ka - 2 Ma	Pre-Pleistocene >2Ma
(a) Continental Deposits					
River channel	Locally variable	Very High	High	Low	Very Low
Flood plain	Locally variable	High	Moderate	Low	Very Low
Alluvial fan and plain	Widespread	Moderate	Low	Low	Very Low
Marine terraces and plains	Widespread	--	Low	Very Low	Very Low
Delta and fan-delta	Widespread	High	Moderate	Low	Very Low
Lacustrine and playa	Variable	High	Moderate	Low	Very Low
Colluvium	Variable	High	Moderate	Low	Very Low
Talus	Widespread	Low	Low	Very Low	Very Low
Dunes	Widespread	High	Moderate	Low	Very Low
Loess	Variable	High	High	High	Unknown
Glacial till	Variable	Low	Low	Very Low	Very Low
Tuff	Rare	Low	Low	Very Low	Very Low
Tephra	Widespread	High	High	--	--
Residual soils	Rare	Low	Low	Very Low	Very Low
Sebkha	Locally variable	High	Moderate	Low	Very Low
(b) Coastal Zone					
Delta	Widespread	Very High	High	Low	Very Low
Estuarine	Locally variable	High	Moderate	Low	Very Low
Beach					
High Wave Energy	Widespread	Moderate	Low	Very Low	Very Low
Low Wave Energy	Widespread	High	Moderate	Low	Very Low
Lagoonal	Locally variable	High	Moderate	Low	Very Low
Fore shore	Locally variable	High	Moderate	Low	Very Low
(c) Artificial					
Uncompacted Fill	Variable	Very High	--	--	--
Compacted Fill	Variable	Low	--	--	--

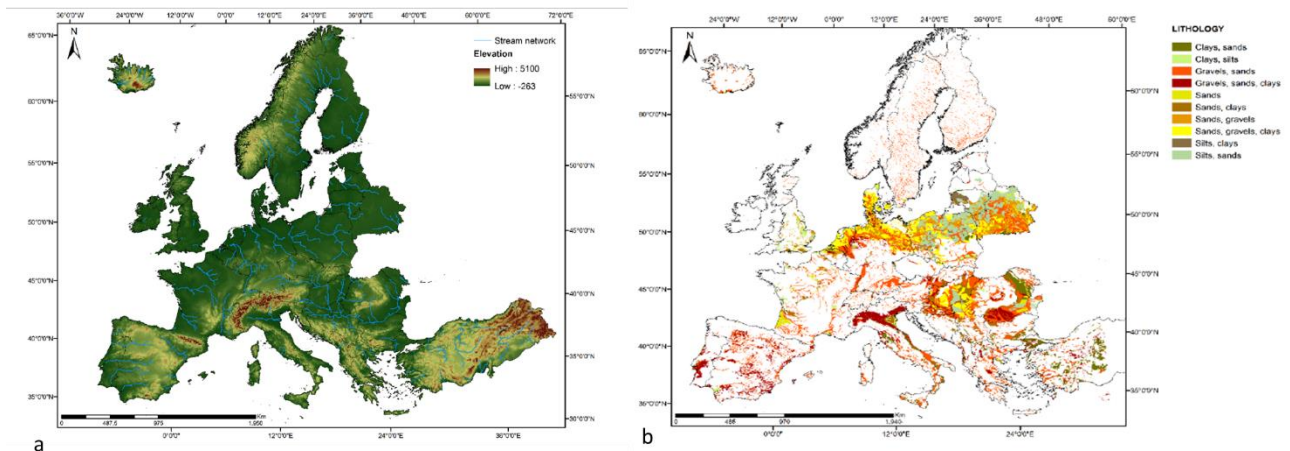


Figure 4-2: a) Stream network derived from Shuttle Radar Topography Mission Digital Elevation Model (SRTM DEM) of European area; b) Lithologies susceptible to liquefaction for the European territory are showed in the Map.



This project has received funding from the European Union's Horizon 2020 research and innovation programme under grant agreement No. 700748

Manual for the assessment of liquefaction risk, defining the procedures to create the database, collect, define, symbolize and store information in the Georeferenced Information System and to perform and represent the risk analysis

Combining the geological and hydrogeological information, a map of the potentially liquefiable lithologies for the European territory can be obtained (Figure 4-2). Such a map shows the spatial distribution of potentially liquefiable lithologies. As can be seen, susceptible subsoil typologies are widely distributed over the continent (Iberian Peninsula, Italy, Balkan region, Greece, Turkey, but also in the Baltic area. Obviously, this result does not imply the occurrence of liquefaction, being the phenomenon dictated by the seismicity of the area.

Among the activities of WP2, an interesting outcome is the creation of the GIS-based catalogue of European manifestations of seismic liquefaction, obtained by collecting all the recorded liquefaction manifestation after the historical earthquakes in Europe. It also includes the main seismological features of the seismic events: date, location, depth, macro-seismic intensity (MCS scale), magnitude. Concerning sites where liquefaction occurred, location, epicentral and hypocentral distances, macro-seismic intensity and type of liquefaction observations (according to Galli, 2000) were stored in such database.

At present this catalogue includes approximately a thousand liquefaction manifestations, mostly located in the Mediterranean area, due to earthquakes of moderate magnitude (M_w ranging from 6 to 6.5).

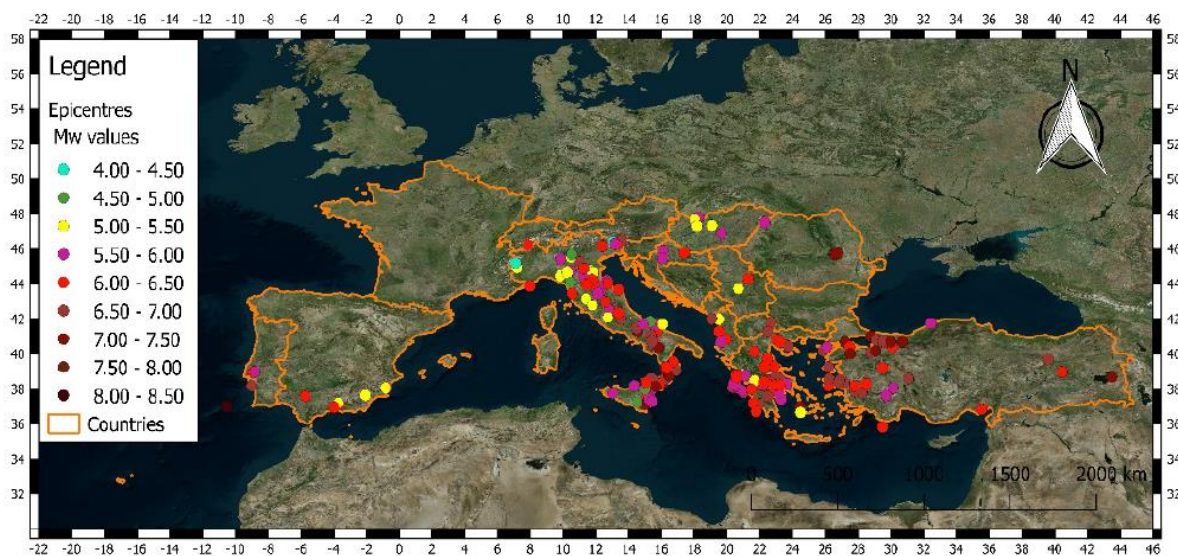


Figure 4-3: Distribution of liquefaction manifestations included in the catalogue across Europe. The colour of the circles is proportional to the event moment magnitude

4.2.2 Liquefaction Susceptibility on the Microzonation Scale

Within the Italian “Guidelines for Seismic Microzonation” (GSM, 2008; Gruppo di Lavoro MS, 2008; English version: SM Working Group, 2015), seismic microzonation (SM) is defined as “the assessment of local seismic hazards by identifying the zones of a given geographic area with homogeneous seismic behaviour”. The strategy outlined in this document identifies three subsequent levels for the seismic microzonation, characterised by an increasing detail of investigation and analysis. SM identifies and characterises the zones in a specified context (a region, city or district) as stable, stable but prone to develop local amplification and prone to instability”.



This project has received funding from the European Union's Horizon 2020 research and innovation programme under grant agreement No. 700748

Manual for the assessment of liquefaction risk, defining the procedures to create the database, collect, define, symbolize and store information in the Georeferenced Information System and to perform and represent the risk analysis

Subsequently a specific document has been produced with regard to liquefaction. The document entitled “LAND USE GUIDELINES FOR AREAS AFFECTED BY LIQUEFACTION (LQ), version I.0” (Technical Commission on Seismic Microzonation, 2018) represents a modification and integration of the “Guidelines for Seismic Microzonation” prepared accounting for the experience of the Emilia-Romagna earthquake that struck in 2012 the area of Po Valley and Reggio Emilia and to incorporate the studies produced in its wake. The primary objective of these guidelines is the definition of general criteria and operative procedures, in coordination with State, Regional and Local Entities, to:

- gather accurate information about the risks induced by the presence of soils susceptible to liquefaction;
- manage risk in undeveloped areas (with or with no plans for development);
- mitigate risk in developed areas.

Regarding the data that can be used for this purpose, the GSM (2008) states that the Map of Seismically Homogenous Microzones (SHM Map) can be prepared at the Level 1 of the study using pre-existing information when sufficient. In the majority of cases, the “minimum informative elements” (this is how pre-existing information are defined) consists of basic data such as the description of lithological units based on visual inspections, water table levels surveyed during perforations, etc. For this reason, the susceptibility to liquefaction in Level 1 SHM Maps is estimated based on immediately available information – gathered in situ – or present in literature or public databases.

On the contrary the level 3 Map of Seismic Microzonation requires the accomplishment of specific investigations and in-depth studies necessary to define soil characteristics. These Guidelines state that methods for data processing must be based on available technical-normative documentation (NTC - Italian National Building Code, 2018 and AGI - Guidelines of Italian Geotechnical Association, 2005) and scientific documentation, while the verification of innovative methodologies must be of proven validity.

The diagram represented in Figure 4-4 is applicable to all possible seismic instabilities (landslides, liquefactions, active and capable faults and differential settlements). It summarises the activities, expected results and type of zone susceptible to instability at the different levels of study of seismic microzonation. Also worth of mention is the opportunity of standardising the identification, significance and denomination of zones susceptible to instability that, as the diagram shows, are of three types:

- Attention Zones (AZ) in SHM Map studies;
- Susceptibility Zones (SZ) in SM Map studies;
- Respect Zones (RZ) in SM Map studies.



This project has received funding from the European Union's Horizon 2020 research and innovation programme under grant agreement No. 700748

Manual for the assessment of liquefaction risk, defining the procedures to create the database, collect, define, symbolize and store information in the Georeferenced Information System and to perform and represent the risk analysis

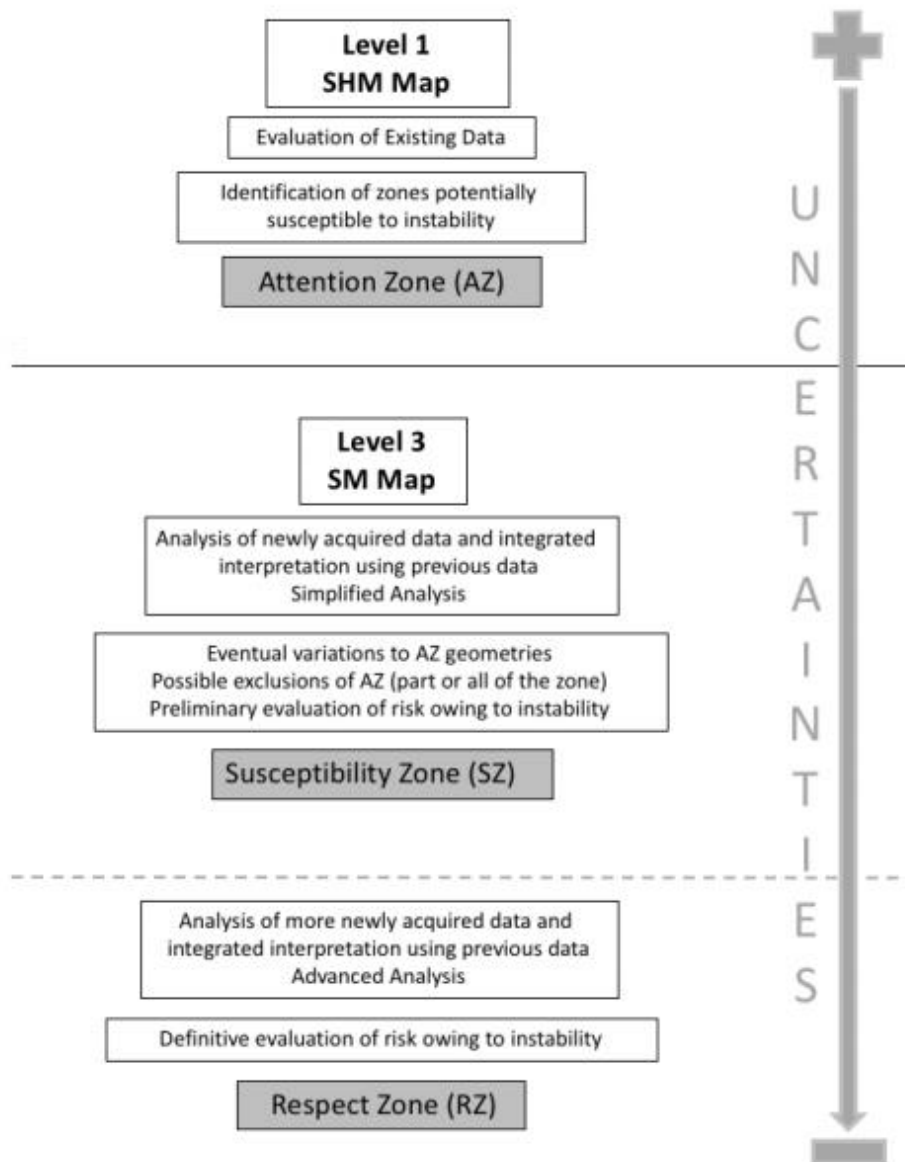


Figure 4-4: Illustrative diagram of instability zone types in SHM Maps and SM Maps. Data gathering and analyses permit a reduction in uncertainties from Level 1 to Level 3 (Technical Commission on Seismic Microzonation, Land Use Guidelines for Areas Affected by Liquefaction (LQ), version 1.0, Rome, 2018.).

Among the activities of Task 2.6 of this project there is the “Validation of the European Liquefaction Hazard Map by detailed analysis at the four testing areas”. For this scope a microzonation procedure which its first step is the characterization of a geological and geotechnical model (Figure 4-5, Figure 4-6), has been defined and applied in WP2 for the Cavezzo municipality (Emilia-Romagna).



This project has received funding from the European Union's Horizon 2020 research and innovation programme under grant agreement No. 700748

Manual for the assessment of liquefaction risk, defining the procedures to create the database, collect, define, symbolize and store information in the Georeferenced Information System and to perform and represent the risk analysis

Identification of source layers for liquefaction

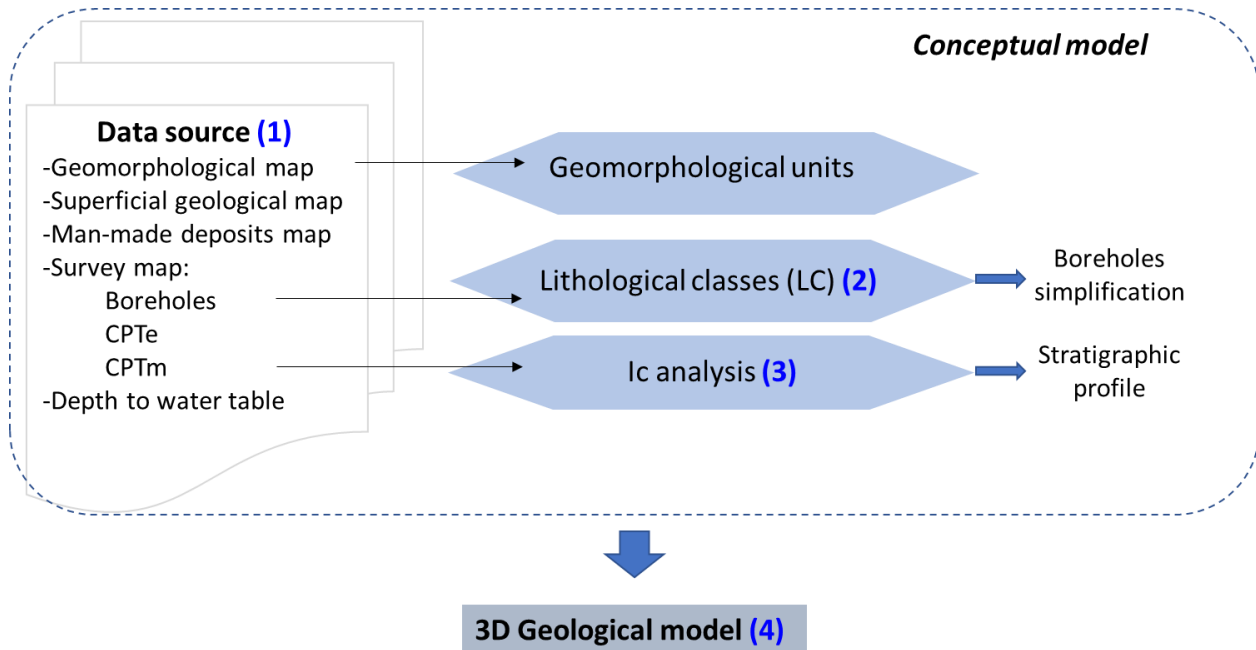


Figure 4-5: Scheme of the procedure to identify layers prone to liquefaction, as defined in WP2 (Task 2.6)

The geological and geotechnical model is aimed at the identification of source layers for liquefaction as much as the definition of zones having homogeneous stratigraphy. Geomorphological and surface geological Maps describe the geomorphology of the area, highlighting the presence of sandy and silty lithologies and of relevant geomorphological elements, such as rivers, levees/paleo-levees and paleochannels. On the other hand, information about the land use, thickness of man-made deposits and the existing survey maps are required to understand the urban development of the study area and to reconstruct the subsoil profiles.

To evaluate the local site effects on ground motion and to assess the liquefaction potential for a given area, a geotechnical model must be defined on the basis of: topography (DEM, DTM), monitoring activities (piezometers, wells), in-situ geotechnical (e.g. Boreholes, SPT, CPT) and geophysical investigations (SASW, MASW, Cross-hole, Down-Hole, Micro-tremors...) and laboratory tests.

In areas where microzonation for liquefaction susceptibility is performed, a convenient number of representative geotechnical vertical profiles should be individuated. The choice of the profiles will depend on the lateral discontinuities and variation of the soil types and their properties, and on the lateral variability of the surface topography. Particular attention should be taken during this phase to be sure whether one-dimensional models are adequate or, instead, two/three-dimensional models should be adopted. In fact, two-dimensional geotechnical models are recommended in valleys and basins where a significant amplification must be expected due to topographical effects.



This project has received funding from the European Union's Horizon 2020 research and innovation programme under grant agreement No. 700748

Manual for the assessment of liquefaction risk, defining the procedures to create the database, collect, define, symbolize and store information in the Georeferenced Information System and to perform and represent the risk analysis

Since liquefaction occurs in loose saturated sandy deposits, a detailed study on the hydrogeology is needed. In particular, the fluctuation over an entire year of the groundwater level should be investigated with in-situ tests performed in different periods (Figure 4-5).

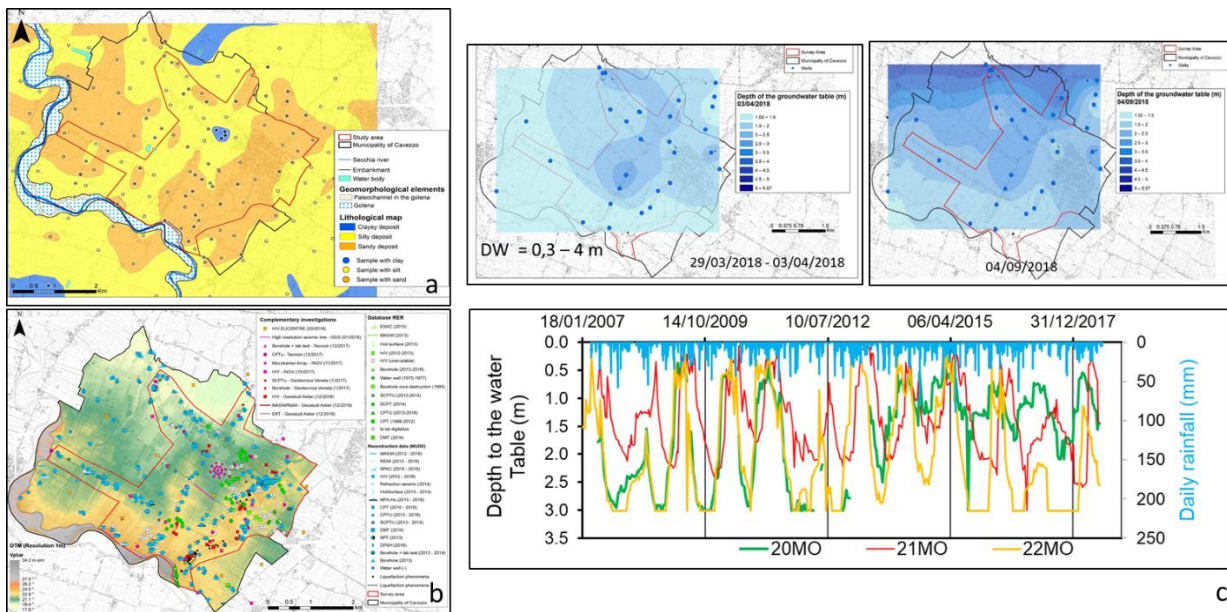


Figure 4-6: Example of main data source to define the geological and geotechnical model, according to the microzonation procedure (WP2); a,b) Superficial geological and surveys map of Mirabello district, c) a campaign of measures and the freatic level fluctuation analysis allowed to identify the position of water table in different seasons

4.2.2.1 Liquefaction susceptibility levels

To quantify liquefaction susceptibility at the geotechnical level, the criteria defined by the University of Ferrara (2014) for the seismic microzonation of S. Agostino (FE), can also be applied. This criterion is based on the evaluation of a non-liquefiable crust thickness (CT) and of a cumulative thickness of liquefiable layers (CTL). As a function of these two parameters (CT and CTL), a level of liquefaction susceptibility can be defined for the soil profile as defined in Table 4-2. Such level of susceptibility is proportional to the thickness of the liquefiable layer and inversely proportional to his depth. Thickness and depth of potentially liquefiable layers can be evaluated from in-situ tests (boreholes and CPT).



This project has received funding from the European Union's Horizon 2020 research and innovation programme under grant agreement No. 700748

Manual for the assessment of liquefaction risk, defining the procedures to create the database, collect, define, symbolize and store information in the Georeferenced Information System and to perform and represent the risk analysis

Table 4-2: Punctual level of liquefaction susceptibility (“CMS” - University of Ferrara, 2014).

Crust Thickness (m)	Thickness of liquefiable layer (m)	Susceptibility level
< 5	> 0.4	L1
5-10	>1	L2
10-15	>2	L3
15-20	≥2	L4
≥ 20	0	N

4.2.2.2 Borehole – based method to assess the liquefaction susceptibility

The term borehole indicates a continuous or a core destruction drill in the soil (ASTM, 2011). The former is aiming at characterizing the stratigraphy of a profile, as well as to take samples for laboratory investigation; logs appropriately divided into segments and stored in boxes in order to carry out identification and other possible mechanical (Figure 4-7).

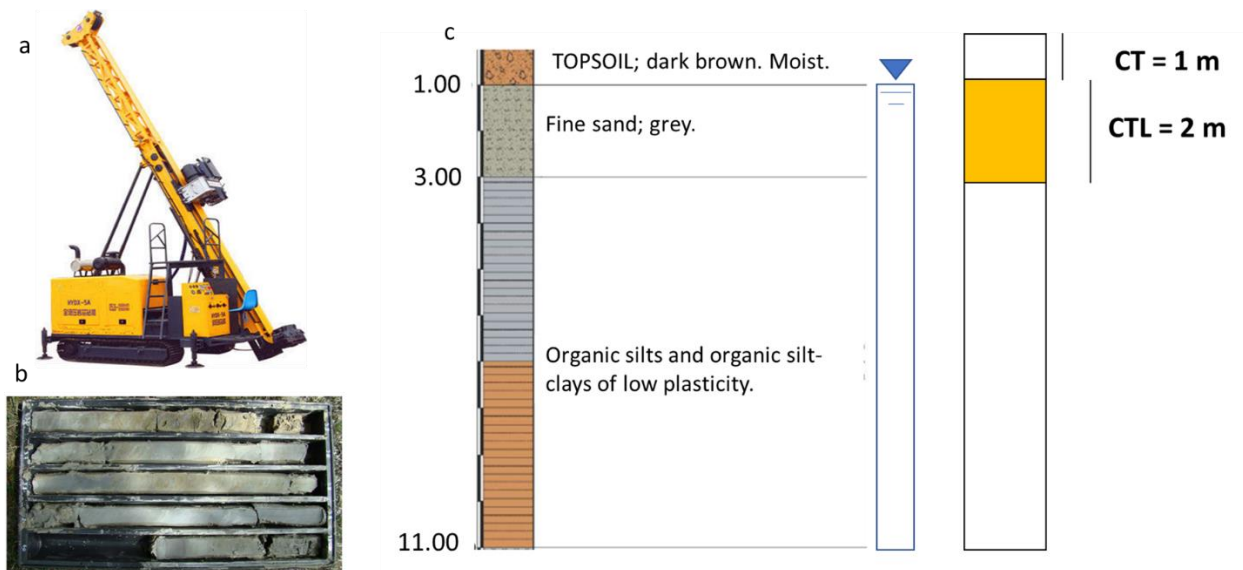


Figure 4-7: a) Example of instrument to carry out a probing hole; b) the obtained carrots are stored in a box to define the stratigraphy. c) Common report of a borehole stratigraphy; depending on the groundwater level and the soil characteristics, the crust thickness and the cumuklative thickness of saturated sandy layer are indicated.

Simultaneously with a borehole, Standard Penetration Tests “SPT” can be also carried out (ASTM, 2011a,b). Despite a continuous effort to standardize SPT procedure and equipment, there are still problems associated with its repeatability and reliability. However, SPT are very popular because many considerable studies (Meyerhof, 1956; Palmer and Stuart, 1957; Yoshida and Kokusho, 1989; Cubrinovski and Ishihara, 2002) and empirical correlations between N_{SPT} and soils properties (D_r , friction angle, V_s) exist.

4.2.2.3 CPT – Based method to assess the liquefaction Susceptibility

The Cone Penetration Test (CPT) and its enhanced versions such as the piezocone (CPTu) and seismic (SCPT), have extensive applications in a wide range of soils. One of their major applications (Robertson, 2015) is for



This project has received funding from the European Union's Horizon 2020 research and innovation programme under grant agreement No. 700748

Manual for the assessment of liquefaction risk, defining the procedures to create the database, collect, define, symbolize and store information in the Georeferenced Information System and to perform and represent the risk analysis

soil profiling and soil type. The CPT cannot provide accurate predictions of soil type based on physical characteristics, such as, grain size distribution but they provide a guide to the mechanical characteristics (strength, stiffness, compressibility) of the soil. However, interpretation criteria exist (e.g. Robertson & Wride, 1998) of CPT data that provide a repeatable index of the aggregate behaviour. Hence, prediction of soil type based on CPT is referred to as Soil Behaviour Type (SBT), obtained through the index I_c defined by Robertson (1990). One of the most known procedures to evaluate the Soil Behaviour Type index from a CPT profile is summarised in Figure 4-8.

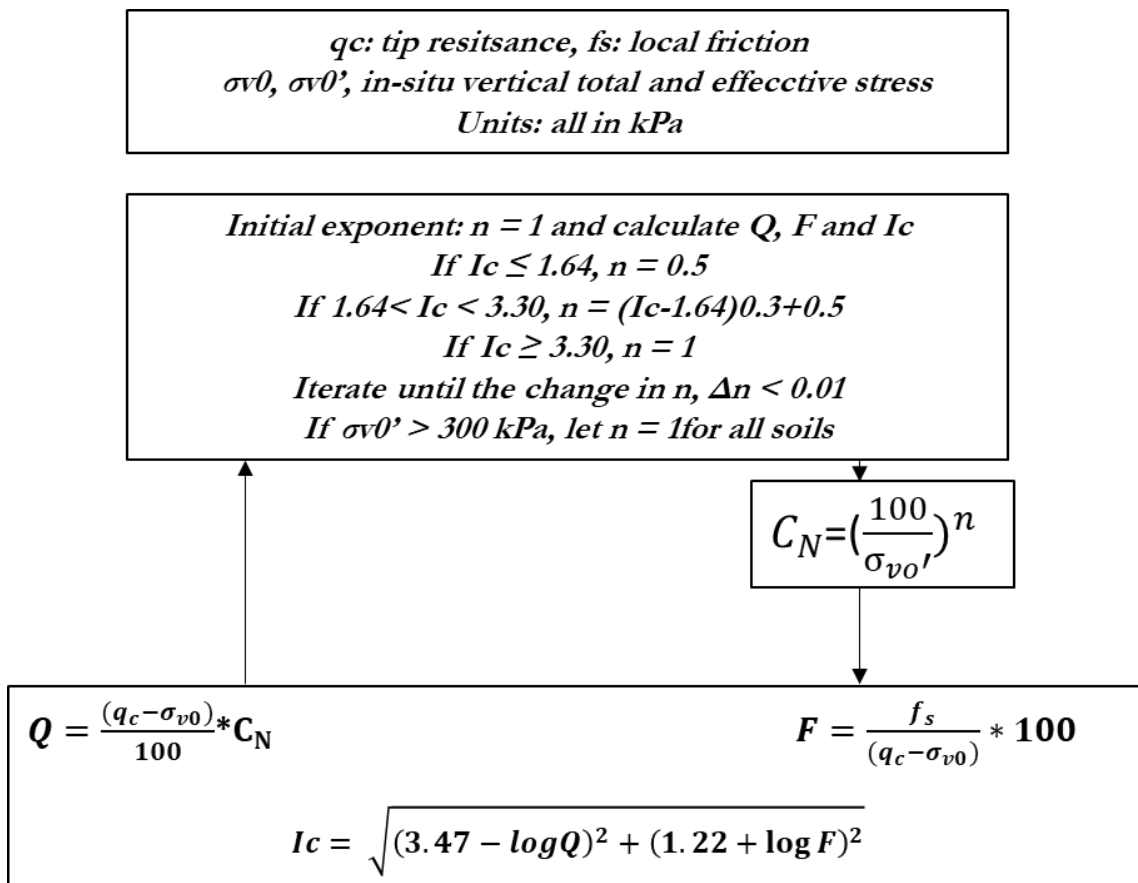


Figure 4-8: Schematic flowchart to evaluate the Soil Behavior Type index (Robertson, 1998).



This project has received funding from the European Union's Horizon 2020 research and innovation programme under grant agreement No. 700748

Manual for the assessment of liquefaction risk, defining the procedures to create the database, collect, define, symbolize and store information in the Georeferenced Information System and to perform and represent the risk analysis

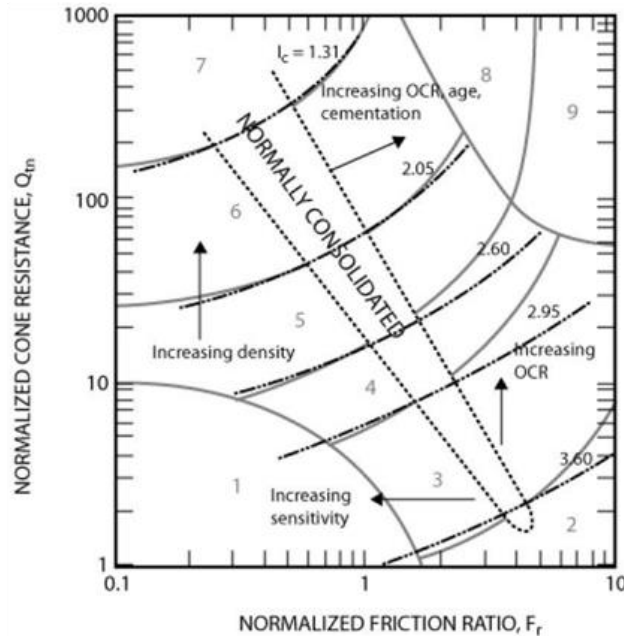


Figure 4-9: Normalized CPT Soil Behavior Type (SBTn) chart, $Q_t - F_r$; (Robertson, 1990)

Table 4-3: Soil behaviour type index ranges and inferred soil types (Robertson & Wride 1998).

Zone	Soil Behaviour Type	I_c
1	Sensitive, fine grained	N/A
2	Organic soils – clay	> 3.6
3	Clays – silty clay to clay	2.95 – 3.6
4	Silt mixtures – clayey silt to silty clay	2.60 – 2.95
5	Sand mixtures – silty sand to sandy silt	2.05 – 2.6
6	Sands – clean sand to silty sand	1.31 – 2.05
7	Gravelly sand to dense sand	< 1.31
8	Very stiff sand to clayey sand	N/A
9	Very stiff, fine grained	N/A

To assess the liquefaction susceptibility, Robertson and Wride (1998) propose a default cut-off of the soil behaviour type index (I_c) equal to 2.6. Beyond this value, the soil can be assumed as non-liquefiable (i.e. not susceptible to liquefaction) being too fine-grained (Liquefiable soils belong to classes 5 and >5 in Figure 4-9). Although this cut-off criterion is generally accepted, it is also acknowledged that soils with $I_c > 2.6$ may undergo liquefaction under certain circumstances.

Robertson and Wride (1998) define a procedure to obtain the I_c profile relating the tip resistance and the sleeve friction to the in-situ tensional state. Accounting also for the groundwater level, the non-liquefiable crust thickness and the cumulative thickness of the potentially liquefiable layers can be evaluated exclusively depending on the lithology (Figure 4-10).



This project has received funding from the European Union's Horizon 2020 research and innovation programme under grant agreement No. 700748

Manual for the assessment of liquefaction risk, defining the procedures to create the database, collect, define, symbolize and store information in the Georeferenced Information System and to perform and represent the risk analysis

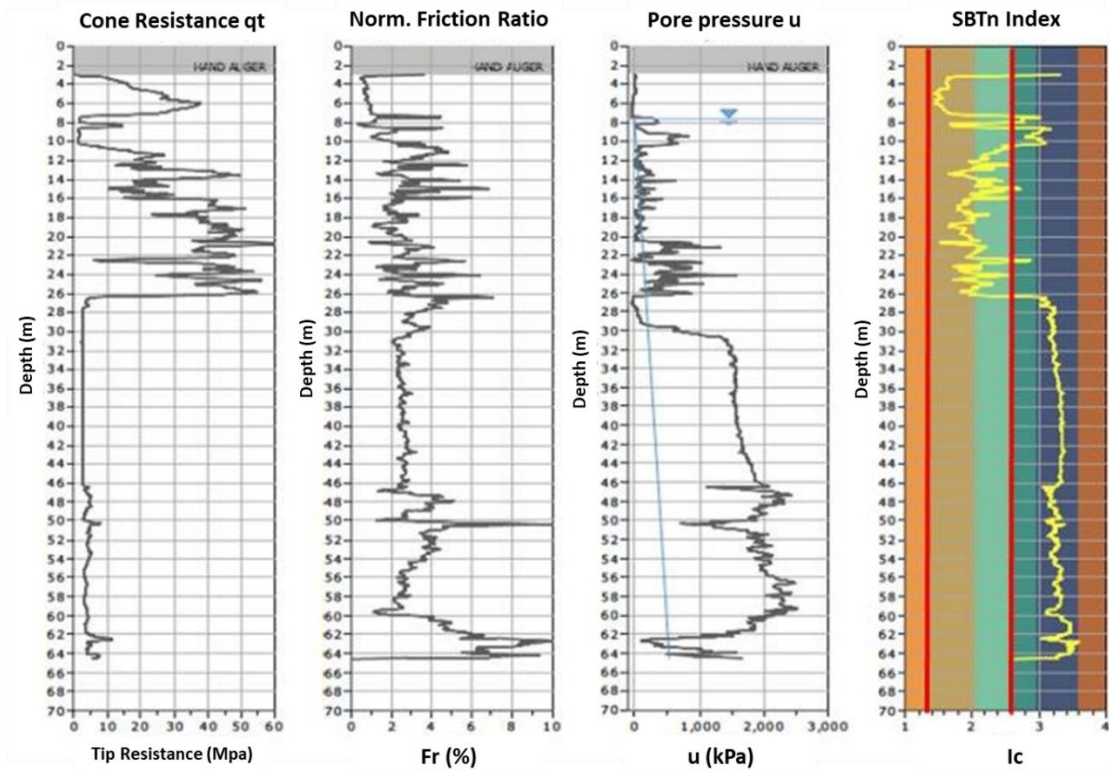


Figure 4-10: Example of q_c , f_s/q_c (%) and pore pressure measures and soil behavior type characterization from CPT.

4.2.2.3.1 Possible corrections of CPT profiles

Even if the application of the electrical Cone Penetration Test (CPTe) and its enhanced versions such as the piezocone (CPTu) and seismic (SCPT), has increased in recent years, many existing databases still include data from mechanical CPTs (CPTm). Considering the amount of data from CPTm and the importance of such databases and also considering that the most common simplified procedures (e.g. Boulanger & Idriss, 2014) are based on electrical CPTs, it is important to identify how critical is the application of these methods to CPTm. The main differences between CPTe and CPTm include:

- Different geometry of the tip, in the application of stab strength and acquiring the information;
- The different size of the investigated soil volume (CPTm measures are spaced 20 cm, while CPTe 2 cm);
- A possible uncontrolled inclination from the initial vertical position for the CPTm.

Based on data from 44 couples of mechanical and electrical CPT profiles performed 1-3 m far each other, Madiat et al. (2016) proposed a procedure to calibrate the results obtained from CPTm and use them for the evaluation of Liquefaction Potential. Based on the analysis of more than 4000 couple of points measured to the same depth, the authors propose to correct the normalized tip resistance ($q_{c1n,cs}$) and the Soil Behaviour Type index I_c as shown in Figure 4-11.



This project has received funding from the European Union's Horizon 2020 research and innovation programme under grant agreement No. 700748

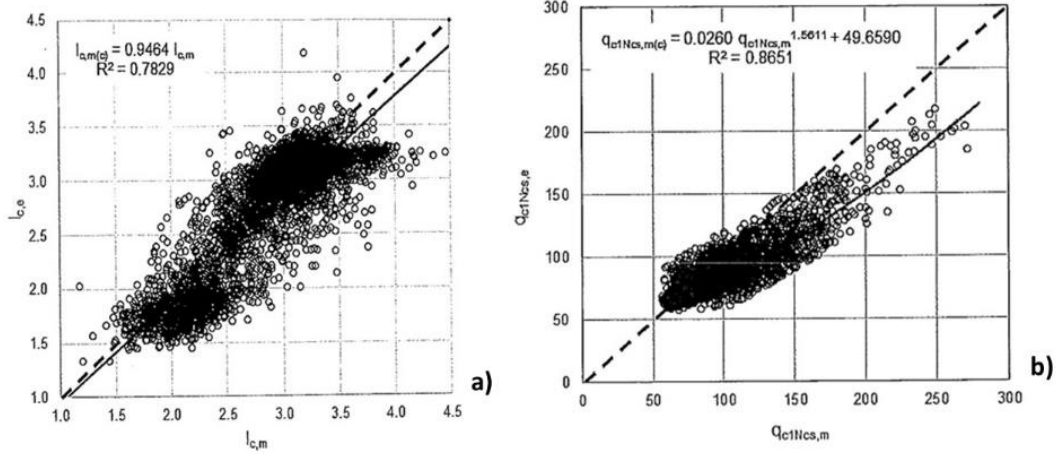


Figure 4-11: a) $I_{c,m}$ values calculated from CPTm and CPTe data and best regression model adapted to mechanical CPT data; b) $qc_{1n,cs}$ values calculated from CPTm and CPTe data by following the procedure of Boulanger & Idriss (2014) and best regression models.

Additionally, the comparison between boreholes and CPT profiles sometimes shows that strata having Soil Behaviour Type index (I_c) slightly higher than 2.6 can be more properly considered as liquefiable.

An example is shown for instance in WP2 for Cavezzo Municipality. Here, a set of boreholes with grain size curves was available. Then a specific - empirical calibration of I_c vs borehole evidence (Lo Presti et al., 2016) was used to correlate the I_c range and the Soil Behaviour Type to the Soil classification (AGI, 1994) which also accounts for the fine content. Then, after interpretations of I_c (Robertson, 2009) obtained from CPTU were compared to borehole stratigraphy, the following relationships were introduced to correct I_c :

$$\Delta I_{c(qt)} = 0.59 * qt^{0.35}$$

Equation 4-1

If $qt \leq 2 \text{ MPa}$

$$I_{c_{corr}}(CPTu) = I_{c(CPTu)} - \Delta I_{c_{error}}$$

If $qt > 2 \text{ MPa}$

$$I_{c_{corr}}(CPTu) = I_{c(CPTu)}$$

If $I_c > 3.5$

$$I_{c_{corr}}(CPTu) = I_{c(CPTu)}$$

It is implicit that the above correction should be derived from case to case and not generalised.



This project has received funding from the European Union's Horizon 2020 research and innovation programme under grant agreement No. 700748

Manual for the assessment of liquefaction risk, defining the procedures to create the database, collect, define, symbolize and store information in the Georeferenced Information System and to perform and represent the risk analysis

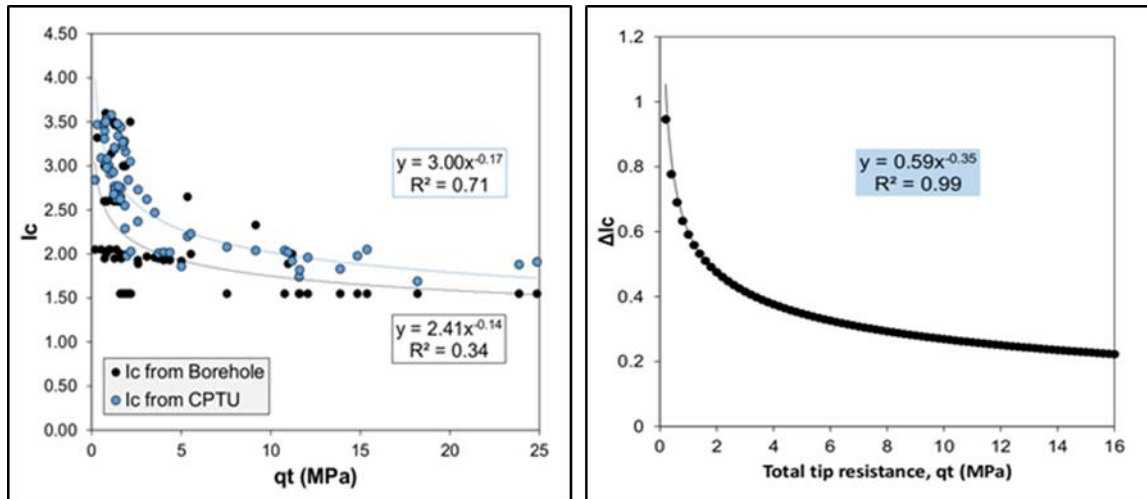


Figure 4-12: Empirical calibration of I_c from CPTu vs I_c from borehole and data regression obtained for Cavezzo Municipality.

4.2.2.4 Example of liquefaction susceptibility assessment based on CPT

To assess the liquefaction susceptibility of an area, all the existing surveys and tests should be collected in vector format file (shapefile) indicating for each of them an identification number (ID), type of the survey, date of execution, location (coordinates according to a system defined in chapter 3 of the present deliverable), investigated depth, link to the raw data, database where data is derived (if publicly available).

Table 4-4 shows an example of data collected from the Emilia-Romagna geognostic database (<https://geoportale.regione.emilia-romagna.it/it>; <https://geo.regione.emilia-romagna.it/geocatalogo/>).

Following the recent major seismic events that produced significant liquefaction damage, such as the 2010-2011 and 2016 the 2012 Emilia-Romagna (Italy) earthquake, the 2016 Kumamoto (Japan) earthquake, the scientific community has decided to support reconstruction strategies by establishing databases in order to facilitate the data sharing among the stakeholders and to support the post-earthquake, political and economic evaluations. One of the most important examples is the Canterbury Geotechnical Database CGD, established and founded by the New Zealand Government (MBIE) and the Earthquake Commission (EQC), after the 2010-2011 Christchurch earthquake Sequence that was characterized by 5 major shocks with extensive evidence of liquefaction. For the Emilia-Romagna Region, a large amount of geological-technical data was already available in numerous and fragmented archives of public and private property, collected to support cognitive investigations of various nature. In recent years, the Region encouraged the collection of the existing data and their loading into numerical archives, that are constantly updated. After the May-June 2012 seismic sequence, a considerable amount of new geotechnical information and surveys, coming from the other platforms (as “Mude Platform”, established to manage the reconstruction of private buildings), have been added to the already existing information. The Geognostic Database includes, at January 2018, more than 85 000 publicly available tests.



This project has received funding from the European Union's Horizon 2020 research and innovation programme under grant agreement No. 700748

Manual for the assessment of liquefaction risk, defining the procedures to create the database, collect, define, symbolize and store information in the Georeferenced Information System and to perform and represent the risk analysis

Data processing phase consists of a semi-automated process to evaluate CT and CTL for each soil profile. For automated processing, all the available information for in situ tests (from the GIS environment) should be organized into a table. In addition to the ID, the folder where all the files are stored needs to be defined. On the other hand, each soil profile (borehole, CPT, SPT, Vs) must be provided in “csv” standardized format.

An example of liquefaction susceptibility, for Christchurch City (New Zealand) and Terre del Reno Municipality (Italy), is represented in Figure 4-13 as cumulative thickness of liquefiable layers evaluated from the CPT profiles available in the existing public databases.

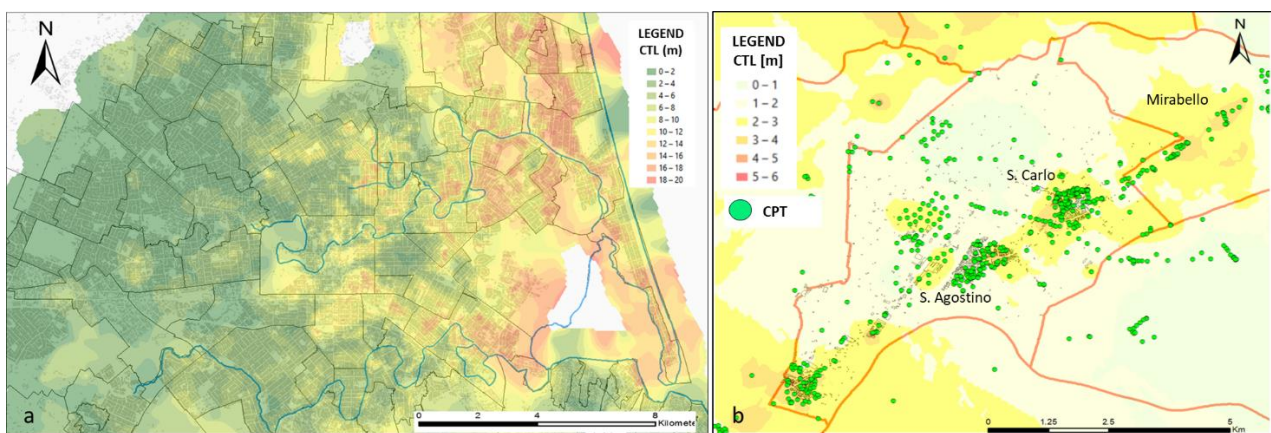


Figure 4-13: Example of geotechnical liquefaction susceptibility. The maps show the cumulative thickness of potentially liquefiable layer for Christchurch City (a) and Terre del Reno district (b).

According to Ishihara (1985), the non-liquefiable crust thickness has been assumed equal to the depth of the first liquefiable sandy layer (if there is a surficial cohesive soil) or equal to ground water depth if it is located within the sand deposits, while the cumulative potentially liquefiable layer is obtained by summing the thickness of all the saturated sandy layers present in the first 20 meters depth.

4.2.2.5 CRR_ESP METHOD

Gerace (2018) analysed the performance of different parameters to defining the strength of a liquefiable layer. In the work package 3 of this project a new semi-automated procedure to derive an equivalent three strata model from a CPTu profile has been proposed. In such a methodology, the Cyclic Resistance Ratio “CRR” (Boulanger and Idriss, 2014) is used as a comparison term. The procedure proposed by WP3 consists of computing every possible three-layered profile and to minimise the difference between the real CRR values and the equivalent three-layered profiles, as schematically illustrated in Figure 4-14.



This project has received funding from the European Union's Horizon 2020 research and innovation programme under grant agreement No. 700748

Manual for the assessment of liquefaction risk, defining the procedures to create the database, collect, define, symbolize and store information in the Georeferenced Information System and to perform and represent the risk analysis

Table 4-4: List of the available geognostic tests from the Emilia-Romagna Region database (<https://geo.regione.emilia-romagna.it/geocatalogo/>).

FID	Shape	GISID	SIGLA	QUOTA P	PROF RAG	DATA ESEC	TETTO GH	TIPO PROVA	COMUNE	CTR	ATTEND U	RISERVATE	LINK PDF	AREA	LEN	X	Y
47	Multipoint	12105	187020T03	-1	0	9 <Null>	0	trivellata manuale	ARIANO NEL POLE	1870	alta	pubblico	http://geo.regione.emilia-romagna.it/gstactico/documenti/prove/geoqnostiche/187/187020T034.pdf	0	0	744516.642401	4985799
48	Multipoint	12107	187020T03	-2	0	9 <Null>	0	trivellata manuale	ARIANO NEL POLE	1870	alta	pubblico	http://geo.regione.emilia-romagna.it/gstactico/documenti/prove/geoqnostiche/187/187020T036.pdf	0	0	744573.650444	4985831
49	Multipoint	16914	200050C05	88.9	4	12/06/1990	2.2	prova CPT con punta meccanica	MONTECHIARIGOL	2000	alta	pubblico	http://geo.regione.emilia-romagna.it/gstactico/documenti/prove/geoqnostiche/200/200050C052.pdf	0	0	610972.477831	4953857
50	Multipoint	16918	200050C05	92.6	3	12/06/1990	1.6	prova CPT con punta meccanica	MONTECHIARIGOL	2000	alta	pubblico	http://geo.regione.emilia-romagna.it/gstactico/documenti/prove/geoqnostiche/200/200050C056.pdf	0	0	610038.083678	4953415
51	Multipoint	17309	200060P40	71.5	101	17/04/1992	1.5	carotaggio continuo	BIBBIANO	2000	alta	pubblico	http://geo.regione.emilia-romagna.it/gstactico/documenti/prove/geoqnostiche/200/200060P402.pdf	0	0	618670.121309	4951990
52	Multipoint	17321	200060P61	60.1	105	25/12/1991	5	pozzo per acqua	SANTILARIO D'ENZ	2000	alta	pubblico	http://geo.regione.emilia-romagna.it/gstactico/documenti/prove/geoqnostiche/200/200060P611.pdf	0	0	616915.326828	4954900
53	Multipoint	17323	200060P61	61.9	130	01/03/1978	28	pozzo per acqua	SANTILARIO D'ENZ	2000	alta	pubblico	http://geo.regione.emilia-romagna.it/gstactico/documenti/prove/geoqnostiche/200/200060P614.pdf	0	0	617650.042019	4953951
54	Multipoint	10446	185160C28	7.8	12	05/01/1995	0	prova CPT con punta meccanica	FERRARA	1851	bassa	pubblico	http://geo.regione.emilia-romagna.it/gstactico/documenti/prove/geoqnostiche/185/185160C281C.pdf	0	0	704700.009685	4965660
55	Multipoint	14875	199040C42	67	5	25/03/1982	4.8	prova CPT con punta meccanica	PARMA	1990	alta	pubblico	http://geo.regione.emilia-romagna.it/gstactico/documenti/prove/geoqnostiche/199/199040C422B.pdf	0	0	602694.735208	4959740
56	Multipoint	14876	199040C42	67.4	5.8	29/03/1982	5.7	prova CPT con punta meccanica	PARMA	1990	alta	pubblico	http://geo.regione.emilia-romagna.it/gstactico/documenti/prove/geoqnostiche/199/199040C423A.pdf	0	0	602658.799457	4959821
57	Multipoint	14895	199040C44	57.7	10.2	28/03/1990	10	prova CPT con punta meccanica	PARMA	1990	alta	pubblico	http://geo.regione.emilia-romagna.it/gstactico/documenti/prove/geoqnostiche/199/199040C440.pdf	0	0	604303.785326	4961162
58	Multipoint	14900	199040D09	82.3	2.4	01/01/1986	2.3	prova dinamica generica	PARMA	1990	alta	pubblico	http://geo.regione.emilia-romagna.it/gstactico/documenti/prove/geoqnostiche/199/199040D094.pdf	0	0	601651.533869	4958598
59	Multipoint	14902	199040D09	83	4.9	01/01/1986	4.7	prova dinamica generica	PARMA	1990	alta	pubblico	http://geo.regione.emilia-romagna.it/gstactico/documenti/prove/geoqnostiche/199/199040D096.pdf	0	0	601679.595296	4958451
60	Multipoint	16805	200040C09	28	12	18/02/1998	0	prova CPT con punta meccanica	CADELBOSCO DI S	2000	alta	pubblico	http://geo.regione.emilia-romagna.it/gstactico/documenti/prove/geoqnostiche/200/200040C091D.pdf	0	0	628817.148524	4959330
61	Multipoint	16807	200040C09	28	12	18/02/1998	0	prova CPT con punta meccanica	CADELBOSCO DI S	2000	alta	pubblico	http://geo.regione.emilia-romagna.it/gstactico/documenti/prove/geoqnostiche/200/200040C091F.pdf	0	0	628832.147831	4959320
62	Multipoint	16816	200040C09	28	10	14/07/1998	0	prova CPT con punta meccanica	CADELBOSCO DI S	2000	alta	pubblico	http://geo.regione.emilia-romagna.it/gstactico/documenti/prove/geoqnostiche/200/200040C097.pdf	0	0	628710.840947	4959360
63	Multipoint	16820	200040C10	35.7	15	29/04/1999	0	prova CPT con punta meccanica	CADELBOSCO DI S	2000	alta	pubblico	http://geo.regione.emilia-romagna.it/gstactico/documenti/prove/geoqnostiche/200/200040C100A.pdf	0	0	626421.510312	4957024
64	Multipoint	16825	200040C10	32	14	30/06/1998	0	prova CPT con punta meccanica	CADELBOSCO DI S	2000	alta	pubblico	http://geo.regione.emilia-romagna.it/gstactico/documenti/prove/geoqnostiche/200/200040C102A.pdf	0	0	626616.68843	4958184
65	Multipoint	16832	200040C10	35.2	10	06/10/1998	0	prova CPT con punta meccanica	CADELBOSCO DI S	2000	alta	pubblico	http://geo.regione.emilia-romagna.it/gstactico/documenti/prove/geoqnostiche/200/200040C106A.pdf	0	0	626355.636376	4959693
66	Multipoint	16837	200040C10	28.1	13.2	30/10/1997	0	prova CPT con punta meccanica	CADELBOSCO DI S	2000	alta	pubblico	http://geo.regione.emilia-romagna.it/gstactico/documenti/prove/geoqnostiche/200/200040C108A.pdf	0	0	630370.326639	4959093
67	Multipoint	16846	200040E01	30.5	25	28/04/1992	0	prova CPT con punta elettrica	REGGIO NELL'EMILIA	2000	alta	pubblico	http://geo.regione.emilia-romagna.it/gstactico/documenti/prove/geoqnostiche/200/200040E010.pdf	0	0	630949.61295	496757
68	Multipoint	16848	200040P08	32.9	4.3	22/07/1997	0	sondaggio a distruzione	EMILIA-ROMAGNA	2000	alta	pubblico	http://geo.regione.emilia-romagna.it/gstactico/documenti/prove/geoqnostiche/200/200040P089.pdf	0	0	626293.016704	4967728
69	Multipoint	16849	200040P40	28.5	29.8	19/03/1992	0	carotaggio continuo	CADELBOSCO DI S	2000	alta	pubblico	http://geo.regione.emilia-romagna.it/gstactico/documenti/prove/geoqnostiche/200/200040P401.pdf	0	0	625552.299583	4960403
70	Multipoint	16934	200050C07	127.4	4	14/06/1990	2.2	prova CPT con punta meccanica	MONTECHIARIGOL	2000	alta	pubblico	http://geo.regione.emilia-romagna.it/gstactico/documenti/prove/geoqnostiche/200/200050C072.pdf	0	0	607114.719878	4950846
71	Multipoint	16938	200050C07	99.7	3	13/06/1990	1.4	prova CPT con punta meccanica	MONTECHIARIGOL	2000	alta	pubblico	http://geo.regione.emilia-romagna.it/gstactico/documenti/prove/geoqnostiche/200/200050C078.pdf	0	0	609276.306863	4959287
72	Multipoint	16943	200050C08	118	5	11/06/1990	3.4	prova CPT con punta meccanica	MONTECHIARIGOL	2000	alta	pubblico	http://geo.regione.emilia-romagna.it/gstactico/documenti/prove/geoqnostiche/200/200050C085.pdf	0	0	610958.541155	4951150
73	Multipoint	16944	200050D01	92.9	1.4	01/09/1992	1.2	prova dinamica generica	MONTECHIARIGOL	2000	alta	pubblico	http://geo.regione.emilia-romagna.it/gstactico/documenti/prove/geoqnostiche/200/200050D018.pdf	0	0	610039.27115	4953305
74	Multipoint	16951	200050D03	115.9	4.3	01/02/1992	3	prova dinamica generica	MONTECHIARIGOL	2000	alta	pubblico	http://geo.regione.emilia-romagna.it/gstactico/documenti/prove/geoqnostiche/200/200050D031.pdf	0	0	611026.413384	4951224
75	Multipoint	16953	200050D03	116.7	5	01/02/1992	5	prova dinamica generica	MONTECHIARIGOL	2000	alta	pubblico	http://geo.regione.emilia-romagna.it/gstactico/documenti/prove/geoqnostiche/200/200050D033.pdf	0	0	610949.791937	495122
76	Multipoint	16955	200050D03	97.9	1.8	01/06/1993	0.7	prova dinamica generica	MONTECHIARIGOL	2000	alta	pubblico	http://geo.regione.emilia-romagna.it/gstactico/documenti/prove/geoqnostiche/200/200050D035.pdf	0	0	609350.365178	4953136
77	Multipoint	16964	200050D04	99.5	2.3	01/06/1993	1	prova dinamica generica	MONTECHIARIGOL	2000	alta	pubblico	http://geo.regione.emilia-romagna.it/gstactico/documenti/prove/geoqnostiche/200/200050D044.pdf	0	0	609234.058665	4959321
78	Multipoint	10453	185160C40	7.9	18	13/09/1982	0	prova CPT con punta meccanica	FERRARA	1851	alta	pubblico	http://geo.regione.emilia-romagna.it/gstactico/documenti/prove/geoqnostiche/185/185160C4010.pdf	0	0	704215.835586	496908
79	Multipoint	10455	185160C40	6.1	9.8	11/12/1987	0	prova CPT con punta meccanica	FERRARA	1851	alta	pubblico	http://geo.regione.emilia-romagna.it/gstactico/documenti/prove/geoqnostiche/185/185160C4012.pdf	0	0	709104.608426	4966199
80	Multipoint	10462	185160C40	7.3	20	07/05/1991	0	prova CPT con punta meccanica	FERRARA	1851	alta	pubblico	http://geo.regione.emilia-romagna.it/gstactico/documenti/prove/geoqnostiche/185/185160C4018.pdf	0	0	706014.939159	496676
81	Multipoint	10488	185160D03	4.3	8	14/11/1985	0	prova dinamica generica	FERRARA	1851	alta	pubblico	http://geo.regione.emilia-romagna.it/gstactico/documenti/prove/geoqnostiche/185/185160D039A.pdf	0	0	709077.046578	496754
82	Multipoint	10501	185160D16	5.7	4	02/01/1981	0	prova dinamica generica	FERRARA	1851	bassa	pubblico	http://geo.regione.emilia-romagna.it/gstactico/documenti/prove/geoqnostiche/185/185160D161C.pdf	0	0	707577.615554	4969045
83	Multipoint	14909	199040D42	67	6	<Null>	5.1	prova dinamica generica	PARMA	1990	alta	pubblico	http://geo.regione.emilia-romagna.it/gstactico/documenti/prove/geoqnostiche/199/199040D422B.pdf	0	0	602714.734276	4959760
84	Multipoint	14912	199040D42	68.4	9.3	19/04/1982	6.3	prova dinamica generica	PARMA	1990	alta	pubblico	http://geo.regione.emilia-romagna.it/gstactico/documenti/prove/geoqnostiche/199/199040D424A.pdf	0	0	602588.240131	4959820
85	Multipoint	14933	199040P13	81.7	4.7	<Null>	3.6	sondaggio a distruzione	PARMA	1990	alta	pubblico	http://geo.regione.emilia-romagna.it/gstactico/documenti/prove/geoqnostiche/199/199040P139.pdf	0	0	601709.593883	4958556
86	Multipoint	14936	199040P14	82.7	5	<Null>	3.5	sondaggio a distruzione	PARMA	1990	alta	pubblico	http://geo.regione.emilia-romagna.it/gstactico/documenti/prove/geoqnostiche/199/199040P142.pdf	0	0	601909.147084	4958297
87	Multipoint	14940	199040P14	76	3.5	01/03/1990	2.2	sondaggio a distruzione	PARMA	1990	alta	pubblico	http://geo.regione.emilia-romagna.it/gstactico/documenti/prove/geoqnostiche/199/199040P147C.pdf	0	0	604210.915463	4967611
88	Multipoint	14946	199040P15	76	3.4	01/03/1990	1.8	sondaggio a distruzione	PARMA	1990	alta	pubblico	http://geo.regione.emilia-romagna.it/gstactico/documenti/prove/geoqnostiche/199/199040P153A.pdf	0	0	604153.480154	4957651
89	Multipoint	14951	199040P15	74.6	4	01/03/1990	1	sondaggio a distruzione	PARMA	1990	alta	pubblico	http://geo.regione.emilia-romagna.it/gstactico/documenti/prove/geoqnostiche/199/199040P157C.pdf	0	0	604093.108407	



This project has received funding from the European Union's Horizon 2020 research and innovation programme under grant agreement No. 700748

Manual for the assessment of liquefaction risk, defining the procedures to create the database, collect, define, symbolize and store information in the Georeferenced Information System and to perform and represent the risk analysis

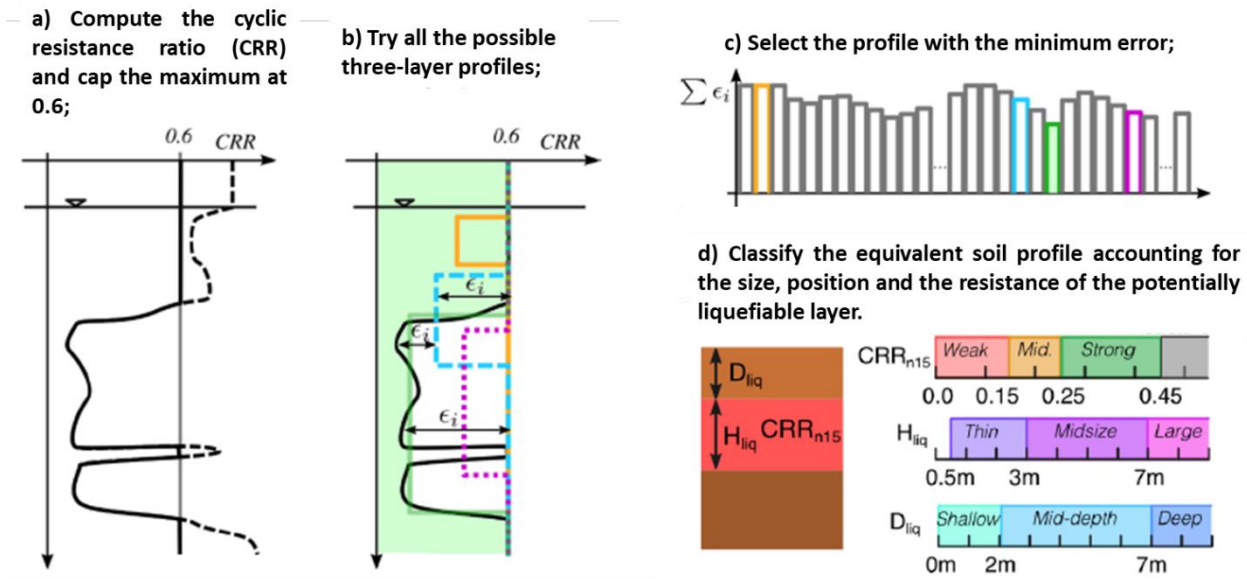


Figure 4-14: Scheme of the procedure to implement the CRR-fitted method and liquefact soil profile classification criteria

$$\delta = \frac{\sum(CRR_{calc,i} - CRR_{fitted,i}) \cdot \Delta H}{CRR_{nonliq} \cdot H_{total}}$$

Equation 4-2

The calculation of the normed error (Equation 4-2) is sensitive to the choice of CRR limit value set for the non-liquefiable soil and the maximum depth of the profile. The CRR limit was set by the authors equal to 0.6, taking the common value suggested in simplified procedures (e.g. Youd et al., 2001; Boulanger and Idriss, 2014). Higher values imply that soil layers with higher CRR would generate some error during fitting (Gerace, 2018). The maximum depth was taken as 20 metres, since surficial consequences of liquefaction below such depths are considered as negligible (Maurer et al., 2015). The increment of depths and CRR should be set small enough that they are not influential on the results. The depth increment was set to 0.1 m and the CRR increments were determined by setting the equivalent cone tip resistance for clean sand to range from 0 to 175 kPa in increments of 5kPa to give a CRR range from 0.061 to 0.6.

The equivalent soil profile found with the above procedure is then classified as in Figure 4-15, where 22 ESP classes are defined accounting for strength, size and position of the potentially liquefiable layer.



This project has received funding from the European Union's Horizon 2020 research and innovation programme under grant agreement No. 700748

Manual for the assessment of liquefaction risk, defining the procedures to create the database, collect, define, symbolize and store information in the Georeferenced Information System and to perform and represent the risk analysis

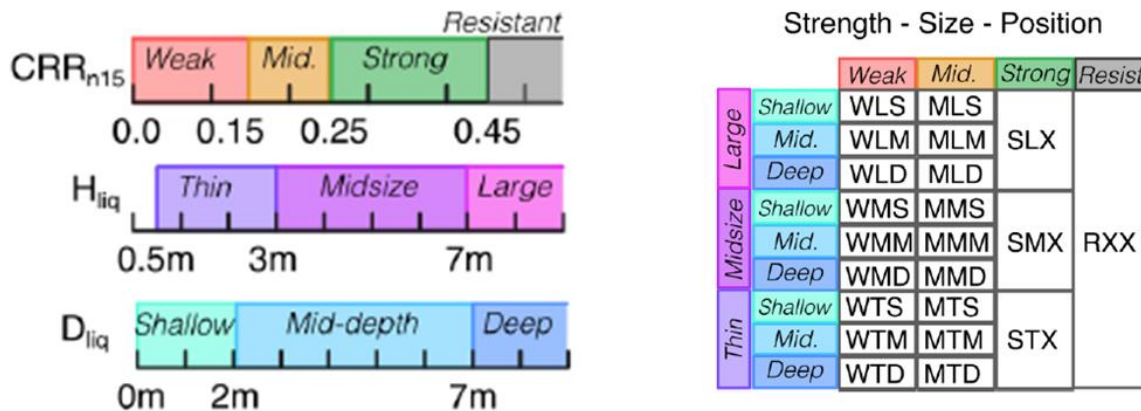


Figure 4-15: Liquefact soil profile classes, as defined by WP3 (D3.3 of this Project). Threshold values for CRR, thickness and depth of liquefiable layer are highlighted in the left part of the Figure

4.2.2.6 Granulometry of liquefiable soils

Liquefaction resistance increases when the grain size becomes coarser due to improved drainage, but also increases as the grain size becomes finer due to increased soil plasticity. Therefore, granulometry plays an important role on the liquefaction susceptibility of soil. For instance, the Eurocode 7 identifies two granulometric zones for soils prone to liquefaction as a function of the coefficient of uniformity U_c : the former is defined for U_c smaller than 3.5 and the latter for U_c greater than 3.5 (Figure 4-16).

When available, the grading curves can be referred to these plots to derive susceptibility. Outside the highlighted zones (Figure 4-16) liquefaction susceptibility is considered negligible, and no further liquefaction analyses are required to estimate triggering.

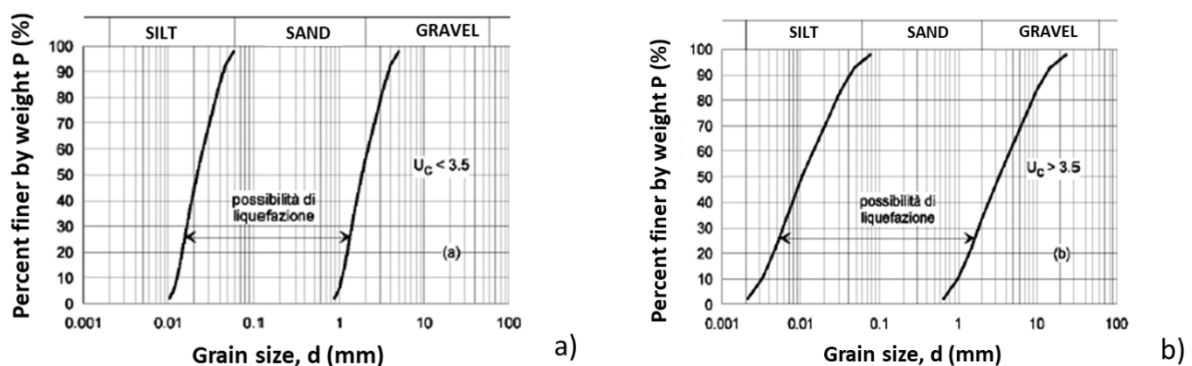


Figure 4-16: Boundaries for potentially liquefiable soils if $U_c < 3.5$ (a) and $U_c > 3.5$ (b), from the Italian Standards (NTC 2018, 7.11).



This project has received funding from the European Union's Horizon 2020 research and innovation programme under grant agreement No. 700748

4.3 Triggering

The fact that a soil is susceptible to liquefaction does not imply that liquefaction will be triggered during an earthquake. Hence a specific analysis is needed to find if the conditions for triggering are fulfilled.

For a given soil profile, the triggering of liquefaction at different depths can be evaluated by applying several approaches. One of these is the cyclic stress approach, which implies the calculation of a liquefaction safety factor (FSL) obtained by dividing the cyclic stress ratio τ/σ'_v producing liquefaction (CRR) with the one induced by the earthquake (CSR). According to this method, seismic liquefaction is triggered in a susceptible soil when the seismic demand (expressed as Cyclic Stress Ratio “CSR”) exceeds the resistance of such soils (expressed as Cyclic Resistance Ratio “CRR”).

The Cyclic Resistance Ratio is a representation of the ability of the soil to resist liquefaction demand and is related to its relative density and Fines Content (FC). It is also recognized that the stress conditions (confining pressure, cyclic shear and initial static shear stresses) play an important role in the liquefaction behaviour of soil, the type of failure mechanism and the mode of development of soil deformation, especially in the case of slopes of sandy deposits.

Site characterization for liquefaction triggering analysis includes collection of information to accurately estimate the values of CRR and earthquake-induced CSR at the site.

The goal of a liquefaction triggering analysis is to evaluate whether liquefaction is expected to occur at a site under a given seismic load. An FSL less than 1.0 is generally assumed to indicate that liquefaction is expected to trigger at that depth. The factor of safety against liquefaction, however, does not give insights into the associated uncertainties and variability related to the calculation of CRR and CSR. In practice, a minimum required FSL for design as low as 1.0 has been required when coupled with an extreme ground motion level. Typical minimum values used in practice are between 1.1 and 1.3.

4.3.1 Ground motion definition

A key point in any seismic risk assessment is the provision of seismic ground motion (level and spectral characteristics of earthquake shaking), Figure 4-17. Ground motion estimates are represented by: (1) contour maps and (2) location-specific values of ground shaking demand. For computational efficiency and improved accuracy, earthquake losses are generally computed using location-specific estimates of ground shaking demand. Contour maps are also developed to provide pictorial representations of the variation in ground motion demand within the study region. When ground motion is based on either probabilistic hazard maps or user-supplied maps, location-specific values of ground shaking demand are interpolated between PGA, PGV or spectral acceleration contours, respectively.

Elastic response spectra (5% damping) are used to characterize ground shaking demand. All these spectra have the same “standard” format defined by a PGA value (at zero period) and spectral response at a period of 0.3 second (acceleration domain) and spectral response at a period of 1.0 second (velocity domain). Ground shaking demand can be also defined in terms of peak ground velocity (PGV).



This project has received funding from the European Union's Horizon 2020 research and innovation programme under grant agreement No. 700748

Manual for the assessment of liquefaction risk, defining the procedures to create the database, collect, define, symbolize and store information in the Georeferenced Information System and to perform and represent the risk analysis

The characterization of a scenario-based approach requires the incorporation of the available information collected in a geological, seismotectonic and geotechnical database of the site of interest as well as advanced physical modelling techniques to provide a reliable and robust deterministic basis both for design application and risk analysis.

The choice of one or a set of scenario earthquakes is a central concept in seismic and liquefaction risk analysis. It includes the following steps:

- Basis for ground shaking
- Selection of hazard parameter(s) to characterise the impact of an earthquake
- Attenuation model for ground shaking
- Incorporation of site effects, and near-field and potential directivity/focusing factors
- Definition of the earthquake(s) scenario

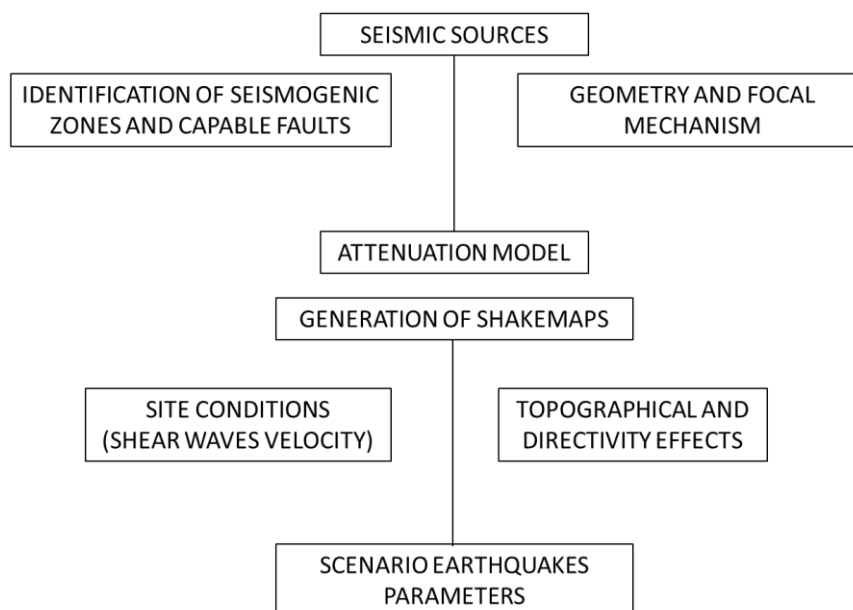


Figure 4-17: Information to characterize a seismic scenario

According to the Manual for Zonation on Seismic Geotechnical Hazards (revised version), prepared by The Technical Committee for Earthquake Geotechnical Engineering (TC4) of the International Society for Soil Mechanics and Geotechnical Engineering (TC4-ISSMGE 1999) three levels of increasing complexity for ground motion microzonation can be performed.

The first level of zonation (“general zonation”) is used for preparing maps with scale in the range 1:1.000.000~1:50.000. Local site effects are evaluated through compilation and interpretation of existing information available from historic documents (i.e. compiled data on the distribution of damage induced during past destructive earthquake), published reports and other available databases (i.e. macroseismic intensities), or by direct reference to the site surface geology.

The second level of zonation (“detailed zonation”) requires the execution of geotechnical investigations. To minimize the effort and expense, existing geotechnical engineering reports from governmental agencies and



This project has received funding from the European Union's Horizon 2020 research and innovation programme under grant agreement No. 700748

Manual for the assessment of liquefaction risk, defining the procedures to create the database, collect, define, symbolize and store information in the Georeferenced Information System and to perform and represent the risk analysis

private companies should be collected and compiled. Therefore, this level of zonation can usually be achieved at reasonable cost and permits a substantial upgrading of the zonation maps to scales of about 1:100.000 to 1:10.000. Such maps are prepared using simplified approaches, including the use of ground classification, microtremor measurements, and shear-wave velocity.

By using complete geotechnical investigations and ground response analyses, the third level of zonation (“rigorous zonation”) is achieved, which allows to produce maps with a scale of 1:25.000-1:5.000. This is a very high and detailed zonation level, which is generally expensive.

4.3.1.1 Basis for ground shaking

Ground motion estimates are generated in the form of contour maps and location-specific seismic demands. Ground motion is characterized by: (1) spectral response, based on a standard spectrum shape, (2) peak ground acceleration and (3) peak ground velocity. The spatial distribution of ground motion can be determined using one of the following methods or sources:

- Scenario Earthquake analysis (Methodology calculation);
- Probabilistic ground motion maps (e.g. Share.eu);
- Other probabilistic or deterministic ground motion maps (user-defined maps).

Deterministic seismic ground motion demands are calculated for user-specified scenario earthquakes. For a given event magnitude, attenuation relationships are used to calculate ground shaking demand for rock sites, which is then amplified by factors based on local soil conditions. This requires V_s profiles, supplied by the user.

Probabilistic ground motion maps include for instance the SHARE PSHA (<http://portal.share.eu.org:8080/opencms/opencms/share/model/>) that represents the current state of knowledge with all its uncertainties and which is subject to updates in future. The new maps include estimates based on the collected information on fault moment release and the dipping geometry of subduction zones. Secondly, the maps include estimates of ground shaking that is caused by the seismic waves propagating through the earth's crust and along the surface.

The amplitudes of seismic waves caused by each earthquake vary with magnitude and distance from the rupture and also depend on the faulting type. Ground motion amplitudes decay with increasing distance from the causative fault; such decay is described with empirical relations, referred to as Ground Motion Prediction Equations (GMPEs), determined from previously measured ground motion.

User-supplied peak ground acceleration (PGA) and spectral acceleration contour maps may also be used. In this case, the user must provide all contour maps in a pre-defined digital format (as shapefile or csv). In such case it is assumed that user-supplied maps already include soil amplification.

4.3.1.1.1 Scenario Earthquake Analysis

For deterministic definition of a scenario Earthquake, the user specifies the location (e.g., Latitude and Longitude of the epicentre), the magnitude of the earthquake and the fault mechanism. Several options to define an appropriate scenario earthquake location are available: the user can (1) define an event based on



This project has received funding from the European Union's Horizon 2020 research and innovation programme under grant agreement No. 700748

Manual for the assessment of liquefaction risk, defining the procedures to create the database, collect, define, symbolize and store information in the Georeferenced Information System and to perform and represent the risk analysis

the European faults catalogue or (2) on a database of the historical earthquakes epicentres, or (3) chose arbitrary the epicentre.

An example of seismic scenarios characterization is shown in the Table 4-5. The main earthquakes of the 2012 Emilian seismic sequence, having M_w greater than 5, are described through the location and depth of the hypocentre, the magnitude and the type of fault mechanism.

Table 4-5: Example of general input file for seismic scenarios characterization. By default, the strike and dip of the fault are set equal to 0.

ID	Lat.	Long.	Focal Depth (km)	Magnitude	Strike	Dip	Fault Mechanism
1	44.89	11.23	6	5.9	0: north	0: horizontal	Inverse
2	44.86	11.37	5	5.1	0: north	0: horizontal	Inverse
3	44.83	11.49	4.7	5.1	0: north	0: horizontal	Inverse
4	44.85	11.09	10.2	5.8	0: north	0: horizontal	Inverse
5	44.89	11.01	6.8	5.3	0: north	0: horizontal	Inverse
6	44.88	10.95	5.4	5.2	0: north	0: horizontal	Inverse
7	44.9	10.94	9.2	5.1	0: north	0: horizontal	Inverse

4.3.1.1.1.1 Seismic sources Database

In cases where risk assessment concerns earthquake scenarios that may occur on an area, a study of the seismo-genic faults is required. In particular, the European database (EDSF; <http://diss.rm.ingv.it/share-edsf/>), which includes a compilation of fault sources deemed to be capable of generating earthquakes of magnitude equal to or larger than 5.5 in the Euro-Mediterranean area, can be used. A “capable fault” is a fault with a significant potential for relative displacement at or near the ground surface.

The selection of the scenario earthquake(s) focused on the largest (magnitude) earthquakes expected from each source. These earthquakes traditionally are called maximum credible earthquakes (MCEs). The use of the MCE ensures that effects from all other magnitudes are explicitly considered. In other words, by virtue of designing a structure to withstand the MCE, it will automatically withstand all other (smaller) earthquakes. The focus on large magnitudes is justified, because the destructive potential of earthquakes primarily depends on its energy content (proportional to the magnitude) and the transfer of this energy into a structure.

4.3.1.1.1.2 Historical Earthquake Database

In addition to the capable faults catalogue, the SHEEC - SHARE European Earthquake catalogue has been compiled. It includes harmonized moment magnitude M_w estimates and provides uncertainty estimates. The SHARE European Earthquake Catalogue, compiled in the frame of the SHARE (<http://www.share-eu.org/>) project (Task 3.1), consists of two portions:

- the SHARE European Earthquake Catalogue (SHEEC) 1000-1899 compiled under the coordination of INGV, Milan, building on the data contained in AHEAD (Archive of Historical Earthquake Data) and



This project has received funding from the European Union's Horizon 2020 research and innovation programme under grant agreement No. 700748

Manual for the assessment of liquefaction risk, defining the procedures to create the database, collect, define, symbolize and store information in the Georeferenced Information System and to perform and represent the risk analysis

with the methodology developed in the frame of the I3, EC project "Network of Research Infrastructures for European Seismology" (NERIES), module NA4.

- the SHARE European Earthquake Catalogue (SHEEC) 1900-2006 compiled by GFZ Potsdam. This part of the catalogue represents a temporal and spatial excerpt of "The European-Mediterranean Earthquake Catalogue" (EMEC) for the last millennium (Grünthal and Wahlström, 2012) with some modifications, which are described in Grünthal et al. (2013).

In addition, the SHARE earthquake catalogue for Central and Eastern Turkey (SHARE-CET), complementing the SHARE European Earthquake Catalogue (SHEEC) has been compiled. For the time-window 1000–2006 the catalogue lists over 30.000 earthquakes in the magnitude range $1.7 \leq M_W \leq 8.5$.

4.3.1.1.2 Probabilistic Seismic Hazard Maps

The available probabilistic seismic hazard contour maps for Euro-Mediterranean Region, developed by the Share consortium, can be used as basis to ground shaking in probabilistic analyses. In fact, SHARE project produced more than sixty time-independent European Seismic Hazard Maps (ESHMs) spanning spectral ordinates from PGA to 10 seconds and exceedance probabilities ranging from 10^{-1} to 10^{-4} yearly probability. An example of SHARE-developed seismic hazard Map is shown in Figure 4-18, in terms of PGA having 10% exceedance probability in 50 years.

The hazard values are referenced to a rock velocity of $V_{s,30} = 800$ m/s at 30 m depth. SHARE models earthquakes as finite ruptures and includes all events with magnitudes $M_W \geq 4.5$ in the computation of hazard values. SHARE introduces an innovative weighting scheme that reflects the importance of the input data sets considering their time horizon, thus emphasizing the geologic knowledge for products with longer time horizons and seismological data for shorter ones.

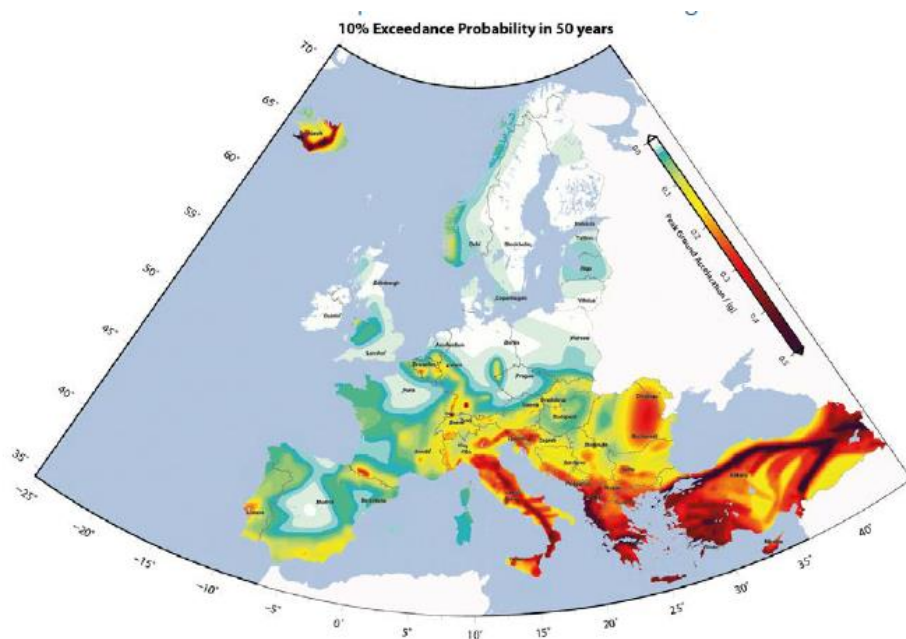


Figure 4-18: - Seismic hazard map depicts the 10% exceedance probability that a peak ground acceleration of a certain fraction of the gravitational acceleration g is observed within the next 50 year



This project has received funding from the European Union's Horizon 2020 research and innovation programme under grant agreement No. 700748

Manual for the assessment of liquefaction risk, defining the procedures to create the database, collect, define, symbolize and store information in the Georeferenced Information System and to perform and represent the risk analysis

4.3.1.1.3 User-Supplied Seismic Hazard Maps

A methodology as much flexible as possible must allow the end user to characterize each specific seismic scenario. This can be defined by providing PGA maps and spectral acceleration contour maps of ground shaking in a pre-defined digital format (i.d. shapefile or csv format). This option allows the user to develop a scenario event that could not be described adequately by the available attenuation relationships, or to replicate historical earthquakes. In this case, maps of PGA and spectral acceleration (periods from 0.1 to 5.0 second) must be provided, also accounting to the soil amplification, Figure 4-19.

Rigorously, as defined by the WP2 microzonation procedure, within the Liquefact project procedure these user-defined maps should result from a local seismic response analysis, corresponding to the third level of a microzonation model for ground shaking.

Latitude	Longitude	PGA (g)	Sa (T=0.1s)	Sa (T=0.2s)	Sa (T=0.3s)	Sa (T=0.4s)	Sa (T=0.5s)	Sa (T=0.75s)	Sa (T=1.0s)	Sa (T=1.5s)	Sa (T=2.0s)	Sa (T=2.5s)	Sa (T=3.0s)	Sa (T=5.0s)
59.959075	11.037236	0.1664	0.291	0.3741	0.3375	0.2886	0.2559	0.207	0.1744	0.1162	0.0872	0.0697	0.0581	0.0349
59.959075	11.040013	0.1793	0.3144	0.4045	0.3617	0.3081	0.2724	0.2188	0.1831	0.122	0.0915	0.0732	0.061	0.0366
59.959131	11.042987	0.1917	0.3368	0.4336	0.385	0.3269	0.2882	0.2302	0.1915	0.1277	0.0958	0.0766	0.0638	0.0383
59.959136	11.046358	0.2073	0.363	0.4668	0.415	0.3512	0.3086	0.2447	0.2021	0.1348	0.1011	0.0809	0.0674	0.0404
59.959114	11.049509	0.2213	0.3875	0.4983	0.4423	0.3734	0.3274	0.2584	0.2124	0.1416	0.1062	0.085	0.0708	0.0425
59.959175	11.05353	0.2386	0.4182	0.5379	0.4733	0.3985	0.3485	0.2737	0.2238	0.1492	0.1119	0.0895	0.0746	0.0448
59.959224	11.057067	0.25	0.4473	0.5756	0.5028	0.4222	0.3685	0.2879	0.2342	0.1562	0.1171	0.0937	0.0781	0.0468
59.957658	11.037612	0.2759	0.4849	0.6242	0.5407	0.4527	0.3941	0.3061	0.2475	0.165	0.1238	0.099	0.0825	0.0495
59.957636	11.041798	0.2947	0.5185	0.6678	0.5767	0.4818	0.4185	0.3236	0.2604	0.1736	0.1302	0.1041	0.0868	0.0521
59.957647	11.046568	0.3188	0.5609	0.7224	0.626	0.5215	0.4518	0.3473	0.2776	0.1851	0.1388	0.111	0.0925	0.0555
59.957686	11.052836	0.3415	0.601	0.774	0.6696	0.557	0.4819	0.3694	0.2943	0.1962	0.1472	0.1177	0.0981	0.0589
59.95768	11.057132	0.3727	0.6559	0.8446	0.7243	0.6022	0.5208	0.3986	0.3172	0.2115	0.1586	0.1269	0.1057	0.0634
59.955651	11.05711	0.4017	0.708	0.9122	0.7764	0.6447	0.5568	0.4251	0.3372	0.2248	0.1686	0.1349	0.1124	0.0674
59.955673	11.051944	0.4401	0.7792	1.0053	0.8531	0.7066	0.609	0.4625	0.3648	0.2432	0.1824	0.1459	0.1216	0.073
59.955772	11.045698	0.4766	0.8424	1.0862	0.9269	0.7664	0.6594	0.4988	0.3918	0.2612	0.1959	0.1567	0.1306	0.0784
59.955866	11.041082	0.5339	0.9386	1.2084	1.0313	0.8522	0.7328	0.5537	0.4343	0.2895	0.2171	0.1737	0.1448	0.0869
59.955976	11.037546	0.585	1.0302	1.327	1.1254	0.9307	0.801	0.6063	0.4766	0.3177	0.2383	0.1906	0.1588	0.0953

Figure 4-19: Example of input file for user-defined seismic scenario

If only PGA contour maps are available, the user can develop the other required maps based on the spectral acceleration response factors (as established in the Standards).

4.3.2 Intensity measures

Performance-based design of civil engineering structures and seismic risk assessment require the identification of critical indices of damage. Since building performance is traditionally assessed in terms of seismically induced permanent displacement, many procedures (e.g. Makdisi and Seed, 1978; Bray et al., 1998) relate them with earthquake intensity measures.

$$P(D > d) = \int_{im} P(D > d|IM) \cdot \left[\sum_i N_i(M_{min}) \cdot \int_m \int_r f(im|M, R) \cdot f(m) \cdot f(r) \cdot dmdr \right] dim$$

Equation 4-3

where $P(D>d)$ = probability of the displacement D exceeding a test value d; $N_i(M_{min})$ = the rate of earthquakes above magnitude M_{min} for the i^{th} source, im and IM = Intensity Measure, m and M = magnitude, r and R = distance, $f(x)$ = probability density function for the random variable X.



This project has received funding from the European Union's Horizon 2020 research and innovation programme under grant agreement No. 700748

Manual for the assessment of liquefaction risk, defining the procedures to create the database, collect, define, symbolize and store information in the Georeferenced Information System and to perform and represent the risk analysis

In National standards, the design basis forces are typically derived from linear-elastic response spectra, accounting for some damping of the structure. These are adjusted by load correction factors for the required application. The anchor point (of a response spectrum for pseudo-spectral accelerations) for scaling a generic design spectrum (often normalised to 1 g) is at a certain high frequency (typically around 33 Hz) and the final design spectrum commonly used by engineers is scaled by peak ground acceleration (PGA). In the past, PGA values were derived from intensity attenuation equations and therefore closely related to observed damage; indeed, it is known that intensities (as a damage characteristic) correlate much better with peak ground velocity (PGV) or with the spectral acceleration corresponding to the first natural frequency of structures.

Concerning the liquefaction triggering analysis, one main question arises on the Intensity Measure relevant for liquefaction. Studying the performance of different IMs on liquefaction versus advanced numerical calculations, Karimi and Dashti (2017) observed that the evolutionary settlements of structures depend on intensity, duration and frequency content of the ground motion and concluded that cumulative energy (Table 4-6) is a more appropriate to represent intensity measure, more than peak variables (Table 4-5). They propose the cumulative absolute velocity (Campbell & Bozorgnia, 2012) as a potential candidate as also recently assumed by Bray and Macedo (2017) and Karamitros et al. (2013). Other authors (e.g. Youd et al., 2002; Youd & Perkins, Bardet et al., 2002; Rauch & Martin, 2000) combine magnitude, distance from the rupture and peak ground acceleration.

The existing semi-empirical procedures to evaluate liquefaction triggering (e.g., Seed and Idriss, 1971; Youd et al., 2001) rely on ground motion IMs that may not be optimum in terms of their ability to reduce variability in the predicted response or their independence from source characteristics. In these procedures, the peak ground acceleration at the surface in the free-field is often used in combination with earthquake moment magnitude (M_w) to characterize the intensity and duration of seismic loading, which are compared with a measure of soil resistance to obtain a factor of safety against liquefaction triggering (FSL) at the site. The same IMs or the resulting FSL are used to evaluate liquefaction-induced soil settlement in the free-field (e.g., Ishihara and Yoshimine, 1992; Tokimatsu and Seed, 1987). The estimation of PGA at the surface of a highly nonlinear soil profile (e.g., susceptible to liquefaction) introduces a great deal of uncertainty in evaluating the liquefaction hazard and the resulting settlements. Further, the influence of traditional IMs (e.g., PGA, FF-Surface) on the variability of the predicted response (e.g., excess pore pressure generation or settlement) is not well understood. Lastly, none of the previous empirical procedures consider the influence of a building and soil-structure interaction (SSI) on the extent of excess pore pressure generation, the liquefaction hazard, and the resulting settlements, which are important near the built facilities.

Table 4-6 and Table 4-7 resume the most known peak and cumulative-energy variables used as seismic Intensity Measures.



This project has received funding from the European Union's Horizon 2020 research and innovation programme under grant agreement No. 700748

Manual for the assessment of liquefaction risk, defining the procedures to create the database, collect, define, symbolize and store information in the Georeferenced Information System and to perform and represent the risk analysis

Table 4-6: Definition of a subset of the principal Intensity Measures present in literature.

IM	Definition	Units
PGA- Peak Ground Acceleration	$\max_t(a(t))$	G
PGV- Peak Ground Velocity	$\max_t(v(t))$	cm/s
PGD – Peak Ground Displacement	$\max_t(d(t))$	Cm
EPV – Effective Peak Velocity (ATC, 1978)	$SV(T_s \approx 1)/2.5$	
SA - Spectral Acceleration	$SA(T_s)$	G
I_c – Characteristic Intensity (Ang, 1990)	$a_{rms}^{1.5}(D_{595})^{0.5}$	$\text{cm}^{1.5} \text{s}^{-2.5}$
T_p – Predominant Period	$T(\max(SA))$	S
D_{595} – Significant Duration (Trifunac & Brady, 1975)	$t(0.95I_a) - t(0.05I_a)$	S

Table 4-7: Definition of a subset of the principal ground motion Cumulative Measure

IM	Definition	Units
I_a - Arias Intensity (Arias 1970)	$\frac{\pi}{2g} \int_0^\infty [a(t)]^2 dt$	cm/s
CAV - Cumulative Absolute Velocity	$\int_0^\infty a(t) dt$	cm/s
CAV,dp – Standardized version of the Cumulative Absolute Velocity (Campbell and Bozorgnia, 2011)	$\sum_{i=1}^N (H(PGA_i) - 0.025) \int_{i-1}^i a(t) dt$	
SI – Response Spectrum Intensity (Housner, 1959)	$\int_{0.1}^{2.5} PSV(\xi = 0.05, T_s) / dT$	Cm
$a_{\max} T^2 N$ - (Karamitros 2013)	$\pi^2 \int v(t) dt$	M
avgSa - mean of the log spectral accelerations at a set of periods of interest (Kazantzi and Vamvatsikos, 2015)	$\frac{1}{N} \sum_{i=1}^N \ln Sa(c_i * T_i)$	g-s
a_{rms} - Root Mean Square Acceleration	$\sqrt{\frac{1}{D_{95}} \int_{T_1}^{T_2} [a(t)]^2 dt}$	G

4.3.3 Attenuation model

For deterministic analysis the spectral ground-motion parameters produced by the scenario earthquake can be evaluated by a selectable ground motion prediction equation (GMPE), accounting for the attenuation of the ground shaking with the distance from the source.



This project has received funding from the European Union's Horizon 2020 research and innovation programme under grant agreement No. 700748

Manual for the assessment of liquefaction risk, defining the procedures to create the database, collect, define, symbolize and store information in the Georeferenced Information System and to perform and represent the risk analysis

These relationships define ground shaking for rock conditions based on earthquake magnitude, M , and other parameters. They provide estimates of the PGA and spectral demand at 0.3 and 1.0 seconds, and with the standard response spectrum shape, fully define 5%-damped demand spectra for a given location.

Since each GMPE is dependent on the particular distance, different types of distances should be computed (Figure 4-20):

- epicentral distance R_{epi} ,
- hypocentral distance R_{hypo} ,
- “Joyner-Boore” distance R_{jb} (shortest distance to the vertical surface projection of the fault rupture plane),
- source-to-site azimuth R_X (sites located on the hanging wall have positive azimuths ranging from 0° to 180° , while sites located on the footwall have negative azimuths ranging from -180° to 0°),
- the depth-to-top of rupture Z_{TOR} , and
- the shortest distance to the subsurface fault rupture plane R_{rup} .

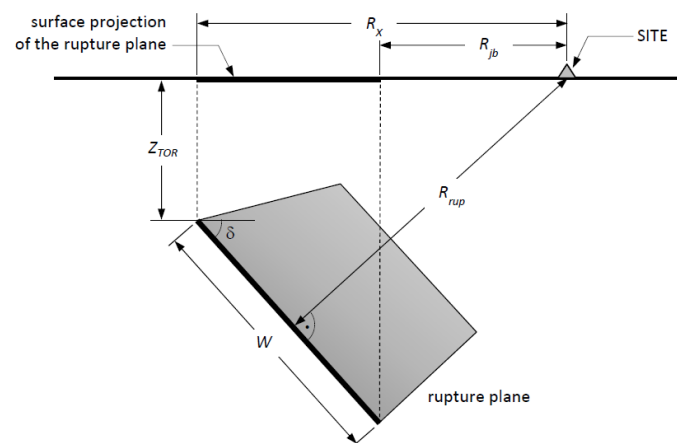


Figure 4-20: Geometric illustration of earthquake source and distance measures using a vertical cross-section through a fault rupture plane.

A considerable number of well-established ground motion prediction equations exists; in addition to these, the user can implement any additional GMPE. It should be noted that, when using the elastic design spectra, all provided prediction relations refer to rock site conditions and thus compute ground motion amplitudes without soil amplification since this is covered in a separate (subsequent) calculation step. On the other hand, when the site-specific response spectra are used, the soil conditions are considered in the ground motion prediction equation and no further amplification is therefore necessary.

4.3.4 Code Design Response spectrum

To describe the seismic action, two different types of design spectra are provided within Eurocode 8 (CEN, 2004a). This is mainly done to account for the differing level of seismic hazard in Europe and the different earthquake types susceptible to occur. In case that earthquakes with a surface-wave magnitude $M_w > 5.5$ are



This project has received funding from the European Union's Horizon 2020 research and innovation programme under grant agreement No. 700748

Manual for the assessment of liquefaction risk, defining the procedures to create the database, collect, define, symbolize and store information in the Georeferenced Information System and to perform and represent the risk analysis

expected, it is suggested to use Spectrum Type 1, else ($M_w \leq 5.5$) Type 2. The question which spectrum type to choose for a specific region should be based upon "(...) the magnitude of earthquakes that are actually expected to occur rather than conservative upper limits defined for the purpose of probabilistic hazard assessment".

$$\begin{aligned}
 Sa(T) &= a_g \cdot S \cdot \left[1 + \frac{T}{T_B} \cdot (\eta \cdot 2.5 - 1)\right] && \text{for } T < T_B \\
 Sa(T) &= a_g \cdot S \cdot \eta \cdot 2.5 && \text{for } T_B < T < T_C \\
 Sa(T) &= a_g \cdot S \cdot \eta \cdot 2.5 \cdot \left[\frac{T}{T_C}\right] && \text{for } T_C < T < T_D \\
 Sa(T) &= a_g \cdot S \cdot \eta \cdot 2.5 \cdot \left[\frac{T_C \cdot T_D}{T^2}\right] && \text{for } T_D < T < 4.0 \text{ s}
 \end{aligned}$$

Equation 4-4

where:

- a_g - design ground acceleration (here: PGA) on soil type A ground;
- T_B, T_C - corner periods of the constant spectral acceleration branch (plateau);
- T_D - corner period defining the beginning of the constant displacement range;
- S - soil amplification factor;
- η - damping correction factor ($\eta = 1.00$ for 5% viscous damping).

The shape of the design spectrum is thus determined by the corner periods, soil amplification factor, and the level of input ground motion. Both, corner periods (T_B, T_C , and T_D) as well as soil amplification factor S are dependent on 'ground type', which is mainly distinguished by the average shear-wave velocity of the uppermost 30 m ($v_{s,30}$) and hence categorized into 5 different soil classes (Table 4-8). Both, soil amplification factor and corner periods for the different soil classes are given in Table 4-9 and Table 4-10 for Type 1 and Type 2 design response spectra, respectively. Figure 4-21 illustrates the corresponding sets of normalized elastic design response spectra.

Given that sedimentary soil materials are present at a site, the seismic ground motion at the ground surface is modified both in amplitude and frequency content. Respective amplification factors and/or corner periods which basically describe the shape of the design spectra for the different soil classes are given in the corresponding code provisions; in many standards (Eurocode 8) soil classes are commonly classified as a function of the shear waves velocity ($v_{s,30}$).

Table 4-8: Ground types provided by Eurocode 8

Ground type	Description of stratigraphic profile	Shear wave velocity $v_{s,30}$ [m/s]
A	Rock or rock-like geological formation, incl. at most 5 m of weaker material at the surface	>800
B	Deposits of very dense sands, gravel, or very stiff clay (at least several tens of m in thickness) characterized by a gradual increase of mechanical properties with depth	360-800
C	with thickness from several tens to many hundreds of m	180-360
D	Deposits of loose-to-medium cohesionless soil (with or without some soft cohesive layers), or of predominantly soft-to-firm cohesive soil	<180
E	Soil profile consisting of a surface alluvium layer with $v_{s,30}$ values of type C or D and thickness H varying between 5–20 m underlain by stiffer material with $v_{s,30} > 800$ m/s	n.a.



This project has received funding from the European Union's Horizon 2020 research and innovation programme under grant agreement No. 700748

Manual for the assessment of liquefaction risk, defining the procedures to create the database, collect, define, symbolize and store information in the Georeferenced Information System and to perform and represent the risk analysis

Table 4-9: Values of the parameters describing Eurocode 8 – Type 1 spectra

Ground Type	Soil factor S	T_B [sec]	T_C [sec]	T_D [sec]
A	1.00	0.15	0.40	2.00
B	1.20	0.15	0.50	2.00
C	1.15	0.20	0.60	2.00
D	1.35	0.20	0.80	2.00
E	1.40	0.15	0.50	2.00

Table 4-10: Values of the parameters describing Eurocode 8 – Type 2 spectra

Ground Type	Soil factor S	T_B [sec]	T_C [sec]	T_D [sec]
A	1.00	0.05	0.25	1.20
B	1.35	0.05	0.25	1.20
C	1.50	0.10	0.25	1.20
D	1.80	0.10	0.30	1.20
E	1.60	0.05	0.25	1.20

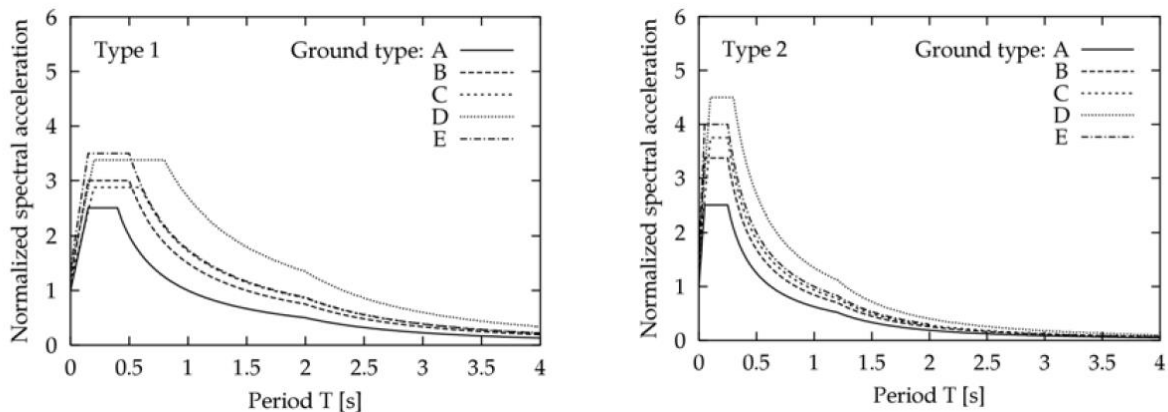


Figure 4-21: Elastic design spectra of Type 1 and Type 2 for ground types A – E.

4.3.4.1 Site-specific (scenario-based) elastic response spectrum

Site-specific elastic response spectra can be either derived from a deterministic earthquake scenario or a probabilistic seismic scenario. In the first case, attenuation relationships are applied to compute the corresponding ground motion estimates using average shear-wave velocity $V_{s,30}$ in order to amplify the ground motion. This $V_{s,30}$ value must be supplied as input file.

In the second case, when a probabilistic scenario is selected, the ground motion provided in the input files is amplified using the soil amplification factors provided by NEHRP (ICC, 2006) by assigning a soil type that agrees with the $V_{s,30}$ value read from the input files.



This project has received funding from the European Union's Horizon 2020 research and innovation programme under grant agreement No. 700748

Manual for the assessment of liquefaction risk, defining the procedures to create the database, collect, define, symbolize and store information in the Georeferenced Information System and to perform and represent the risk analysis

Ground Amp. Profile	Latitude	Longitude	Soil (Vs30 m/s)
VP-0001	42.3534	11.56788	200

Figure 4-22: To amplify the seismic action accounting for the stratigraphy, values of Vs30 must be assigned to some profiles within the study area

Few international seismic building codes address the topic of topographic amplification effects. In general, each of these provisions tackles this topic in a very simplified way by solely adding a period-independent topographic amplification factor to the elastic design spectrum. This factor, often called AT or ST, requires that the topographic relief can be represented as a simplified 2D feature. Each of the respective design codes mention that irregular complex shapes will require specific studies.

Eurocode 8 (EN 1998-5:2003, CEN 2004b) provides some simplified topographic amplification factors, called ST. Factors ST are considered independent of the fundamental period of vibration and are used as a constant scaling factor for the ordinates of the elastic design response spectrum. These should be used in cases that the slope belongs to 2D topographic irregularities, such as long ridges and cliffs of heights $H \geq 30$ m.

Table 4-11: Topographic amplification factors according to Eurocode 8 (EN 1998-5:2003, CEN 2004b).

Description	Building location	Topographic amplification factor ST
flat or average slope angles of less than $\sim 15^\circ$	-	1.0
isolated cliffs and slopes	Near the top edge	≥ 1.2 ¹⁾
ridges with crest widths significantly less than the base width	Near the top of the slope	≥ 1.4 ¹⁾ for angles greater than 30°
		≥ 1.2 ¹⁾ for angles 15° to 30°

¹⁾ Increase by 20% in presence of a loose surface layer.

The value of ST may be assumed to decrease as a linear function of the height above the base of the cliff or ridge, and to be unity at the base.

4.4 Earthquake induced Cyclic Stress Ratio

For a given soil profile, the triggering of liquefaction at each depth can be evaluated by applying simplified methods. The most popular implies the calculation of a liquefaction safety factor (FSL), obtained by dividing the cyclic stress ratio τ/σ'_v producing liquefaction (CRR) with the one induced by the earthquake (CSR). A simplified method to estimate the CSR profile was developed by Seed and Idriss (1971) based on the maximum ground surface acceleration (a_{max}) at the site.

$$CSR_{M=7.5}(z) = 0.65 * \left(\frac{a_{max}}{g}\right) * \left(\frac{\sigma_{vo}(z)}{\sigma_{vo}(z)'}\right) * r_d(z) \quad \text{Equation 4-5}$$

Where:

$\sigma_{vo}, \sigma_{vo}'$ = vertical total and effective stress at depth z , a_{max}/g = maximum horizontal acceleration (as a fraction of gravity) at the ground surface, and r_d is the shear stress reduction factor that accounts for the dynamic response of the soil profile.



This project has received funding from the European Union's Horizon 2020 research and innovation programme under grant agreement No. 700748

Manual for the assessment of liquefaction risk, defining the procedures to create the database, collect, define, symbolize and store information in the Georeferenced Information System and to perform and represent the risk analysis

The cyclic stress ratio required to initiate liquefaction (i.e., the liquefaction resistance, CRR) decreases with increasing number of cycles of loading; therefore, the seismic loading must be associated with a number of loading cycles. Earthquake magnitude is used as a proxy for the number of loading cycles because the duration of shaking and the associated number of loading cycles correlate with earthquake magnitude. The CSR is adjusted using a magnitude scaling factor (MSF) to compute an equivalent CSR for a reference $M = 7.5$.

$$CSR_{M=7.5}(z) = CSR_{M=m}(z) * \frac{1}{MSF} = 0.65 * \left(\frac{a_{max}}{g}\right) * \left(\frac{\sigma_{vo}(z)}{\sigma'_{vo}(z)}\right) * r_d(z) * \frac{1}{MSF} \quad \text{Equation 4-6}$$

The magnitude scaling factor (MSF) accounts for duration effects (i.e., number and relative amplitudes of loading cycles) on the triggering of liquefaction. Several formulations (Andrus and Stokoe, 1997; Idriss and Boulanger, 2008) have been proposed to evaluate the Magnitude Scaling Factor, after the first developed by Seed and Idriss (1982), Figure 4-22.

For instance, the MSF for sands used by Boulanger and Idriss (2014) was developed by Idriss (1999), who derived the following relationship:

$$MSF = 6.9 \cdot \exp\left(\frac{-M}{4}\right) - 0.058 \leq 1.8 \quad \text{Equation 4-7}$$

An upper limit for the MSF is assigned to very-small-magnitude earthquakes for which a single peak stress can dominate the entire time series. The value of 1.8 is obtained by considering the time series of stress induced by a small magnitude earthquake to be dominated by single pulse of stress (i.e., 1/2 to 1 full cycle, depending on its symmetry), with all other stress cycles being sufficiently small to neglect.

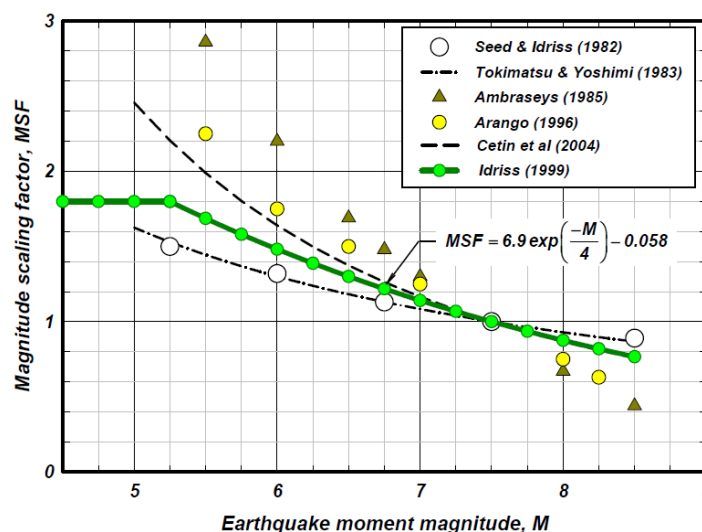


Figure 4-23: Magnitude scaling factor (MSF) relationships.

After parametric site response analyses, Idriss (1999) concluded that the shear stress reduction coefficient, r_d , can be calculated using two functions of the depth, z , within the soil profile, namely $\alpha(z)$ and $\beta(z)$, and the earthquake magnitude, M .



This project has received funding from the European Union's Horizon 2020 research and innovation programme under grant agreement No. 700748

$$r_d = \exp[\alpha(z) + \beta(z) \cdot M]$$

Equation 4-8

$$\alpha(z) = -1.012 - 1.126 \sin\left(\frac{z}{11.73} + 5.133\right)$$

Equation 4-9

$$\beta(z) = 0.106 + 0.118 \sin\left(\frac{z}{11.28} + 5.142\right)$$

Equation 4-10

The depth-dependent shear stress reduction coefficient, r_d , accounts for the nonrigid response of the soil deposit (characterized in the small strain regime by the shear wave velocity [Vs] profile at the site) as well as for the characteristics of the earthquake waves traveling through the soil. Seed and Idriss (1971) initially proposed a relationship between r_d and depth developed from a limited number of dynamic response analyses for a range of generic site conditions. Using additional site response analyses, Idriss (1999) modified the Seed and Idriss (1971) r_d relationship, introducing also the magnitude. The Idriss (1999) relationship is used to develop the triggering relationships of Idriss & Boulanger (2008) and Boulanger & Idriss (2014), Figure 4-24.

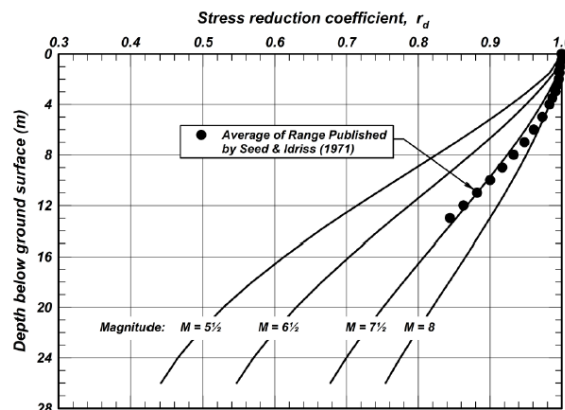


Figure 4-24: Shear stress reduction factor, r_d , relationships (Boulanger and Idriss, 2014).

The 0.65 factor found in Equation 4-5 was originally proposed as a way to relate the number of loading cycles from an irregular earthquake loading to the number of loading cycles from uniform cyclic loading. Although this value is somewhat arbitrary and was unnecessary once MSFs were introduced, 0.65 is still the standard due to historical precedent.

CSR evaluation requires estimates of PGA, M_w , and r_d ; since the required PGA is at the ground surface, it must account for the effects of the near-surface soil conditions on ground shaking.

4.5 Cyclic Resistance Ratio “CRR”

Several empirical procedures (Robertson, 1998; Boulanger and Idriss, 2014) were proposed to evaluate the CRR starting from geotechnical and geophysical in-situ tests (CPT, SPT and Vs profile). In particular, Boulanger and Idriss (2014) provide an empirical formulation of the Cyclic Resistance Ratio based on the survey of



This project has received funding from the European Union's Horizon 2020 research and innovation programme under grant agreement No. 700748

Manual for the assessment of liquefaction risk, defining the procedures to create the database, collect, define, symbolize and store information in the Georeferenced Information System and to perform and represent the risk analysis

liquefaction and the results of the most common in-situ tests (CPT and SPT), while Andrus and Stokoe (2000) propose a method to evaluate the CRR starting from Vs profiles.

Therefore, calculation of the CRR requires geotechnical and geophysical in-situ tests (measurement of the profile of SPT blow count, CPT tip resistance and sleeve friction, Vs profiles) as a function of depth and at multiple locations across the site. Then, correction factors are applied; for instance, to the measured SPT blow count, a first correction factor is required to define a stress- and energy-corrected SPT resistance $(N_1)_{60}$ based on the test setup. Furthermore, SPT blow counts recorded in hollow stem auger borings below the water table are particularly susceptible to error due to soil disturbance and may result in abnormally low blow count values. The SPT provides measurements at widely spaced intervals (often 1.5 m, but never less than the length of the split spoon sampler, 0.45 m), which limits the ability to use SPT measurements to identify thinner layers or detailed variations within a soil profile. On the contrary, the CPT provides continuous measurements along a profile, representing a very powerful mean to characterize thinner layers and detailed variations within strata. Pore-pressure data from piezocone penetration testing (CPTu) can provide additional information, both qualitative (e.g., whether soil is dilatant or not) and quantitative (e.g., the steady-state porewater pressure).

Depending on the method of measurement, Vs may be used to identify thin layers and variations within strata, even if it has not the detail and the resolution of the CPT.

A rigorous soil type characterization is required to perform liquefaction triggering analyses. Rigorously, since CPT and Vs methods do not provide a direct measure of soil type, additional boring and sampling, or sampling using a special sampler adapted for use with CPT rigs, are needed to determine soil type directly. When using liquefaction triggering methods that require Vs values to calculate the earthquake-induced CSR from site response analysis (e.g., Andrus and Stokoe, 2000; Cetin and Seed, 2004), Vs should be measured directly and not estimated by correlations with the SPT or the CPT. A comprehensive site investigation for liquefaction triggering could include all three characterization techniques: borings with SPT sampling (with hammer energy measurements—a stricter requirement than use of the automatic hammer) to obtain blow counts and soil type; CPT soundings to obtain detailed profiles of in situ resistance; and Vs profiles to accurately assess the earthquake-induced CSR and to provide additional insights into the CRR.

4.5.1 CPT-Based liquefaction triggering analysis

One of the most popular CPT-based procedure to evaluate the Factor of Safety against liquefaction at each depth of a soil profile is the Boulanger and Idriss (2014), which is summarized in Figure 4-25.

Boulanger and Idriss (2014) calculate the Cyclic Resistance Ratio (CRR) from the measured CPT tip resistance, q_c , the CPT sleeve friction, f_s , and the effective vertical stress, σ'_v , in the soil. These are used to estimate an overburden correction factor, CN, and correct the tip resistance to account for the overburden stress, q_{c1} . The normalized overburden stress, q_{c1N} , is q_{c1} divided by the atmospheric pressure ($p_a=100$ kPa). During the iteration (usually about 3 cycles), q_{c1} is always based on the measured tip resistance, q_c , while CN is based on the iteratively updated value for q_{c1N} . A second correction is made for the fines content, FC. With the assumed flat ground or uniform surcharge for the regional-scale analysis, the correction for the effects of an initial static shear stress ratio is $K\alpha=1$.



This project has received funding from the European Union's Horizon 2020 research and innovation programme under grant agreement No. 700748

Manual for the assessment of liquefaction risk, defining the procedures to create the database, collect, define, symbolize and store information in the Georeferenced Information System and to perform and represent the risk analysis

To characterize the soil behaviour type (SBT) and to evaluate the percentage of fines content, FC , the empirical correlations defined by Robertson (2015) are used.

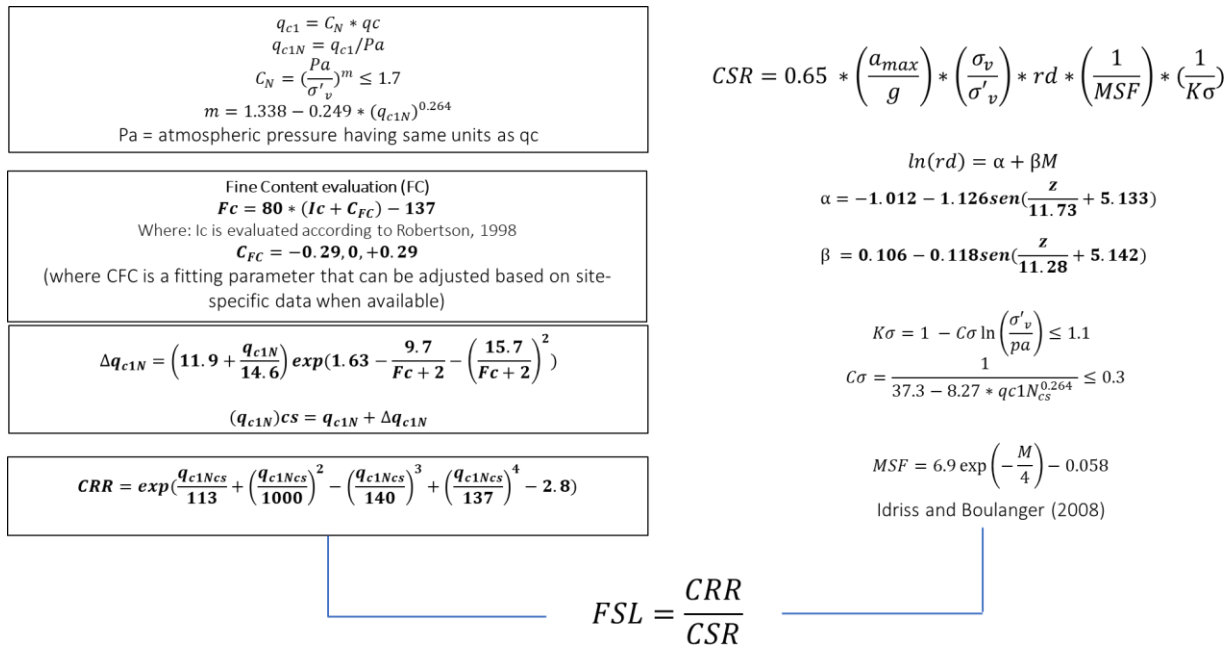


Figure 4-25: Flowchart of the Boulanger & Idriss (2014) CPT-based procedure.

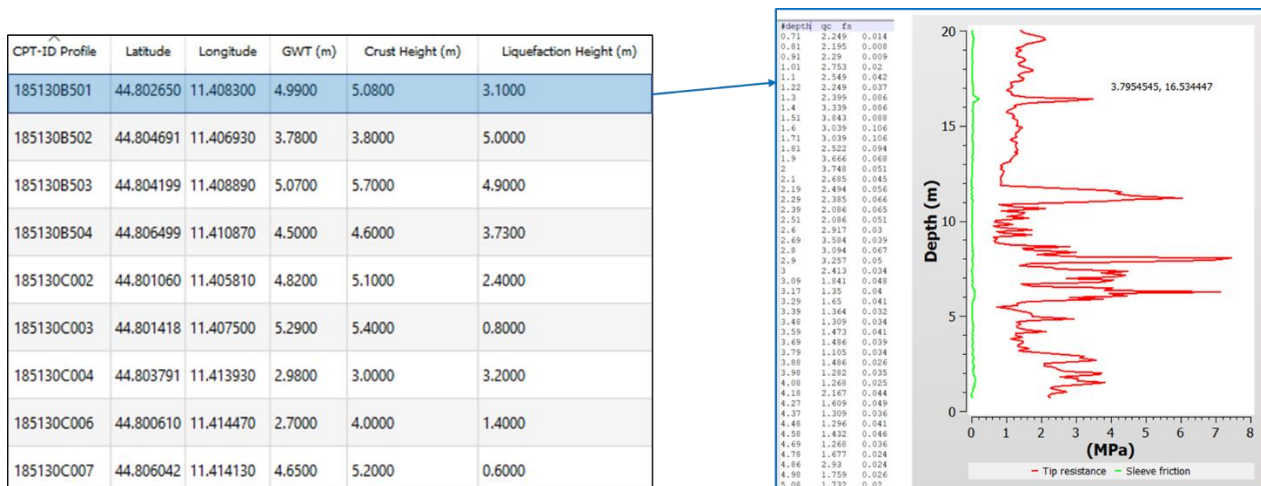


Figure 4-26: Example of input table for CPT-based liquefaction hazard evaluation. For each CPT, the tip resistance, sleeve friction and pore pressure must be provided in ASCII format

4.5.2 SPT-Based liquefaction triggering analysis

Boulanger and Idriss (2014) also propose a SPT-based procedure to evaluate the CRR (Figure 4-27) starting from the number of blows N_{160} , normalized with respect to the atmospheric pressure P_a and increased to account for the fine content. In this case, the soil behavior type index I_c can be evaluated with numerous empirical correlations between in-situ tests and geotechnical parameters.



This project has received funding from the European Union's Horizon 2020 research and innovation programme under grant agreement No. 700748

Manual for the assessment of liquefaction risk, defining the procedures to create the database, collect, define, symbolize and store information in the Georeferenced Information System and to perform and represent the risk analysis

$$(N_1)_{60cs} = CN \cdot CE \cdot CB \cdot CR \cdot CS \cdot N + \Delta(N_1)_{60} \quad \text{Equation 4-11}$$

where CN is the correction factor to adjust the blow count to a reference stress of one atmosphere; CE is a correction factor for the kinetic energy of the hammer (i.e. hammer weight and height of fall); CB is a correction factor for the borehole diameter; CR is a rod length correction factor; CS is a correction factor for the configuration of the SPT sampler; N is the recorded blow count; and $\Delta(N_1)_{60}$ is the correction factor for the fines content. There is uncertainty in the computed FS from a stress-based analysis not only because of the uncertainty in the location of the CRR relationship but also because the values of the parameters in the CSR and $(N_1)_{60cs}$ equations are not known precisely. In fact, explicit consideration of uncertainty associated with a correction factor may even increase the uncertainty associated with the liquefaction potential assessment.

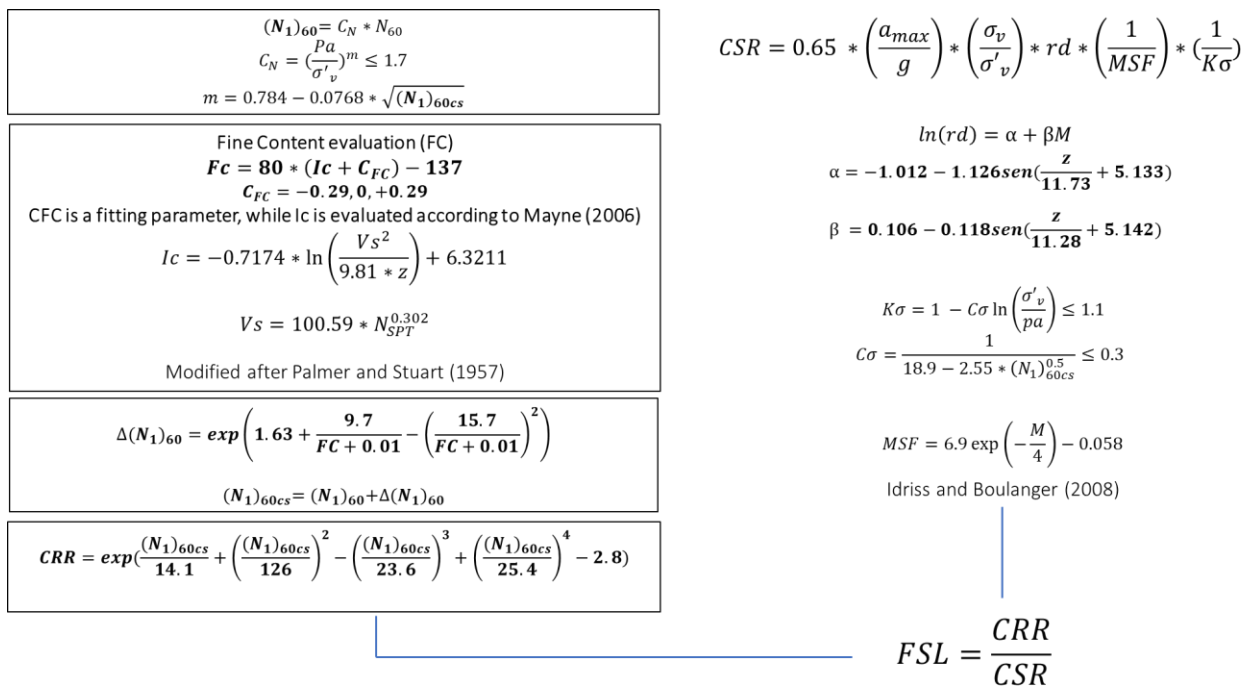


Figure 4-27: Flowchart of the Boulanger & Idriss (2014) SPT-based procedure for liquefaction triggering analysis.

Vs – ID PROFILE	Latitude	Longitude	GWT (m)	γ (kN/m ³)	Crust Height (m)	Liquefaction Height (m)
ID-001	44.80376	11.406520	2.00	19.00	3.50	5.00
ID-002	44.80470	11.410773	1.80	19.00	4.00	3.00
ID-003	44.804765	11.410672	3.50	19.00	3.50	2.00
ID-004	44.804765	11.410502	3.00	19.00	10.00	4.00
ID-005	44.804659	11.410680	2.80	19.00	9.00	2.20
ID-006	44.800881	11.408108	2.50	20.00	6.00	1.50
ID-007	44.804154	11.409344	1.00	20.00	2.00	3.00

Figure 4-28: General input file for SPT-based liquefaction triggering analysis



This project has received funding from the European Union's Horizon 2020 research and innovation programme under grant agreement No. 700748

Manual for the assessment of liquefaction risk, defining the procedures to create the database, collect, define, symbolize and store information in the Georeferenced Information System and to perform and represent the risk analysis

SPT (ID – 000)

z [m]	N _{SPT}	Upper boundary [m]	Lower boundary [m]
3.5	25	3.5	4
6	23	5	9
10	18	9.6	11
13	19	12.5	13.5
15	28	14	17
18	31	18	21

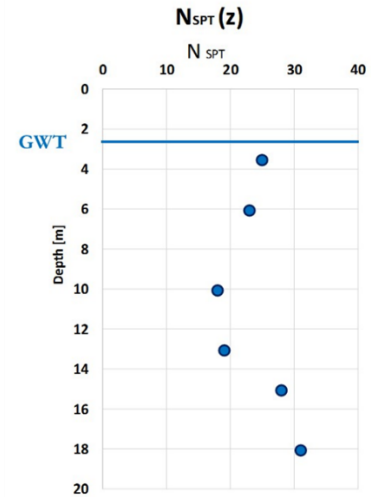


Figure 4-29: Example of SPT input file for liquefaction triggering analysis.

4.5.3 Vs-based liquefaction triggering analysis

Measuring shear wave velocity (V_s) is another test used to characterize soils in situ. V_s refers to the speed at which a shear wave (one type of wave generated by an earthquake) propagates through the ground. The speed of wave propagation depends on the density of the soil, the directions of wave propagation and particle motion, and the effective stresses in those two directions. V_s , by convention, refers to the shear wave speed at very small amplitudes. V_s is related to the shear modulus of the soil at small strain, G_{max} , and the mass density of the soil, ρ , by the equation:

$$V_s = \sqrt{\frac{G_{max}}{\rho}} \quad \text{Equation 4-12}$$

Where ρ is equal to the total unit weight of the soil divided by the acceleration of gravity.

V_s measurements are economical and non-invasive, since they do not need to penetrate the ground surface to make the measurement. The latter capability can be beneficial if soil profiles contain inclusions (i.e., gravel or cobble inclusions) that can make testing difficult or even prohibit SPTs and CPTs. There are many V_s measurement techniques, including downhole measurements (ASTM International, 2014a), cross-hole measurements (ASTM International, 2014b), suspension logging (Nigbor and Imai, 1994), and non-invasive methods (Stokoe and Santamarina, 2000). Because non-invasive V_s tests do not provide soil samples, however, some drilling and sampling may still be required as part of a subsurface investigation.

Andrus and Stokoe (2000) define an alternative method for calculating CRR using shear-wave velocity, V_s .

$$CRR = \left[0.022 \left(\frac{V_{s1}}{100} \right)^2 + 2.8 \left(\frac{1}{V_{s1}^* - V_{s1}} - \frac{1}{V_{s1}^*} \right) \right] \quad \text{Equation 4-13}$$

in which: V_{s1} is the stress-corrected shear wave velocity; V_{s1}^* is the limiting upper value of V_{s1} for cyclic liquefaction occurrence, which varies between 200-215m/s depending on the fines content of the soil.



This project has received funding from the European Union's Horizon 2020 research and innovation programme under grant agreement No. 700748

Manual for the assessment of liquefaction risk, defining the procedures to create the database, collect, define, symbolize and store information in the Georeferenced Information System and to perform and represent the risk analysis

$$V_{S1} = V_s \left(\frac{pa}{\sigma'_v} \right)^{0.25}$$

$$V_{S1,csa1} = \frac{V_{S1}}{Ka1}$$

Pa = atmospheric pressure (kPa); σ'_v effective vertical stress (kPa).

ka1 is the correction factor accounting for the age of the deposit

Time (years)	Soil aging factor (Ka1)
1	1.09
10	1.01
100	0.94
1 000	0.88
10 000	0.83
100 000	0.78

$$CRR = 0.022 * \left(\frac{V_{S1,csa1}}{100} \right)^2 + 2.8 * \left(\frac{1}{V_{S1}^* - V_{S1,csa1}} - \frac{1}{V_{S1}^*} \right)$$

V_{S1}^* is the limiting upper value of $V_{S1,csa1}$ for cyclic liquefaction occurrence, which varies between 200-215 m/s depending on the fines content of the soil.

$$CSR = 0.65 * \left(\frac{a_{max}}{g} \right) * \left(\frac{\sigma_v}{\sigma'_v} \right) * rd * \left(\frac{1}{MSF} \right) * \left(\frac{1}{K\sigma} \right)$$

$$rd = 1 - 0.00765z \quad \text{if } z < 9.2m$$

$$rd = 1.174 - 0.0267z \quad \text{if } z \geq 9.2m$$

Liao and Whitman (1986)

$$K\sigma = 1 - C\sigma \ln \left(\frac{\sigma'_v}{pa} \right) \leq 1.1 \quad C\sigma = \frac{1}{18.9 - 3.1 * \left(\frac{V_{S1}}{100} \right)^{1.976}} \leq 0.3$$

$$MSF = \left(\frac{Mw}{7.5} \right)^{-2.56}$$

Andrus and Stokoe (1997)

$$FSL = 1.4 * \frac{CRR}{CSR}$$

Juang et al. (2005)

Figure 4-30: Flowchart of the Andrus & Stokoe (2000) procedure for liquefaction triggering evaluation

To evaluate the soil behavior type index, the procedure proposed by Mayne (2006) can be applied:

$$Ic = -0.7174 \cdot \ln[Vs^2 / (9.81 \cdot z)] + 6.3211$$

Equation 4-14

Then, the fine content FC can be evaluated by applying the following correlation (Robertson and Fear, 1995):

$$FC (\%) = 42.4179 \cdot Ic - 54.8574$$

Equation 4-15

About the Factor of Safety, Juang et al. (2005) found that the traditional FSL is conservative for calculating CRR, resulting in lower factors of safety and over-prediction of liquefaction occurrence. To account for this, they introduce a multiplication factor of 1.4 to obtain a more realistic estimate of the factor of safety.

After an 11-years period of Vs site data collection and the development of probabilistic correlations for seismic liquefaction occurrence, new correlations for probabilistic/deterministic assessment of liquefaction potential from shear wave velocity were proposed by Kayen et al. (2013).

Data coming from 301 liquefaction field case histories in China, Taiwan, Japan, Grece and the United States were merged to previously published case histories to build a global catalog of 422 case histories of Vs liquefaction performance. Then, after Bayesian regression and structural reliability methods a probabilistic treatment of the Vs catalog for performance-based engineering applications was developed.



This project has received funding from the European Union's Horizon 2020 research and innovation programme under grant agreement No. 700748

Manual for the assessment of liquefaction risk, defining the procedures to create the database, collect, define, symbolize and store information in the Georeferenced Information System and to perform and represent the risk analysis

Vs – ID PROFILE	Latitude	Longitude	GWT (m)	Soil Ageing (years)
ID-001	44.80376	11.406520	2.00	1000
ID-002	44.80470	11.410773	1.80	1000
ID-003	44.804765	11.410672	3.50	1000
ID-004	44.804765	11.410502	3.00	1000
ID-005	44.804659	11.410680	2.80	1000
ID-006	44.800881	11.408108	2.50	1000
ID-007	44.804154	11.409344	1.00	1000

Figure 4-31: General input file for Vs-based liquefaction triggering analysis

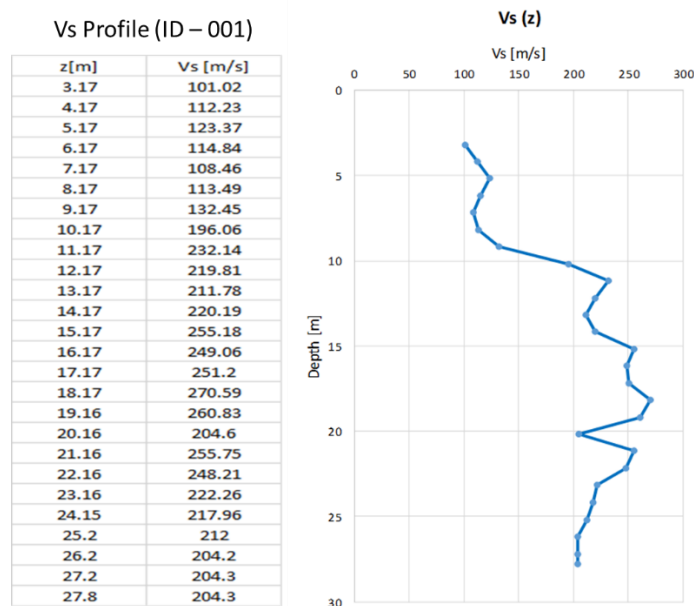


Figure 4-32: Example of Vs Profile

4.6 Liquefaction Severity Indicators

Once the Factor of Safety (FSL) has been calculated at each depth, synthetic indicators of the liquefaction severity on the ground (free field) can be evaluated. These integrate the contribution to the liquefaction of each layers, generally for the first 20 meters of depth, giving a measure of the liquefaction severity on the surface (free field).

In general terms, a liquefaction severity indicator (Eq. 4.16) can be defined as the integral of the product between a function of the Factor of Safety against Liquefaction $f_1(FSL)$ and a weight function that emphasizes the severity of liquefaction at a lower depth, Table 4-12.

$$INDEX = \int_{z_{max}} f_1(FSL) * w(z) dz$$

Equation 4-16



This project has received funding from the European Union's Horizon 2020 research and innovation programme under grant agreement No. 700748

Manual for the assessment of liquefaction risk, defining the procedures to create the database, collect, define, symbolize and store information in the Georeferenced Information System and to perform and represent the risk analysis

Table 4-12: The most widespread indicators, except the LDI which was defined for lateral spreading, quantify the damage to the ground by integrating the estimated effects of liquefaction in the first 20 m depth

INDEX	REFERENCE	$f_1(FSL)$	$w(z)$	Z
LPI	Iwasaki et al., 1978	$\begin{cases} 1 - FSL & \text{if } FSL < 1 \\ 0 & \text{if } FSL \geq 1 \end{cases}$	$10 - 0.5z$	$Z_{min} = 0$ $Z_{max} = 20m$
LPI_{ISH}	Maurer, 2015	$\begin{cases} 1 - FSL & \text{if } FSL \leq 1 \cap H_1 \cdot m(FSL) \leq 3 \\ 0 & \text{otherwise} \end{cases}$ <p>Where:</p> $m(FSL) = \exp\left(\frac{5}{25.56(1 - FSL)}\right) - 1$	$\frac{25.56}{z}$	$Z_{min} = H_1$ $Z_{max} = 20m$
S	Zhang et al., 2002	$\varepsilon_v = \varepsilon_v(FSL, q_{C1Ncs})$	-	$Z_{min} = 0$ $Z_{max} = \text{max depth}$
LDI	Zhang et al., 2004	$\gamma_{max} = \gamma_{max}(FSL, q_{C1N})$	-	$Z_{min} = 0$ $Z_{max} < 23m$
LSN	van Ballegooy et al., 2014	$\varepsilon_v = \varepsilon_v(FSL, q_{C1Ncs})$	$\frac{1000}{z}$	$Z_{min} = 0$ $Z_{max} = 20m$

Various liquefaction severity or damage potential indicators were proposed in literature to provide a measure of the liquefaction-induced surficial evidence, based on the cumulative liquefaction response of a soil profile.

The most used of them are: Liquefaction Potential Index “LPI” (Iwasaki et al., 1978); Ishihara-inspired Liquefaction Potential Index “ LPI_{ISH} ” (Maurer et al., 2015); one-dimensional volumetric reconsolidation settlement “S” (Zhang et al., 2002); Lateral Displacement Index “LDI” (Zhang et. al, 2004); Liquefaction Severity Number “LSN” (van Ballegooy et al., 2014).

Such indicators are defined and discussed in the following sections.

4.6.1 Liquefaction Potential Index LPI (Iwasaki, 1978)

The Liquefaction Potential Index LPI is the summation of liquefaction severity in each soil layer, which in turn is a function of the Factor of Safety (FSL), weighted by a depth factor that decreases linearly from 10 to 0 over the top 20 m. The LPI value is between 0 (representing no liquefaction expected) and 100 (representing extreme liquefaction effects expected to the ground surface). By weighting soils to have an increasing influence on LPI as depth decreases, this parameter is able to represent the beneficial effects of an increasing non-liquefied surface layer thickness, or crust.

Iwasaki et al. (1978) defined the Liquefaction Potential Index (LPI) of a 20 m deep soil profile as:



This project has received funding from the European Union's Horizon 2020 research and innovation programme under grant agreement No. 700748

Manual for the assessment of liquefaction risk, defining the procedures to create the database, collect, define, symbolize and store information in the Georeferenced Information System and to perform and represent the risk analysis

$$LPI = \int_0^{20m} F_1(z) \cdot W(z) dz$$

Equation 4-17

where:

$$W(z) = 10 - 0.5z$$

$$F_1(z) = \begin{cases} 1 - F_0S & \text{if } F_0S < 1 \\ 0 & \text{if } F_0S \geq 1 \end{cases}$$

z = the depth below the ground surface in metres;

F₀S(z) = the Factor of Safety against Liquefaction FSL (z).

There are no LPI adjustments when the CPT profile is less than 20 m deep. Iwasaki proposed four classes to quantify the liquefaction risk to the ground, ranging from no-very low to very high (Table 4-13).

Table 4-13: Iwasaki observed that LPI values can range from 0 to 100, with the following indicators of liquefaction induced damage.

LPI Range	Liquefaction Risk
LPI = 0	Very low
LPI < 5	Low
5 < LPI ≤ 15	High
LPI > 15	Very high

4.6.2 LPI Ishihara Inspired

Ishihara (1985), recognized the important role of the upper non-liquefiable crust's thickness (H₁) in mitigating the surficial liquefaction manifestations. The thinner the crust near the ground surface, the more the pore water pressure from the underlying liquefied sand deposit will be able to disrupt it, resulting in sand boils and cracks. Plotting observations of liquefaction surface effects where the thicknesses of the non-liquefied capping layer (H₁) and the liquefied strata (H₂) were known, Ishihara (1985) proposed boundary curves for predicting liquefaction manifestation as a function of H₁, H₂ and peak ground acceleration. These boundary curves indicate that for a given PGA, there is a limiting H₁ beyond which surface manifestations do not form regardless of H₂. It means that the liquefied deposit needed to be both sufficiently thick and close enough to the ground surface for the resulting excess pore water pressure to erupt at ground surface.

Moving from Ishihara experience, Maurer et al. (2015) derived a new index to assess liquefaction-induced ground manifestations: the Ishihara inspired LPI, LPI_{ISH}, developed as a result of the rebuilding efforts in Christchurch. The modifications proposed to the LPI framework try to better capture the trends in the Ishihara boundary curves, to include the influence of the thickness of the non-liquefied crust (i.e., H₁) on the surficial liquefaction manifestations.

Maurer et al. (2015) defined LPI_{ISH} as:



This project has received funding from the European Union's Horizon 2020 research and innovation programme under grant agreement No. 700748

Manual for the assessment of liquefaction risk, defining the procedures to create the database, collect, define, symbolize and store information in the Georeferenced Information System and to perform and represent the risk analysis

$$LPI_{ISH} = \int_0^{20m} F(FS) \frac{25.56}{z} dz \quad \text{Equation 4-18}$$

Where:

$$F(FS) = \begin{cases} 1 - FS & \text{if } FS \leq 1 \cap H_1 \cdot m(FS) \leq 3 \\ 0 & \text{otherwise} \end{cases} \quad \text{Equation 4-19}$$

$$m(FS) = \exp\left(\frac{5}{25.56(1 - FS)}\right) - 1 \quad \text{Equation 4-20}$$

Where:

- H_1 is defined the same as H_1 in the Ishihara (1985) procedure;
- z is the depth to the layer of interest in meters below the ground surface
- FS is the factor of safety against liquefaction, $FSL(z)$;

As compared to the Iwasaki et al. (1978) LPI procedure, LPI_{ISH} incorporates the concept of a limiting cap thickness and also utilizes a power law, rather than linear, depth weighting function. In Figure 4-32, the depth weighting function used in the existing LPI framework is compared to that proposed herein. LPI_{ISH} weighs the contribution of liquefaction triggering towards producing surficial manifestation more for depths between 0 and 3 m, and less for depths between 3 and 17 m.

It can be shown that $LPI_{ISH} = 100$ for a profile with $FS = 0$ over the entire 20 m, and with groundwater at a depth of 0.4 m. Because of the powerlaw form of the depth weighting function, the authors recommend that a minimum H_1 of 0.4 m should be used in computing LPI_{ISH} , regardless of whether liquefiable soils are present at shallower depths. The new LPI_{ISH} framework has been validated using a total of 60 liquefaction case studies from the 1989 Loma Prieta (USA), 1994 Northridge (USA), 1999 Kocaeli (Turkey), 1999 Chi-Chi (Taiwan), 2010 Darfield (New Zealand) and 2011 Christchurch (New Zealand) earthquakes. Case histories were selected from the literature based on the availability of CPT soundings in digital-format; Factors of Safety against liquefaction (i.e. FS) were evaluated according to the CPT based liquefaction evaluation procedure of Robertson and Wride (1998), using the I_c to identify the Soil Behavior Type (SBT) and assuming a cut-off value of 2.6, because soils having $I_c > 2.6$ were considered too plastic to liquefy.

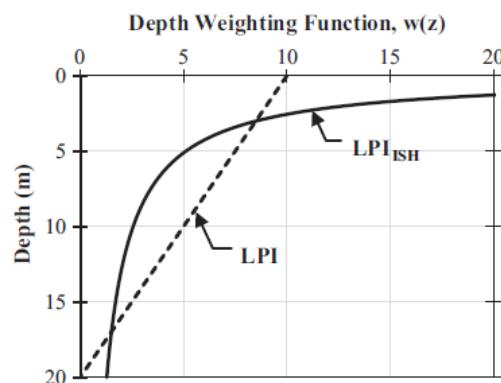


Figure 4-33: Comparison of depth weighting functions used in the LPI and LPIISH procedures (Maurer et al., 2014).



This project has received funding from the European Union's Horizon 2020 research and innovation programme under grant agreement No. 700748

For the 2010-2011 Christchurch Earthquake Sequence case study, after liquefaction triggering assessments of selected CPT profiles, LPI_{ISH} was found to be consistent with observed surface effects showing improvement over the existing LPI procedure, especially in reducing false-positive predictions (cases where manifestations were predicted but not observed), as shown in Figure 4-33.

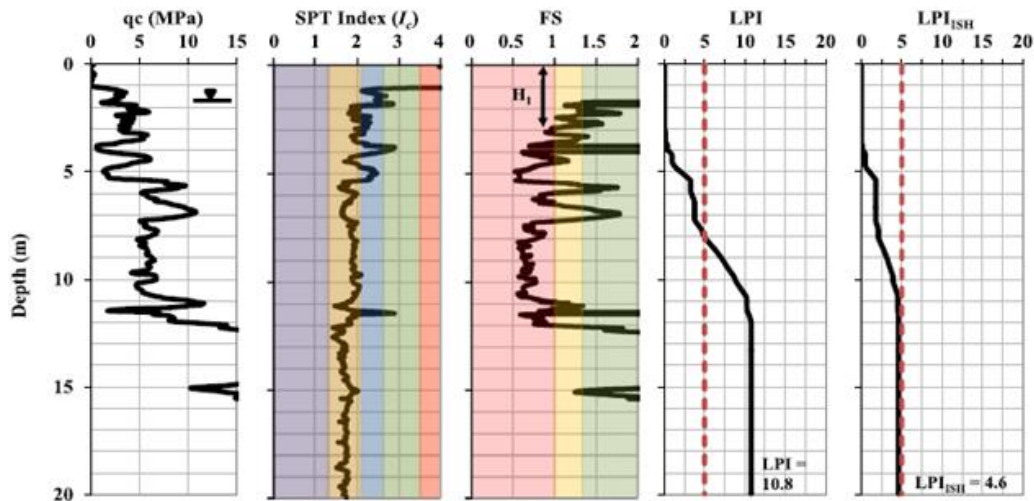


Figure 4-34: Example of CPT data for a site that showed no surficial manifestations of liquefaction during the 2010 Darfield earthquake (Maurer et al., 2015).

4.6.3 Liquefaction-induced ground settlements

Liquefaction-induced ground settlements are essentially vertical deformations of superficial soil layers caused by the densification and compaction of loose granular soils following earthquake loading. Several methods have been proposed to calculate liquefaction-induced ground deformations, including numerical and analytical methods, laboratory modeling and testing, and field-testing-based methods.

The expense and difficulty associated with obtaining and testing high quality samples of loose sandy soils may only be feasible for high-risk projects where the consequences of liquefaction may result in severe damage and large costs. Semi-empirical approaches using data from field tests are likely best suited to provide simple, reliable, and direct methods to estimate liquefaction-induced ground deformations for low to medium-risk projects and also to provide preliminary estimates for higher risk projects. The post-liquefaction volumetric strain can then be estimated using Equation 4-20, that correspond to Figure 4-35, for every reading in the CPT sounding.

For sites with level ground, far from any free face (e.g., river banks, seawalls), it is reasonable to assume that little or no lateral displacement occurs after the earthquake, such that the volumetric strain will be equal or close to the vertical strain. If the vertical strain in each soil layer is integrated with depth using the following equation:

$$S = \sum_{i=1}^j \varepsilon_{vi} \cdot \Delta Z_i$$

Equation 4-21



This project has received funding from the European Union's Horizon 2020 research and innovation programme under grant agreement No. 700748

Where:

- S is the calculated liquefaction-induced ground settlement at the CPT location;
- ϵ_{vi} is the post-liquefaction volumetric strain for the soil sublayer i;
- Δz_i is the thickness of the sublayer i;
- j is the number of soil sublayers the result should be an appropriate index of potential liquefaction-induced ground settlement at the CPT location due to the design earthquake.

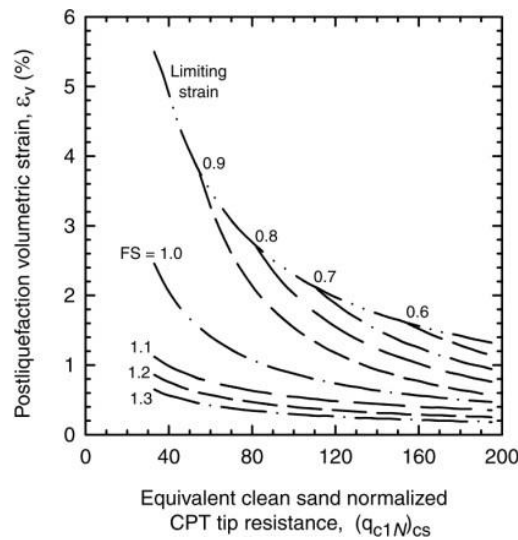


Figure 4-35: Relationship between post-liquefaction volumetric densification strains, ϵ_v , and the normalized CPT tip resistance, qc_{1N} , for selected factors of safety, FS (Zhang et al., 2002).

At each layer, the Factor of Safety (FS) and the normalised tip resistance, qc_{1N} , are used to calculate the post-liquefaction volumetric densification strain, ϵ_v . These strains are interpolated from the curves proposed by Zhang et al. (2002), except that the CPT tip resistance is corrected to remove the effect of overburden stress using the iterative Idriss and Boulanger (2014) procedure.

if	$FS \leq 0.5,$	$\epsilon_v = 102(q_{c1N})_{cs}^{-0.82}$	for	$33 \leq (q_{c1N})_{cs} \leq 200$
if	$FS = 0.6,$	$\epsilon_v = 102(q_{c1N})_{cs}^{-0.82}$	for	$33 \leq (q_{c1N})_{cs} \leq 147$
if	$FS = 0.6,$	$\epsilon_v = 2411(q_{c1N})_{cs}^{-1.45}$	for	$147 \leq (q_{c1N})_{cs} \leq 200$
if	$FS = 0.7,$	$\epsilon_v = 102(q_{c1N})_{cs}^{-0.82}$	for	$33 \leq (q_{c1N})_{cs} \leq 110$
if	$FS = 0.7,$	$\epsilon_v = 1701(q_{c1N})_{cs}^{-1.42}$	for	$110 \leq (q_{c1N})_{cs} \leq 200$
if	$FS = 0.8,$	$\epsilon_v = 102(q_{c1N})_{cs}^{-0.82}$	for	$33 \leq (q_{c1N})_{cs} \leq 80$
if	$FS = 0.8,$	$\epsilon_v = 1690(q_{c1N})_{cs}^{-1.46}$	for	$80 \leq (q_{c1N})_{cs} \leq 200$
if	$FS = 0.9,$	$\epsilon_v = 102(q_{c1N})_{cs}^{-0.82}$	for	$33 \leq (q_{c1N})_{cs} \leq 60$
if	$FS = 0.9,$	$\epsilon_v = 1430(q_{c1N})_{cs}^{-1.48}$	for	$60 \leq (q_{c1N})_{cs} \leq 200$
if	$FS = 1.0,$	$\epsilon_v = 64(q_{c1N})_{cs}^{-0.93}$	for	$33 \leq (q_{c1N})_{cs} \leq 200$
if	$FS = 1.1,$	$\epsilon_v = 11(q_{c1N})_{cs}^{-0.65}$	for	$33 \leq (q_{c1N})_{cs} \leq 200$
if	$FS = 1.2,$	$\epsilon_v = 9.7(q_{c1N})_{cs}^{-0.69}$	for	$33 \leq (q_{c1N})_{cs} \leq 200$
if	$FS = 1.3,$	$\epsilon_v = 7.6(q_{c1N})_{cs}^{-0.71}$	for	$33 \leq (q_{c1N})_{cs} \leq 200$
if	$FS = 2.0,$	$\epsilon_v = 0.0$	for	$33 \leq (q_{c1N})_{cs} \leq 2009$

Equation 4-22



This project has received funding from the European Union's Horizon 2020 research and innovation programme under grant agreement No. 700748

Manual for the assessment of liquefaction risk, defining the procedures to create the database, collect, define, symbolize and store information in the Georeferenced Information System and to perform and represent the risk analysis

Equations for the relationships plotted in Figure 4-35 are given by Zhang et al., 2002.

Table 4-14: The following additional constraints are applied to the volumetric densification calculations using the equations given in Appendix A of Zhang et al. (2002)

CALCULATION ISSUE	DESCRIPTION OR REFERENCE
Strain equation are only provided for $q_{c1}/q_{c1ncs} \geq 33$	For $q_{c1ncs} < 33$, strain is bounded by the limiting value, calculated using $q_{c1ncs} = 33$
Strain equations are only provided for specific Factors of Safety	Linear interpolation is used between the published equations
Limits on values	Maximum strain = $102 q_{c1ncs}^{-0.82}$

The Settlement indicator integrates the volumetric densification strains, ϵ_v , calculated using the Zhang et al. (2002) method, over the total depth of the CPT profile, Z , using:

$$S_{V1,d} = \int_0^Z \epsilon_v(z) dz \quad \text{Equation 4-23}$$

Where:

- $\epsilon_v(z)$ = the volumetric densification strain at depth, z , based on Zhang et al. (2002);
- Z = the total depth of the CPT profile;
- z = the depth in metres below the round surface.

There are always volumetric densification strains when the excess pore pressure rises during shaking, so strains are included for all factors of safety up to FoS = 2.0 (i.e. including non-liquefied layers). Settlements calculated using this method for deeper CPT profiles are typically greater than settlements calculated for shallower CPT profiles. The calculated values are therefore not strictly comparable between CPT profiles.

4.6.4 Liquefaction Severity Number (LSN) (van Ballegooy et al., 2014)

The LSN indicator was developed to assess the performance of residential land in Canterbury in future earthquakes and was validated against the residential land damage observed in Canterbury. The LSN depends on the seismic load, depth to groundwater and geological profile. The LSN is defined as:

$$LSN = 1000 \int_0^{20m} \frac{\epsilon_v(z)}{z} dz \quad \text{Equation 4-24}$$

Where:

- $\epsilon_v(z)$ = the volumetric densification strain at depth, z , based on Zhang et al. (2002);
- z = the depth in metres below the ground surface.

LSN is defined as the summation of the post-liquefaction volumetric reconsolidation strains calculated for each soil layer divided by the depth to the midpoint of that layer. The value of LSN is theoretically between 0 (representing no liquefaction vulnerability) to a very large number (representing extreme liquefaction



This project has received funding from the European Union's Horizon 2020 research and innovation programme under grant agreement No. 700748

Manual for the assessment of liquefaction risk, defining the procedures to create the database, collect, define, symbolize and store information in the Georeferenced Information System and to perform and represent the risk analysis

vulnerability). The hyperbolic depth weighting function ($1/z$) can yield a very large value only when the groundwater table is very close to the ground surface and soil layers immediately below the ground surface liquefy.

LSN is an extension of the LPI philosophy. It attempts to quantify the effects of liquefaction and consequent land damage using volumetric strains (adopted in conventional settlement calculations, e.g., Zhang et al. 2002). The hyperbolic function gives much greater weight to liquefaction at shallow depths and considers shallow liquefaction (<6 m) to be the key contributor in the overall damage to land and relatively light residential buildings supported on shallow foundations.

Table 4-15: LSN Ranges and observed land effects.

LSN Range	Predominant performance
0-10	Little to no expression of liquefaction, minor effects
10-20	Minor expression of liquefaction, some sand boils
20-30	Moderate expression of liquefaction, with sand boiling and some structural damage
30-40	Moderate to severe expression of liquefaction, settlement can cause structural damage
40-50	Major expression of liquefaction, undulations and damage to ground surface, severe total and differential settlement of structures
50+	Severe damage, extensive evidence of liquefaction at surface, severe total and differential settlements affecting structures

4.6.5 Liquefaction Severity Number and Equivalent Soil Profile method

Graphs showing the correspondence between ESP classes and LSN values were provided (D3.2 of this project) to allow the backward estimate of likely ESPs in a region given a liquefaction severity estimate. In fact, for the investigated profiles, the LSN was computed for four different hazard level representing: low, moderate, high and severe seismicity (PGA values equal to 0.1g, 0.2g, 0.35g, 0.5g and M_w equal to 7.5). By applying the Bayes theorem, the conditional probability of finding each ESP class for a given LSN range was evaluated and plotted for the before mentioned four levels of seismicity. The PGA values from different magnitude events can be converted to an equivalent magnitude 7.5 event using the magnitude scaling factor (Idriss and Boulanger (2008)).

The charts were simplified accounting for the original liquefaction severity classes (defined by from Tonkin and Taylor, 2013); by aggregating LSN values (Table 4-15), just four liquefaction severity classes can be obtained (Table 4-16). The simplified charts are shown in for the different expected seismic and liquefaction severity.



This project has received funding from the European Union's Horizon 2020 research and innovation programme under grant agreement No. 700748

Manual for the assessment of liquefaction risk, defining the procedures to create the database, collect, define, symbolize and store information in the Georeferenced Information System and to perform and represent the risk analysis

Table 4-16: Liquefaction severity classes for ESP classification from macro-zonation (D3.2 of this project).

SEVERITY	LSN RANGE	Tonkin and Taylor (2013) Description
Low	0-10	"Little to no expression of liquefaction, minor effects"
Moderate	10-30	"Minor expression of liquefaction, some sand boils" to "Moderate expression of liquefaction, with sand boils and some structural damage"
High	30-50	"Moderate to severe expression of liquefaction, settlement can cause structural damage" to "Major expression of liquefaction, undulations and damage to ground surface, severe total and differential settlement of structures"
Severe	>50	"Severe damage, extensive evidence of liquefaction at surface, severe total and differential settlements affecting structures, damage to services."

It can be seen (Figure 4-36) that in all cases there are many different ESP classes present. If seismic and liquefaction severity are provided at multiple return periods, then average of multiple charts can be used to be estimate the distribution of profiles.

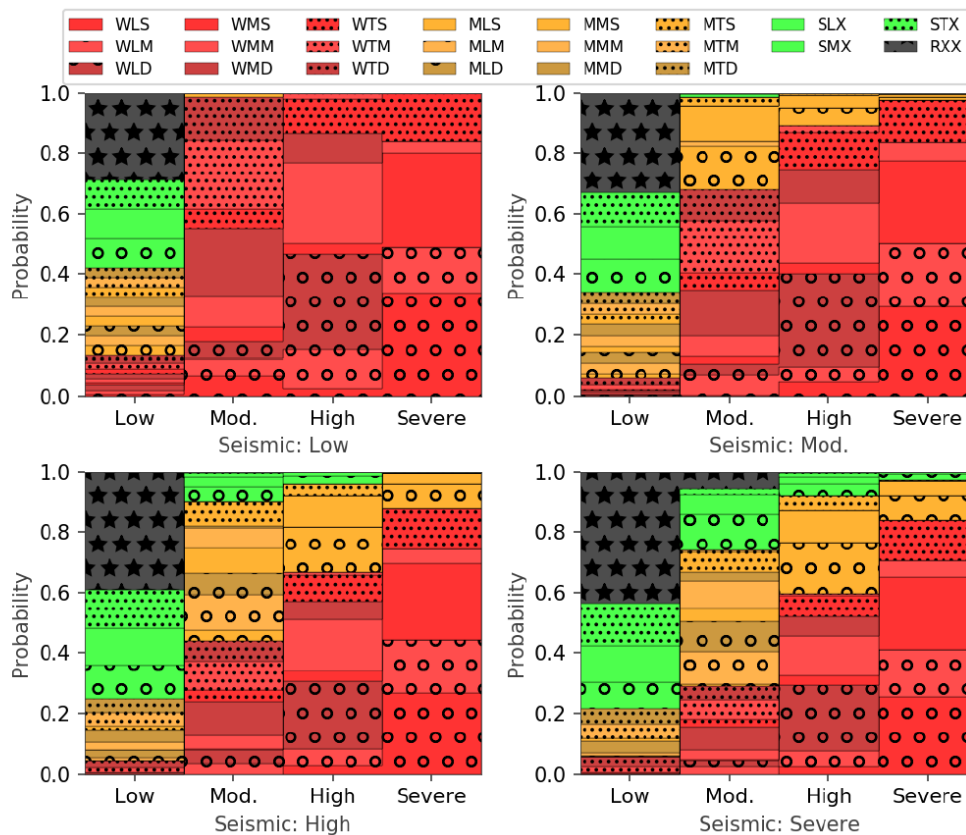


Figure 4-36: Liquefaction severity vs equivalent soil profile class for different levels of seismic hazard.

4.6.6 Zhang et al. (2004) procedure

Zhang et al. (2004) proposed a semiempirical approach to estimate liquefaction-induced lateral displacements using standard penetration test or cone penetration test. The approach combines available SPT- and CPT-based methods to evaluate liquefaction potential with laboratory test results for clean sands



This project has received funding from the European Union's Horizon 2020 research and innovation programme under grant agreement No. 700748

to estimate the potential maximum cyclic shear strains for saturated sandy soils under seismic loading. A lateral displacement index (LDI), obtained by integrating the maximum cyclic shear strains with depth, is introduced.

Such procedure can be summarized in the following four steps.

Step 1: Assess the liquefaction potential using either the NCEER SPT- or CPT-based methods.

Step 2: Calculate the Lateral Displacement Index (LDI)

$$LDI = \int_0^{Z_{max}} \gamma_{max} dz$$

Equation 4-25

Where:

- Z_{max} [m] is the maximum depth below all the potential liquefiable layers with a calculated $FS < 2.0$ (in any case minor than 23 m that is beyond the range of liquefaction);
- γ_{max} is the maximum cyclic shear strain.

Relationship between maximum cyclic shear strain and factor of safety for different relative densities D_r for clean sands (after Ishihara and Yoshimine, 1992) are proposed in Equation 4-26 (and Figure 4-37).

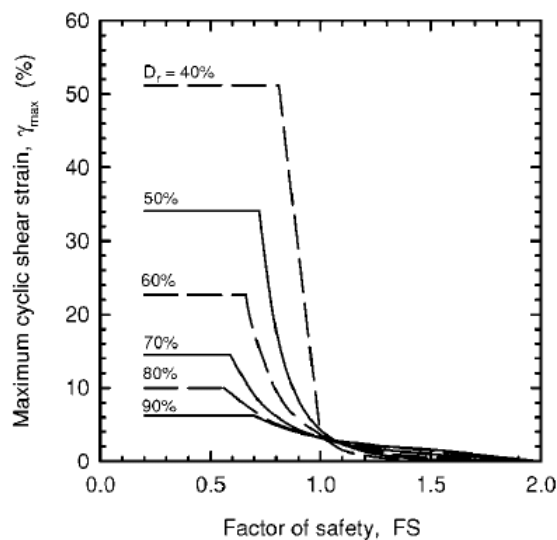


Figure 4-37: Relationship between maximum cyclic shear strain and factor of safety for different relative densities D_r for clean sands (Zhang et al., 2004).



This project has received funding from the European Union's Horizon 2020 research and innovation programme under grant agreement No. 700748

Manual for the assessment of liquefaction risk, defining the procedures to create the database, collect, define, symbolize and store information in the Georeferenced Information System and to perform and represent the risk analysis

<i>if</i> $Dr = 90\%$	$\gamma_{max} = 3.26 \cdot (FS)^{-1.80}$	<i>for</i> $0.7 \leq FS \leq 2.0$
<i>if</i> $Dr = 90\%$	$\gamma_{max} = 6.2$	<i>for</i> $FS \leq 0.7$
<i>if</i> $Dr = 80\%$	$\gamma_{max} = 3.22 \cdot (FS)^{-2.08}$	<i>for</i> $0.56 \leq FS \leq 2.0$
<i>if</i> $Dr = 80\%$	$\gamma_{max} = 10$	<i>for</i> $FS \leq 0.56$
<i>if</i> $Dr = 70\%$	$\gamma_{max} = 3.2 \cdot (FS)^{-2.89}$	<i>for</i> $0.59 \leq FS \leq 2.0$
<i>if</i> $Dr = 70\%$	$\gamma_{max} = 14.5$	<i>for</i> $FS \leq 0.59$
<i>if</i> $Dr = 60\%$	$\gamma_{max} = 3.58 \cdot (FS)^{-4.42}$	<i>for</i> $0.66 \leq FS \leq 2.0$
<i>if</i> $Dr = 60\%$	$\gamma_{max} = 22.7$	<i>for</i> $FS \leq 0.66$
<i>if</i> $Dr = 50\%$	$\gamma_{max} = 4.22 \cdot (FS)^{-6.39}$	<i>for</i> $0.72 \leq FS \leq 2.0$
<i>if</i> $Dr = 50\%$	$\gamma_{max} = 34.1$	<i>for</i> $FS \leq 0.72$
<i>if</i> $Dr = 40\%$	$\gamma_{max} = 3.31 \cdot (FS)^{-7.97}$	<i>for</i> $1.0 \leq FS \leq 2.0$
<i>if</i> $Dr = 40\%$	$\gamma_{max} = 250 \cdot (1 - FS) + 3.5$	<i>for</i> $0.81 \leq FS \leq 1.0$
<i>if</i> $Dr = 40\%$	$\gamma_{max} = 51.2$	<i>for</i> $FS \leq 0.81$

Equation 4-26

Zhang et al. (2004) suggest adopting the correlation between Dr and cone tip resistance q_c of Tatsuoka et al. (1990).

$$Dr = -85 + 76 \log(q_{c1N}) \quad (q_{c1N} \leq 200)$$

Equation 4-27

where q_{c1N} is the normalized CPT tip resistance corrected for effective overburden stresses corresponding to 100 kPa (Robertson and Wride, 1998). This correlation provides slightly smaller and more conservative estimates of relative density than the correlation by Jamiolkowski et al. (1985) when q_{c1N} is less than about 100.

Although LDI has the units of displacement, it is intended only to provide an index to quantify potential lateral displacements for a given soil profile, soil properties, and earthquake characteristics. The actual magnitude of lateral displacement depends on both LDI and geometric parameters characterizing ground geometry.

Step 3: Knowing ground slope (S) or/and free face height (H) and the distance to a free face (L), estimate the lateral displacement (LD) using either:

$$LD = (S + 0.2) \cdot LDI \quad \text{for } (0.2\% < S < 3.5\%)$$

Equation 4-28

for gently sloping ground without a free face, or:

$$LD = 6 \cdot \left(\frac{L}{H}\right)^{-0.8} \cdot LDI \quad \text{for } (4 < L/H < 40)$$

Equation 4-29

for level ground with a free face (Figure 4-37).

The proposed approach is recommended within the ranges of earthquake properties and ground conditions, namely moment magnitude of earthquake between 6.4 and 9.2, peak surface acceleration between 0.19g and 0.6g, and free face heights less than 18 m (Figure 4-37).



This project has received funding from the European Union's Horizon 2020 research and innovation programme under grant agreement No. 700748

Manual for the assessment of liquefaction risk, defining the procedures to create the database, collect, define, symbolize and store information in the Georeferenced Information System and to perform and represent the risk analysis

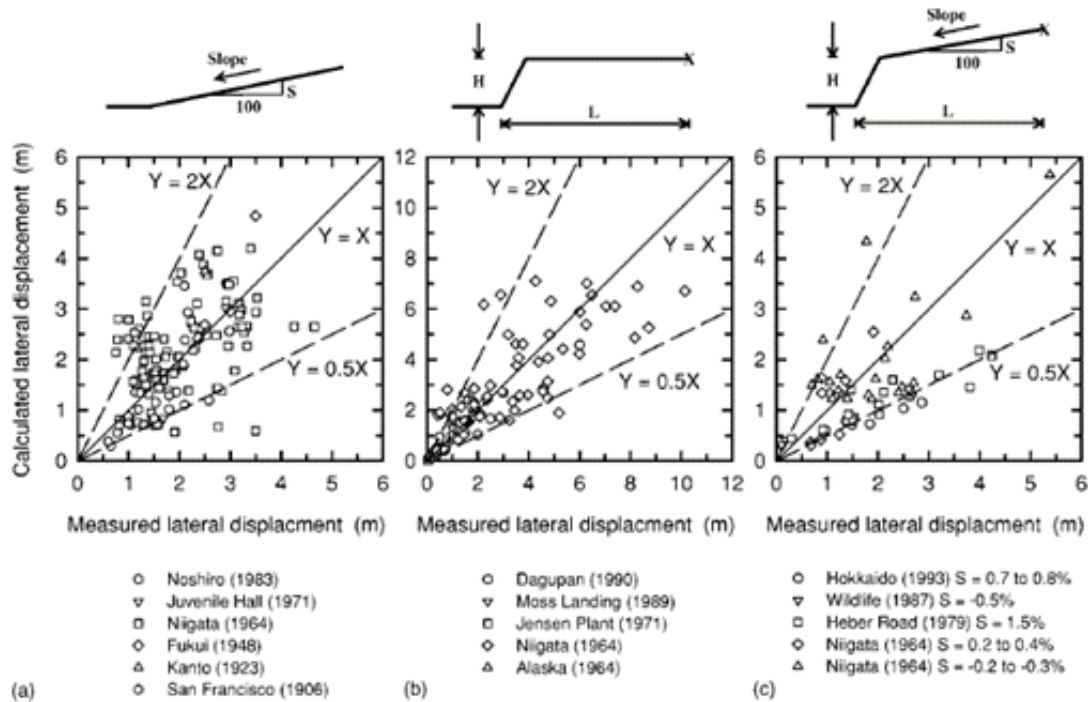


Figure 4-38: Comparison of measured lateral displacements less than 1 m and calculated lateral displacements for the available case histories for: a) gently sloping ground without a free face; b) level ground with a free face; and c) gently sloping ground with a free face (Zhang et al., 2004).

Given the complexity of liquefaction-induced lateral spreads, considerable variations in magnitude and distribution of lateral displacements are expected. As observed by the authors after the analysis of the available case histories, the calculated lateral displacements using the LDI approach showed variations between 50 and 200% of measured values. The accuracy of “measured” lateral displacements for most case histories is about ± 0.1 to ± 1.92 m.

4.6.7 Zhu et al. (2015) method

Alternative to the liquefaction potential indicators, empirical functions (Zhu et al., 2015) can be employed to predict liquefaction probability specifically for use in rapid response and loss estimation over large areas.

They use predictor variables that are readily accessible, such as $V_{s,30}$ and do not require any specialist knowledge to be applied. For a given set of predictor variables, the probability of liquefaction is given by the function:

$$P [liq] = \frac{1}{1 + e^{-x}} \quad \text{Equation 4-30}$$

where X is a linear function of the predictor variables accounting for the geology and the expected seismicity of an area. Concerning the X function, Zhu et al. (2015) proposed three linear models that are applicable to the Canterbury region: a specific local model for Christchurch; a regional model for use in coastal sedimentary basins (including Christchurch) and a global model that is applicable more generally.



This project has received funding from the European Union's Horizon 2020 research and innovation programme under grant agreement No. 700748

Manual for the assessment of liquefaction risk, defining the procedures to create the database, collect, define, symbolize and store information in the Georeferenced Information System and to perform and represent the risk analysis

Within the Liquefact project, a specific model applicable to the European territory was developed and proposed by WP2.

For applicability within the insurance sector, this model presents an advantage over traditional indicators since it was defined for large scale problems and the only parameter that requires engineering judgment is the selection of ground motion prediction equation if ShakeMap or equivalent data is not available.

4.7 Summary of the procedure for the assessment of Liquefaction Hazard

The above defined methodology, with the subsequent evaluation of susceptibility, triggering and hazard and the preparation of microzonation maps is summarised in the flowchart of Figure 4-39. Figure 4-40 reports an example of database preparation with reference of CPT, SPT and V_s tests, Figure 4-41 reports an example of susceptibility analysis, Figure 4-42 shows an example of characterisation of seismic scenario, and Figure 4-43 a typical output of liquefaction hazard analysis.



This project has received funding from the European Union's Horizon 2020 research and innovation programme under grant agreement No. 700748

Manual for the assessment of liquefaction risk, defining the procedures to create the database, collect, define, symbolize and store information in the Georeferenced Information System and to perform and represent the risk analysis

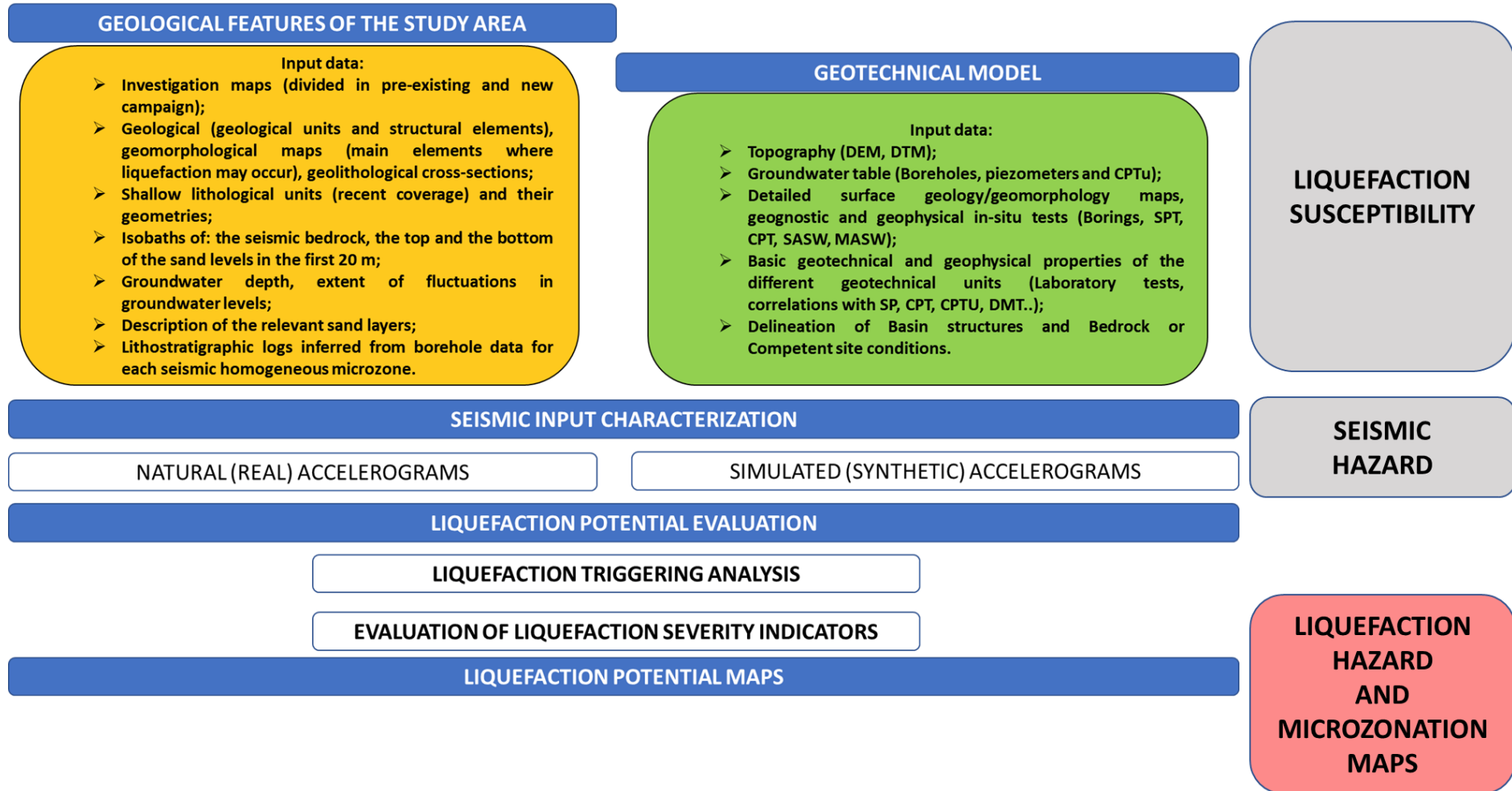


Figure 4-39: Flowchart of the general methodology to evaluate the liquefaction potential on a given area, according to criteria defined for microzonation studies



This project has received funding from the European Union's Horizon 2020 research and innovation programme under grant agreement No. 700748

Manual for the assessment of liquefaction risk, defining the procedures to create the database, collect, define, symbolize and store information in the Georeferenced Information System and to perform and represent the risk analysis

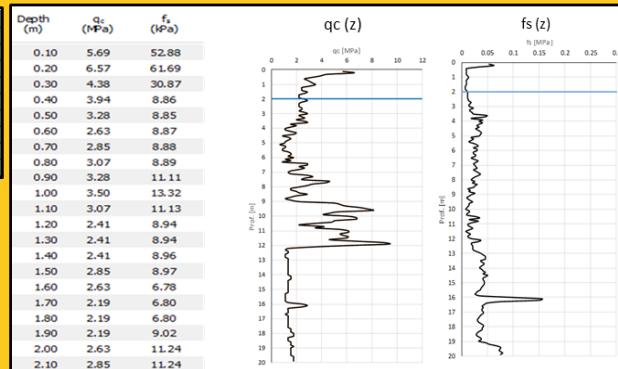
INPUT DATA PREPARATION GENERAL INPUT DATA

ID-PROFILE	Long.	Lat.	TEST	Groundwater depth (m)
001	11.4073	44.8041	BOREHOLE	2.00
002	11.4101	44.7992	CPT	1.50
003	11.4088	44.8101	SPT	2.00
004	11.4090	44.8056	Vs PROFILE	3.20

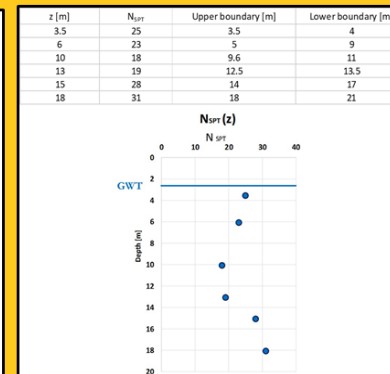
EXAMPLE OF BOREHOLE INPUT DATA

N. Strata	Upper limit (m)	Lower limit (m)	SBT
1	0.00	2.00	3
2	2.00	4.00	4
3	4.00	7.10	2
4	7.10	13.90	3
5	13.90	18.90	6
6	18.90	24.00	3
7	24.00	29.00	5
8	29.00	37.00	3
9	37.00	40.00	6

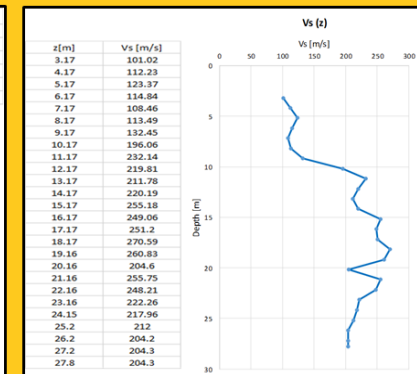
EXAMPLE OF CPT PROFILE



EXAMPLE OF SPT PROFILE



EXAMPLE OF VS PROFILE



*Both general and specific Input data must be given in .csv format.

Figure 4-40: Example of input data preparation



This project has received funding from the European Union's Horizon 2020 research and innovation programme under grant agreement No. 700748

Manual for the assessment of liquefaction risk, defining the procedures to create the database, collect, define, symbolize and store information in the Georeferenced Information System and to perform and represent the risk analysis

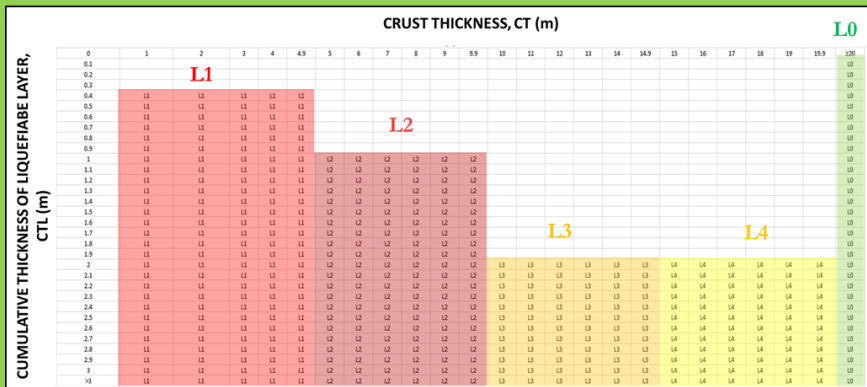
LIQUEFACTION SUSCEPTIBILITY ANALYSIS

Semi-automated procedures to define a three strata profile, by evaluating the crust thickness ($H1$) and the cumulative thickness of liquefiable layer ($H2$).

METHODOLOGIES

Microzonation Criteria

- BOREHOLE and CPT - based



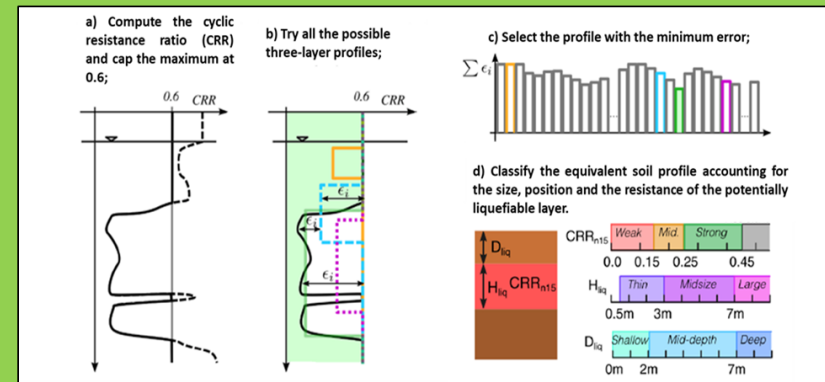
OUTPUT

Punctual level of Liquefaction Susceptibility

Maps of liquefaction susceptibility (in terms of $H1$, $H2$ and/or mean CRR) can be obtained through geostatistical interpolation of the results.

Equivalent Soil Profile method

- CPT - based



OUTPUT

Definition of an Equivalent Soil Profile

Figure 4-41: Example of liquefaction susceptibility analysis



This project has received funding from the European Union's Horizon 2020 research and innovation programme under grant agreement No. 700748

Manual for the assessment of liquefaction risk, defining the procedures to create the database, collect, define, symbolize and store information in the Georeferenced Information System and to perform and represent the risk analysis

CHARACTERIZATION OF SEISMIC SCENARIOS

METHODOLOGY CALCULATIONS SHAKEMAPS

ID	Lat.	Long.	Focal Depth (km)	Magnitude	Strike	Dip	Fault Mechanism
1	44.89	11.23	6	5.9	0: north	0: horizontal	Inverse
2	44.86	11.37	5	5.1	0: north	0: horizontal	Inverse
3	44.83	11.49	4.7	5.1	0: north	0: horizontal	Inverse
4	44.85	11.09	10.2	5.8	0: north	0: horizontal	Inverse
5	44.89	11.01	6.8	5.3	0: north	0: horizontal	Inverse
6	44.88	10.95	5.4	5.2	0: north	0: horizontal	Inverse
7	44.9	10.94	9.2	5.1	0: north	0: horizontal	Inverse

➤ Definition of:

Latitude, Longitude, Focal Depth, Magnitude and Fault Mechanism.

➤ Selection of GMPE.

USER-DEFINED SHAKEMAPS

Latitude	Longitude	PGA (g)	Sa(T=0,1s)	Sa(T=0,2s)	Sa(T=0,3s)	Sa(T=0,4s)	Sa(T=0,5s)	Sa(T=0,75s)
59,959075	11,037236	0,1664	0,291	0,3741	0,3375	0,2886	0,2559	0,207
59,959075	11,040013	0,1793	0,3144	0,4045	0,3617	0,3081	0,2724	0,2188
59,959131	11,042987	0,1917	0,3368	0,4336	0,385	0,3269	0,2882	0,2302
59,959136	11,046358	0,2073	0,363	0,4668	0,415	0,3512	0,3086	0,2447
59,959114	11,049509	0,2213	0,3875	0,4983	0,4423	0,3734	0,3274	0,2584
59,959175	11,05353	0,2386	0,4182	0,5379	0,4733	0,3985	0,3485	0,2737
59,959224	11,057067	0,255	0,4473	0,5756	0,5028	0,4222	0,3685	0,2879
59,957658	11,037612	0,2759	0,4849	0,6242	0,5407	0,4527	0,3941	0,3061
59,957636	11,041798	0,2947	0,5185	0,6678	0,5767	0,4818	0,4185	0,3236
59,957647	11,046568	0,3188	0,5609	0,7224	0,626	0,5215	0,4518	0,3473
59,957686	11,052836	0,3415	0,601	0,774	0,6696	0,557	0,4819	0,3694
59,95768	11,057132	0,3727	0,6559	0,8446	0,7243	0,6022	0,5208	0,3986
59,955651	11,05711	0,4017	0,708	0,9122	0,7764	0,6447	0,5568	0,4251
59,955673	11,051944	0,4401	0,7792	1,0053	0,8531	0,7066	0,609	0,4625
59,955772	11,045698	0,4766	0,8424	1,0862	0,9269	0,7664	0,6594	0,4988
59,955866	11,041082	0,5339	0,9386	1,2084	1,0313	0,8522	0,7328	0,5537
59,955976	11,037546	0,585	1,0302	1,327	1,1254	0,9307	0,801	0,6063
59,953929	11,037503	0,6636	1,1668	1,5023	1,2776	1,0562	0,9087	0,6873

➤ Definition of PGA and Sa (from 0.1 to 5s),
(.csv or .shp format).

PRE-DEFINED SEISMIC HAZARD MODEL

➤ Choice of a Return
Period (T).

Ground Amplification Profiles (through Vs₃₀ values)

Ground Amp. Profile	Latitude	Longitude	Soil (Vs30 m/s)
VP-0001	42.3534	11.56788	200

Figure 4-42: Example of characterization of seismic scenarios.



This project has received funding from the European Union's Horizon 2020 research and innovation programme under grant agreement No. 700748

Manual for the assessment of liquefaction risk, defining the procedures to create the database, collect, define, symbolize and store information in the Georeferenced Information System and to perform and represent the risk analysis

LIQUEFACTION HAZARD ANALYSIS

Semi-automated procedures to evaluate the most known liquefaction severity indicators (LPI , LPI_{ish} , w , LSN , LDI).

METHODOLOGIES

- CPT - based

Boulanger & Idriss, 2014

- SPT - based

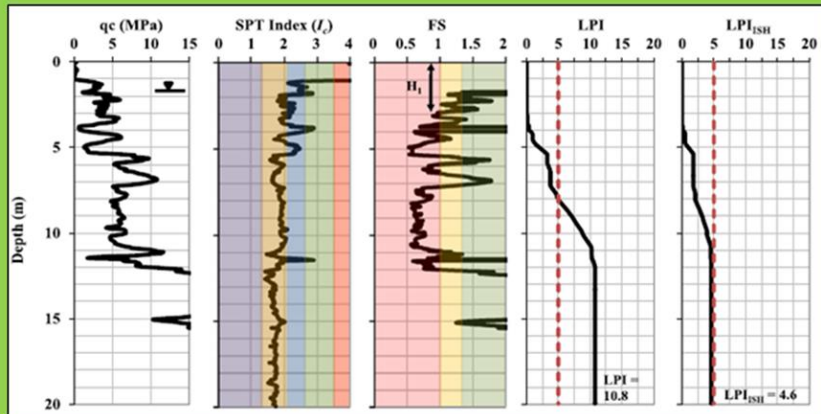
Boulanger & Idriss, 2014

- V_s - based

Andrus & Stokoe, 2000

OUTPUT

Liquefaction Potential of each profile



Example of Liquefaction potential assessed for a CPT profile.

Spatial Analysis



Example of Liquefaction Severity Map over an urban scale.

Figure 4-43: Example of liquefaction hazard analysis



This project has received funding from the European Union's Horizon 2020 research and innovation programme under grant agreement No. 700748

5. HAZARD AND RISK

5.1 Introduction

Risk measures the expected value of an undesirable outcome and is obtained as the combination into a single value of the probabilities of various possible events with the corresponding harm:

$$\text{Risk} = \text{Probability of an undesired event} * \text{Loss estimated for the event} \quad \text{Equation 5-1}$$

There are many formal methods to quantify risk. Often the probability of a negative event is estimated by using the frequency of past similar events, but for rare failures this approach becomes cumbersome. This makes risk assessment difficult in hazardous systems where the frequency of failures is rare, while harmful consequences of failure are severe. Statistical methods may also require the use of a cost function, which in turn may require the calculation of the cost for instance of human life losses.

The definition given by the United Nations Disaster Relief Office (UNDRO, 1979) states that risk is the expected number of lives lost, persons injured, damage to property and disruption of economic activity due to a natural phenomenon (like earthquakes and liquefaction). From an operative viewpoint, risk can be computed as the product of specific risk and elements at risk combining Hazard, Exposure and Vulnerability, as follows:

$$\text{Risk} = \text{Hazard} * \text{Vulnerability} * \text{Exposure} \quad \text{Equation 5-2}$$

As shown in chapter 4, liquefaction susceptibility, triggering and ground effects are deterministically evaluated without explicitly considering the uncertainty related to the various components of the analysis or the performance metric. However, considering this issue is central as the knowledge of nearly all factors, ground motion, subsoil and building properties is affected by aleatory and epistemic uncertainties. Performance-based earthquake engineering offers a rational and consistent way to consider uncertainty through probabilistic evaluations. For a generic system with its lifecycle, a risk of any nature can be computed writing the following convolution integral that convolutes the probability of demand $p(D)$ (Hazard) and the consequent losses connected to the demand $P(L|D)$ (Vulnerability):

$$P(L) = \int_D P(L|D) * p(D) \quad \text{Equation 5-3}$$

A correct application of Equation 5-3 should separately disclose and quantify the uncertainties on:

- the potentially critical scenarios
- the models describing the response of the system
- the quantification of relevant parameters
- the risk evaluation



This project has received funding from the European Union's Horizon 2020 research and innovation programme under grant agreement No. 700748

For seismic risk, Equation 5-3 can be expressed applying the performance-based earthquake assessment (PEBA) cascade methodology defined by the Pacific Earthquake Engineering Research (PEER) Center (Cornell & Krawinkler 2000) and depicted in figure 2.6. Equation 5-3 is transformed as follows where the function $p(D)$ is exploded considering the different factors defining the cascade phenomenon:

$$P(L) = \int_{IM} \int_{EDP} \int_{DM} P(VD|DM) * p(DM|EDP) * p(EDP|IM) * p(IM) \quad \text{Equation 5-4}$$

$p(IM)$ is the probability that a seismic event of intensity measure IM occurs during the lifecycles of the system, $p(EDP|IM)$ is the density probability of the engineering demand parameter (EDP) for the given IM , $p(DM|EDP)$ is the probability that a physical damage occurs on the structural component of the system for a given EDP and $P(VD|DM)$ is an cumulative probability of the assumed evaluator of the system performance for a given damage DM (Lee and Mosalam 2006; Moehle 2003; Porter 2003; Comerio 2005; Krawinkler 2005; Mitrani-Reiser et al. 2006).

Considering the sequence of subsystems involved in seismic liquefaction (see Figure 2-7 and Figure 2-11), the PEBA methodology can be expressed quantifying the uncertainties on earthquake intensity, ground motion, structural response, physical damage, and economic or human losses. In particular, the earthquake can be considered as the primary hazard factor and liquefaction occurs if the soil has specific characteristics, namely a grain size distribution composed of sand with limited fine content, sufficiently low density and saturation. Therefore, the combination of earthquake and subsoil response determines the demand for the structure positioned at the ground level. However, physical damage for the latter can be computed considering the subsoil-structures as a unique coupled system or evaluating the response of the two components separately. In the first case the earthquake intensity measure IM becomes also the engineering demand parameter EDP and the vulnerability function $p(DM|EDP)$ quantifies the response of the subsoil-structure system for the given seismic input. In the second case, the soil response provides the demand function $p(EDP|IM)$ for the structure and physical vulnerability is computed considering the $p(DM|EDP)$ function for the sole structure. HAZUS code (FEMA 1998) adopts this second approach considering soil liquefaction in a group of secondary hazards called ground failures affecting building assets and infrastructure networks.

Physical damage represents the demand for the delivery capability of the system whose vulnerability is defined by a function that relates the loss of serviceability to the different levels of damage. Finally, the latest level of risk assessment concerns the community: it is harmed by the loss of safety and serviceability and risk can be assessed in terms of deaths, injuries, loss of incomes, damage to cultural and environmental heritage.

The terms of Equation 5-4 can be quantified in different manners, sometimes with probabilistic inference of statistical observations, sometimes applying theoretical models with stochastically variable inputs, sometimes with less objective procedures. For instance, it is customary to express severity of damage in terms of financial losses based on expert judgement, qualitative estimates or even rules of thumb that make the process unavoidably subjective.

Some of the relations of Equation 5-4 (e.g. $p(A|B)$ with A and B indicating generic variables) can be established on a deterministic basis ($A=f(B)$). In this case $p(A|B)$ can be expressed with a Dirac function, i.e. equal to ∞



This project has received funding from the European Union's Horizon 2020 research and innovation programme under grant agreement No. 700748

for $A=f(B)$ or 0 for $A \neq f(B)$. The above issues are addressed in the next paragraphs looking at the different factors concurring to determine liquefaction.

Seismic Hazard (UNDRO, 1977) is the occurrence probability, for a given system in a specific timelength, of a certain potentially damaging earthquake scenario. Applying the same definition, liquefaction hazard can be quantified for a generic system (a building, an infrastructure, a district, a community) as the probability that a given liquefaction severity (identified with a demand parameter) will be produced during the lifetime of the structure. In chapter 4 liquefaction demand has been expressed through different indicators following a logic applied in many countries (e.g. DPC 2017, MBIE 2016, Yasuda and Ishikawa, 2018). However, it must be pointed out that these indicators are computed for free field conditions, i.e. without considering the characteristics of the structure under concern, and thus neglecting an important contribution to the response of the system.

Vulnerability is the possibility that damage in structures/infrastructure, potential human and/or financial loss occur in the assessed area when exposed to a particular hazard. This is generally represented in the form of fragility/vulnerability curves which show the relationship between the level of earthquake effect and the level of damage/loss of either one of the previously mentioned entities. For instance, building fragility curves are lognormal functions that describe the probability of reaching, or exceeding, structural and nonstructural damage states, for a given median estimates of IM or EDP. These curves take into account the variability and uncertainty associated with capacity curve properties, damage states and ground shaking. The Hazus (FEMA 1999) fragility curves distribute damage among Slight, Moderate, Extensive and Complete damage states. For any given value of spectral response, discrete damage-state probabilities are calculated as the difference of the cumulative probabilities of reaching, or exceeding, successive damage states (Figure 5-1). The probabilities of a building reaching or exceeding the various damage levels at a given response level sum to 100%.

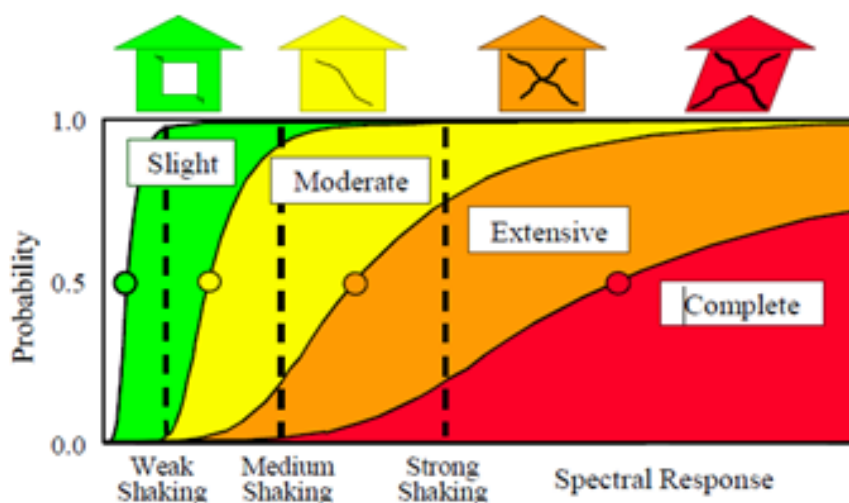


Figure 5-1: Qualitative example Fragility Curves for Slight, Moderate, Extensive and Complete Damage (FEMA, 1999).

Those functions can be constructed both on the basis of the observed damages experienced in past seismic events and of the non-linear structural analyses. In the past, empirical approach was largely adopted worldwide. The major shortcoming of the empirical approach is however its accuracy and completeness, since the database of damage observations may not include all the possible cases.



This project has received funding from the European Union's Horizon 2020 research and innovation programme under grant agreement No. 700748

Exposure is a quantification of the entities in the assessed area. This includes the people and buildings, the number and type of important infrastructures and the amount of industrial and commercial activities.

Given the above, the basic steps in a liquefaction risk assessment (Figure 5-2) are:

- Hazard Analysis that includes the identification of earthquake sources, modelling of the occurrence of earthquakes from these sources, estimation of the attenuation of ground motions between these sources and the study area, evaluation of the site effects of soil amplification, evaluation of liquefaction susceptibility, triggering and liquefaction-induced permanent ground deformations (PGDf). Since Hazard analysis was the focus of the previous chapter, it will not be discussed in the following.
- Inventory Collection (depending on the study detail level): identification of structures and infrastructure exposed to damage, classification of the built asset according to their vulnerability to damage, classification of the occupancy of the buildings and facilities.
- Damage Modelling: modelling of the performance of the inventory classes under ground shaking and seismic liquefaction, development of damage functions (relationship between levels of damage and corresponding demand), estimation of the combined damage to the inventory by introducing relationships between damage and a series of earthquake intensity measures (IMs) or Liquefaction Severity Indicators. In principle seismic and liquefaction hazard cannot be decoupled, although they produce different effects on buildings and infrastructures. The issue of combined ground shaking and liquefaction has been largely debated. More often buildings that have undergone liquefaction do not exhibit ground shaking damage, giving the idea that a base isolation could be induced by the liquefied soil on the building. However, evidences of buildings damaged by both shaking and liquefaction suggest that severe ground shaking might take place before the groundwater pressure builds up. Bird et al. (2005) claim that the differential settlement induced by liquefaction on framed buildings causes a drift of columns additional to that produced by shaking and thus structures previously affected by shaking are more vulnerable to liquefaction. Following this idea, these authors propose a cumulative analytical methodology considering permanent shaking deformation as a reduction of the building capacity against liquefaction. The connection between the two mechanisms is even more evident for masonry structures.
- Loss Estimation: estimation of direct losses due to damage repair costs, estimation of indirect losses due to loss of function of the inventory, estimation of casualties caused by the selected scenario and estimation of social impact on the whole community.



This project has received funding from the European Union's Horizon 2020 research and innovation programme under grant agreement No. 700748

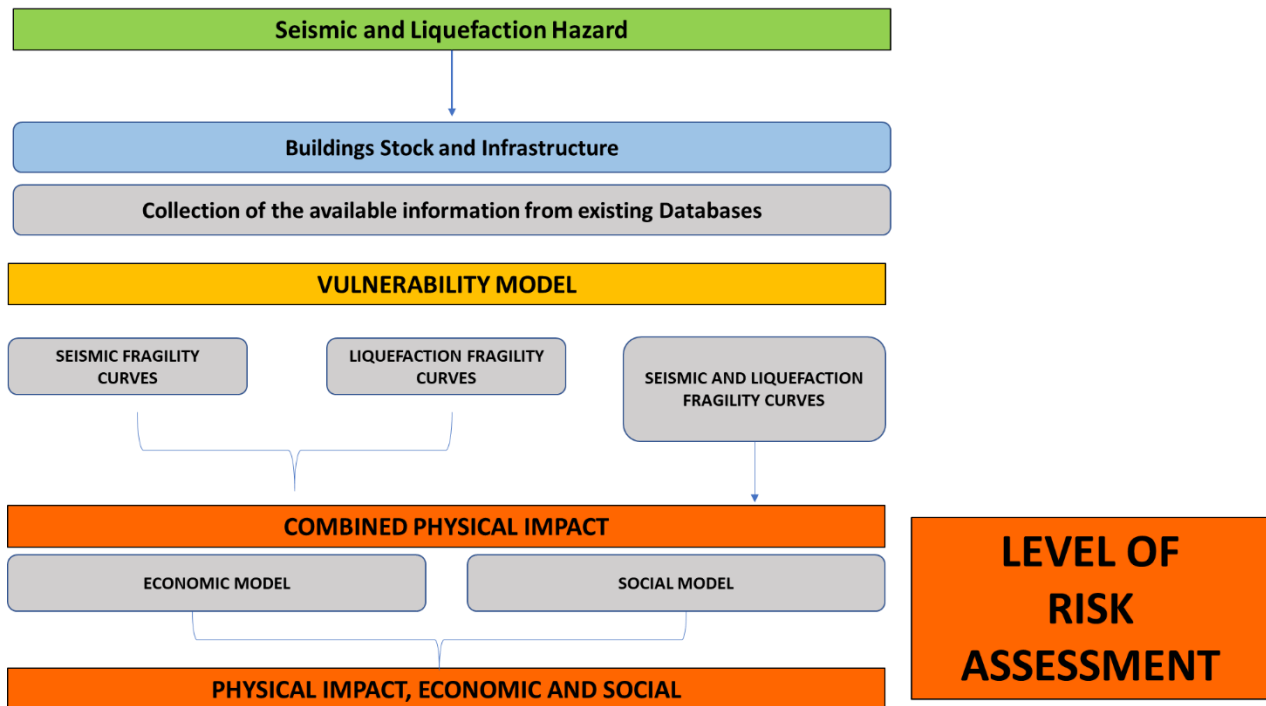


Figure 5-2: Flowchart for the risk assessment

5.2 Inventory Collection and scale level definition

5.2.1 Scale level definition

Earthquake damage and loss studies can be conducted at different scales and resolution. However, in contrast to seismic hazard studies, risk studies have certain restrictions with respect to the maximum size of the study area under consideration. For instance, the study of a scenario earthquake is constricted to a certain region where seismic hazard and local site response is known. As shown in chapter 4, the study of local effects requires to collect the most detailed subsoil information. Additionally, performing risk assessment over larger areas increases the required inventory data, efforts for data preparation as well as computation time. Considering that one of the major components of earthquake risk is exposure, this implies that risk assessment must be restricted to those areas where physical assets are located, i.e. buildings and infrastructure components, and people are living, neglecting country areas possibly affected by significant hazard but limited or nil risk. In this respect, seismic or liquefaction risk studies significantly differ from hazard studies which solely consider earthquake activity and the expected ground motion, or the permanent ground deformation, estimates likely to occur at any site whether populated or not. In addition to the total extent of the study area, the study's resolution will be of importance. Earthquake Loss Estimation studies can however be conducted for an entire country, a region, a city (or a city block) or individual project (house, industrial facility etc.), Figure 5.3.



This project has received funding from the European Union's Horizon 2020 research and innovation programme under grant agreement No. 700748

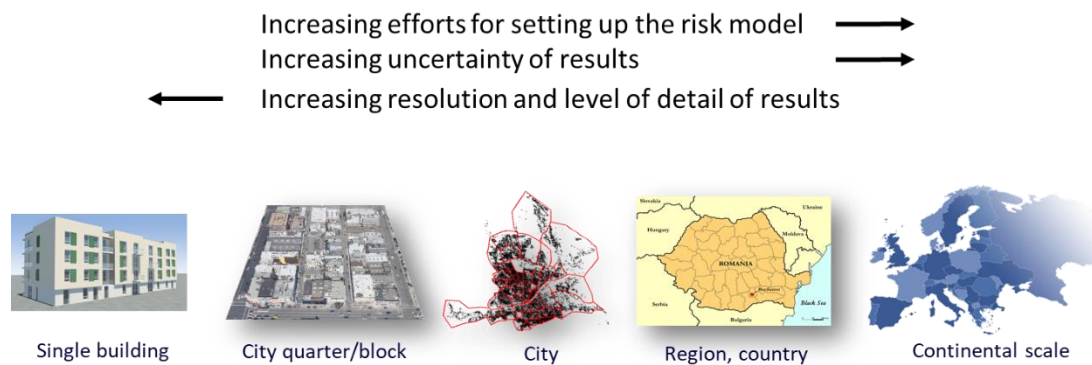


Figure 5-3: Different levels of the study area size can be selected. The extent of the study area affects the resolution and efforts to make. It is directly related to the needed resolution and level of detail of the end results (Lang, 2012).

The highest level of resolution is generally achieved on individual buildings (or individual elements constituting a network) where inventory databases and computational capacities become more precise and sophisticated. In this case, the mechanical response of soil-structure interaction can be analysed deterministically choosing the most detailed constitutive models.

On the other extreme, bigger study areas like entire regions or urban and rural inventory settings will require several assumptions and simplifications with respect to the inventory database. This means that structures will not be characterised individually with all their structural peculiarities but will be merged into classes that are believed to show, on average, the same damage behaviour under earthquake demands. This procedure of course strongly affects the reliability of the results derived for the individual structure that will be seen in probabilistic terms. An example is given by the fragility curves shown in Figure 5-1.

For this assessment, the study area generally must be divided into a number of subsets, called geo-units. They should be (Lang & Aldea, 2011) as many as possible to identify local variations in damage and loss estimates providing sufficient detail.

In a practical situation, the size of the study area will be governed by the respective geographical conditions and by the interest dictating the analysis. The resolution of the study and its results will however be decided by the level of detail of available inventory data or how much effort one is willing to spend while generating an inventory database. The resolution will further depend on the study's initial purpose and the end users of the derived results (strengthening and mitigation studies, emergency response, (re)insurance).

5.2.2 Inventory of element at risk

Once the study area is defined, an exposure model of the element at risk needs to be developed to perform risk and loss assessment. Based on RISK-UE experience, emphasis must be made on:

- Population density repartition.
- Main institutional actors and decision makers.



This project has received funding from the European Union's Horizon 2020 research and innovation programme under grant agreement No. 700748

- Public buildings.
- Utility systems: Water, Sanitation, Electricity, Gas, Liquid fuel, Radio, Telecommunication, ...
- Transportation: Roadways, Railways, Harbours, Airports, ...
- Essential facilities: Critical facilities (dangerous plants or industries); Strategic constructions in terms of crisis management (hospitals, fire, etc.); Main economic issues or facilities in terms of employment, production, trade and services (industrial plants, trade centres, main services, etc.).
- Cultural and historical patrimony.

Concerning the element at risk, the HAZUS-MH (FEMA, 2003) Methodology defines the following classes:

- General building stock: the commercial, industrial and residential buildings in the studied region are not considered individually when calculating losses. Instead, they are grouped together into 36 model building types and 28 occupancy classes and degrees of damage are computed for groups of buildings.
- Essential facilities: these include medical care facilities, emergency response facilities and schools. Specific information is compiled for each building so the loss-of function is evaluated in a building-by-building basis.
- Transportation lifeline systems: these include highways, railways, light rail, bus systems, ports, ferry system and airports and they are broken in components such as bridges, stretches of roadway or track, terminal, and port warehouses. The damage and losses are computed for each component of each lifeline.
- Utility lifeline systems: these include potable water, electric power, waste water, communications, and liquid fuels (oil and gas) and are treated in a manner similar to transportation lifelines.
- High-potential loss facilities: these include dams, nuclear power plants, or military installations which need supplementary specific studies to be evaluated.

5.3 Damage modelling

Since the earthquake represents a demand for structures and infrastructures, vulnerability is the link between such demand and the expected/observed damage. To assess the expected physical damage to the considered element at risk (building, bridge, embankment, water supply etc...) for a given input parameter, e.g. PGA, Intensity Measure or permanent ground deformation (PGD), fragility curves are commonly used in seismic and liquefaction risk assessment. They relate the demand for the structure/infrastructure to predefined damage states.

In general terms, fragility curves are lognormal functions that describe the probability of reaching, or exceeding, structural and nonstructural damage states, given median estimates of spectral response, for example spectral acceleration or displacement.

For instance, building damage varies from “none” to “complete” as a continuous function of building deformations (building response). Wall cracks may vary from invisible or “hairline cracks” to cracks of several inches wide. Since it is not practical to describe building damage as a continuous function, the Hazus - Methodology predicts a structural and nonstructural damage state in terms of one of four ranges of damage or “damage states”: Slight, Moderate, Extensive, and Complete. For example, the Slight damage state



This project has received funding from the European Union's Horizon 2020 research and innovation programme under grant agreement No. 700748

extends from the threshold of Slight damage up to the threshold of Moderate damage. Damage predictions resulting from this physical damage estimation method are then expressed in terms of the probability of a building being in any of these four damage states.

The flowchart shown in Figure 5-4 summarizes the main steps in evaluating liquefaction-induced physical damage for buildings, embankments and pipelines. Firstly, the selected element at risk or network must be described in terms of geometry, material and function. This step is common to each risk assessment procedure, allowing to group buildings (building typologies), facilities and infrastructure that show comparable overall performance during earthquake shaking, i.e. that demonstrate similar vulnerability. On the other hand, liquefaction fragility curves are defined also accounting for the subsoil condition and the soil-building interaction. In a simplified three strata model, a soil profile can be characterized by defining a non-liquefiable crust thickness (H_c) and a cumulative thickness of the liquefiable layer (H_{liq}). By joining such available fragility curves, the probability of reaching, or exceeding, structural and nonstructural damage states can be evaluated for a given EDP.

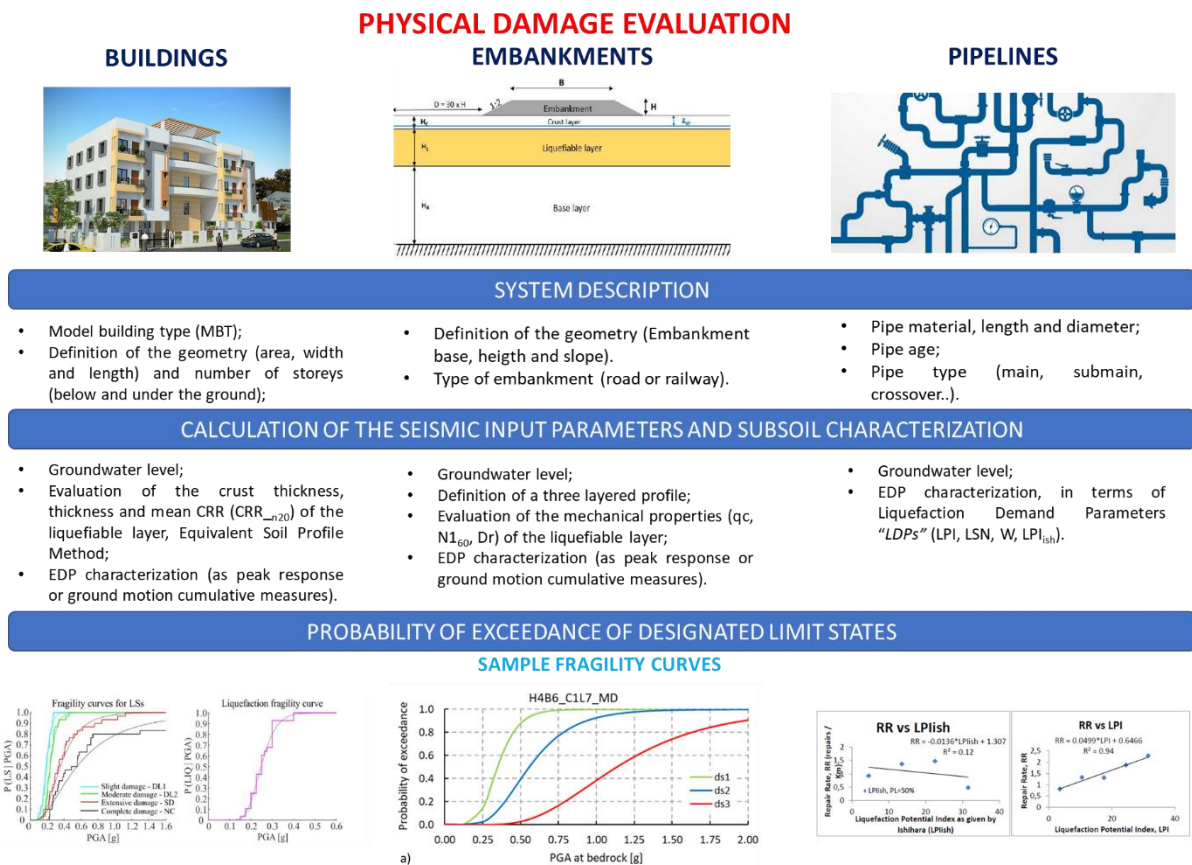


Figure 5-4: Schematic procedure to evaluate liquefaction-induced physical damage for buildings, embankments and pipelines.



This project has received funding from the European Union's Horizon 2020 research and innovation programme under grant agreement No. 700748

5.3.1 Single building

Referring to the single building scale, risk analyses can be carried out following several approaches, characterized by an increasing level of detail:

- Fragility curves – based damage assessment;
- Analytical methods (Karamitros, 2013; Bray & Macedo, 2017 formula) to evaluate the expected liquefaction-induced settlements;
- Non linear dynamic effective stress analysis with numerical modelling.

As discussed in the previous sections, for applications over large areas (regions, cities or city quarters), fragility curves are often employed to relate an engineering demand parameter (EDP) with the expected probability of reaching or exceeding a predefined damage level. More recently, analytical procedures (Karamitros, 2013; Bray and Macedo, 2017; Bullock et al., 2018) based on parametric studies and numerical modelling, were proposed to improve the reliability of results with reasonable computational efforts. Although they are expeditious, the obtained results are affected by several simplifying hypotheses.

Therefore, given the complexity of the liquefaction phenomenon, the numerical analyses are the most adequate to characterize the complex soil-structure interaction. In order to simulate the seismic response of liquefiable soils, constitutive models able to describe the complex development of liquefaction phenomenon must be used in numerical modelling. The selection and calibration of the most appropriate constitutive models is a key point in analysis.

According to Kramer and Elgamal (2001), a soil liquefaction constitutive model should account for the following features:

- nonlinear inelastic shear stress-strain response;
- dependence of shear and volumetric stiffness on effective confining pressure;
- contraction of the soil skeleton during the early stages of loading;
- dilation of the soil skeleton at large strain excursions;
- the critical state at which shearing occurs with neither contractive nor dilative tendencies,
- controlled accumulation of cyclic shear strain when cyclic loading is superimposed upon static stresses;
- post-liquefaction void-ratio redistribution (dilative and, as the liquefied soil re-consolidates, contractive);
- the coupling response of the soil skeleton and porewater;
- the effect of the permeability of the soil on the rate at which volume change can occur.

To implement advanced numerical analyses able to reproduce the development of liquefaction phenomenon, the Fast Lagrangian Analysis of Continua, FLAC V.7 (Itasca, 2017) code was used in this project. It is a numerical modelling software which uses the finite difference method for the computation of advanced geotechnical calculations, as the coupled stress-flows problems, and it is applicable to many situations such as problems that consist of several construction stages, large displacements and strains, non-linear material behaviour or unstable systems (Itasca, 2017). The software is capable of modelling the coupling response



This project has received funding from the European Union's Horizon 2020 research and innovation programme under grant agreement No. 700748

Manual for the assessment of liquefaction risk, defining the procedures to create the database, collect, define, symbolize and store information in the Georeferenced Information System and to perform and represent the risk analysis
v. 1.0

between the soil skeleton and the pore fluid and can model the redistribution of pore pressure during shaking in either two- or three-dimensions. It also features the so called “FISH scripting”, which enables the user to interact with and manipulate the numerical models, as well as Python scripting. User-defined constitutive models can be also implemented in the software.

The *PM4Sand* is a sand plasticity model implemented in FLAC specially developed for geotechnical earthquake engineering applications (Boulanger and Ziotopoulou, 2013). The model follows the basic framework of the stress-ratio controlled, critical state compatible, bounding surface plasticity model for sand presented by Dafalias and Manzari (2004). Modifications to the Dafalias-Manzari model were developed and implemented to improve its ability to approximate stress-strain responses important for geotechnical earthquake engineering applications.

The calibration of *PM4Sand* model and its implementation in the software FLAC was presented by Ziotopoulou and Boulanger (2013), later updated to Version 3.0 (Boulanger and Ziotopoulou, 2015). Ziotopoulou and Boulanger (2015) discuss validation protocols for constitutive modelling of liquefaction, and emphasise the importance of rigorous element-level validations against experimental data. A comparison of the performance of *PM4Sand* model against other constitutive models, i.e. the Dafalias-Manzari model, the PDMY model, and the UBCSAND model, was presented by Ziotopoulou et al. (2014). The formulation of the model focuses on approximating the empirical correlations and design relationships that are frequently adopted to represent the engineering behaviour of sand.

The *PM4Sand* model has three primary input parameters: relative density (D_r), shear modulus coefficient (G_0), and contraction rate parameter (h_{po}). In the dynamic phase, the *PM4Sand* model can be calibrated by fitting the parameters of the Boulanger and Idriss (2016) curve that relates the cyclic resistance ratio “CRR” with the Number of cycles. The 18 secondary model parameters retained the default values recommended by Boulanger and Ziotopoulou (2015).

The *Manzari Dafalias* material (implemented in OpenSees after the work of Dafalias and Manzari, 2004) is a simple stress-ratio controlled, critical state compatible sand plasticity model suitable for simulation of soil liquefaction. Dafalias and Manzari (2004) also provided the suggested input parameters for the model.

The *CycLiqCPSP* material is implemented in OpenSees and is an extended version of the previous material *CycLiqCP*. The constitutive models were proposed by Zhang and Wang (2012) and Wang et al. (2014), respectively, and were specially designed for simulation of large post-liquefaction shear-deformations. Wang et al. (2014) and Wang et al. (2015) presented the implementation of the models in OpenSees, and validated their results against experimental results. A centrifuge experiment on a single pile in liquefiable ground was examined and the model showed promising prediction capabilities.

The effective stress (modified) Mohr-Coulomb model is implemented in FLAC as the Finn-Byrne model and adopts the pore pressure generation model presented by Martin et al. (1975), later modified by Byrne (1991).

Multi-spring and *Cocktail glass* models are formulated on a basis of strain space multiple mechanism model. This model consists of a multitude of simple shear mechanisms with each oriented in an arbitrary direction



This project has received funding from the European Union's Horizon 2020 research and innovation programme under grant agreement No. 700748

and can describe the behaviour of granular materials under complicated loading paths, including the effect of rotation of principal stress axes (lai et al., 2011).

On the other hand, emphasis should be given to the characteristics of the earthquake ground motions that largely determine the seismic response of the ground and structure, and hence, play a significant role in the amount of liquefaction-induced building settlement that is produced.

For this reason, a site-specific seismic response characterization which accounts for the subsoil stiffness is required to evaluate the time history acceleroerogram at the base of the model. Such analyses can be performed through continuous layer models, that consider the soil as a continuous multistrata material, where each layer is assumed homogeneous and with linear viscoelastic behaviour. The parameters that characterize each layer i are: the thickness h_i , the density ρ_i , the shear modulus $G_i = (\rho_i V_s^2)$ and the damping factor D_i , linked to the viscosity coefficient η_i of the continuous model.

If strong motion records are not availbale at the site of interest, appropriate attenuation laws should be implemented to transfer the acceleroerogram from the nearest strong motion station.

In the present study, the Equivalent-linear Earthquake site Response Analyses EERA software (Bardet & Lin, 2000), is employed that analyses the local seismic response on a horizontally layered soil deposit.

The following steps of calculation were defined in the FLAC v7to run the analysis:

- Initialization of the tensional state;
- Foundation (soil excavation) and building construction;
- Constitutive models (PM4 to the sandy layer, Hystheretic Mohr Coulomb to the clayey layers) assignment and parameters for the decay of stiffness function and Damping module (L1-L2);
- Introduction of extra-variables;
- Seismic input application at the base of the model;
- Consolidation phenomenon.

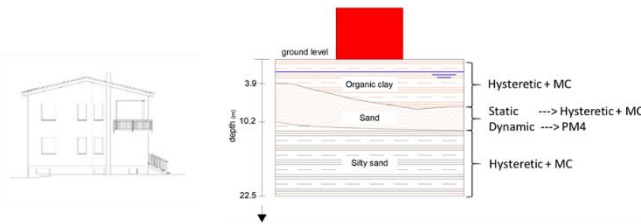
Figure 5-5presents the main steps of a detailed numerical analysis to assess risk for a given element (such as a single building), which are listed in the following:

- Description of the element at risk (Geometry definition, structural features)
- Geotechnical model and subsoil characterization (Stratigraphy, appropriate constitutive models selection and calibration)
- Site response seismic analysis
- Implementation of the case study in the FLAC v7 code
- Validation of results.

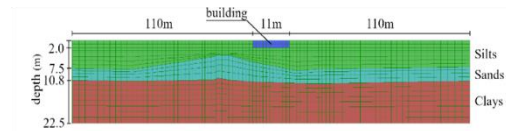


This project has received funding from the European Union's Horizon 2020 research and innovation programme under grant agreement No. 700748

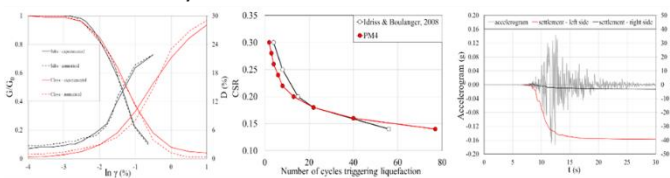
a) Geometry discretization and subsoil characterization



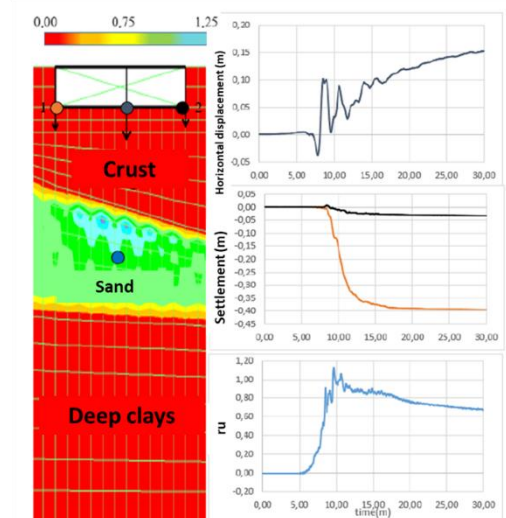
d) Analysis



b) Calibration of the constitutive models



e) Output



c) Site response seismic analysis

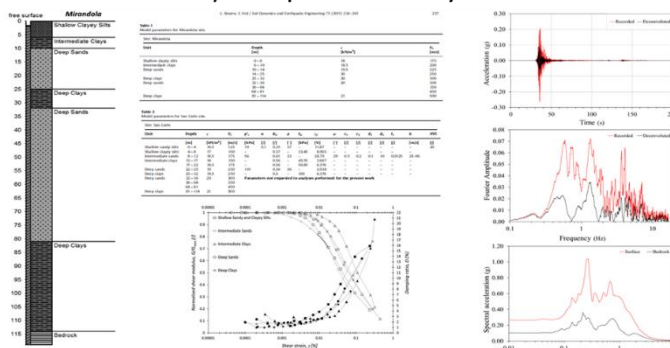


Figure 5-5: – Flowchart of the methodology outlined, among the WP7 activities, to evaluate the liquefaction-induced settlement on the single building scale

5.3.2 General Building Stock – Buildings fragility curves

The main purpose of any classification is to group buildings (building typologies), facilities and infrastructure that show comparable overall performance during earthquake shaking, i.e. that demonstrate similar vulnerability.

The main classifications of European buildings that were used in past risk assessment research and projects (e.g. RISK-UE, LESSLOSS) were reviewed in the European FP7 research project NERA “Network of European Research Infrastructures for Earthquake Risk Assessment and Mitigation” (Crowley et al., 2010).

The GEM Building Taxonomy is a uniform classification system supported by the Global Earthquake Model (www.globalquakemodel.org) that can be applied to buildings across the globe. A genetic code (genome) that is a unique description for a building, or a building typology can be generated using this taxonomy. This code is defined by 13 main attributes and each attribute corresponds to a specific building characteristic that affects its seismic performance such as material, lateral load-resisting system, building height, etc.



This project has received funding from the European Union's Horizon 2020 research and innovation programme under grant agreement No. 700748

Manual for the assessment of liquefaction risk, defining the procedures to create the database, collect, define, symbolize and store information in the Georeferenced Information System and to perform and represent the risk analysis
v. 1.0

A distinctive feature for Europe, besides a large presence in some areas of various types of masonry structures, is the domination of RC building types. Over the last several decades they have been dominating, and still dominate European construction practice. They rapidly increase in number and concentration, altering gradually or in some cases even substituting completely the masonry building typology in urban areas.

Steel structures (S1-S5) used for other than industrial uses are quite rare in Europe. Wooden (W) as well as adobe (M2) structures are exceptionally rare in urban areas of Europe. Those that exist are used either for temporary structures, structures of auxiliary function or are completely abandoned. Thus, they are out of interest for large-scale urban damage/loss assessments.

The confined masonry (M4) is also scarce in Europe, thus not of interest for large – scale damage/loss assessments. As typology, it has been developed and implemented in USA, where significant stock of these buildings exists. For these reasons, in the Risk-UE Deliverable (WP4), the use of HAZUS (1997,1999) fragility curves is recommended for steel (S1-S5), wooden (W) and confined masonry (M4) building classes. Even if the initially RISK-UE BTM consists of 23 building classes (10 masonry, 7 reinforced concrete, 5 steel and 1 wooden building class), the BTM prevailing RISK-UE Cities dominantly comprises of masonry and RC building types (Table 5-1).



This project has received funding from the European Union's Horizon 2020 research and innovation programme under grant agreement No. 700748

Manual for the assessment of liquefaction risk, defining the procedures to create the database, collect, define, symbolize and store information in the Georeferenced Information System and to perform and represent the risk analysis
v. 1.0

Table 5-1: RISK-UE Building Typology Matrix.

No.	Label	Description	Name	Height classes	
				No. of Stories	Height Range (m)
1	M11L	Rubble stone, fieldstone	Low-Rise	1 – 2	≤ 6
2	M11M		Mid-Rise	3 – 5	6 – 15
3	M12L		Low-Rise	1 – 2	≤ 6
4	M12M	Simple stone	Mid-Rise	3 – 5	6 – 15
5	M12H		High-Rise	6+	> 15
6	M13L	Massive stone	Low-Rise	1 – 2	≤ 6
7	M13M		Mid-Rise	3 – 5	6 – 15
8	M13H		High-Rise	6+	> 15
9	M2L	Adobe	Low-Rise	1 – 2	≤ 6
10	M31L	Wooden slabs URM	Low-Rise	1 – 2	≤ 6
11	M31M		Mid-Rise	3 – 5	6 – 15
12	M31H		High-Rise	6+	> 15
13	M32L	Masonry vaults URM	Low-Rise	1 – 2	≤ 6
14	M32M		Mid-Rise	3 – 5	6 – 15
15	M32H		High-Rise	6+	> 15
16	M33L	Composite slabs URM	Low-Rise	1 – 2	≤ 6
17	M33M		Mid-Rise	3 – 5	6 – 15
18	M33H		High-Rise	6+	> 15
19	M34L	RC slabs URM	Low-Rise	1 – 2	≤ 6
20	M34M		Mid-Rise	3 – 5	6 – 15
21	M34H		High-Rise	6+	> 15
22	M4L	Reinforced or confined masonry	Low-Rise	1 – 2	≤ 6
23	M4M		Mid-Rise	3 – 5	6 – 15
24	M4H		High-Rise	6+	> 15
25	M5L	Overall strengthened masonry	Low-Rise	1 – 2	≤ 6
26	M5M		Mid-Rise	3 – 5	6 – 15
27	M5H		High-Rise	6+	> 15
28	RC1L	RC moment frames	Low-Rise	1 – 2	≤ 6
29	RC1M		Mid-Rise	3 – 5	6 – 15
30	RC1H		High-Rise	6+	> 15
31	RC2L	RC shear walls	Low-Rise	1 – 2	≤ 6
32	RC2M		Mid-Rise	3 – 5	6 – 15
32	RC2H		High-Rise	6+	> 15
34	RC31L	Regularly infilled RC frames	Low-Rise	1 – 2	≤ 6
35	RC31M		Mid-Rise	3 – 5	6 – 15
36	RC31H		High-Rise	6+	> 15
37	RC32L	Irregular RC frames	Low-Rise	1 – 2	≤ 6
38	RC32M		Mid-Rise	3 – 5	6 – 15
39	RC32H		High-Rise	6+	> 15



This project has received funding from the European Union's Horizon 2020 research and innovation programme under grant agreement No. 700748

Manual for the assessment of liquefaction risk, defining the procedures to create the database, collect, define, symbolize and store information in the Georeferenced Information System and to perform and represent the risk analysis
v. 1.0

No.	Label	Description	Name	Height classes	
				No. of Stories	Height Range (m)
40	RC4L	RC dual systems	Low-Rise	1 – 2	≤ 6
41	RC4M		Mid-Rise	3 – 5	6 – 15
42	RC4H		High-Rise	6+	> 15
43	RC5L	Precast concrete tilt-up walls	Low-Rise	1 – 2	≤ 6
44	RC5M		Mid-Rise	3 – 5	6 – 15
45	RC5H		High-Rise	6+	> 15
46	RC6L	Precast concrete frames with concrete shear walls	Low-Rise	1 – 2	≤ 6
47	RC6M		Mid-Rise	3 – 5	6 – 15
48	RC6H		High-Rise	6+	> 15
49	S1L	Steel moment frames	Low-Rise	1 – 2	≤ 6
50	S1M		Mid-Rise	3 – 5	6 – 15
51	S1H		High-Rise	6+	> 15
52	S2L	Steel braced frames	Low-Rise	1 – 2	≤ 6
53	S2M		Mid-Rise	3 – 5	6 – 15
54	S2H		High-Rise	6+	> 15
55	S3L	Steel frames with URM infill walls	Low-Rise	1 – 2	≤ 6
56	S3M		Mid-Rise	3 – 5	6 – 15
57	S3H		High-Rise	6+	> 15
58	S4L	Steel frames with cast-in-place concrete shear walls	Low-Rise	1 – 2	≤ 6
59	S4M		Mid-Rise	3 – 5	6 – 15
60	S4H		High-Rise	6+	> 15
61	S5L	Steel and RC composite systems	Low-Rise	1 – 2	≤ 6
62	S5M		Mid-Rise	3 – 5	6 – 15
63	S5H		High-Rise	6+	> 15
64	WL	Wooden structures	Low-Rise	1 – 2	≤ 6
65	WM		Mid-Rise	3 – 5	6 – 15



This project has received funding from the European Union's Horizon 2020 research and innovation programme under grant agreement No. 700748

5.3.2.1 Liquefact Fragility Curves for RC buildings

In the definition of a method for Rapid Risk Identification (RRI), fragility curves for reinforced concrete (RC) frames with masonry infills referred to designated limit state (LSs) were developed by Work Package 3 of the present project.

Non-linear soil-foundation-structure interface were considered as reference structures for analysis. Each analysis considered a structure and a specific combination of soil profile and input motion, and calculation method for the pore pressure, surface motion, and imposed settlement.

One example of fragility curves for the reference RC structure, built on a three-strata subsoil is shown in Figure 5-6, in terms of both shaking and liquefaction fragility curves. Such curves consider PGA as input variable.

For shaking fragility four damage states were considered. The limit states of the building are based on structural damage, foundation rotations and settlements. In the example, four limit states are examined: i) slight damage (DL1), ii) moderate damage (DL2), iii) extensive damage (SD), and iv) complete damage (NC). Note that the complete damage state corresponds to the near collapse (NC) limit state according to EC8 (CEN, 2004) and not to the actual collapse of the building, which cannot be directly simulated with the simplified model. The limit states related to structural damage due to ground shaking are defined based on the peak rotations in the inelastic rotational spring at the base of the buildings.

The limit states related to ground deformations, i.e. peak rigid body foundation rotations, peak θ_{LS} and settlements, $U_{z,LS}$, are defined according to the recommendations by Bird et al. (2006).

In addition to the fragility curves for the designated limit states, the so-called liquefaction fragility curve, which defines the probability of attaining liquefaction for a given value of peak ground acceleration (a_g), is also computed based on the results of the liquefaction triggering procedure.

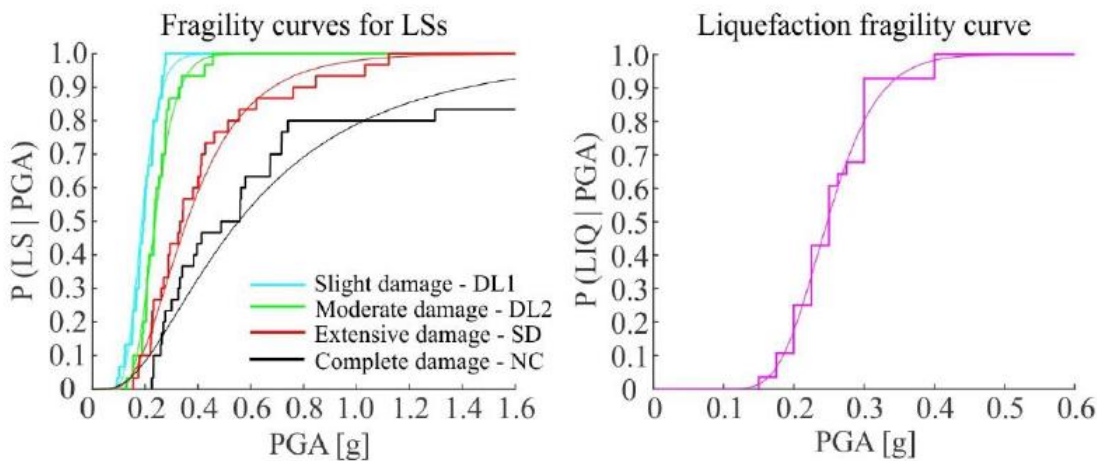


Figure 5-6: Sample fragility curves for designated limit states (left) and the liquefaction fragility curve (right) obtained based on the assumption of lognormal distribution of the fragility function (thin lines) and based on the empirical CDF (thick lines), as defined in D3.2 of this project.



This project has received funding from the European Union's Horizon 2020 research and innovation programme under grant agreement No. 700748

In recent years, several simplified analytical methodologies have been proposed to estimate liquefaction-induced building settlements during seismic shaking. Among these, the Karamitros (2013) and Bray & Macedo (2017) procedures are shown in the following.

5.3.2.2 Karamitros et al. formula (2013)

Based on the results of numerical analyses, Karamitros et al. (2013) gives a simplified analytical formula for the computation of the seismic settlements of strip and rectangle footings resting on liquefiable soil with a clay crust. Such settlement is associated to a "sliding-block" type of punching failure through the clay crust and within the liquefied sand layer.

In particular, liquefaction-induced settlements are correlated to the seismic excitation characteristics and the post-shaking degraded static factor of safety, while the effect of shear-induced dilation of the liquefied subsoil is also taken into account.

The proposed expression for the dynamic settlement ρ_{dyn} (i.e. the settlement during shaking) is shown in Equation 5-5, being c a foundation aspect ratio correction (Equation 5-6, where $c'=0.003$), a_{max} the peak bedrock acceleration, T the representative period of the motion, N the number of cycles of the excitation, Z_{liq} the thick liquefiable sand layer, B the structure width and FS_{deg} the degraded static factor of safety of the foundation.

$$\rho_{dyn} = c a_{max} T^2 N \left(\frac{Z_{liq}}{B} \right)^{1,5} \cdot \left(\frac{1}{FS_{deg}} \right)^3 \quad \text{Equation 5-5}$$

$$c = c' \left(1 + 1,65 \cdot \frac{L}{B} \right) \leq 11,65 c' \quad \text{Equation 5-6}$$

$$a_{max} T^2 N = \int_{t=0}^t |v(t)| dt \quad \text{Equation 5-7}$$

FS_{deg} can be calculated through of the static loading ratio (Equation 5-8), the degraded bearing capacity ($q_{ult,deg}$) divided by the bearing pressure (q). The foundation bearing capacity failure mechanism is simulated by the Meyerhof and Hanna (1978) model for a crust on a weak layer using the degraded friction angle in Equation 5-9 where U is the average excess pore pressure ratio of the liquefied sand and ϕ_0 is the initial friction angle. Superficial crust is beneficial and there is an upper bound beyond where failure occurs entirely within the crust and does not get affected by the liquefiable layer.

$$FS_{deg} = \frac{q_{ultdeg}}{q} \quad \text{Equation 5-8}$$

$$\phi_{deg} = \tan^{-1}[(1 - U)\tan\phi_0] \quad \text{Equation 5-9}$$

Such methodology was evaluated against results from a large number of relevant centrifuge and large-scale experiments, as well as against observations of the performance of shallow foundations in the City of Adapazari, during the 1999 Kocaeli Earthquake. Even if good agreement was found among analytical predictions and liquefaction-induced settlements, in future applications the parameters of the numerical analyses should be respected.



This project has received funding from the European Union's Horizon 2020 research and innovation programme under grant agreement No. 700748

5.3.2.3 Bray & Macedo (2017)

After an extensive in-situ, experimental and analytical work, Bray and Macedo (2017) propose a method to evaluate the shear-induced building settlement (D_s) due to liquefaction below the building. The simplified procedure for estimating liquefaction-induced building settlement involves these steps:

- Perform a liquefaction triggering assessment and calculate the safety factor against liquefaction (FSL) for each potentially liquefiable soil layer preferably using a CPT-based method (e.g., Boulanger and Idriss 2016).
- Calculate the post-liquefaction bearing capacity factor of safety (FS) using the simplified two-layer solution of Meyerhof and Hanna (1978), where the average shear strength of the non-liquefied crust layer represents the top layer and the post-liquefaction residual shear strength of the liquefied soil layer represents the bottom layer. If the post-liquefaction bearing capacity FS is less 1.0 for light or low buildings or less than 1.5 for heavy or tall buildings, large movements are possible, and the potential seismic building performance can generally be judged to be unsatisfactory.
- Estimate the likelihood of sediment ejecta developing at the site by using ground failure indices such as LSN, LPI, or the Ishihara (1985) ground failure design chart. If the amount of sediment ejecta is significant, estimate the amount of building settlement as a direct result of loss of ground due to the formation of sediment ejecta (D_e). This can best be done using relevant case histories to estimate the amount of ejecta and then assuming that the ejecta has been removed below the building foundation.
- Estimate the amount of volumetric-induced building settlement (D_v) preferably using a CPT-based method (e.g., Zhang et al. 2002).
- Estimate the shear-induced building settlement (D_s) due to liquefaction below the building using Equation 5-10, which is repeated below:

$$\ln(D_s) = c_1 + 4.59 \cdot \ln(Q) - 0.42 \cdot \ln(Q)^2 + c_2 \cdot LBS + 0.58 \cdot \ln(\tanh(HL)) - 0.02 \cdot B + 0.84 \cdot \ln(CAV_{dp}) + 0.41 \cdot \ln(S_a) + \varepsilon \quad \text{Equation 5-10}$$

$$LBS = \int W * \frac{\varepsilon_{shear}}{z} dz \quad \text{Equation 5-11}$$

where D_s is in mm, LBS is calculated with Equation 5-11, $c_1 = -8.35$ and $c_2 = 0.072$ for $LBS \leq 16$, and $c_1 = -7.48$ and $c_2 = 0.014$ otherwise. Q is in units of kPa, HL is in m, B is in m, CAV_{dp} is in g-s, and S_a is in g; ε is a normal random variable with zero mean and 0.50 standard deviation in Ln units. CAV_{dp} is the standardised Cumulate Absolute Velocity as defined in Campbell and Bozorgnia (2012) where N is the number of discrete 1 second time intervals, x is $PGAi - 0.025$ ($PGAi$ is the value of the peak ground acceleration (g) in time interval i , inclusive of the first and last values) and $H(x)$ is 0 if $x < 0$ or 1 otherwise, (table 4.6). LBS (Equation 5-11) is an index of equivalent liquefaction-induced shear strain on the free-field (ε_{shear}), defined as the integration along the soil column of the strain estimated by means of the CPT-based procedure proposed in Zhang et al. (2004), weighted by the depth in order to provide more importance to the soil close to the foundation). ε_{shear} is calculated based on the estimated D_r of the liquefied soil layer and the calculated safety factor against liquefaction triggering (FSL). z (m) is the depth measured from the ground surface > 0 and W is a foundation-weighting factor



This project has received funding from the European Union's Horizon 2020 research and innovation programme under grant agreement No. 700748

wherein $W = 0.0$ for z less than D_f , which is the embedment depth of the foundation, and $W = 1.0$ otherwise.

Finally, the total liquefaction-induced building settlement (D_t) can be estimated from Equation 5-12, as:

$$D_t = D_e + D_v + D_s$$

Equation 5-12

5.3.3 Transportation System

Risk Assessment Procedures also emphasize the damage on the utilities and transportation systems, since they play an important role in the economic development of a territory and in the connection between communities.

In the Hazus Methodology, Transportation System includes the following systems:

- Highway;
- Railway;
- Light Rail;
- Bus;
- Port;
- Ferry;
- Airport.

For instance, the Highway System direct damage output includes probability estimates of (1) component functionality and (2) physical damage expressed in terms of the component's damage ratio. In the Hazus Methodology, damage functions or fragility curves for all three highway system components (Road, Bridges and Tunnels) are modelled as lognormally-distributed functions that give the probability of reaching or exceeding different damage states for a given level of ground motion or ground failure. Each fragility curve is characterized by a median value of ground motion or ground failure and an associated dispersion factor (lognormal standard deviation).

Ground motion is quantified in terms of peak ground acceleration (PGA) and spectral acceleration (S_a), and ground failure is quantified in terms of permanent ground displacement (PGD).

- For roadways, fragility curves are defined in terms of PGD.
- For bridges, fragility curves are defined in terms of S_a (0.3 sec), S_a (1.0 sec) and PGD.
- For tunnels, fragility curves are defined in terms of PGA and PGD.

5.3.3.1 Liquefact Fragility Curves for Embankments

In general terms, the road network is composed of a number of nodes and edges. All of them are vulnerable to seismic shaking or geotechnical hazards, with pavements that can rupture due to surface ground deformation. Some types of edges or road segments, like those identified below have specific types of



This project has received funding from the European Union's Horizon 2020 research and innovation programme under grant agreement No. 700748

response to seismic action and associated vulnerability. The main identified system components within the Syner-G (<http://www.vce.at/SYNER-G/files/project/proj-overview.html>) project are:

- Bridge
- Tunnel
- Embankment (road on)
- Trench (road in)
- Unstable slope (road on, or running along)
- Road pavement (ground failure)
- Bridge abutment

During seismic shaking the general movement of an embankment is towards the free face or down the slope. The movement is driven by an in-balance of support force where the earth-pressure is less on the free face or downward slope, thus under cyclic loading the embankment more easily overcomes the static resistance in one direction and moves more in that direction. Cyclic loading, especially in the case of loose liquefiable soil deposits, can result in severe weakening of the soil and can trigger flow-like behaviour where the static shear stress caused by a free face or downward slope can result in large strains and contractive soil behaviour, eventually leading to a dramatic loss of soil shear strength. The behaviour under these conditions is extremely complex as the shear strains are very large and variable throughout the deposit, and some level of drainage, pore pressure dissipation and void redistribution can be expected (Kramer and Wang, 2015). Earth structures such as highway and railway embankments can spread laterally and settle, resulting in opening of cracks in the road pavement or displacement of the railway tracks. The list of possible damage patterns is unlimited.

Therefore, as it is expressed by Pitilakis and Argyroudis (2014) in their synthesis of Syner-G project, classification of damage and the subsequent definition of specific damage states are important in the vulnerability assessment as the seismic intensity is correlated to the expected damage level through the fragility or vulnerability functions. Again, the form of the fragility functions depends on the typology of the element at risk. For common structures (e.g. buildings, bridges) and other not extended elements (e.g. cranes, tanks, substations), the fragility curves describe the response and damage level of particular subcomponents (e.g. columns, transformers) or of the entire structure. For linear elements of extended networks such as gas pipelines, the fragility functions describe the number of expected damages along a certain length (i.e. per km).

An example of fragility curve for embankments is presented in Figure 5.8. Embankments fragility curves are mostly developed for permanent vertical ground displacement in the middle point of embankment crest as damage parameter and PGA at bedrock (alternatively Arias intensity) for intensity measure.

To use adequate fragility curves, the influence of variation of some model parameters (crest width, embankment height, thickness of liquefiable layer, presence of crust layer and relative density of sandy layer) must be examined. A general layout of the model geometry is presented in Figure 5-7, consisting of a traffic embankment underlain by three horizontal soil layers. Under upper clayey crust layer, a sandy layer susceptible to liquefaction is placed, while lower layer represents base of stiff clay. Additionally, the ground water level and embankment slope inclination (vertical/horizontal) must be defined.



This project has received funding from the European Union's Horizon 2020 research and innovation programme under grant agreement No. 700748

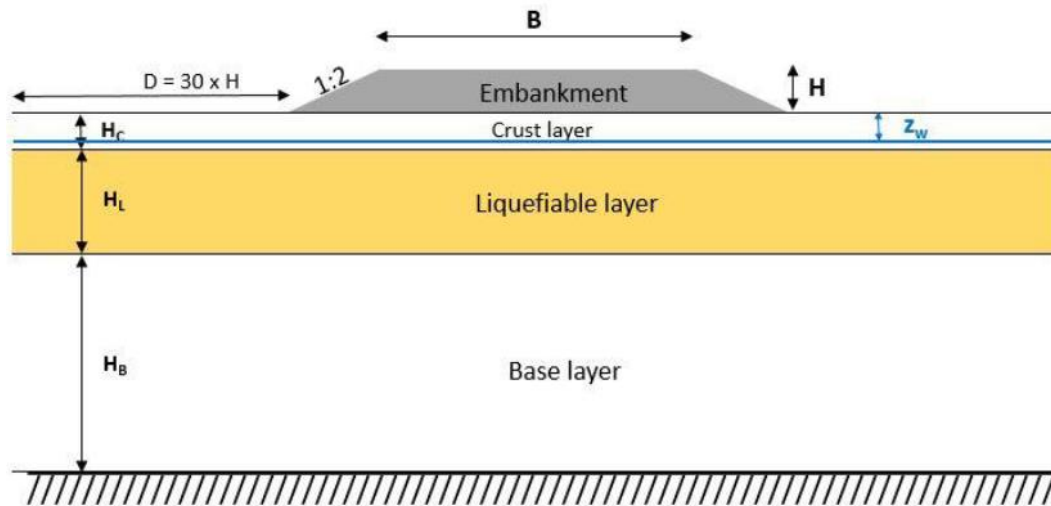


Figure 5-7: Embankment geometry adopted by University of Ljubana in the procedure to develop fragility curves

Based on the results of numerical analyses (Deliverable 3.2), in the activities of WP3 the following was found:

- With increasing embankment height (2, 4, 6 and 8 m) or thickness of liquefiable layer (2, 4, and 7 m) crest settlements increase and fragility curves move to the left. In the absence of crust layer, even higher probability of exceedance of the set damage state was observed.
- The increase of crest width (6, 12 and 24 m) decreases vertical displacement in the centre of the embankment crest. Fragility curves move to the right with larger crest width.
- Denser liquefiable layer produces smaller deformations at the crest in comparison with loose material. Consequently, fragility curves move to the left for cases with loose sand.

Fragility curves were prepared for road and railway embankments based on the SYNER-G criteria (SYNER-G, 2013). They define the damage states as shown in Table 5-2.

Table 5-2: Damage states for traffic embankments (SYNER-G, 2013).

Road embankments				Railway embankments			
Damage state	Permanent vertical ground displacement [m]			Damage state	Permanent vertical ground displacement [m]		
	min	max	mean		min	max	mean
ds1 – minor	0.02	0.08	0.05	ds1 – minor	0.01	0.05	0.03
ds2 – moderate	0.08	0.22	0.15	ds2 – moderate	0.05	0.10	0.08
ds3 – extensive	0.22	0.58	0.40	ds3 – extensive	0.10	0.30	0.20

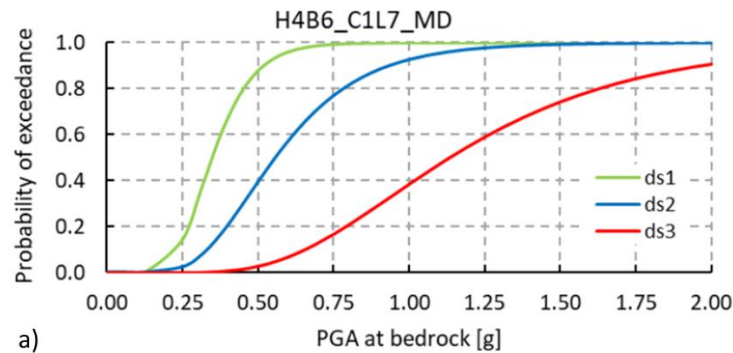
Figure 5-8 shows a set of fragility curves for both Road and Railway Embankments, as a function of the PGA. The same are built also considering the Arias Intensity as input IM.

It can be observed that the titles of the graphs use the following notation: H-B-C-L-, where:

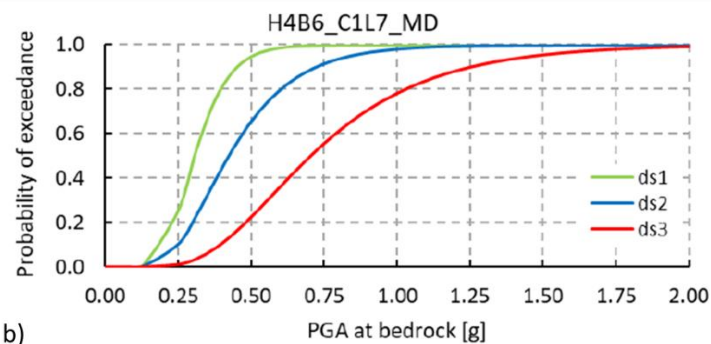


This project has received funding from the European Union's Horizon 2020 research and innovation programme under grant agreement No. 700748

- H – is the embankment height [m];
- B – is the crest width [m];
- C – is the thickness of crust layer [m];
- L – is the thickness of liquefiable (sandy-silty) layer [m];
- MD or L – refers to medium dense or loose density state of the liquefiable layer.



a)



b)

Figure 5-8: Example of fragility curves for road (a) and railway embankments (b). Damage states are defined according the SYNER-G (2013) criteria

5.3.4 Lifeline System and Pipelines

Lifeline system is made by a set of components, including pipelines, water treatment plants, wastewater treatment plants etc. Nature of pipelines is complex with a variation in its pipe materials, pipe diameters, pipe lengths, pipeline laying years and depths, and most importantly its spatial variation. Pipelines carry these variable attributes all across a city, which makes study of pipelines much more complex in nature. Occurrence of an earthquake can cause extensive damage to pipelines. Damage rates vary with pipeline depths, materials, diameters, and age. The burial and connected nature of pipelines makes it very vulnerable to earthquakes and its hazards. Pipeline damage is given as Repair Rate (RR) or individual pipeline damage (a binary term, damage or no damage).

Liquefaction causes severe damage to pipelines, due to eventual ground deformations, sand boils, lateral spreading. Pipeline damage prediction is not a simple process or a spatially similar process. Several past studies have developed correlations between Repair Rates (RR) of pipelines and various intensity measures. Intensity measures like Peak Ground Velocity (PGV), which represents transient ground deformations (Toprak et al., 2017), Permanent Ground Deformation (PGD), angular distortion, lateral strain, Liquefaction Severity



This project has received funding from the European Union's Horizon 2020 research and innovation programme under grant agreement No. 700748

Number (LSN), Settlement have been used in developing fragility curves for pipeline damage (Eguchi, 1991; Eiding, 1998; Ioyama et al., 2000; O'Rourke et al., 2012; Toprak et al., 2017; Bagriacik et al., 2018). Most commonly used are PGV and PGD. Eguchi et al., 1991 was the first to develop relationship between RR and PGD for different pipe materials (Eguchi et al., 1991). Angular distortion and Lateral strain were used by O'Rourke et al., 2012, which have a good correlation with pipeline damage, but they are typically difficult to measure and their predictions are variable due to their dependency on surveying instruments (Toprak et al., 2017).

5.3.4.1 Liquefact Empirical Fragility Curves for Pipelines

Within Liquefact.eu Project, several types of fragility curves are proposed by merging the evaluations of the most used liquefaction severity indicators (LPI, LSN, Settlement and LPI_{SH}) with the pipeline number of repairs per km after the 2010-2011 Christchurch Earthquake Sequence. In such study these indicators are collectively called as Liquefaction Demand Parameters (LDPs), which are a synonym to Intensity Measures (IM). The study aims develop correlations between RR (Mains) pipeline network of Christchurch City and Liquefaction Severity Indicators for the 22nd February 2011 earthquake.

A conceptual fragility model framework is shown in Figure 5.9; this framework describes the relationship between pipeline damage and LDPs and is also a guide in developing fragility functions for pipelines. It is built upon Bagriacik et al. (2018), which says pipeline damage is an interaction of earthquake hazard, pipeline exposure and pipeline vulnerability. In the WP3 study earthquake hazard includes Liquefaction demand Parameters. LDPs are permanent ground deformations (PGD) or measures of liquefaction severity given by settlement, LSN, LPI, LPI_{SH}, which require ground motion, liquefaction susceptibility and groundwater depth data for its computation (Bagriacik et al., 2018).

Pipeline vulnerability includes pipe material, pipe type, pipe diameter and year pipe was laid (Bagriacik et al., 2018). Pipeline length gives the pipe exposure, by incorporating the spatial differential behaviour of interaction of pipelines and liquefaction severity. Pipe exposure and vulnerability collectively fall under pipeline data, forming our total pipeline dataset. The measure of pipeline damage is given by pipe damage (a binary term, pipe is damaged or not). Different variables are assigned to different factors influencing pipeline damage as shown in Figure 5-9.

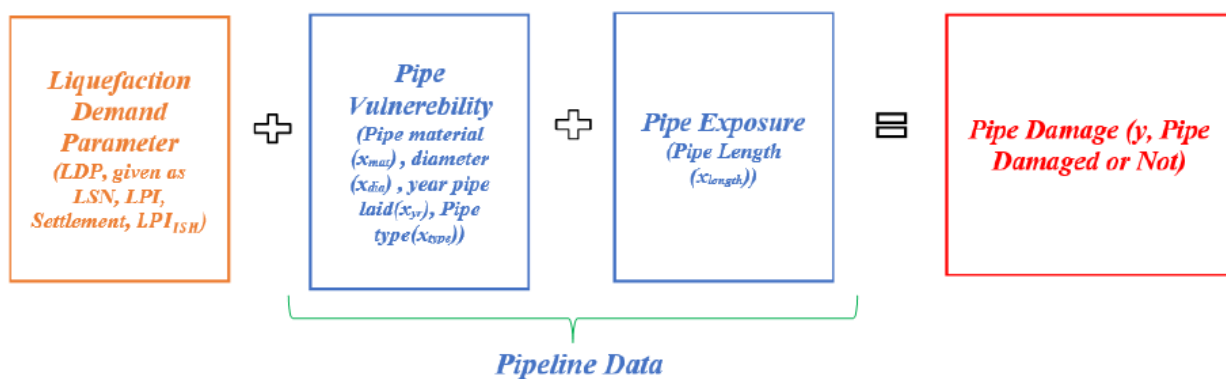


Figure 5-9: General framework to develop the fragility model for pipelines, as defined by WP3



This project has received funding from the European Union's Horizon 2020 research and innovation programme under grant agreement No. 700748

The 2010-2011 Christchurch (N. Z.) Earthquake Sequence caused extensive damage to infrastructures and lifelines. Most of such damage is due to liquefaction, that caused ground deformations, lateral spreading along the Avon river, sand boils, differential settlements, etc.

An extensive pipeline damage was observed during the CES (Figure 5-10). February 2011 earthquake shows the highest number of repairs (Table 5-3), this is due to its proximity (4-10 Km within city boundary) to the Christchurch City. The water supply pipeline network is divided into pipe types of mains, submains, trunk mains and crossovers. Mains are approx. 1700 Km in length laid on the carriageway, 2-2.5m from the kerb and submains are approx. 2000 Km laid beneath the footpaths, 150mm from boundaries. Mains have pipe diameters from 100mm to 600mm, while submains have diameters of 50 mm and 63mm. Crossovers are 50 mm in diameter, serve to submains located at the fire hydrants. Watermains are laid in trenches 200-300 mm wider than the pipe diameter, at shallow depths. The cover thickness depends on the pipe size, location and material, but is usually about 800mm (at least 750mm, but no more than 1.5m for the standard watermains diameters). Typical thickness of cover for submains is 300-500 mm. The trenches are backfilled with native soils and are compacted to 95%, 90% and 70% of the material's maximum dry density (NZS 4402.4.1.1) for trafficked, pedestrian and landscape areas, respectively. The year of laying these pipes varies from 1890's to present.

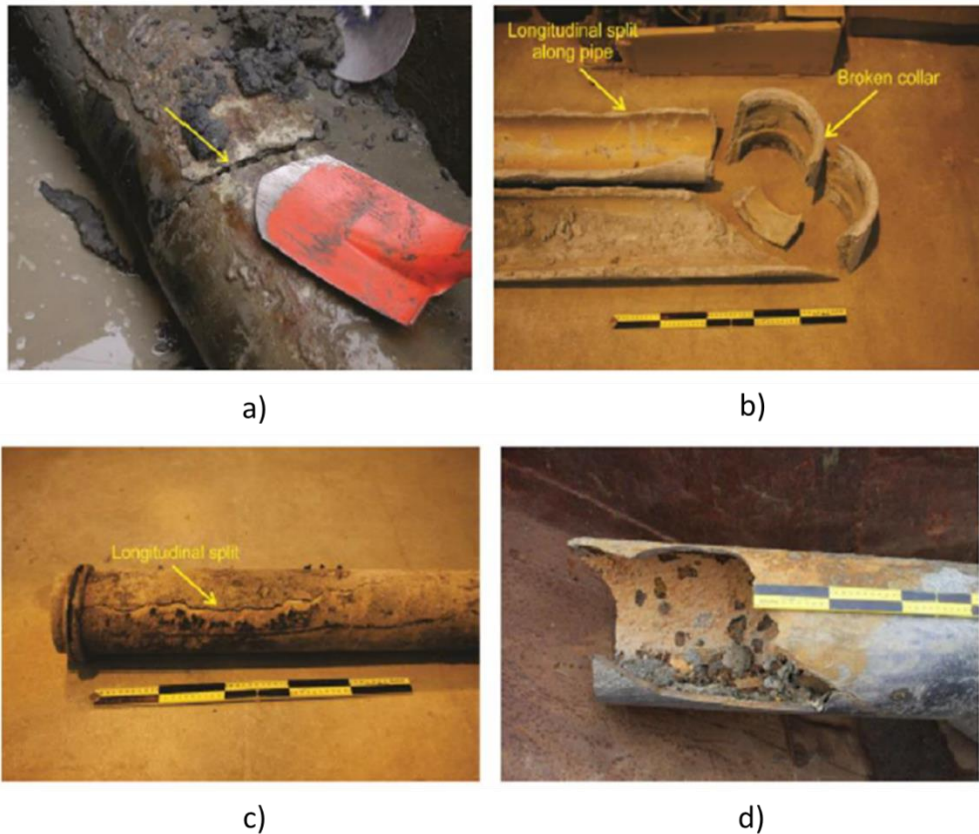


Figure 5-10: Examples of observed damage to the pipelines: a) Circumferential split on AC main, Rowan Avenue, b) AC main broken collar and longitudinal split (Cubrinovski et al., 2015); c) Longitudinal split on AC main, d) Broken CI main (Curbrinovski et al., 2014).



This project has received funding from the European Union's Horizon 2020 research and innovation programme under grant agreement No. 700748

Manual for the assessment of liquefaction risk, defining the procedures to create the database, collect, define, symbolize and store information in the Georeferenced Information System and to perform and represent the risk analysis
v. 1.0

The damage observed to the water supply pipeline was due to three factors namely, earthquake, soil and pipe parameters. Earthquake factors like closeness of the epicentre, magnitude and depth affect the damage to the pipelines. Higher damage was seen for long duration of ground shaking and shallow events, closely associated with occurrence of liquefaction.

Pipe parameters like pipeline direction, pipe age, pipe material, pipeline joints, pipeline diameter affect the damage of the pipelines. Pipeline direction if vertical or almost vertical to the fault causes higher damage. Also, brittle pipe material was observed to be more vulnerable to earthquake shaking. Flexible pipes like PE and PVC suffered 3-5 times less damage than AC, steel and GI pipelines. Older pipelines suffer corrosion, hence vulnerable to damage. The Repair rates are observed to be higher for pipe dia (less than 12 inches) than in large diameter pipelines. Large diameter pipelines suffer less damage due it higher wall thickness. Pipelines in general with less connections, fittings and irregularity suffer less damage. AC pipelines suffered damage to the pipe body itself (62%), commonly circumferential and longitudinal splits type damage. The damage to pipe fittings was observed to be 38%. The pipes which suffered damage to pipe fittings, property connections, coupler, gibaults were HDPE (82%), MDPE80 (90%), PVC (80%), CI (79%), GI (58%). Table 5.3 shows the different types of pipes with its number of repairs.

The total number of pipelines in the database is 146772 nos, with approx. 3800 repairs seen only for the Feb 2011 earthquake.

Table 5-3: Table showing (a) Lengths of different pipe types (b) Repairs conducted after each event of CES (c) Lengths of different Pipe Materials.

Pipe Type	Length (Km)
Main	1700
Submains	1522
Cross Overs	143
Trunk Mains	291

(a)

CES Event	Number of Repairs
Sept 2010	Approx. 98
Feb 2011	Approx. 3800
June 2011	Approx. 1500

(b)

Pipe Material	Pipe Length(Km)	Pipe Material	Pipe Length(Km)
ABS	0.0699	HDPE	931.1103
AC	872.0984	LDPE	2.7341
AL	0.0712	MDPE100	3.7232
API	0.2346	MDPE80	470.4203
CI	208.2447	MLDI	2.5401
CLDI	8.8321	MPVC	149.2289
CLS	53.6754	PE	0.9758
CONC	0.1501	PE100	9.9621
DI	51.2643	PVC	282.9397
GALV	173.7273	RCRR	0.172
Unknown	0.0558	STEEL	41.9845
UPVC	130.3438	WI	0.0064

(c)

On the other hand, the assessment of LDPs resulted from the available CPT within the NZGD <https://nzgd.org.nz> data processing. Liquefaction triggering method can be applied to develop independent regional-scale maps of different liquefaction vulnerability indicators, herein called Liquefaction Demand Parameters (LDP), for a range of earthquake scenario's, groundwater table surfaces and soil properties (Tonkin & Taylor, 2013). The most used LDPs are as follows (Taylor & Taylor, 2013):



This project has received funding from the European Union's Horizon 2020 research and innovation programme under grant agreement No. 700748

- Settlement (S) - Based on Zhang, Robertson and Brachman (2002);
- Liquefaction Severity Number (LSN) - As defined in Tonkin & Taylor (2013);
- Liquefaction Potential Index (LPI) - As defined by Iwasaki et al. (1978);
- Liquefaction Potential Index (LPIISH) - Using the Ishihara inspired LPI method developed by Maurer et al. (2014a).

These LDPs should be evaluated for each seismic scenario and mapped in GIS platform. Since values could not be extracted on the pipelines due to its polyline shape in GIS, it is necessary to convert the pipelines to points, assigning the point at the mid of the polyline. These points contained all attributes of the pipelines but created an uncertainty when LDP values were extracted for pipelines.

At this point, each LDP values need to be matched with the damage parameter, namely Repair Rate (RR, which represents the number of repairs per km of the pipeline).

In Figure 5-11 a set of pipelines fragility curves derived by WP3 is shown. In particular, PGA distribution given by Bradley (Bradley et al., 2012), a fine content calibration factor $C_{FC} = 0.0$ and a probability of liquefaction $PL = 50\%$ were considered as liquefaction triggering parameters.

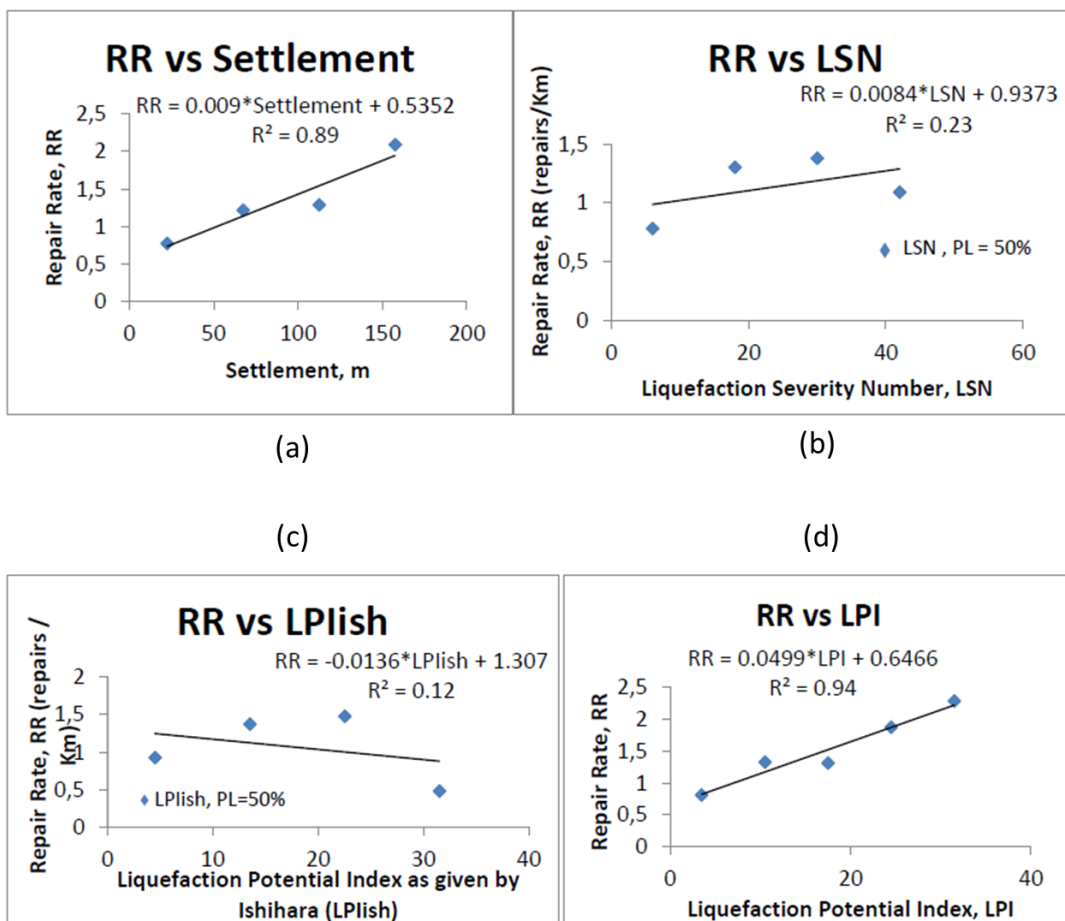


Figure 5-11: Samples of empirical fragility curves for pipelines, obtained for the Christchurch case study: (a) RR vs Settlement, (b) RR vs LSN, (c) RR vs LPIISH, (d) RR vs LPI.



This project has received funding from the European Union's Horizon 2020 research and innovation programme under grant agreement No. 700748

5.4 Physical damage

The above presented seismic and liquefaction fragility curves allow to estimate the earthquake or liquefaction-induced physical damage on a given element (building, road/railway embankment and networks). For buildings and embankments such physical damage is defined through the achievement of predefined limit states (CEN, 2004; Pitilakis and Argyroudis, 2014), while for pipelines the repairs ratio (representing the expected number of repairs per km) is introduced.

It can be observed that damage limit states are related to Earthquake Intensity Measures (IMs), such as PGA, Spectral acceleration, velocity or displacement, Arias Intensity and so on. For pipelines instead, the repairs ratio is defined as a function of the most used Liquefaction Demand Parameters (LDPs): Settlement (Zhang et al., 2002); LPI (Iwasaki et al., 1978), LSN (van Ballegooy, 2014), LPI_{ISH} (Maurer, 2014).

In risk assessment analyses, the annual probability of exceeding designated limit states is computed by convolution of fragility functions and the hazard functions. By using numerical integration, the probability of exceedance of designated limit states can be defined as:

$$P_{LS} = \int_0^{\infty} P(LS | IM = im) \cdot \left| \frac{dH(im)}{d(im)} \right| \cdot d(im) \quad \text{Equation 5-13}$$

where $P(LS | IM = im)$ is the probability of exceeding the limit state if the intensity measure IM takes the value equal to im, and the hazard curve $H(im)$ is the annual rate of exceedance of im. In the computation of P_{LS} , the fragility functions were defined based on both empirical cumulative distributions of limit-state peak ground accelerations or ground motion cumulative measures.

The following flowchart (Figure 5-12) summarizes the main steps in evaluating liquefaction-induced physical damage for buildings, embankments and pipelines. Firstly, the selected element at risk or network must be described in terms of geometry, material and function. This step is common to each risk assessment procedure, allowing to group buildings (building typologies), facilities and infrastructure that show comparable overall performance during earthquake shaking, i.e. that demonstrate similar vulnerability. On the other hand, liquefaction fragility curves are defined also accounting for the subsoil condition and the soil-building interaction. In a simplified three strata model, a soil profile can be characterized by defining a non-liquefiable crust thickness (H_c) and a cumulative thickness of the liquefiable layer (H_{liq}). By joining such available fragility curves, the probability of reaching, or exceeding, structural and nonstructural damage states can be evaluated for a given EDP.

An example of methodology to quantify the physical damage on a building asset is shown in Figure 5-12. Firstly, the element at risk are georeferenced and characterized by indicating the geometry, the model building type, the use and number of storeys. On the other hand, the interaction with the subsoil is accounted through the application of the Equivalent Soil Profile Method, where 22 classes of subsoil are defined. Then, the specific ESP fragility curves are used to evaluate the probability of reaching pre-defined shaking/liquefaction-induced damage levels.

Note that such fragility curves were defined considering seismic Intensity Measures *IMs* (PGA, I_a , S_a , etc.) as input parameters.



This project has received funding from the European Union's Horizon 2020 research and innovation programme under grant agreement No. 700748

Manual for the assessment of liquefaction risk, defining the procedures to create the database, collect, define, symbolize and store information in the Georeferenced Information System and to perform and represent the risk analysis

RISK ANALYSIS

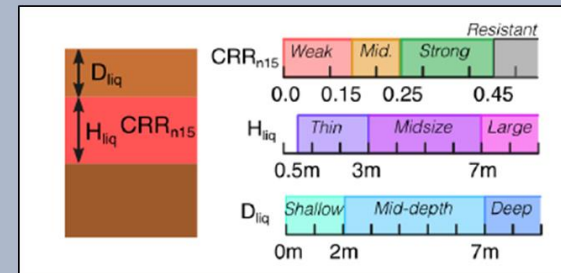
1. RISK PORTFOLIO DATA

ID	lat	lon	DISTRICT	MUNICIPAL	CITY	REGION	postalcode
ID-0001	44,80541666	11,408199	Ferrara	SANCARLO	SANTAGOSTINO	EMILIA-ROMAGNA	4407
ID-0002	44,80735013	11,40139128	Ferrara	SANCARLO	SANTAGOSTINO	EMILIA-ROMAGNA	4407
ID-0003	44,8022905	11,41200315	Ferrara	SANCARLO	SANTAGOSTINO	EMILIA-ROMAGNA	4407
ID-0004	44,80457932	11,40858983	Ferrara	SANCARLO	SANTAGOSTINO	EMILIA-ROMAGNA	4407
ID-0005	44,80469574	11,40868849	Ferrara	SANCARLO	SANTAGOSTINO	EMILIA-ROMAGNA	4407
ID-0006	44,8023033	11,41120737	Ferrara	SANCARLO	SANTAGOSTINO	EMILIA-ROMAGNA	4407
ID-0007	44,80367723	11,40955683	Ferrara	SANCARLO	SANTAGOSTINO	EMILIA-ROMAGNA	4407
ID-0008	44,80497537	11,4081969	Ferrara	SANCARLO	SANTAGOSTINO	EMILIA-ROMAGNA	4407
ID-0009	44,80508723	11,4140857	Ferrara	SANCARLO	SANTAGOSTINO	EMILIA-ROMAGNA	4407
ID-0010	44,80566064	11,40780893	Ferrara	SANCARLO	SANTAGOSTINO	EMILIA-ROMAGNA	4407
ID-0011	44,80405856	11,41410674	Ferrara	SANCARLO	SANTAGOSTINO	EMILIA-ROMAGNA	4407
ID-0012	44,80526434	11,40894626	Ferrara	SANCARLO	SANTAGOSTINO	EMILIA-ROMAGNA	4407
ID-0013	44,80374477	11,41382836	Ferrara	SANCARLO	SANTAGOSTINO	EMILIA-ROMAGNA	4407
ID-0014	44,8035615	11,41406211	Ferrara	SANCARLO	SANTAGOSTINO	EMILIA-ROMAGNA	4407
ID-0015	44,80192248	11,413496	Ferrara	SANCARLO	SANTAGOSTINO	EMILIA-ROMAGNA	4407
ID-0016	44,80578813	11,41197567	Ferrara	SANCARLO	SANTAGOSTINO	EMILIA-ROMAGNA	4407
ID-0017	44,8011481	11,41234284	Ferrara	SANCARLO	SANTAGOSTINO	EMILIA-ROMAGNA	4407
ID-0018	44,80531448	11,40787935	Ferrara	SANCARLO	SANTAGOSTINO	EMILIA-ROMAGNA	4407
ID-0019	44,80507833	11,40745276	Ferrara	SANCARLO	SANTAGOSTINO	EMILIA-ROMAGNA	4407
ID-0020	44,80219934	11,41264125	Ferrara	SANCARLO	SANTAGOSTINO	EMILIA-ROMAGNA	4407

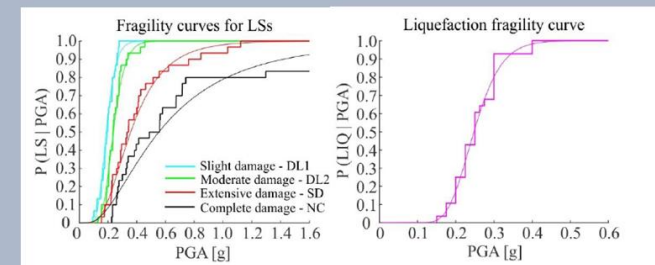
RISK ID	Lat.	Long.	Typology	Use	Width (m)	Length (m)	Height (m)	Storeys above ground	Storeys Below ground
ID-001	59,955532	11,046895	RCFhr	Residential	15	20	40	15	2
ID-002	59,954825	11,046573	CMmr	Governmental	8	15	10	4	0
ID-003	59,955263	11,043518	RMhr	Education	15	20	15	6	1
ID-004	59,956731	11,049535	RCFlr	Business	8	15	6	2	0
ID-005	59,95511	11,044884	URMmr	Health System	10	15	12	4	0
ID-006	59,953441	11,04087	CMlr	Business Center	15	20	30	10	2
ID-007	59,95582	11,04972	RMIr	Residential	6	10	3	1	0

*Building types and administrative information must be given in .csv format.

2. SUBSOIL CHARACTERIZATION



3. FRAGILITY MODEL



4. PHYSICAL DAMAGE EVALUATION

$$P_{LS} = \int_0^{\infty} P(LS | IM = im) \cdot \left| \frac{dH(im)}{d(im)} \right| \cdot d(im)$$

Figure 5-12: Simplified flowchart to evaluate the physical damage on a user-defined building portfolio, for a selected earthquake scenario.



This project has received funding from the European Union's Horizon 2020 research and innovation programme under grant agreement No. 700748

6. LOSSES AND RELIABILITY OF INFRASTRUCTURES

6.1 Critical infrastructures

Critical Infrastructures are the organizations delivering goods and services that is fundamental to the functioning of society. All people consume goods and services on a constant basis, whether this is electric or water or roads. When these goods and services become unavailable, the community and people are acutely aware of the change. Some other CIs like those related to personal and public health (e.g. hospitals) or safety (Police) are not used on an ordinary basis. However, people are even more concerned when they become unavailable because of the vulnerability or exposure generated by their absence.

The first industrial classification schemes of the industrial sector were developed in North America soon after World War II to establish a comprehensive and fully integrated system of economic reporting, in support of post-war reconstruction programmes. In 1994, the advent of the North American Free Trade Agreement (NAFTA) generated a strong requirement for a harmonized classification scheme to support cross-border trade. The North American Industry Classification System (NAICS) developed in 2002 is an industry naming scheme shared among NAFTA countries containing classifications for 20 sectors, 103 subsectors, 328 industry groups, 728 industries, and 928 national industries. Macaulay (2009) proposes a potential top-level list of ten CI sectors that reconciles with NAICS classifications.

- Bank and finance
- Energy
- Information and communication
- Transportation
- Safety and security
- Health service
- Water supply
- Government
- Manufacturing
- Food supply

Murray and Grubestic (2007) add the following:

- National Monuments and Icons
- Nuclear Power Plants
- Dams
- Government Facilities
- Key Commercial Assets

Because the operability of these systems can be vulnerable to disasters or accidents, there is a need to understand how a critical infrastructure and its functionality might be impacted when subjected to disruption. Additionally, the interdependent nature of functionality among different infrastructure is clearly of concern. If a single system is disrupted, secondary failures might occur in interdependent infrastructures



This project has received funding from the European Union's Horizon 2020 research and innovation programme under grant agreement No. 700748

and thus there is a significant need to both measure and monitor the reliability and potential vulnerabilities of these infrastructure systems. Given the massive presence of economic, transportation, telecommunication, energy and medical networks in the industrialized world, it is important to have a spectrum of techniques capable of identifying potential vulnerabilities in singular network elements, or more generalized systematic weaknesses to be protected or fortified.

Reliability and vulnerability are complementary concepts related to the ability of critical infrastructures to provide continuity in operation. Reliability can be expressed as the probability that a given element in a critical infrastructure system is functional at any given time. In this way it is a probabilistic measure of elements in a system and their ability to not fail or malfunction, given a series of established benchmarks or performance guidelines. Vulnerability is a more wide-ranging concept, with much broader implications. While reliability focuses on the possibility of maintaining the performance of critical infrastructure elements, vulnerability focuses on the potential for disrupting these elements or degrading them to a point where performance is diminished. This is a subtle, yet important difference but both reliability and vulnerability are important to the continuity of critical infrastructure operations.

The above concepts impact directly on the losses produced by the physical damage of a critical infrastructure. A unique definition of the losses for all critical infrastructure is impossible as it depends on the type of infrastructure and on its societal role. Broadly, the following categories of losses can be distinguished:

- direct social losses deriving from casualties
- direct economic losses connected with the repair/replacement of the damaged component of the infrastructure
- indirect economic losses connected with the shortage of supply (e.g. displaced households due to loss of housing habitability and short-term shelter needs, lack of service for users, reduced income for a company)
- indirect long-term economic losses connected with the reduced value of the critical infrastructure (e.g. the reduced value of buildings located in a highly valuable area of the city, the loss of market share for a company).

The relative weight of each loss category cannot be uniquely defined as it depends on the relevance of the infrastructure function for the life of people and the adaptive capability of the critical infrastructure.

6.2 Annualized losses

An appropriate cost-benefit analysis of mitigation should consider that while the budget for countermeasures are sustained immediately, or in relatively short time, the advantage is spread over the entire lifecycle of the system (whether a structure, an infrastructure, a lifeline etc.), So expenses and saved repair costs must be expressed on an annual basis to become comparable. As an example, when a company buys a good destined to be used for a prolonged period (typically several years), the relative sustained cost is divided in as many shares as the years of exercises in which the good will presumably be used. Otherwise, the cost would be charged entirely in the year when it is purchased, disregarding the principle of the economic competence of the income components.



This project has received funding from the European Union's Horizon 2020 research and innovation programme under grant agreement No. 700748

There are different criteria to compute the annualized cost of mitigation, one of the most adopted is to equally distribute the invested capital over the lifecycle of the structure adding the interest rate (fixed or variable). The question can be seen as equivalent to borrow the capital necessary for mitigation from a bank at a fixed rate mortgage and pay it back with a constant annual amount. In this way the annualized cost sustained for mitigation is the amount paid by the borrower every year that ensures that the loan is paid off, in full of interest, at the end of its term. The annual payment can be computed with the following formula:

$$AC = C \cdot (1 + MR)^n \frac{MR}{(1 + MR)^n - 1}$$

Equation 6-1

where AC is the annual cost sustained by the investor, C is the capital necessary to cover the expenses of mitigation, MR is the fixed mortgage rate, n is the lifecycle length expressed in years.

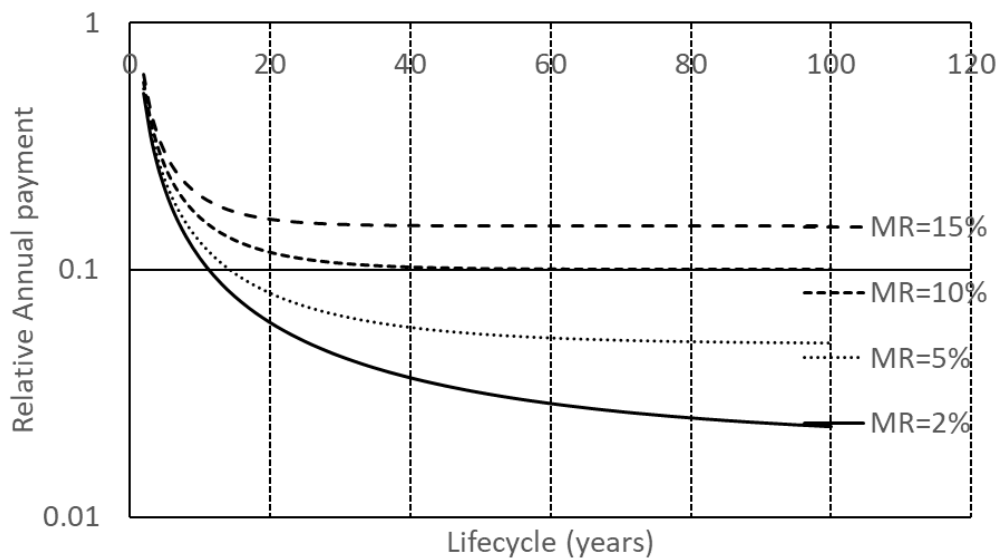


Figure 6-1: Annual expenses for mitigation

This cost should be compared with the annualized benefit, i.e. the earthquake losses saved per each year. HAZUS (FEMA, 2003) computes this amount integrating the product between losses given by earthquakes of different intensity and their annual occurrence probability. In details the hazard, expressed as PGA and spectral acceleration for periods T equal to 0.3 and 1 sec, is evaluated for different return periods (100, 250, 500, 750, 1000, 1500, 2000, and 2500 years) or correspondingly for the exceedance frequency in a year (Table 6-1). These data are then used to transform the losses from all eight scenarios into Annualized Earthquake Loss (AEL) each value computed considering local site effects and structural types. A plot like the one in Figure 6-2 is finally drawn and the area delimited by the AEL-curve, equivalent to taking the summation of the losses multiplied by their annual probability of occurrence represents an approximation to the AEL.



This project has received funding from the European Union's Horizon 2020 research and innovation programme under grant agreement No. 700748

Manual for the assessment of liquefaction risk, defining the procedures to create the database, collect, define, symbolize and store information in the Georeferenced Information System and to perform and represent the risk analysis v. 1.0

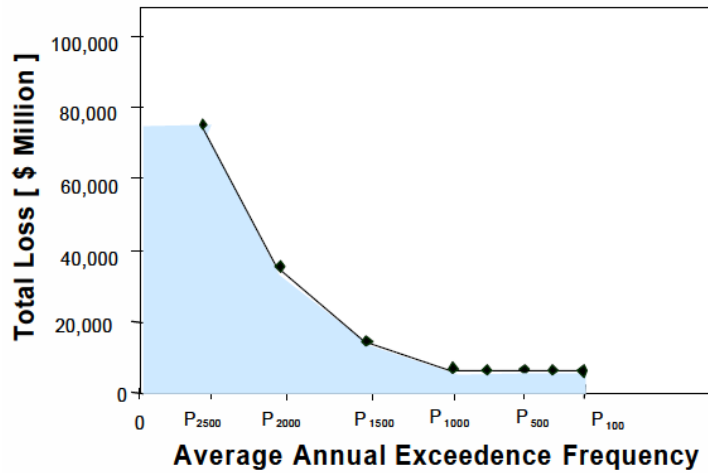


Figure 6-2: Probabilistic loss curve (FEMA, 2003).

Table 6-1: Example of USGS hazard data (FEMA, 2003).

#	Ground Motion Data					
	PGA	AFE	SA (0.3 sec)	AFE	SA (1.0 sec)	AFE
1	5.00E-03	2.49E-02	5.00E-03	3.28E-02	2.50E-03	2.85E-02
2	7.00E-03	2.07E-02	7.50E-03	2.89E-02	3.75E-03	2.37E-02
3	9.80E-03	1.65E-02	1.13E-02	2.40E-02	5.63E-03	1.84E-02
4	1.37E-02	1.25E-02	1.69E-02	1.85E-02	8.44E-03	1.34E-02
5	1.92E-02	8.76E-03	2.53E-02	1.30E-02	1.27E-02	9.24E-03
6	2.69E-02	5.86E-03	3.80E-02	8.45E-03	1.90E-02	6.25E-03
7	3.76E-02	3.87E-03	5.70E-02	5.29E-03	2.85E-02	4.23E-03
8	5.27E-02	2.64E-03	8.54E-02	3.36E-03	4.27E-02	2.95E-03
9	7.38E-02	1.90E-03	1.28E-01	2.27E-03	6.41E-02	2.14E-03
10	1.03E-01	1.43E-03	1.92E-01	1.63E-03	9.61E-02	1.60E-03
11	1.45E-01	1.08E-03	2.88E-01	1.19E-03	1.44E-01	1.18E-03
12	2.03E-01	7.73E-04	4.32E-01	8.28E-04	2.16E-01	8.08E-04
13	2.84E-01	5.06E-04	6.49E-01	5.03E-04	3.24E-01	4.83E-04
14	3.97E-01	2.88E-04	1.30E+00	1.30E-04	4.87E-01	2.36E-04
15	5.56E-01	1.35E-04	1.95E+00	3.84E-05	7.30E-01	9.04E-05
16	7.78E-01	4.88E-05	2.92E+00	7.62E-06	1.09E+00	2.60E-05
17	1.09E+00	1.32E-05	4.38E+00	9.76E-07	1.64E+00	5.08E-06
18	1.52E+00	2.80E-06	6.57E+00	8.61E-08	2.46E+00	6.62E-07

* AFE = Annual Frequency of Exceedence \cong 1/ Return Period



This project has received funding from the European Union's Horizon 2020 research and innovation programme under grant agreement No. 700748

6.3 Buildings

Buildings affected by earthquakes and in particular by liquefaction undergo structural and non-structural repair costs caused by damage to the structural and non-structural components, damage of building contents and business inventory. The restriction of the building's ability to function properly represents another (indirect) relevant source of losses. Direct and indirect losses of buildings are subdivided into the following categories:

- Casualties
- Repair/replacement costs
- Content losses
- Inventory losses
- Indirect economic losses for temporary housing (shelter)

6.3.1 Estimate of casualties

There are different methodologies to estimate the number casualties produced by an earthquake. One of the most popular is the one defined in HAZUS (FEMA, 2003) and depicted by the flow chart of Figure 6-3. Injuries are categorized into four different severity levels, from a slight (level #1) requiring paramedical assistance to instantaneous death (level #4). The code considers 36 different building types and for each of them and a given earthquake scenario defines four possible damage states depending on the building vulnerability. The key point for the calculation is the probability of injury level associated to the building damage, given in a series of tables. The example of Figure 6-3 reports two such tables for complete structural damage, with or without collapse, and the probability of collapse for buildings falling in the fourth damage state. The number of people injured at the different severity levels is thus computed multiplying the probability of injuries times the occupancy of the building.

However, it must be noticed that this methodology applies for the damage induced by shaking and that for liquefaction similar tables do not exist. As widely acknowledged by the experience of past earthquakes, the number of casualties directly induced by liquefaction is limited (or even nil) mostly because damaged buildings rarely reach collapse. So, the above described procedure could be adapted modifying the tables giving the percentage of building collapse related to the fourth damage state.

6.3.2 Economic losses

For building related items, direct losses include:

- Building Repair and Replacement Costs
- Building Contents Losses
- Business Inventory Losses

Time dependent losses to be also calculated for:

- Relocation Expenses
- Loss of Proprietors' Income
- Rental Income Losses



This project has received funding from the European Union's Horizon 2020 research and innovation programme under grant agreement No. 700748

Manual for the assessment of liquefaction risk, defining the procedures to create the database, collect, define, symbolize and store information in the Georeferenced Information System and to perform and represent the risk analysis

Table 13.6: Indoor Casualty Rates by Model Building Type for Complete Structural Damage (No Collapse)

#	Building Type	Casualty Severity Level			
		Severity 1 (%)	Severity 2 (%)	Severity 3 (%)	Severity 4 (%)
1	W1	5	1	0.01	0.01
2	W2	5	1	0.01	0.01
3	S1L	5	1	0.01	0.01
4	S1M	5	1	0.01	0.01
5	S1H	5	1	0.01	0.01
6	S2L	5	1	0.01	0.01
7	S2M	5	1	0.01	0.01
8	S2H	5	1	0.01	0.01
9	S3	5	1	0.01	0.01
10	S4L	5	1	0.01	0.01
11	S4M	5	1	0.01	0.01
12	S4H	5	1	0.01	0.01
13	S5L	5	1	0.01	0.01
14	S5M	5	1	0.01	0.01
15	S5H	5	1	0.01	0.01
16	C1L	5	1	0.01	0.01
17	C1M	5	1	0.01	0.01
18	C1H	5	1	0.01	0.01
19	C2L	5	1	0.01	0.01
20	C2M	5	1	0.01	0.01
21	C2H	5	1	0.01	0.01
22	C3L	5	1	0.01	0.01
23	C3M	5	1	0.01	0.01
24	C3H	5	1	0.01	0.01
25	PC1	5	1	0.01	0.01
26	PC2	5	1	0.01	0.01
27	PC3	5	1	0.01	0.01
28	PC4	5	1	0.01	0.01
29	PC5	5	1	0.01	0.01
30	PC6	5	1	0.01	0.01
31	PC7	5	1	0.01	0.01
32	PC8	5	1	0.01	0.01
33	PC9	5	1	0.01	0.01
34	UR1	10	2	0.02	0.02
35	UR2	10	2	0.02	0.02
36	UR3	5	1	0.01	0.01
80	Major Bridge	17	20	17	7
81	Continuous Bridge	17	20	17	7
82	S.S. Bridge	7	27	20	9

Table 13.7: Indoor Casualty Rates by Model Building Type for Complete Structural Damage (With Collapse)

#	Building Type	Casualty Severity Level			
		Severity 1 (%)	Severity 2 (%)	Severity 3 (%)	Severity 4 (%)
1	W1	40	20	5	7
2	W2	40	20	5	10
3	S1L	40	20	5	10
4	S1M	40	20	5	10
5	S1H	40	20	5	10
6	S2L	40	20	5	10
7	S2M	40	20	5	10
8	S2H	40	20	5	10
9	S3	40	20	5	7
10	S4L	40	20	5	10
11	S4M	40	20	5	10
12	S4H	40	20	5	10
13	S5L	40	20	5	10
14	S5M	40	20	5	10
15	S5H	40	20	5	10
16	C1L	40	20	5	10
17	C1M	40	20	5	10
18	C1H	40	20	5	10
19	C2L	40	20	5	10
20	C2M	40	20	5	10
21	C2H	40	20	5	10
22	C3L	40	20	5	10
23	C3M	40	20	5	10
24	C3H	40	20	5	10
25	PC1	40	20	5	10
26	PC2	40	20	5	10
27	PC3	40	20	5	10
28	PC4	40	20	5	10
29	PC5	40	20	5	10
30	PC6	40	20	5	10
31	PC7	40	20	5	10
32	PC8	40	20	5	10
33	PC9	40	20	5	10
34	UR1	40	20	5	10
35	UR2	40	20	5	10
36	UR3	40	20	5	7
80	Major Bridge	N/A	N/A	N/A	N/A
81	Continuous Bridge	N/A	N/A	N/A	N/A
82	S.S. Bridge	N/A	N/A	N/A	N/A

Table 13.8: Collapse Rates by Model Building Type for Complete Structural Damage

Model Building Type	Probability of Collapse Given a Complete Damage State ^a	
1	W1	0.0%
2	W2	0.0%
3	S1L	0.0%
4	S1M	0.0%
5	S1H	0.0%
6	S2L	0.0%
7	S2M	0.0%
8	S2H	0.0%
9	S3	0.0%
10	S4L	0.0%
11	S4M	0.0%
12	S4H	0.0%
13	S5L	0.0%
14	S5M	0.0%
15	S5H	0.0%
16	C1L	0.0%
17	C1M	0.0%
18	C1H	0.0%
19	C2L	0.0%
20	C2M	0.0%
21	C2H	0.0%
22	C3L	0.0%
23	C3M	0.0%
24	C3H	0.0%
25	PC1	0.0%
26	PC2	0.0%
27	PC3	0.0%
28	PC4	0.0%
29	PC5	0.0%
30	PC6	0.0%
31	PC7	0.0%
32	PC8	0.0%
33	PC9	0.0%
34	UR1	0.0%
35	UR2	0.0%
36	UR3	0.0%

Table 13.1: Injury Classification Scale

Injury Severity Level	Injury Description
Severity 1	Injuries requiring basic medical aid that could be administered by paraprofessionals. These types of injuries would require bandages or observation. Some examples are: a sprain, a severe cut requiring stitches, a minor burn (first degree or second degree on a small part of the body), or a bump on the head without loss of consciousness. Injuries of lesser severity that could be self treated are not estimated by HAZUS.
Severity 2	Injuries requiring a greater degree of medical care and use of medical technology such as x-rays or surgery, but not expected to progress to a life threatening status. Some examples are third degree burns or second degree burns over large parts of the body, a bump on the head that causes loss of consciousness, fractured bone, dehydration or exposure.
Severity 3	Injuries that pose an immediate life threatening condition if not treated adequately and expeditiously. Some examples are: uncontrolled bleeding, punctured organ, other internal injuries, spinal column injuries, or crush syndrome.
Severity 4	Instantaneously killed or mortally injured

POPULATION DISTRIBUTION
Table 13.2

INVENTORY

VULNERABILITY

CASUALTY

CASUALTY

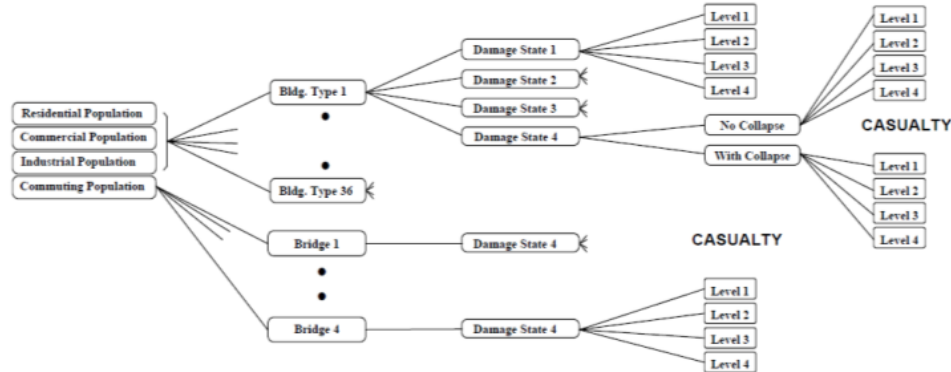


Figure 6-3: Flow chart describing the Hazus methodology to estimate casualties (FEMA, 2003).



This project has received funding from the European Union's Horizon 2020 research and innovation programme under grant agreement No. 700748

6.3.2.1 Direct economic losses

Once physical damage of buildings is estimated in the form of probabilities of each structural and non-structural damage state, conversion to monetary losses requires inventory information and economic data. Hazus (FEMA, 2003) classifies the building typology into 33 classes described in Table 6-2 to determine the non-structural element make-up of the buildings and the nature and value of their contents.

Table 6-2: Building occupancy classes (FEMA, 2003).

No.	Label	Occupancy Class	Description
		Residential	
1	RES1	Single Family Dwelling	Detached House
2	RES2	Mobile Home	Mobile Home
3-8	RES3a-f	Multi Family Dwelling	Apartment/Condominium
9	RES4	Temporary Lodging	Hotel/Motel
10	RES5	Institutional Dormitory	Group Housing (military, college), Jails
11	RES6	Nursing Home	
		Commercial	
12	COM1	Retail Trade	Store
13	COM2	Wholesale Trade	Warehouse
14	COM3	Personal and Repair Services	Service Station/Shop
15	COM4	Professional/Technical Services	Offices
16	COM5	Banks/Financial Institutions	
17	COM6	Hospital	
18	COM7	Medical Office/Clinic	Offices
19	COM8	Entertainment & Recreation	Restaurants/Bars
20	COM9	Theaters	Theaters
21	COM10	Parking	Garages
		Industrial	
22	IND1	Heavy	Factory
23	IND2	Light	Factory
24	IND3	Food/Drugs/Chemicals	Factory
25	IND4	Metals/Minerals Processing	Factory
26	IND5	High Technology	Factory
27	IND6	Construction	Office
		Agriculture	
28	AGR1	Agriculture	
		Religion/Non-Profit	
29	REL1	Church	
		Government	
30	GOV1	General Services	Office
31	GOV2	Emergency Response	Police/Fire Station
		Education	
32	EDU1	Schools	
33	EDU2	Colleges/Universities	Does not include group housing

6.3.2.1.1 Repair/replacement cost

In the common belief, the true cost of buildings damaged or destroyed is their loss of market value, reflecting the age of the building, depreciation, and the architectural/historical value. Market value includes factors such as locations of high land cost, building age that often depreciates the value but sometimes give additional value due to craftsmanship or architectural relevance. Replacement cost is the budget that should be sustained to reconstruct the building and is equal to the extension of the buildings (typically expressed in square meters) multiplied for the building unit cost. The latter is estimated based on complex socio-economic models, adopting data from the census related with the construction classes. In general, it varies depending



This project has received funding from the European Union's Horizon 2020 research and innovation programme under grant agreement No. 700748

with the used materials and on the cost of manufacture. Different categories of buildings can be broadly defined to define this cost (Economy, Average, Custom and Luxury) but a dependency on the local situation must be taken into account.

The replacement cost is one of the most frequently requested output in loss estimation studies, because it gives an immediately understandable picture of the community building losses.

Then cost for structural and non-structural repair can be then computed as follows:

$$rc_i = RC_i \left(\sum_{ds} P_{i_ds} \cdot [(rc_{str}/RC)_{ds_i} + (rc_{non\ str}/RC)_{ds_i}] \right) \quad \text{Equation 6-2}$$

where:

- rc_i is the repair cost for the building type i (see for instance the categorization given in Table 6-2)
- RC_i is the replacement cost for the building type i
- P_{i_ds} is the probability that a building type i is affected by a damage state ds
- $(rc_{str}/RC)_{ds_i}$ and $(rc_{non\ str}/RC)_{ds_i}$ are the ratio between structural and non-structural repair costs and the replacement cost RC for building type i and damage state ds .

Examples of repair cost ratios for earthquake damages on the building categories defined in Table 6-2 are reported in Table 6-3 (HAZUS by FEMA, 2003). The code adopts structural and non-structural repair, distinguishing the latter in acceleration and drift sensitive damage. Application to the study of liquefaction impact should reconsider these costs neglecting those due to acceleration sensitive phenomena and recalibrating the other values differently (the sum of the different percentages pertaining to a building category and damage state must be always 100).



This project has received funding from the European Union's Horizon 2020 research and innovation programme under grant agreement No. 700748

Manual for the assessment of liquefaction risk, defining the procedures to create the database, collect, define, symbolize and store information in the Georeferenced Information System and to perform and represent the risk analysis

Table 6-3: Cost ratios for structural, non-structural (acceleration and drift sensitive) repairs expressed as percentage of replacement costs (FEMA, 2003).

Table 15.2: Structural Repair Cost Ratios (in % of building replacement cost)

No.	Label	Occupancy Class	Structural Damage State			
			Slight	Moderate	Extensive	Complete
Residential						
1	RES1	Single Family Dwelling	0.5	2.3	11.7	23.4
2	RES2	Mobile Home	0.4	2.4	7.3	24.4
3-8	RES3a-f	Multi Family Dwelling	0.3	1.4	6.9	13.8
9	RES4	Temporary Lodging	0.2	1.4	6.8	13.6
10	RES5	Institutional Dormitory	0.4	1.9	9.4	18.8
11	RES6	Nursing Home	0.4	1.8	9.2	18.4
Commercial						
12	COM1	Retail Trade	0.6	2.9	14.7	29.4
13	COM2	Wholesale Trade	0.6	3.2	16.2	32.4
14	COM3	Personal and Repair Services	0.3	1.6	8.1	16.2
15	COM4	Professional/Technical/Business Services	0.4	1.9	9.6	19.2
16	COM5	Banks/Financial Institutions	0.3	1.4	6.9	13.8
17	COM6	Hospital	0.2	1.4	7.0	14.0
18	COM7	Medical Office/Clinic	0.3	1.4	7.2	14.4
19	COM8	Entertainment & Recreation	0.2	1.0	5.0	10.0
20	COM9	Theaters	0.3	1.2	6.1	12.2
21	COM10	Parking	1.3	6.1	30.4	60.9
Industrial						
22	IND1	Heavy	0.4	1.6	7.8	15.7
23	IND2	Light	0.4	1.6	7.8	15.7
24	IND3	Food/Drugs/Chemicals	0.4	1.6	7.8	15.7
25	IND4	Metals/Minerals Processing	0.4	1.6	7.8	15.7
26	IND5	High Technology	0.4	1.6	7.8	15.7
27	IND6	Construction	0.4	1.6	7.8	15.7
Agriculture						
28	AGR1	Agriculture	0.8	4.6	23.1	46.2
Religion/Non-Profit						
29	REL1	Church/Membership Organization	0.3	2.0	9.9	19.8
Government						
30	GOV1	General Services	0.3	1.8	9.0	17.9
31	GOV2	Emergency Response	0.3	1.5	7.7	15.3
Education						
32	EDU1	Schools/Libraries	0.4	1.9	9.5	18.9
33	EDU2	Colleges/Universities	0.2	1.1	5.5	11.0

Table 15.3: Acceleration Sensitive Non-structural Repair Cost Ratios (in % of building replacement cost)

No.	Label	Occupancy Class	Acceleration Sensitive Non-structural Damage State			
			Slight	Moderate	Extensive	Complete
Residential						
1	RES1	Single Family Dwelling	0.5	2.7	8.0	26.6
2	RES2	Mobile Home	0.8	3.8	11.3	37.8
3-8	RES3a-f	Multi Family Dwelling	0.8	4.3	13.1	43.7
9	RES4	Temporary Lodging	0.9	4.3	13.0	43.2
10	RES5	Institutional Dormitory	0.8	4.1	12.4	41.2
11	RES6	Nursing Home	0.8	4.1	12.2	40.8
Commercial						
12	COM1	Retail Trade	0.8	4.4	12.9	43.1
13	COM2	Wholesale Trade	0.8	4.2	12.4	41.1
14	COM3	Personal and Repair Services	1.0	5	15	50.0
15	COM4	Professional/Technical/Business Services	0.9	4.8	14.4	47.9
16	COM5	Banks/Financial Institutions	1.0	5.2	15.5	51.7
17	COM6	Hospital	1.0	5.1	15.4	51.3
18	COM7	Medical Office/Clinic	1.0	5.2	15.3	51.2
19	COM8	Entertainment & Recreation	1.1	5.4	16.3	54.4
20	COM9	Theaters	1.0	5.3	15.8	52.7
21	COM10	Parking	0.3	2.2	6.5	21.7
Industrial						
22	IND1	Heavy	1.4	7.2	21.8	72.5
23	IND2	Light	1.4	7.2	21.8	72.5
24	IND3	Food/Drugs/Chemicals	1.4	7.2	21.8	72.5
25	IND4	Metals/Minerals Processing	1.4	7.2	21.8	72.5
26	IND5	High Technology	1.4	7.2	21.8	72.5
27	IND6	Construction	1.4	7.2	21.8	72.5
Agriculture						
28	AGR1	Agriculture	0.8	4.6	13.8	46.1
Religion/Non-Profit						
29	REL1	Church/Membership Organization	0.9	4.7	14.3	47.6
Government						
30	GOV1	General Services	1.0	4.9	14.8	49.3
31	GOV2	Emergency Response	1.0	5.1	15.1	50.5
Education						
32	EDU1	Schools/Libraries	0.7	3.2	9.7	32.4
33	EDU2	Colleges/Universities	0.6	2.9	8.7	29.0

Table 15.4: Drift Sensitive Non-structural Repair Costs (in % of building replacement cost)

No.	Label	Occupancy Class	Drift Sensitive Non-structural Damage State			
			Slight	Moderate	Extensive	Complete
Residential						
1	RES1	Single Family Dwelling	1.0	5.0	25.0	50.0
2	RES2	Mobile Home	0.8	3.8	18.9	37.8
3-8	RES3a-f	Multi Family Dwelling	0.9	4.3	21.3	42.5
9	RES4	Temporary Lodging	0.9	4.3	21.6	43.2
10	RES5	Institutional Dormitory	0.8	4.0	20.0	40.0
11	RES6	Nursing Home	0.8	4.1	20.4	40.8
Commercial						
12	COM1	Retail Trade	0.6	2.7	13.8	27.5
13	COM2	Wholesale Trade	0.6	2.6	13.2	26.5
14	COM3	Personal and Repair Services	0.7	3.4	16.9	33.8
15	COM4	Professional/Technical/Business Services	0.7	3.3	16.4	32.9
16	COM5	Banks/Financial Institutions	0.7	3.4	17.2	34.5
17	COM6	Hospital	0.8	3.5	17.4	34.7
18	COM7	Medical Office/Clinic	0.7	3.4	17.2	34.4
19	COM8	Entertainment & Recreation	0.7	3.6	17.8	35.6
20	COM9	Theaters	0.7	3.5	17.6	35.1
21	COM10	Parking	0.4	1.7	8.7	17.4
Industrial						
22	IND1	Heavy	0.2	1.2	5.9	11.8
23	IND2	Light	0.2	1.2	5.9	11.8
24	IND3	Food/Drugs/Chemicals	0.2	1.2	5.9	11.8
25	IND4	Metals/Minerals Processing	0.2	1.2	5.9	11.8
26	IND5	High Technology	0.2	1.2	5.9	11.8
27	IND6	Construction	0.2	1.2	5.9	11.8
Agriculture						
28	AGR1	Agriculture	0.0	0.8	3.8	7.7
Religion/Non-Profit						
29	REL1	Church/Membership Organization	0.8	3.3	16.3	32.6
Government						
30	GOV1	General Services	0.7	3.3	16.4	32.8
31	GOV2	Emergency Response	0.7	3.4	17.1	34.2
Education						
32	EDU1	Schools/Libraries	0.9	4.9	24.3	48.7
33	EDU2	Colleges/Universities	1.2	6.0	30.0	60.0



This project has received funding from the European Union's Horizon 2020 research and innovation programme under grant agreement No. 700748

Manual for the assessment of liquefaction risk, defining the procedures to create the database, collect, define, symbolize and store information in the Georeferenced Information System and to perform and represent the risk analysis

6.3.2.1.2 Building content and business inventory losses

Normally liquefaction does not produce acceleration capable of damaging building contents such as furniture, equipment, computers, supplies or other business inventory. Normally it is assumed that most contents damage, such as overturned cabinets and equipment sliding off tables and counters, is a function of building accelerations and thus acceleration sensitive non-structural damage is a good indicator of contents damage for earthquakes induced shaking.

When acceleration is limited, like in the case of building located on liquefied soil, it is unlikely that there will be such a damage on the content. Content can be normally retrieved, unless for the case of complete collapse when the building has to be demolished.

Similar consideration applies to the business inventory losses that can be computed as follows:

$$INV_DAM_i = Prod_i \cdot (INV/Prod)_i \cdot INV_damage \cdot P_{i_collapse}$$

Equation 6-3

where:

- INV_DAM_i is the inventory losses for the business activity i (see for instance the categorization given in Table 6-2)
- $Prod_i$ is the annual gross sales of the business activity. Unless specific studies are performed, this datum is provided by statistical reports performed at the national level.
- $(INV/Prod)_i$ is the business inventory as a percentage of annual gross sales for business type i (Table 6-4 reports the values given in HAZUS, FEMA 2003)
- INV_damage is the fraction of damaged inventory. In general, it is related to the damage state of the building. For complete damage, Hazus fixes this fraction equal to 50%.
- $P_{i_collapse}$ is the probability that a building type i is affected by complete collapse.

Table 6-4: Business inventory as percentage of annual gross sales (FEMA, 2003).

No.	Label	Occupancy Class	Business Inventory (%)
		Commercial	
7	COM1	Retail Trade	13
8	COM2	Wholesale Trade	10
		Industrial	
17	IND1	Heavy	5
18	IND2	Light	4
19	IND3	Food/Drugs/Chemicals	5
20	IND4	Metals/Minerals Processing	3
21	IND5	High Technology	4
22	IND6	Construction	2
		Agriculture	
23	AGR1	Agriculture	8



This project has received funding from the European Union's Horizon 2020 research and innovation programme under grant agreement No. 700748

Manual for the assessment of liquefaction risk, defining the procedures to create the database, collect, define, symbolize and store information in the Georeferenced Information System and to perform and represent the risk analysis

6.3.2.2 Indirect economic losses

6.3.2.2.1 Interruption of function

Indirect costs of damaged buildings are related to the interruption of the functions carried out in the building. They depend on the time necessary to restore the original conditions of the business, being this time dictated by the repair of the building and the time necessary for decision making, negotiating financial issues with insurance, obtaining permissions, negotiating with construction companies etc. An example of recovery time given in Hazus (FEMA, 2003) for the different occupancies listed in Table 6-2 is reported in Table 6-5.a. However, some activities can reduce this time relocating elsewhere their operative site. Table 6-5.b provides indication of this reducing factor for different activities. The functionality loss time for a generic activity can be thus computed as:

$$FLT_i = BRT_i \cdot SIM_i$$

Equation 6-4

where FLT_i is the functionality loss time for the generic activity

BRT_i is the building recovery time for the generic activity

SLM_i is the service interruption multiplier for the generic activity

Table 6-5: Recovery time (in days) for different categories of building (a) and time interruption multipliers (b) for different activities (FEMA, 2003).

Table 15.10: Building Recovery Time (Time in Days)

No.	Label	Occupancy Class	Recovery Time				
			None	Slight	Moderate	Extensive	Complete
Residential							
1	RES1	Single Family Dwelling	0	5	120	360	720
2	RES2	Mobile Home	0	5	20	120	240
3-8	RES3a-f	Multi Family Dwelling	0	10	120	480	960
9	RES4	Temporary Lodging	0	10	90	360	480
10	RES5	Institutional Dormitory	0	10	90	360	480
11	RES6	Nursing Home	0	10	120	480	960
Commercial							
12	COM1	Retail Trade	0	10	90	270	360
13	COM2	Wholesale Trade	0	10	90	270	360
14	COM3	Personal and Repair Services	0	10	90	270	360
15	COM4	Professional/Technical/Business Services	0	20	90	360	480
16	COM5	Bank/Financial Institutions	0	20	90	180	360
17	COM6	Hospital	0	20	135	540	720
18	COM7	Medical Office/Clinic	0	20	135	270	540
19	COM8	Entertainment & Recreation	0	20	90	180	360
20	COM9	Theater	0	20	90	180	360
21	COM10	Parking	0	5	60	180	360
Industrial							
22	IND1	Heavy	0	10	90	240	360
23	IND2	Light	0	10	90	240	360
24	IND3	Food/Drug/Chemicals	0	10	90	240	360
25	IND4	Metal/Mineral Processing	0	10	90	240	360
26	IND5	High Technology	0	20	135	360	540
27	IND6	Construction	0	10	60	160	320
Agriculture							
28	AGR1	Agriculture	0	2	20	60	120
Religion/Non-Profit Organization							
29	REL1	Church/Membership Organization	0	5	120	480	960
Government							
30	GOV1	General Services	0	10	90	360	480
31	GOV2	Emergency Response	0	10	60	270	360
Education							
32	EDU1	Schools/Libraries	0	10	90	360	480
33	EDU2	Colleges/Universities	0	10	120	480	960

(a)

Table 15.11: Building and Service Interruption Time Multipliers

No.	Label	Occupancy Class	Construction Time				
			None	Slight	Moderate	Extensive	Complete
Residential							
1	RES1	Single Family Dwelling	0	0	0.5	1.0	1.0
2	RES2	Mobile Home	0	0	0.5	1.0	1.0
3-8	RES3a-f	Multi Family Dwelling	0	0	0.5	1.0	1.0
9	RES4	Temporary Lodging	0	0	0.5	1.0	1.0
10	RES5	Institutional Dormitory	0	0	0.5	1.0	1.0
11	RES6	Nursing Home	0	0	0.5	1.0	1.0
Commercial							
12	COM1	Retail Trade	0.5	0.1	0.1	0.3	0.4
13	COM2	Wholesale Trade	0.5	0.1	0.2	0.3	0.4
14	COM3	Personal and Repair Services	0.5	0.1	0.2	0.3	0.4
15	COM4	Professional/Technical/Business Services	0.5	0.1	0.1	0.2	0.3
16	COM5	Bank/Financial Institutions	0.5	0.1	0.05	0.03	0.03
17	COM6	Hospital	0.5	0.1	0.5	0.5	0.5
18	COM7	Medical Office/Clinic	0.5	0.1	0.5	0.5	0.5
19	COM8	Entertainment & Recreation	0.5	0.1	1.0	1.0	1.0
20	COM9	Theater	0.5	0.1	1.0	1.0	1.0
21	COM10	Parking	0.1	0.1	1.0	1.0	1.0
Industrial							
22	IND1	Heavy	0.5	0.5	1.0	1.0	1.0
23	IND2	Light	0.5	0.1	0.2	0.3	0.4
24	IND3	Food/Drug/Chemicals	0.5	0.2	0.2	0.3	0.4
25	IND4	Metal/Mineral Processing	0.5	0.2	0.2	0.3	0.4
26	IND5	High Technology	0.5	0.2	0.2	0.3	0.4
27	IND6	Construction	0.5	0.1	0.2	0.3	0.4
Agriculture							
28	AGR1	Agriculture	0	0	0.05	0.1	0.2
Religion/Non-Profit Organization							
29	REL1	Church/Membership Organization	1	0.2	0.05	0.03	0.03
Government							
30	GOV1	General Services	0.5	0.1	0.02	0.03	0.03
31	GOV2	Emergency Response	0.5	0.1	0.02	0.03	0.03
Education							
32	EDU1	Schools/Libraries	0.5	0.1	0.02	0.05	0.05
33	EDU2	Colleges/Universities	0.5	0.1	0.02	0.03	0.03

(b)

The loss of income can be thus estimated as:



This project has received funding from the European Union's Horizon 2020 research and innovation programme under grant agreement No. 700748

Manual for the assessment of liquefaction risk, defining the procedures to create the database, collect, define, symbolize and store information in the Georeferenced Information System and to perform and represent the risk analysis

$$LI_i = FA_i \cdot INC_i \cdot \sum_{ds} FLT_i \cdot P_{i_ds}$$

Equation 6-5

where LI_i is the loss of income for the generic activity

FA_i is floor are of the generic activity

INC_i is the income per unit area and per day of the generic activity (variable from region to region)

FLT_i is the functionality loss time for the generic activity (Equation 6-4)

P_{i_ds} is the probability that a building type i is affected by a damage state ds

Finally, relocation implies another cost that is sustained partly by the holder of an activity partly by the building owner. Independently on the subject who pays each cost, the total cost for the community is given by the sum of disruption, that include the cost of shifting and transferring the activity, and the rental of temporary space. The sum of these two costs is given by the following expression:

$$RC_i = FA_i \cdot \sum_{ds} (DC_i + RENT_i \cdot FLT_i) \cdot P_{i_ds}$$

Equation 6-6

where RC_i is the relocation cost for the generic activity

FA_i is floor are of the generic activity

DC_i is the disruption cost per unit area

$RENT_i$ is the rental cost per unit area and per day (variable from site to site depending on the local market conditions)

FLT_i is the functionality loss time for the generic activity (Equation 6-4)

P_{i_ds} is the probability that a building type i is affected by a damage state ds

6.3.2.2.2 Shelter needs

Uninhabitability of dwelling units depends on the actual structural damage and on the uninhabitability perceived by their occupants. The methodology defined by Hazus (FEMA, 2003) considers all dwelling units located in completely damaged buildings to be uninhabitable. For dwelling units located in moderately and extensively damaged multi-family structures uninhabitability depends on the fact that renters perceive it even if the level of damage is moderate. On the other hand, people living in single-family homes are much more likely to tolerate damage and continue to live in their home.

By applying an occupancy rate (households vs. dwelling units), the total number of displaced households (#DH) is calculated by the following relationship.



This project has received funding from the European Union's Horizon 2020 research and innovation programme under grant agreement No. 700748

Manual for the assessment of liquefaction risk, defining the procedures to create the database, collect, define, symbolize and store information in the Georeferenced Information System and to perform and represent the risk analysis

$$DH = HH \cdot \left(\frac{SFU \cdot SF + MFU \cdot MF}{SFU + MFU} \right)$$

Equation 6-7

Where

HH is the total number of households, SFU and MFU are respectively the total Number of Single-Family Dwelling Units and of Multi-Family Dwelling Units. SF and MF are the fraction of uninhabitable Single and Multiple Family Dwelling Units, that can be computed as follows.

$$SF = w_{SFM} \cdot SFM + w_{SFE} \cdot SFE + w_{SFC} \cdot SFC$$

Equation 6-8

$$MF = w_{MFM} \cdot MFM + w_{MFE} \cdot MFE + w_{MFC} \cdot MFC$$

Equation 6-9

Where

SFM, SFE and SFC are the probability of Single-Family Unit to be in respectively moderate, extensive and collapse structural damage state.

Analogously MFM, MFE and MFC are the probability of Multiple Family Unit to be in respectively moderate, extensive and collapse structural damage state

The weighting factors are given in Table 6-6.

Table 6-6: Default values for damage state probabilities (FEMA, 2003).

Weight Factor	Default Value
w_{SFM}	0.0
w_{SFE}	0.0
w_{SFC}	1.0
w_{MFM}	0.0
w_{MFE}	0.9
w_{MFC}	1.0

The model considered in Hazus to compute the number of households seeking short term public shelter is derived from the observation of past disasters and includes information on income, ethnicity, ownership of the dwelling and age. The computation of people requiring short term housing STP is based on the following formula:

$$STP = POP \cdot \frac{DH}{HH} \cdot \sum_{i=1}^5 \sum_{j=1}^5 \sum_{k=1}^2 \sum_{l=1}^3 (\alpha_{ijkl} \cdot HI_i \cdot HE_j \cdot HO_k \cdot HA_l)$$

Equation 6-10



This project has received funding from the European Union's Horizon 2020 research and innovation programme under grant agreement No. 700748

Manual for the assessment of liquefaction risk, defining the procedures to create the database, collect, define, symbolize and store information in the Georeferenced Information System and to perform and represent the risk analysis

Where POP is the population in census tract

H_i - Percentage of population in the i^{th} income class

HE_j - Percentage of population in the j^{th} ethnic class

HO_k - Percentage of population in the k^{th} ownership class

HA_l - Percentage of population in the l^{th} age class

α_{ijkl} - is a weight factor computed through the following relation:

$$\alpha_{ijkl} = (IW \cdot IM_i) + (EW \cdot EM_j) + (OW \cdot OM_k) + (AW \cdot AM_l)$$

Equation 6-11

with the factors and given in Table 6-7 and Table 6-8.

Table 6-7: Shelter category weights (FEMA, 2003).

Class	Description	Default
IW	Income Weighting Factor	0.73
EW	Ethnic Weighting Factor	0.27
OW	Ownership Weighting Factor	0.00
AW	Age Weighting Factor	0.00

Table 6-8: Shelter relative modification factors (FEMA, 2003)

Class	Description	Default
Income		
IM_1	Household Income < \$10000	0.62
IM_2	\$10000 < Household Income < \$15000	0.42
IM_3	\$15000 < Household Income < \$25000	0.29
IM_4	\$25000 < Household Income < \$35000	0.22
IM_5	\$35000 < Household Income	0.13
Ethnic		
EM_1	White	0.24
EM_2	Black	0.48
EM_3	Hispanic	0.47
EM_4	Asian	0.26
EM_5	Native American	0.26
Ownership		
OM_1	Own Dwelling Unit	0.40
OM_2	Rent Dwelling Unit	0.40
Age		
AM_1	Population Under 16 Years Old	0.40
AM_2	Population Between 16 and 65 Years Old	0.40
AM_3	Population Over 65 Years Old	0.40

SYNER-G (2013) adopts a different model where the first decision step in leaving or staying at home after an earthquake (building habitability) is determined as a combination of the functionality of buildings (building usability), utility services and impending weather conditions. It implies a interrelated approach where building usability is derived from a simplified semi-empirical approach as a function of the severity of



This project has received funding from the European Union's Horizon 2020 research and innovation programme under grant agreement No. 700748

observed damage to structural and non-structural elements of buildings. In this procedure, each building is firstly classified as Fully Usable, Partially Usable and Non-Usable depending on the structural damage. Then non-usable buildings are considered non-habitable, partially or fully usable buildings can be habitable or not depending on the availability of utilities. The utility loss UL is defined averaging with weight factors w_j the losses of the different utilities UL_j (gas, potable and waste water, electricity), each given by the ratio of unsatisfied over required demand:

$$UL = \sum_{j=1}^N UL_j \cdot w_j \quad \text{Equation 6-12}$$

The percentage fully or partially usable buildings that are non-habitable (NH_{FU} , or NH_{PU}) is thus determined as the portion of buildings which have utility losses greater than the utility loss threshold value (U_{L_ULT}). The Uninhabitable Building Index (UBI) is computed as the ratio of occupants of buildings that are uninhabitable to the total population (N) according to the following relationship:

$$BHI = N \cdot (N_{FU} \cdot NH_{FU} + N_{PU} \cdot NH_{PU} + NU - N_d) \quad \text{Equation 6-13}$$

where:

N_{FU} , N_{PU} , N_{NU} are the numbers of occupants in buildings that are fully, partially and non-usable

NH_{FU} , NH_{PU} are the fractions of fully or partially usable buildings that are non-habitable due to the condition $UL > ULT$

N_d is the number of dead persons estimated in a selected casualty model.

6.4 Transportation networks

6.4.1 Direct economic losses

The direct economic losses on transportation lifelines such as highways and railroads depend on the inventory data providing the location of all nodes and links and on the models adopted to quantify damage. Losses are computed considering the probabilities of exceeding a certain damage state ($P[D_s \geq ds_i]$), the replacement value of the damaged components and the level of damage (the ratio DR_i) for each damage state, ds_i . Economic losses are evaluated by multiplying the compounded damage ratio (DR_c) by the replacement value. The compounded repair cost is computed as the probabilistic combination of damage ratios as follows:

$$Trc_i = TRC_i \left(\sum_{ds} P_{i_ds} \cdot D_{i_ds} \right) \quad \text{Equation 6-14}$$

where:

Trc_i is the repair cost for the i^{th} component

TRC_i is the replacement cost for the i^{th} component



This project has received funding from the European Union's Horizon 2020 research and innovation programme under grant agreement No. 700748

Manual for the assessment of liquefaction risk, defining the procedures to create the database, collect, define, symbolize and store information in the Georeferenced Information System and to perform and represent the risk analysis

$P_{i_{ds}}$ is the probability that the i^{th} component is affected by a damage state ds

$D_{i_{ds}}$ is the damage ratio of the i^{th} component for a given damage state ds (i.e the ratio between damage and replacement cost).

The replacement costs of each component (node or link) should be evaluated case by case depending on the specific situation (country, typology of the component, manufacturing etc.). FEMA (2003) provides a list of costs for the main components of highways, railways etc. computed for the standard situation of 1994 US dollars (see Table 6-9). Similarly, the damage ratios are provided by FEMA (2003) for different damage states affecting highway or railway systems.

Table 6-9: Replacement costs and damage ratios for highway and railway systems (FEMA, 2003).

Table 15.16: Default Replacement Values of Transportation System Components

System	Replacement Value (thous. \$)	Label	Component Classification	
Highway	10,000	HRD1	Major Road (value based on one km length, 4 lanes)	
	5,000	HRD2	Urban Street (value based on one km length, 2 lanes)	
	20,000	HWB1/HWB2	Major Bridges	
	5,000	HWB3, 9, 10, 11, 15, 16, 20, 21, 22, 23, 26, 27		
	1,000	HWB5, 4, 5, 6, 7, 12, 13, 14, 17, 18, 19, 24, 25, 28	Continuous Bridges	
			Other Bridges	
	20,000	HTU1	Highway Bored/Drilled Tunnel (value based on liner)	
	20,000	HTU2	Highway Cut and Cover Tunnel (value based on liner)	
	Rail	1,500	ERT1	Rail Track (value based on one km length)
		5,000	EBR1	Rail Bridge - Seismically Designed
5,000		EBR2	Rail Bridge - Conventionally Designed	
10,000		RTU1	Rail Bored/Drilled Tunnel (value based on liner)	
10,000		RTU2	Rail Cut and Cover Tunnel (value based on liner)	
2,000		RST1	Rail Urban Station (C2L)	
2,000		RST2	Rail Urban Station (S2L)	
2,000		RST3	Rail Urban Station (S1L)	
2,000		RST4	Rail Urban Station (S5L)	
2,000		RST5	Rail Urban Station (PC1)	
2,000		RST6	Rail Urban Station (C3L)	
2,000		RST7	Rail Urban Station (W1L)	
3,000		RFF1	Rail Fuel Facility w/ Anchored Tanks, w/ BU Power	
3,000		RFF2	Rail Fuel Facility w/ Anchored Tanks, w/ BU Power	
3,000		RFF3	Rail Fuel Facility w/ Unanchored Tanks, w/ BU Power	
3,000		RFF4	Rail Fuel Facility w/ Unanchored Tanks, w/ BU Power	
3,000		RFF5	Rail Fuel Facility w/ Buried Tanks	
3,000		RDF1	Rail Dispatch Facility w/ Anchored Sub-Comp., w/ BU Power	
3,000		RDF2	Rail Dispatch Facility w/ Anchored Sub-Comp., w/ BU Power	
3,000		RDF3	Rail Dispatch Facility w/ Unanchored Sub-Comp., w/ BU Power	
3,000		RDF4	Rail Dispatch Facility w/ Unanchored Sub-Comp., w/0 BU Power	
2,800		RMF1	Rail Maintenance Facility (C2L)	
2,800		RMF2	Rail Maintenance Facility (S1L)	
2,800		RMF3	Rail Maintenance Facility (S2L)	
2,800		RMF4	Rail Maintenance Facility (S3L)	
2,800		RMF5	Rail Maintenance Facility (PC1)	
2,800		RMF6	Rail Maintenance Facility (C3L)	
2,800		RMF7	Rail Maintenance Facility (W1)	

Table 15.16: Default Replacement Values of Transportation System Components (con't)

System	Replacement Value (thous. \$)	Label	Component Classification
Light Rail	1,500	LTR1	Light Rail Track
	5,000	LBR1	Light Rail Bridge - Seismically Designed/Retrofitted
	5,000	LBR2	Light Rail Bridge - Conventionally Designed
	10,000	LTU1	Light Rail Bored/Drilled Tunnel (value based on liner)
	10,000	LTU2	Light Rail Cut and Cover Tunnel (value based on liner)
	2,000	LDC1	Light Rail DC Substation w/ Anchored Sub-Components
	2,000	LDC2	Light Rail DC Substation w/ Unanchored Sub-Comp.
	3,000	LDF1	Lt Rail Dispatch Fac w/ Anchored Sub-Comp., w/ BU Power
	3,000	LDF2	Lt Rail Dispatch Fac w/ Anchored Sub-Comp., w/ BU Power
	3,000	LDF3	Lt Rail Dispatch Fac w/ Unanchored Sub-Comp., w/ BU Power
	3,000	LDF4	Lt Rail Dispatch Fac w/ Unanchored Sub-Comp., w/ BU Power
	2,600	LMF1	Light Rail Maintenance Facility (C2L)
	2,600	LMF2	Light Rail Maintenance Facility (S2L)
	2,600	LMF3	Light Rail Maintenance Facility (S1L)
	2,600	LMF4	Light Rail Maintenance Facility (S3L)
	2,600	LMF5	Light Rail Maintenance Facility (PC1)
	2,600	LMF6	Light Rail Maintenance Facility (C3L)
2,600	LMF7	Light Rail Maintenance Facility (W1)	
Bus	1,000	BPT1	Bus Urban Station (C2L)
	1,000	BPT2	Bus Urban Station (S2L)
	1,000	BPT3	Bus Urban Station (S1L)
	1,000	BPT4	Bus Urban Station (S5L)
	1,000	BPT5	Bus Urban Station (PC1)
	1,000	BPT6	Bus Urban Station (C3L)
	1,000	BPT7	Bus Urban Station (W1)
	150	BFF1	Bus Fuel Facility w/ Anchored Tanks, w/ BU Power
	150	BFF2	Bus Fuel Facility w/ Anchored Tanks, w/ BU Power
	150	BFF3	Bus Fuel Facility w/ Unanchored Tanks, w/ BU Power
	150	BFF4	Bus Fuel Facility w/ Unanchored Tanks, w/ BU Power
	150	BFF5	Bus Fuel Facility w/ Buried Tanks
	400	BDF1	Bus Dispatch Fac. w/ Anchored Sub-Comp., w/ BU Power
	400	BDF2	Bus Dispatch Fac. w/ Anchored Sub-Comp., w/ BU Power
	400	BDF3	Bus Dispatch Fac. w/ Unanchored Sub-Comp., w/ BU Power
	400	BDF4	Bus Dispatch Fac. w/ Unanchored Sub-Comp., w/ BU Power
	1,300	BMF1	Bus Maintenance Facility (C2L)
	1,300	BMF2	Bus Maintenance Facility (S2L)
	1,300	BMF3	Bus Maintenance Facility (S1L)
	1,300	BMF4	Bus Maintenance Facility (S3L)
1,300	BMF5	Bus Maintenance Facility (PC1)	

Table 15.19: Damage Ratios for Railway System Components

Table 15.18: Damage Ratios for Highway System Component

Classification	Damage State	Best Estimate Damage Ratio	Range of Damage Ratios
Roadways	slight	0.05	0.01 to 0.15
	moderate	0.20	0.15 to 0.4
	extensive/ complete	0.70	0.4 to 1.0
Tunnel's Lining	slight	0.01	0.01 to 0.15
	moderate	0.30	0.15 to 0.4
	extensive/ complete	0.70	0.4 to 0.8
Bridges	slight	0.03	0.01 to 0.03
	moderate	0.08	0.02 to 0.15
	extensive/ complete	0.25	0.10 to 0.40
	complete	1.00*	0.30 to 1.00

Classification	Damage State	Best Estimate Damage Ratio	Range of Damage Ratios
Bridges	slight	0.12	0.01 to 0.15
	moderate	0.19	0.15 to 0.4
	extensive	0.40	0.4 to 0.8
	complete	1.00	0.8 to 1.0
Fuel Facilities	slight	0.15	0.01 to 0.15
	moderate	0.39	0.15 to 0.4
	extensive	0.80	0.4 to 0.8
	complete	1.00	0.8 to 1.0
Dispatch Facilities	slight	0.04	0.01 to 0.15
	moderate	0.4	0.15 to 0.4
	extensive	0.8	0.4 to 0.8
	complete	1.00	0.8 to 1.0
Urban Stations and Maintenance Facilities	slight	0.10	0.01 to 0.15
	moderate	0.40	0.15 to 0.4
	extensive	0.80	0.4 to 0.8
	complete	1.00	0.8 to 1.0



This project has received funding from the European Union's Horizon 2020 research and innovation programme under grant agreement No. 700748

Manual for the assessment of liquefaction risk, defining the procedures to create the database, collect, define, symbolize and store information in the Georeferenced Information System and to perform and represent the risk analysis

6.4.2 Indirect economic/social losses

The physical losses on transportation infrastructures turn into a deficiency of function that may have severe implications on the usage of the infrastructure, from a decay of the performance to the complete interruption of the service. Depending on the time necessary to restore the original conditions, these effects may cause economic and social losses to the community. Studying this impact requires the characterization and modelling of the transportation network, with the identification of parameters describing its operative conditions, a model that transforms the physical damage into the loss of functionality and a metric to evaluate the performance of the damaged infrastructure in comparison with the original conditions.

A multi-level strategy to analyze losses has been proposed in Syner-G (2013). It requires first to identify the system components, i.e. all edges that are vulnerable to seismic shaking or geotechnical hazards (i.e. ground failure due to liquefaction, landslides and fault rupture):

- *RDN01*: Bridge [Points or edges]
- *RDN02*: Tunnel [Edges]
- *RDN03*: Embankment (road on) [Edges]
- *RDN04*: Trench (road in a) [Edges]
- *RDN05*: Unstable slope (road on, or running along) [Edges]
- *RDN06*: Road pavements [Edges]
- *RDN07*: Bridges abutments [Points or edges]

Information on the Road Transportation network can be schematically stores as described in Table 6-10.

Table 6-10: Main attributes/properties of the road Transportation network class (Syner G, 2013).

Group	Attribute(s)	Description
Global properties	tripDemand	Origin-destination matrix built from the TAZ nodes
Pointers	roadBlockageModel	Road blockage model to be used
	roadBlockageCoefficients	Coefficients of road blockage model to be used
	road, trench, embank, unstSlope, tunnel, bridge	Pointers to all road pavements, trenches, embankments, unstable slopes, tunnels, bridges, which are assigned specific fragility functions
	intersection	Pointers to all intersections, objects from the Intersection class
	external	Pointers to all external stations, objects from the ExternalStation class
	taz	Pointers to all Traffic Analysis Zones, objects from the TAZ class
Edge properties stored at RDN level	speed, lanes, dependency, hierarchy	Length, centroid, etc. are attributes inherited from the Directed Network class. Here the network-specific properties are listed (free-flow speed, number of lanes, classification, etc.)
Node properties stored at RDN level	tazType	Type of Traffic Analysis Zones (type of trip demand)
State variables recording RDN state	states	$n_E \times 1$ collection of properties that describe the current state for each of the n_E events (fields: damage state, isBroken, isBlocked, SCL, WCL, isolatedTAZ, etc.)



This project has received funding from the European Union's Horizon 2020 research and innovation programme under grant agreement No. 700748

Manual for the assessment of liquefaction risk, defining the procedures to create the database, collect, define, symbolize and store information in the Georeferenced Information System and to perform and represent the risk analysis

The analysis of the functionality of the transportation network can be performed at one of the following three levels:

- Level 0 (Vulnerability analysis):

is a basic vulnerability analysis aimed at quantifying the physical performance of a single component of the network (e.g. damages to roads, tunnel or bridges)

- Level I (Connectivity analysis):

the integrity of the network is studied in terms of pure connectivity, focusing on the services provided by the network, e.g. the rescue function immediately after the earthquake. This analysis may be of interest to identify critical portions of the network, components necessary to keep the connectivity between fundamental points of the networks.

- Level IIa (Capacity analysis):

compared with the previous level, this analysis is widened to consider the network capacity to accommodate traffic flows. An example of this approach (Shinozuka et al., 2003) is aimed at determining the direct and indirect economic loss due to damage to a transportation network. Direct loss is related to physical damage to vulnerable components, while indirect loss is related to functionality of the transportation system, whose degradation is measured in terms of a system-level performance index called Driver's delay (DD), i.e., the increase in total daily travel time for all travelers. Another example (Chang et al., 2011) goes beyond the pre-earthquake origin-destination matrix and considers the post-quake traffic scenario determined by the damage of transportation infrastructures.

- Level IIb (Serviceability analysis):

this very challenging approach aims at obtaining a realistic estimate of total loss, inclusive of direct physical damage to the built environment (residential and industrial buildings as well as network components), loss due to reduced activity in the economic sectors (industry, services), and losses due to (increased travel time). Economic interdependencies must be accounted for, such as the reduction in demand and supply of commodities (due to damaged factories, etc.), hence in the demand for travel, and due to the increased travel costs. At this level the relevance and the complexity of the economic models become dominant over that of the transportation network. This is a full systemic study requiring important inputs from the economic disciplines.

Fragility curves like the one reported in Figure 6-4 can then be defined (as in the deliverable 3.3) to compute the probability that a sector of the network undergoes a damage state.



This project has received funding from the European Union's Horizon 2020 research and innovation programme under grant agreement No. 700748

Manual for the assessment of liquefaction risk, defining the procedures to create the database, collect, define, symbolize and store information in the Georeferenced Information System and to perform and represent the risk analysis

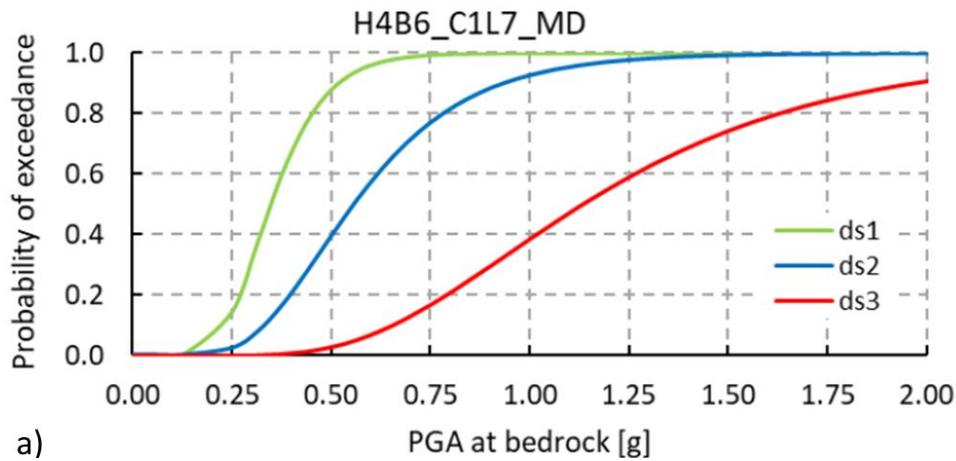


Figure 6-4: Example of fragility curve for road embankment

Alternatively, the level of performance for embankments of road and railway can be defined as in Table 6-11 (SYNER-G, 2013) depending on the crest settlement. The thresholds differ for railways compared to roads considering the different sensitivity of trains to the deformation of the pavement/tracks.

Table 6-11: Damage states for road and railway embankments (SYNER-G, 2013).

Road embankments				Railway embankments			
Damage state	Permanent vertical ground displacement [m]			Damage state	Permanent vertical ground displacement [m]		
	min	max	mean		min	max	mean
ds1 – minor	0.02	0.08	0.05	ds1 – minor	0.01	0.05	0.03
ds2 – moderate	0.08	0.22	0.15	ds2 – moderate	0.05	0.10	0.08
ds3 – extensive	0.22	0.58	0.40	ds3 – extensive	0.10	0.30	0.20

6.5 Lifelines

6.5.1 Direct economic losses

The direct economic losses on lifelines such as pipelines depend on the inventory data providing the location of all nodes and links and on the models adopted to quantify damage. Losses are computed considering the probabilities of exceeding a certain damage state ($P[D_s \geq ds_i]$), the replacement value of the damaged components and the level of damage (the ratio DR_i) for each damage state, ds_i . Economic losses are evaluated by multiplying the compounded damage ratio (DR_c) by the replacement value. The compounded repair cost is computed as the probabilistic combination of damage ratios as follows:

$$Lrc_i = LRC_i \left(\sum_{ds} P_{i,ds} \cdot D_{i,ds} \right)$$

Equation 6-15

where:

Lrc_i is the repair cost for the i^{th} component of the lifeline



This project has received funding from the European Union's Horizon 2020 research and innovation programme under grant agreement No. 700748

Manual for the assessment of liquefaction risk, defining the procedures to create the database, collect, define, symbolize and store information in the Georeferenced Information System and to perform and represent the risk analysis

LRC_i is the replacement cost for the i^{th} component of the lifeline

$P_{i_{ds}}$ is the probability that the i^{th} component of the lifeline is affected by a damage state ds

$D_{i_{ds}}$ is the damage ratio of the i^{th} component for a given damage state ds (i.e the ratio between damage and replacement cost).

The replacement costs of each component of the lifeline should be evaluated case by case depending on the specific situation (country, typology of the component, manufacturing etc.). FEMA (2003) provides a list of costs for the main components of potable water distribution and for wastewater computed for the standard situation of 1994 US dollars (see Table 6-12). Similarly, the damage ratios are provided by FEMA (2003) for different damage states affecting highway or railway systems.

Table 6-12: Replacement costs and damage ratios for utility lifelines (FEMA, 2003).

Table 15.17: Default Replacement Values of Utility System Components

System	Replacement Value (thous \$)	Label	Component Classification
Potable Water	1	PWP1	Brittle Pipe (per break)
	1	PWP2	Ductile Pipe (per break)
	30,000	PWT1	Small WTP with Anchored Components < 50 MGD
	30,000	PWT2	Small WTP with Unanchored Components < 50 MGD
	100,000	PWT3	Medium WTP with Anchored Components 50-200 MGD
	100,000	PWT4	Medium WTP with Unanchored Components 50-200 MGD
	360,000	PWT5	Large WTP with Anchored Components > 200 MGD
	360,000	PWT6	Large WTP with Unanchored Components > 200 MGD
	400	PWE1	Wells
	1,500	PST1	On Ground Anchored Concrete Tank
	1,500	PST2	On Ground Unanchored Concrete Tank
	800	PST3	On Ground Anchored Steel Tank
	800	PST4	On Ground Unanchored Steel Tank
	800	PST5	Above Ground Anchored Steel Tank
	800	PST6	Above Ground Unanchored Steel Tank
	30	PST7	On Ground Wood Tank
	150	PPP1	Small Pumping Plant with Anchored Equipment < 10 MGD
150	PPP2	Small Pumping Plant with Unanchored Equipment < 10 MGD	
525	PPP3	Medium/Large Pumping Plant with Anchored Equipment > 10 MGD	
525	PPP4	Med./Large Pumping Plant with Unanchored Equipment > 10 MGD	
Waste Water	1	WWP1	Brittle Pipe (per break)
	1	WWP2	Ductile Pipe (per break)
	60,000	WWT1	Small WWTP with Anchored Components < 50 MGD
	60,000	WWT2	Small WWTP with Unanchored Components < 50 MGD
	200,000	WWT3	Medium WWTP with Anchored Components 50-200 MGD
	200,000	WWT4	Medium WWTP with Unanchored Components 50-200 MGD
	720,000	WWT5	Large WWTP with Anchored Components > 200 MGD
	720,000	WWT6	Large WWTP with Unanchored Components > 200 MGD
	300	WLS1	Small Lift Stations with Anchored Components < 10 MGD
	300	WLS2	Small Lift Stations with Unanchored Components < 10 MGD
	1,050	WLS3	Medium/Large Lift Stations with Anchored Components > 10 MGD
	1,050	WLS4	Med./Large Lift Stations with Unanchored Components > 10 MGD
	Oil	1	OEP1
1		OEP2	Welded Steel Pipe with Arc Welded Joints (per break)
175,000		ORF1	Small Refinery with Anchored Equipment < 100,000 bl/day
175,000		ORF2	Small Refinery with Unanchored Equipment < 100,000 bl/day
750,000		ORF3	Medium/Large Refinery with Anchored Equipment > 100,000 bl/day
750,000		ORF4	Medium/Large Refinery with Unanchored Equipment > 100,000 bl/day
1,000		OPP1	Pumping Plant with Anchored Equipment
1,000	OPP2	Pumping Plant with Unanchored Equipment	
2,000	OTF1	Tank Farms with Anchored Tanks	
2,000	OTF2	Tank Farms with Unanchored Tanks	

Table 15.25: Damage Ratios for Potable Water Systems

Classification	Damage State	Best Estimate Damage Ratio	Range of Damage Ratios
Pipelines	leak	0.10*	0.05 to 0.20
	break	0.75*	0.5 to 1.0
Water Treatment Plants	slight	0.08	0.01 to 0.15
	moderate	0.4	0.15 to 0.4
	extensive	0.77	0.4 to 0.8
Tanks	complete	1.00	0.8 to 1.0
	slight	0.20	0.01 to 0.15
	moderate	0.40	0.15 to 0.4
Wells and Pumping Plants	extensive	0.8	0.4 to 0.8
	complete	1.00	0.8 to 1.0
	slight	0.05	0.01 to 0.15
	moderate	0.38	0.15 to 0.4
	extensive	0.8	0.4 to 0.8
	complete	1.00	0.8 to 1.0

* % of the replacement cost for one 20 ft. pipe segment

Table 15.26: Damage Ratios for Waste Water Systems

Classification	Damage State	Best Estimate Damage Ratio	Range of Damage Ratios
Underground Sewers & Interceptors	leak	0.10	0.05 to 0.20
	break	0.75	0.5 to 1.0
Waste Water Treatment Plants	slight	0.10	0.01 to 0.15
	moderate	0.37	0.15 to 0.4
	extensive	0.65	0.4 to 0.8
	complete	1.00	0.8 to 1.0



This project has received funding from the European Union's Horizon 2020 research and innovation programme under grant agreement No. 700748

Manual for the assessment of liquefaction risk, defining the procedures to create the database, collect, define, symbolize and store information in the Georeferenced Information System and to perform and represent the risk analysis

6.5.2 Indirect economic/social losses

The physical losses on utility lifelines may cause a deficiency of function that may have severe implications on the usage of the infrastructure, from a decay of the performance to the complete interruption of the service. Depending on the time necessary to restore the original conditions, these effects may cause economic and social losses to the community. Studying this impact requires the characterization and modelling of the transportation network, with the identification of parameters describing its operative conditions, a model that transforms the physical damage into the loss of functionality and a metric to evaluate the performance of the damaged lifeline in comparison with the original conditions.

A multi-level strategy to analyze losses has been proposed in Syner-G (2013) for different systems. For instance, the water-supply system as a whole is composed of a number of point-like critical facilities (Water sources, Treatment plants, Pumping stations, Storage tanks) and of the Water distribution network itself. The internal logic of the critical facilities and their function in the management of the whole system should be modelled explicitly. The identified system components are:

- WSS01: Source (Springs, shallow or deep wells, rivers, natural lakes, and impounding reservoirs) [Points]
- WSS02: Treatment Plant [Points, critical facility]
- WSS03: Pumping station [Points, critical facility]
- WSS04: Storage Tank [Points]
- WSS05: Pipe [Edges]
- WSS06: Tunnel [Edges]
- WSS07: Canal [Edges]
- WSS08: SCADA system [System]

Information on the utility network can be schematically stores as described in Table 6-13.

Table 6-13: Main attributes/properties of the potable water supply system class (Syner G, 2013).

Group	Attribute(s)	Description
Global properties	sourceHead	Water head at source nodes
	endUserDemand, hydricEquipment	Required water flow at demand nodes, either assigned or evaluated by aggregating over tributary cells, employing population and hydricEquipment for the region (expressed in [l/inhab./day])
Pointers	refEPNnode	Pointers to EPN node(s) feeding power to pumping stations (for inter-dependence modelling)
	pipe	Pointers to all the pipes in the system, objects from the pipe class
	demand	Pointers to all end-user nodes, objects from the DistributionNode class
	source	Pointers to all sources in the system, in general objects from the ConstantHeadSource and VariableHeadSource (for finite reservoirs) classes
Edge properties stored at WSS level	edgeMaterial, edgeDiameter, edgeRoughness, edgeDepth	Length, centroid, etc. are attributes inherited from the Network class. Here the network-specific properties are listed (roughness, diameter, laying depth, etc.)
Node properties stored at WSS level	nodeMinimalHead	Minimal head required at nodes for delivery of the assigned demand water flow; this property is a function of the average building elevation in the region of interest
State variables recording WSS state	nodeDepth, states	– $n_E \times 1$ collection of properties that describe the current state for each of the n_E events (fields: demandFlow, outFlow, average head ratio, system serviceability index, number of leaks, number of breaks, etc.)



This project has received funding from the European Union's Horizon 2020 research and innovation programme under grant agreement No. 700748

Manual for the assessment of liquefaction risk, defining the procedures to create the database, collect, define, symbolize and store information in the Georeferenced Information System and to perform and represent the risk analysis

As for other infrastructures (e.g. transportation) the seismic reliability of water networks can be assessed at different level: vulnerability, connectivity and serviceability. Connectivity analyses measure the post-earthquake integrity of the system, i.e., the extent to which links and nodes are still connected. Serviceability analyses estimate the post-earthquake capacity between selected source-to-sink nodes.

Closely related to reliability is redundancy, i.e. the existence of backup capacities and alternatives routing to demand nodes in case of breaks in the main supply links. Reliability assessment could be performed to prioritize mitigation procedures adopting multi-criteria analysis (MCA) or traditional cost-benefit analysis.

The following methods to address the risk of Water Supply Systems imply a different modelling of the network, progressively more complete with the level of analysis:

- Level 0 (Vulnerability Analysis)

The scope is to estimate the percentage of physical damages to the Water Supply System based on the vulnerability analysis of water network components, which can be estimated through appropriate fragility curves or/and Monte-Carlo technique. Most of the Level 0 studies imply simple physical vulnerability studies of water system components and express the performance with the “Damage Ratio”, i.e. the expected number of failures per unit of length (for pipes) or as percentage of collapsed links or nodes of the system.

- Level I (Connectivity Analysis)

In this level of analysis, the concern is the system connectivity between supplying (sources, pumping systems) to demand nodes through undamaged pipes. Considering the removal from the network of damaged components, the “Damage Ratio” (Level 0) and “Service Ratio” (Level I) can be computed to quantify the performance of the network. Service Ratio can be expressed as the ratio of houses supplied after the earthquake over the total number in the system. Other performance indicators can be computed on a probabilistic basis, like the “Connectivity Loss” that quantifies the average decrease of the ability of distribution vertices to receive flow from the generation vertices, the “Reachability” of water indicating the probability that a certain amount of water flow would reach key locations (nodes).

- Level II (Flow Analysis/Serviceability Analysis)

At this level, the concern is the ability of the system to provide the service to the users. Typically, physical-based indicators such as water head, flow rate at each demand node are calculated under intact (pre-earthquake) conditions computing the flow rate and head loss in each pipe. After computing the physical damages of the network (breaks leakages), the flow analysis is repeated assuming that a shutdown device is automatically activated to prevent water in broken pipes while assuming the capacity of the supplying nodes unchanged. Vulnerability and damage estimations of water system components, with the resulting flow analysis can be thus repeated for different seismic intensities using Monte-Carlo simulations.

The results are returned as ratios of post- to pre- earthquakes measures of flow rate and water pressure in each node, giving the percentage reduction of functionality as damage indicator. Other potential performance indicators are the ratio of available water flow or pressure over the required ones at given demands (e.g. fire outbreak) or the probabilistic distribution of the percentage of customers who would lose



This project has received funding from the European Union's Horizon 2020 research and innovation programme under grant agreement No. 700748

Manual for the assessment of liquefaction risk, defining the procedures to create the database, collect, define, symbolize and store information in the Georeferenced Information System and to perform and represent the risk analysis

their service after a specific earthquake. The methodology proposed in SYNER-G (2013) is depicted in Table 6-14.

Table 6-14: Methodology for the assessment of risk in potable water supply systems defined in SYNER-G (2013).

Method	Description
computeDemand	Aggregates demand from tributary cells in demand nodes
isBreakAndLeaksNumber	Evaluates the damage state of each pipeline segment employing the corresponding set of fragility functions and the current intensity at the centroid
computeLeakageArea	Computes the amount of leakage from the numbers of leaks in each pipe segment
updateConnectivity	Updates the adjacency matrix based on the pipe breaks and/or the failure of the nodes (e.g. pumping stations, reservoirs)
computeFlow	Computes the actual flow from the sources to the demand nodes based on an optimization algorithm, using the demand level and the leakage amount
computePerformanceIndicator	Computes the different PIs at component- and system-level

The seismic performance of a network and the planning of mitigation actions needs to be quantified with indicators expressing the damage on the network and the relevance of each component. Several indicators have been proposed in the literature. One of them is the Head ratio (HR) at the junctions/nodes, expressed as follows:

$$HR_i = \frac{H_{si}}{H_{0i}} \quad \text{Equation 6-16}$$

Where H_{si} is the water head in seismically damaged network and H_{0i} is the reference value for the non-seismic, normal operations conditions. Its calculation implies a flow analysis of the network. Hence this index may express the functional consequence in the i -th component of the physical damage to all other components of the water supply system.

A cumulative indicator connected to the above index is the Average Head Ratio (AHR) defined as the average over the network nodes of the HR index

$$AHR = \frac{1}{n} \sum_{i=1}^n HR_i \quad \text{Equation 6-17}$$

Another indicator is the System Serviceability Index (SSI), variable between 0 and 1, being defined as the ratio of the sum of the satisfied customer demands after an earthquake over the ones before the earthquake:

$$SSI = \frac{\sum_{i=1}^n Q_i}{\sum_{i=1}^{n_0} Q_i} \quad \text{Equation 6-18}$$

where n and n_0 are the number of satisfied demand nodes after and before the earthquake, and Q_i is the demand at the i^{th} node. A single value can be determined for a given condition of the network assuming that the demand remains fixed before and after the earthquake. Its probabilistic characterization, in terms of either its full distribution or its expected value $E[SSI]$, requires running multiple simulations for different earthquake realizations.



This project has received funding from the European Union's Horizon 2020 research and innovation programme under grant agreement No. 700748

Manual for the assessment of liquefaction risk, defining the procedures to create the database, collect, define, symbolize and store information in the Georeferenced Information System and to perform and represent the risk analysis

Given the definition of eq. 6.17, the complement of SSI to 1 ($1-SSI$) represents an indicator of the serviceability loss given by the damages. In particular, the Damage Consequence Index can be computed for a generic pipe i^{th} to provide the impact of the pipe on the overall system serviceability and to identify critical links that may affect the system's seismic performance. It is computed as follows:

$$DCI_i = \frac{E[SSI] - E[SSI|L_i]}{1 - E[SSI]} \quad \text{Equation 6-19}$$

- in which $E[SSI]$ is the expected value of SSI from a set of simulations (for instance generated with the Monte Carlo method) in which the i^{th} pipe might be randomly damaged or not;

- $E[SSI|L_i]$ is the conditional expectation of SSI from another set of simulations under the same seismic hazard, but assuming the i^{th} pipe as damaged.

Similarly, the Upgrade Benefit Index, can be defined as an index of the impact of an upgrade of an individual pipe on the overall system serviceability. It is defined as:

$$UBI_i = \frac{E_{upgrade}[SSI] - E[SSI|L_i]}{1 - E[SSI]} \quad \text{Equation 6-20}$$



This project has received funding from the European Union's Horizon 2020 research and innovation programme under grant agreement No. 700748

Manual for the assessment of liquefaction risk, defining the procedures to create the database, collect, define, symbolize and store information in the Georeferenced Information System and to perform and represent the risk analysis

7. MITIGATION

7.1 Introduction

The decision-making to mitigate risk applies to the above defined holistic model including the multiscale connections outlined in Figure 7-1. Briefly recalling the fundamental steps, liquefaction is triggered when a relatively high seismic hazard combines with susceptible subsoil. The phenomenon may turn or not into damage of buildings and infrastructures depending on their physical fragility. Damaged systems become progressively unable to withstand their function and thus, depending on its severity physical damage turns into lack of serviceability. The consequences for the society depend on the relevance of the function provided by the infrastructure for the served community, on the repairability/replaceability of this function or, in more general terms, on the preparedness of the community to withstand its absence.

Interrupting this chain is the scope of mitigation, acting separately on one component of the system or undertaking a holistic strategy aimed at reducing the overall impact on the society. The Japan Geotechnical Society (JGS, 1998) envisages three different classes of intervention (Figure 7-2), acting respectively on auxiliary facilities supporting/replacing the function of the concerned infrastructure, on the physical reinforcement of the structures or of the ground.

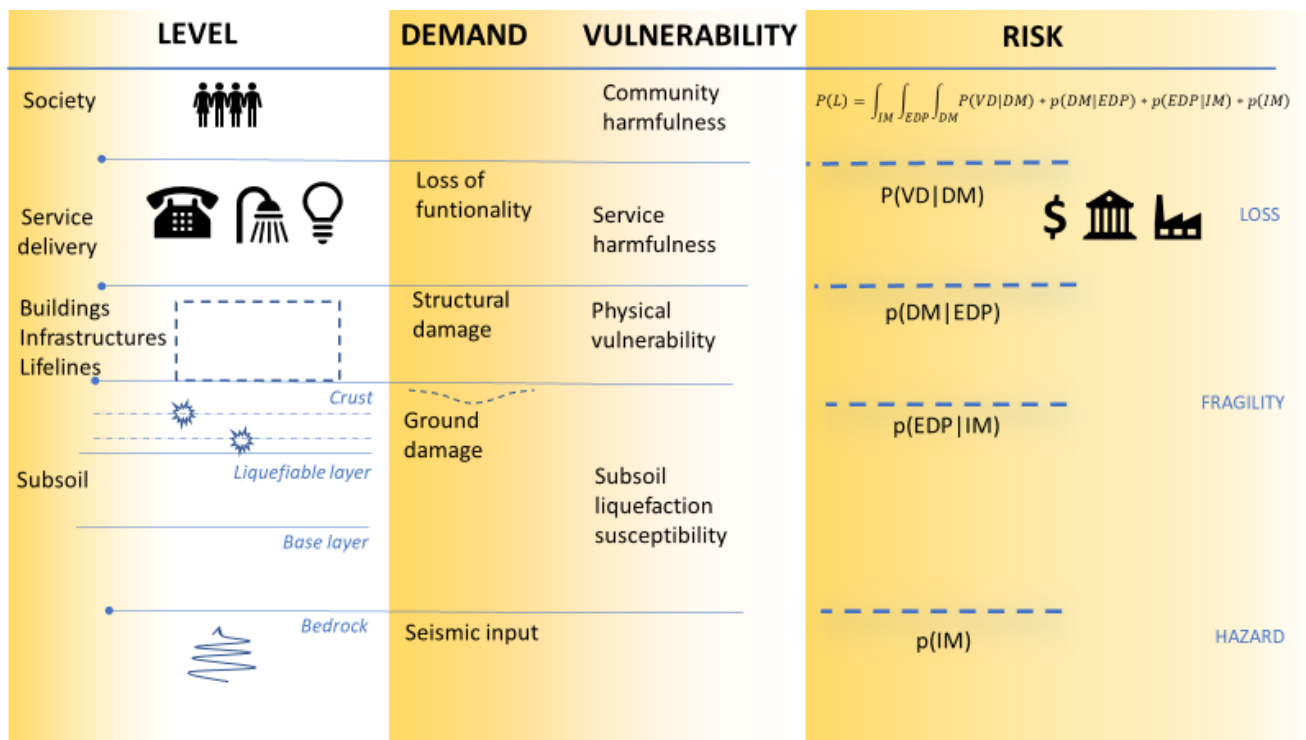


Figure 7-1: Liquefaction risk model.



This project has received funding from the European Union's Horizon 2020 research and innovation programme under grant agreement No. 700748

Manual for the assessment of liquefaction risk, defining the procedures to create the database, collect, define, symbolize and store information in the Georeferenced Information System and to perform and represent the risk analysis

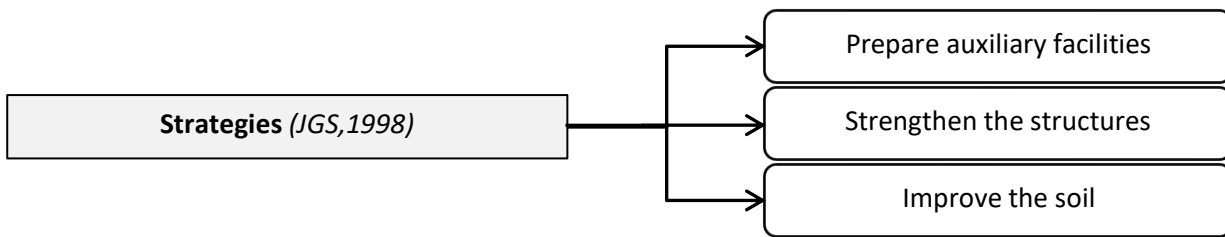


Figure 7-2: Strategies for liquefaction risk mitigation.

The Japan Geotechnical Society (JGS, 2011) reports several situations that did not undergo liquefaction during the big 2011 earthquake, thanks to mitigation undertaken at different level.

- a) Elevated structures (i.e., RC framework structures), bridges, for railways (Keiyo Line, etc.), roads (Bay Shore Route of the Metropolitan Expressway and national road) and multi-purpose conduits crossing recently reclaimed land in the Tokyo Bay area was not damaged by soil liquefaction. Only at Higashi-Ohgishima, the Maihama ramp, and Ichikawa parking area, there was some deformation of the road surface due to soil liquefaction. This was rapidly restored within a few days. No measures were taken against soil liquefaction in these areas at the design stage.
- b) Pile-supported medium-and high-rise buildings (including residential buildings) as well as a UR residential development (RC wall 2-story housing estate with ground improvement by the sand compaction pile method in Urayasu City) in the Tokyo Bay area was not damaged by soil liquefaction.
- c) Buildings at Tokyo Disneyland and elsewhere in the Tokyo Bay area - Urayasu city where ground improvement had been applied was not damaged by soil liquefaction.
- d) At Sendai Airport's runway B, assessment of soil liquefaction had been carried out and, based on the results, countermeasures against soil liquefaction below the runway were carried out by cement-mixing. The runway suffered from no damage. In an untreated area, ground settlement was caused by soil liquefaction (Fig. 3-2).
- e) In the seismically strengthened quays at Takamatsu Wharf in Sendai's Shiogama Port and the Hitachinaka section of Ibaraki Port, countermeasures had been carried out based on results of soil liquefaction analysis of the backfill soil and the wall supporting strata. These quays suffered little damage, so a few days after the earthquake they were already in use as landing points for emergency supplies.
- f) The bearing stratum for major structures of industrial facilities including chemical plants and tanks in the coastal area that were prepared for soil liquefaction were not damaged by soil liquefaction.
- g) Kasumigaura water pumping station, which is supported on piles (Japan Water Agency), was not damaged by soil liquefaction that took place in the supporting ground.
- h) Large-diameter pipelines for agricultural use (diameter 1.5 to 2.6 m) suffered from little damage by soil liquefaction where they had been backfilled with crushed gravelly soil.

Figure 7-3: Situations where mitigation against liquefaction was effective during the big 2011 earthquake in Japan (JGS, 2011).

However, the effectiveness of mitigation should be also evaluated from the cost/benefit viewpoint, i.e. comparing on a financial basis the budget spent on mitigation with the reduction of losses. Considering that mitigation, when undertaken, is a cost while losses depend on the probability of liquefaction occurrence, the



This project has received funding from the European Union's Horizon 2020 research and innovation programme under grant agreement No. 700748

Manual for the assessment of liquefaction risk, defining the procedures to create the database, collect, define, symbolize and store information in the Georeferenced Information System and to perform and represent the risk analysis

comparison should be performed on an annual basis considering the residual lifecycle of the infrastructure under concern, as explained in Chapter 6.

In general, mitigation actions can be subdivided in two main categories, strategic or non-technical when aimed at improving the functionality of the considered system with the creation of auxiliary facilities or with a modified management to face critical situations, or technical when operating on the physical systems with structural reinforcement or ground improvement. These two categories are dealt in the following chapter.

7.2 Strategic mitigation

Non-technical strategies generally require an analysis of the behaviour of a system under critical scenarios and to prepare a series of actions able to reduce the impact on the community and to improve its resilience.

7.2.1 Resilience assessment and Improvement Framework (RAIF)

Resilience Assessment and Improvement Framework (RAIF) can be used by built assets owners and/or managers to assess the antecedent vulnerability, resilience and adaptive capacity of their built assets (buildings and infrastructure) to EILD events. The same framework can also be used by EU, national, regional and local decision makers to assess vulnerability, resilience and adaptive capacity of urban communities to EILD events. RAIFs provide the theoretical basis for the development of a range of decision support tools. The RAIF developed for the LIQUEFACT project (Deliverable D.1.3 of the present project) is based on the risk/resilience framework developed by Prof Jones in the CREW project, which examined the factors that affected community resilience to extreme weather events (CREW, 2012). The CREW project developed and tested a six stages adaptation framework that was integrated into a built asset management model that would allow building owners/managers to identify and programme interventions (physical and social) to improve the resilience of their built assets to extreme weather events. Whilst the stressor behind the disaster risk associated with the LIQUEFACT project is different to that used in the CREW project the general theory supporting the adaptation framework is similar. The underlying theory is based on Cutter's (2008) Disaster Resilience of Place model (Figure 7-4) in which antecedent conditions, including coping response and absorptive capacity, directly affect speed of recovery and system resilience. The LIQUEFACT project has re-interpreted the adaptation framework developed in the CREW project to reflect the specific characteristics associated with EILD events to provide guidance on the metrics, tools and models that need to be developed (WP's 2, 3, 4 and 5) to operationalise the RAIF and provide the input into the SELENA-LRG software toolkit and wider guidance documentation.



This project has received funding from the European Union's Horizon 2020 research and innovation programme under grant agreement No. 700748

Manual for the assessment of liquefaction risk, defining the procedures to create the database, collect, define, symbolize and store information in the Georeferenced Information System and to perform and represent the risk analysis

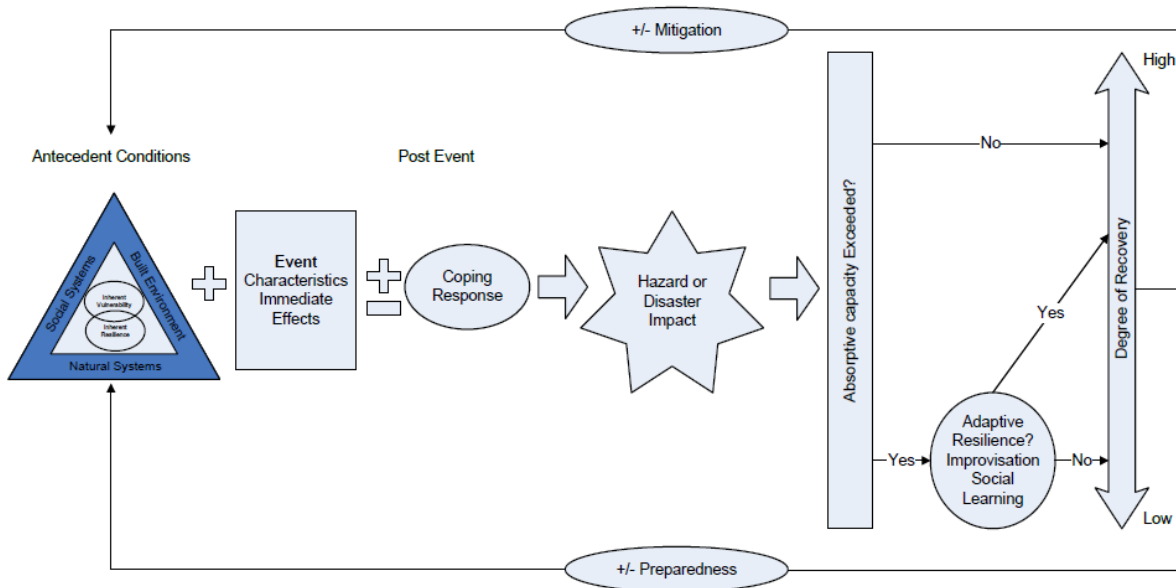


Figure 7-4: Schematic representation of the disaster resilience of place (DROP) model (Cutter et al., 2008).

The RAIF is based on the SENDAI Framework for Disaster Risk Reduction 2015-2030 (UN General Assembly, 2015), whose stated intention is to support a "... substantial reduction of disaster risk and losses in lives, livelihoods and health and in the economic, physical, social, cultural and environmental assets of persons, businesses, communities and countries". When developing implementation plans the SENDAI Framework suggest that national states should focus on 4 priority areas for action.

- PRIORITY 1: Understand the disaster risk
- PRIORITY 2: Strengthen disaster governance to manage risk
- PRIORITY 3: Invest in disaster risk reduction to improve resilience
- PRIORITY 4: Enhance disaster preparedness and build-back-better

Pre-planning is essential for an effective recovery, rehabilitation and reconstruction following a disaster event, but also represents an ideal opportunity to build-back-better by integrating disaster risk reduction into development and reconstruction projects. Preparedness for disaster events requires contingency plans and programmes to be developed and tested routinely across the community. These plans need to consider forecasting and early warning systems as well as communication systems and channels. Policies to improve the resilience of existing critical infrastructure should be developed and implemented as part of routine refurbishment. Logistics required immediately after a disaster event should be stockpiled and a distribution system established for their release immediately following a disaster event. The SENDAI Framework also emphasises the role of stakeholders in disaster risk reduction; identifying particularly society; volunteers, organised voluntary work organisations, and community-based organisations; businesses; professional associations; financial institutions; and media organisations as critical components to community resilience. A better understanding of how risks escalate over time and particularly the social, economic and institutional factors that contribute to risk and the transfer of risk between stakeholders.

Assessment of vulnerability implies to check the conditions listed in Table 7-1.



This project has received funding from the European Union's Horizon 2020 research and innovation programme under grant agreement No. 700748

Manual for the assessment of liquefaction risk, defining the procedures to create the database, collect, define, symbolize and store information in the Georeferenced Information System and to perform and represent the risk analysis

Table 7-1: Factors affecting vulnerability, adaptive capacity and resilience of urban communities (from D.1.3).

Technical factors	Organizational factors	Social factors	Economic factors
Poor design and construction of buildings	Early warning system	Education	Empowerment
Unregulated land use planning	Risk assessment	Disaster preparedness	Disaster insurance
Lack of building codes	Trained staff	Social cohesion	Funding mechanism
Protection of critical infrastructures	Emergency response plan	Social support	Business continuity plan
Protection of built assets	Public information	Social networks	Ability to mobilising resources
Building stock assessment and retrofitting	Hazard mitigation plan	Poverty	
Network redundancy	Effective leadership	Collaboration with research institution	
Proximity to disaster prone areas	Pre-Disaster planning	Public participation in decisions	
Building typology			

Once vulnerability of the system has been assessed a series of potential mitigation interventions can be identified to reduce failure probabilities (and the consequences of failure) and to improve the resilience of the system. The analysis will produce another Kiviat diagram (Figure 7-5) in which it is possible to assess how the mitigation measures affect the overall system vulnerability, both positively and/or negatively. The new diagram shows how the adoption of the selected mitigation measures change the values of the system.

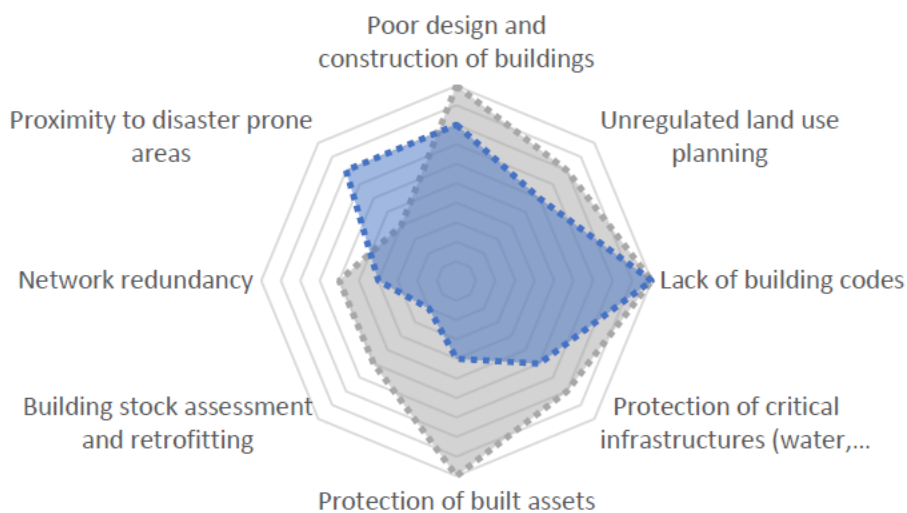


Figure 7-5: Schematic representation of the disaster resilience of place (DROP) model (Cutter et al., 2008).



This project has received funding from the European Union's Horizon 2020 research and innovation programme under grant agreement No. 700748

7.2.2 Urban planning

Urban planning represents one of the most effective mitigation actions against risk, in particular that deriving from liquefaction. As part of territorial and urban planning, Microzonation studies integrate the knowledge of components that determine the seismic risk, as well as provide some selection criteria aimed at its prevention and reduction, according to a gradual and programmatic approach to the various scales and to the various planning levels. On an urban scale, the identification of local seismic hazard, associated with the knowledge of the different levels of vulnerability of the elements and of the systems exposed, is crucial for the evaluation of the areas at risk and, therefore, to introduce safety elements as key factors development and location choices. In Italy (DPC, 2008), Seismic Microzonation studies are applied at the planning of various territorial levels as follows:

- large area planning (provincial plans and other territorial plans)

In the specific area of seismic risk, large area planning: transposes the objectives of seismic risk reduction defined at regional and national level; assumes and defines for the territory of competence, methodologies and procedures defined from the regional legislation; identifies priority areas of intervention and investigation, as well as the levels of required in-depth analysis, also planning resources; contributes to define the cognitive framework of the territory.

In addition to contributing to the formation of over-communal level choices, risk assessment contributes to define a knowledge base useful for municipal level planning. Studies serve to provide for any in-depth investigations and their methods of use; orient and verify planning decisions and locations of supra-municipal importance; orient the location of the primary operational, logistic and infrastructural elements for emergency planning; provide municipal planning with a cognitive map of their territory to be used in plan formation process; integrate hazard studies with other cognitive areas of risk analysis seismic.

- municipal level

Municipal planning defines the existing historical-cultural, environmental, infrastructural and built-asset invariants of the territory, the strategies and general objectives of transformation, specific objectives and intervention policies, the methods and areas of transformation, the priorities and phases of the planning process. In this framework risk assessment can contribute to the definition of the following contents: general and/or sectorial urban planning strategies, articulated in choices for the specific location and explicitly including the targets for seismic risk reduction. Risk assessment is intended to address the choices for:

- guiding the choice of new forecast areas;
- defining eligible interventions in a given area with related procedures;
- orienting the location of the primary operational, logistic and infrastructural elements for planning emergency;
- preparing any in-depth investigation programs.

From an operative viewpoint, seismic risk analysis defined address choices regarding:

- new building areas;
- eligible interventions in individual areas and their methods;



This project has received funding from the European Union's Horizon 2020 research and innovation programme under grant agreement No. 700748

Manual for the assessment of liquefaction risk, defining the procedures to create the database, collect, define, symbolize and store information in the Georeferenced Information System and to perform and represent the risk analysis

- intervention methods in already urbanized areas;
- prescriptive content with reference to areas whose transformability is limited by instability.

The introduction of seismic risk assessment in the municipal planning in Italy is described in Figure 7-6 derived from DPC (2008).

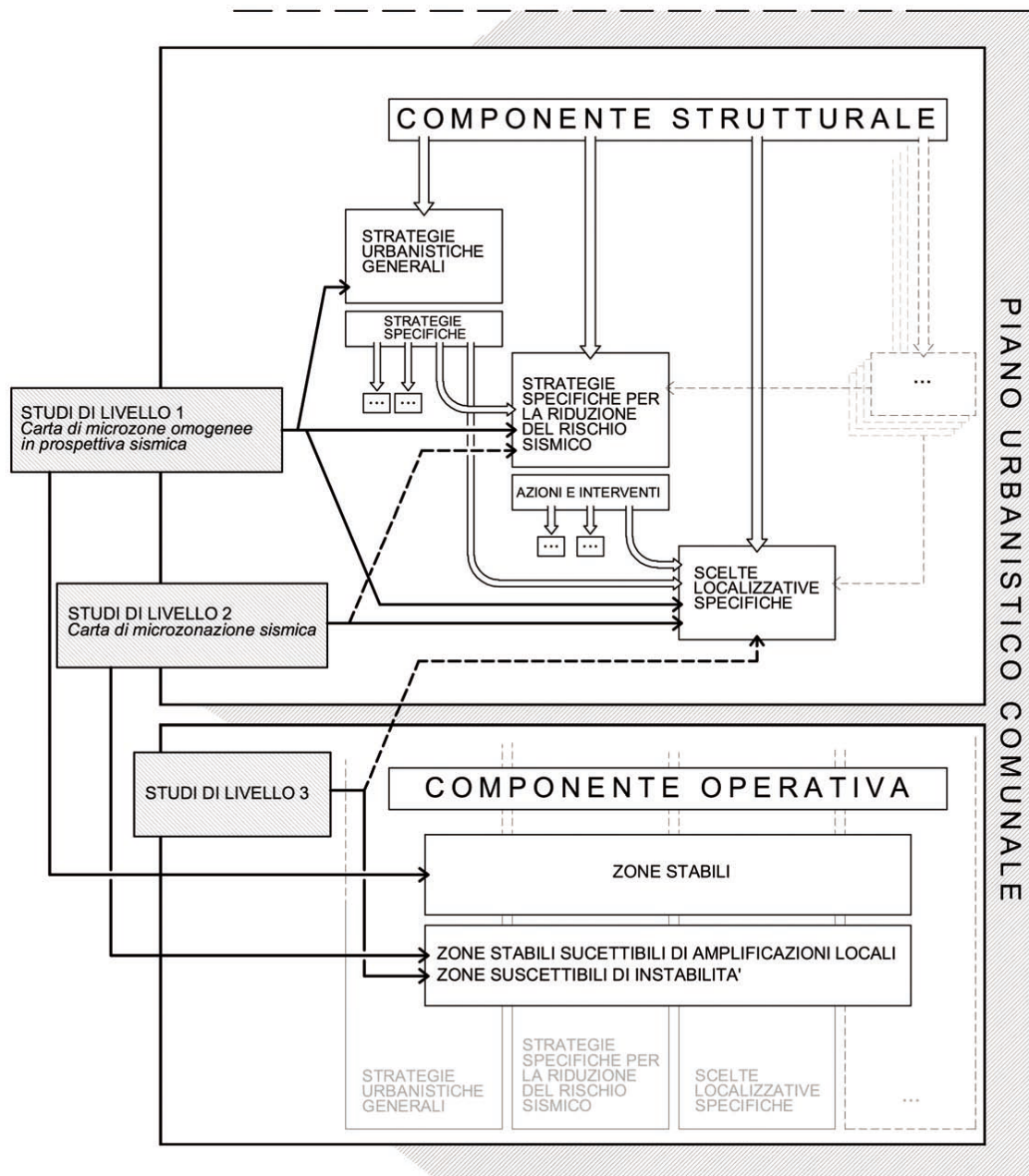


Figure 7-6: Scheme for the use of seismic microzonation studies in the municipal planning (from DPC, 2008).



This project has received funding from the European Union's Horizon 2020 research and innovation programme under grant agreement No. 700748

7.2.3 Management of lifelines

The liquefaction risk for critical lifelines (see the list in paragraph 1.2.2) can be also faced by re-thinking the physical and operative set-up of the infrastructure. The risk felt by operators stems partly from the cost necessary to repair the damaged physical support of the service (roads, pipelines, electric or communication cables etc.), moreover from the reduced or interrupted operability of the system. Considering as paramount the “reliability of the infrastructure”, i.e. the probability that a given element in a critical infrastructure system is functional at any given time” (Murray & Grubestic, 2007), an interruption of the service, or even its temporary reduction, determines a variety of financial losses related not only to the missed income from the users of the service, but also for the credibility of the provider. The question becomes even more severe considering the interconnection with other services and the criticality of the infrastructure for the life of the community.

Together with the technical remediation of the structures and subsoil shown in paragraph 7.3, the above risk can be mitigated with a more rational planning of the service. In case of punctual infrastructures or vital nodes for network systems, like for instance power plants, antennas for telecommunication, water purification plants and reservoirs or sanitary centres (clinics and hospitals), the relocation or duplication in less hazardous areas could represent a convenient alternative to a very costly technical mitigation.

For horizontally distributed infrastructures like transportation networks, aqueducts and gas pipelines, sewers, electric and telecommunication lines, a detailed analysis of the systems and of their working conditions in case of earthquake induced liquefaction damage leads to envisage alternative distributions, with the redirection of the flows towards less hazardous areas, and the reinforcement of specific directions. For freshwater distribution pipes, closed meshes are more flexible than open trees systems and are thus able to redistribute flows and supply service in case of local disconnection. For road networks, the enlargement of secondary roads, the duplication of critical interconnections (e.g. bridges) can be achieved to mitigate the reduction of traffic speed caused by the reduced serviceability of the main roads.

7.2.4 Insurance

In addition to seismic provisions for new construction and retrofitting of existing structures, insurance represents an option to face and mitigate financial risk. The principle of this mitigation action is that risk for economic/financial consequences and for fluctuation/variability of a stakeholder’s asset caused by contingencies is transferred to a third subject (accompany or a public/semi-public institution). Typically, the contract establishes that the owner of an asset pays an annual premium to the insurer and receives compensation upon the occurrence of specific loss events. In the context of earthquake insurance, the occurrence of seismic damage cost, exceeding a specified deductible, triggers the pay-out from an insurer. A typical pay-out function includes deductible, cap, and co-insurance factor. The earthquake insurance premium consists of pure premium, which is equivalent to the expected damage cost, and risk premium (plus transaction cost). The risk premium is an overcharge requested by an insurer for undertaking low-probability and high consequence events and can be much greater than pure premium. The appreciation of benefit from purchasing earthquake insurance coverage varies significantly, depending on risk attitudes, financial status, personal experience, and many other factors (Palm 1995). Therefore, even when the overall premium is reasonably priced, not so many stakeholders voluntarily purchase earthquake risk coverage.



This project has received funding from the European Union's Horizon 2020 research and innovation programme under grant agreement No. 700748

Manual for the assessment of liquefaction risk, defining the procedures to create the database, collect, define, symbolize and store information in the Georeferenced Information System and to perform and represent the risk analysis

From a general viewpoint, insurance against earthquakes can be seen as a non-technical measure to face losses, but policies differ largely from country to country, being insurance strongly promoted or even compulsory in some countries, poorly adopted in some others.

Insurances (public and private), differentiating the premium, may contribute to control the quality of design and construction. Several models for the application of insurance are available and practiced throughout the world. Essentially, one can have centralized bodies as practiced in Spain by the Consorcio de Compensación de Seguros (CCS, 2018), or a moderate centralized scheme such as the Solidarity Fund created in the EU in the aftermath of the large Central Europe floods of summer 2002. But the most practiced case is the existence of individual national or international companies with pools through international re-insurance.

Convenience of this mitigation action mainly depends on the occurrence probability of an event and on the related severity, in a few words on the outcomes of the risk assessment. Cost-benefits analyses performed with the criteria shown in chapter 6 should be performed to estimate the advantages of insuring an asset in comparison with providing a technical mitigation, considering the general principle that higher risk correspond to higher premium to be paid to the insurer.

In general, for high risk given by a high likelihood coupled with the possibility of producing severe damage and casualties, technical mitigation like those described in paragraph 7.3 should be preferable also from a financial viewpoint. However, they could be conveniently coupled with an insurance to face unforeseen occurrences. On the other hand, low probability events mostly if not associated with casualties, could be more conveniently covered by insurance compared with costly technical mitigation.



This project has received funding from the European Union's Horizon 2020 research and innovation programme under grant agreement No. 700748

7.3 Technical mitigation

7.3.1 Reduction of subsoil susceptibility by ground improvement

As repeatedly shown in the previous chapters, high energy seismic excitation on loose sands triggers volume contraction that in saturated conditions turns into an accumulation of pore water pressures. When the natural drainage capacity of the system is unable to exhaust the pore pressures, the total overburden stress may be entirely carried out by water with the result that the effective stresses, index of the contact forces between grains, nullify and the sand matrix loses its shear resistance and starts behaving like a viscous fluid. The consequence turns to be more dramatic when sandy layers are sloped and covered by an impermeable crust. Being the phenomenon ruled by the concurrence of different factors, i.e. non plastic soil in a loose state, saturation, hampered drainage, various mitigation techniques may be carried out to interrupt the chain of mechanisms responsible for the phenomenon. Soil susceptibility may be reduced decreasing the contractive tendency upon cyclic loading, e.g. by means of dynamic compaction (Mayne, 1984), vibratory techniques (Kirsch and Kirsch, 2016) or blasting (Lyman, 1942) or adding a finer plastic material (El Mohtar et al., 2013) to reduce the mobility of grains upon shaking. Triggering may be avoided by preventing the excess pore pressure build-up with induced partial desaturation (Mele et al., 2018) or facilitating its exhaust with horizontal and vertical drains (Chang *et al.*, 2004). Other possible countermeasures consist in limiting the impact on the superstructure by reinforcing foundations with piles, columnar or lattice wall inclusions created with jet grouting (Yamauchi *et al.*, 2017), deep soil mixing (Nguyen *et al.*, 2012) or stone columns (Dappolonia, 1954). Reinforcements have the twofold scope of reducing shear strains in susceptible soils and transfer loads to deeper non liquefiable strata.

A list of possible ground improvement solutions describing principles, drawbacks and costs is provided by the JGS (2011) (Table 7-2). From a purely mechanical viewpoint, the function of ground improvement can be classified as follows, being the single ground improvement technique able to reach one or more of the following goals:

- **Densification:** reducing the volume contraction tendency of the soil upon shaking
- **Stabilisation:** reducing the mobility of grain and volume contraction tendency of the soil upon shaking
- **Drainage:** reducing the pore pressure build-up
- **Desaturation:** preventing the pore pressure build-up
- **Reinforcement:** reducing the shear strain into liquefiable soil and transferring loads to more competent strata



This project has received funding from the European Union's Horizon 2020 research and innovation programme under grant agreement No. 700748

Manual for the assessment of liquefaction risk, defining the procedures to create the database, collect, define, symbolize and store information in the Georeferenced Information System and to perform and represent the risk analysis

Table 7-2: Classification of ground improvement methods for soil liquefaction countermeasure (JGS, 2011).

Basic principle	Technique	Outline	General cost (JPY/m ³)	Noise, Vibration	Disturbance of soil	Machine size	Displacement control
Densification	Sand compaction method	Compacted sand piles are installed by driving down and extracting up a vibrating steel shaft.	1,000 ~ 2,000	Higher	More	Big	More
	Vibro compaction	A vibrator implemented at tip of extension tube carries out compaction at designated depths.	1,000 ~ 2,000	Higher	More	Big	More
	Quiet compaction	Casing pipe is penetrated and withdrawn a little at a time with rotational force to achieve soil compaction.	2,000 ~ 3,000	Lower	More	Big	More
	Compaction grouting	A very stiff grout mix, with an almost zero slump, is injected under relatively high-pressure to compact surrounding soil.	10,000 ~ 15,000	Lower	More	Small	More
Drain	Gravel drain	Gravel piles are vertically installed into the ground to accelerate the dissipation of excess pore water pressure induced by seismic events.	2,000 ~ 4,000	Lower	Less	Big	Less
	Artificial drain	Artificial drains such as PVD are installed into the ground to accelerate the dissipation of excess pore water pressure induced by seismic events.	2,000 ~ 4,000	Lower	Less	Middle	Less
Replacement	Pre-mixed soil	Stabilized grounds are constructed using soils mixed with chemical agent such as cement prior to placing in dry or slurry form.	3,000 ~ 4,000	Lower	More	Big	More
	Light weight soil	Stabilized grounds are constructed using soil mixed with cement along with foam or light weight material.	8,000 ~ 12,000	Lower	More	Big	More
Solidifying	Deep soil mixing	In-situ soils are mixed with a binder, such as cement or lime supplied in dry or slurry form, using rotating blade.	4,000 ~ 6,000	Lower	Less	Big	More
	Jet grout	A high pressure fluid is jetted out from the tip of extension rod, to allow in-situ soils eroded and mixed with cement grout.	20,000 ~ 60,000	Lower	Less	Small	More
	Chemical grouting	Chemical grouts, composed of additives such as sodium silicate or polymer, are injected into ground to improve its strength or lower its permeability.	20,000 ~ 30,000	Lower	Less	Small	Less
	Permeation grouting	Durable chemical grouts, specially manufactured to remove anti-durable factor, is injected into ground to increase liquefaction resistance.	20,000 ~ 30,000	Lower	Less	Small	Less
Reinforcing	Additional piles	Additional pile installation or reinforcing around pile heads increase structural resistance.	(20,000 ~ 50,000)	Lower	Less	Small	More
	Sheet pile reinforcing	Sheet piling surrounding structures works to protect its foundation; also effectively works as a stopper of the excess pore water pressure during seismic events.	(20,000 ~ 50,000)	Lower	Less	Small	More
	Solidifying reinforcing	Solidifying soils around foundations works, in some degrees, as structural reinforcing.	(20,000 ~ 50,000)	Lower	Less	Small	More



This project has received funding from the European Union's Horizon 2020 research and innovation programme under grant agreement No. 700748

Manual for the assessment of liquefaction risk, defining the procedures to create the database, collect, define, symbolize and store information in the Georeferenced Information System and to perform and represent the risk analysis

As for any ground improvement application, suitable techniques should be chosen scrutinizing the problem from different perspectives, i.e. not only considering mechanical effectiveness, but also the temporal/permanent function of treatments, their invasiveness, durability, cost-effectiveness and executability, mostly existing structures are of concern. Whatever the adopted technique, the international standards (e.g. EN1997-1, 2004) state the following basic principle: “the effectiveness of the ground improvement shall be checked against the acceptance criteria by determining the induced changes in the appropriate ground properties”. Although general, this sentence features a strategy that may be adopted to drive in a consistent framework the three phases of ground improvement application, design, execution and control of treatments (Croce et al., 2014). Therefore, depending on the scope of ground improvement, the hydraulic/mechanical performance should be identified with a property (or more than one), originally inadequate and modifiable with ground improvement, and its adjustment motivated with quantitative design analyses.

Usually ground improvement techniques bring advantages, producing positive modification to the ground properties. Sometimes they are accompanied by limitations and drawbacks that must be seriously considered as they may hamper the effectiveness of the technique. One of the main aspects to be considered is the applicability of the candidate technique on existing structures. Some techniques produce in fact significant disturbance to the surrounding soil at a point that their execution is impossible near or below existing buildings or infrastructures, while others can be conveniently applied due to low invasiveness.

Apart from the induced modification, another relevant issue concerns the execution of the technique, i.e. the setting of the optimal treatment parameters necessary to achieve a prescribed goal. Each technique is achieved with a treatment that can be characterised with a set of geometrical and mechanical parameters (e.g. the intensity and duration of shaking and the spacing between boreholes for vibratory compaction, the injection pressure and spacing between holes for grouting etc.).

The choice of parameters dictates the cost of the treatment, which is a relevant issue to judge economic convenience. In some cases, charts exist to define the above parameters starting from the characteristics of the soil to be treated and to the desired goal. In some other cases, a significant degree of uncertainty remains that must be necessarily solved with an experimental assessment (field trial) to be performed before treatment is executed. This preliminary activity has the twofold scope of ensuring the feasibility of treatment and establishing the best procedures for execution.

Finally, but not less important, the effectiveness of ground improvement must be proven with simple, fast, reliable and non-invasive control tests. The controlling technique must be chosen depending on the modification applied to the soil. Most commonly, penetration resistance tests (SPT, CPT) executed prior and after treatment are suitable for assessing improvement, also because they are widely used for liquefaction assessment. Sonic tests based on the propagation of compression and shear waves can be also used, provided the technique determines an increase of the propagation velocity.

The main factors characterising the use of a ground improvement technique for liquefaction mitigation can be synthetically described in charts, an example of which is given in Figure 7-7. Normally, ground improvement requires a protocol procedure to choose, design and apply the selected technique. For risk assessment the fundamental choice concerns the economical convenience of mitigation, that should be



This project has received funding from the European Union's Horizon 2020 research and innovation programme under grant agreement No. 700748

Manual for the assessment of liquefaction risk, defining the procedures to create the database, collect, define, symbolize and store information in the Georeferenced Information System and to perform and represent the risk analysis

estimated performing a cost/benefit analysis as described in the flow chart of Figure 7-8. One of the main variables that must be known and considered to determine a sufficiently approximate estimate of costs is the volume of subsoil to be treated. This information, together with the unit cost of treatment (typically expressed as cost/volume) forms the total cost of mitigation.

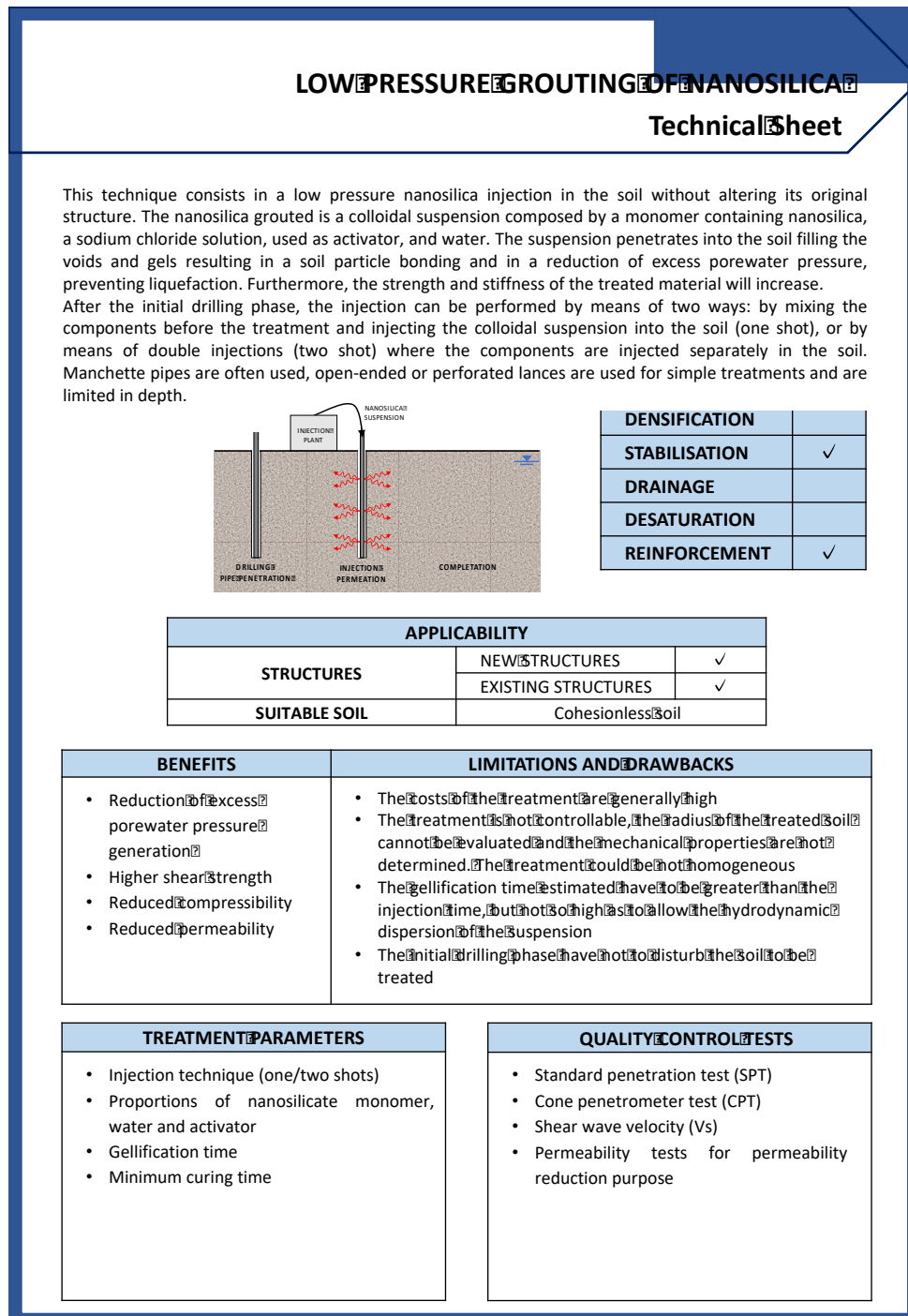


Figure 7-7: Example of technical chart describing the ground improvement technique.



This project has received funding from the European Union's Horizon 2020 research and innovation programme under grant agreement No. 700748

Manual for the assessment of liquefaction risk, defining the procedures to create the database, collect, define, symbolize and store information in the Georeferenced Information System and to perform and represent the risk analysis

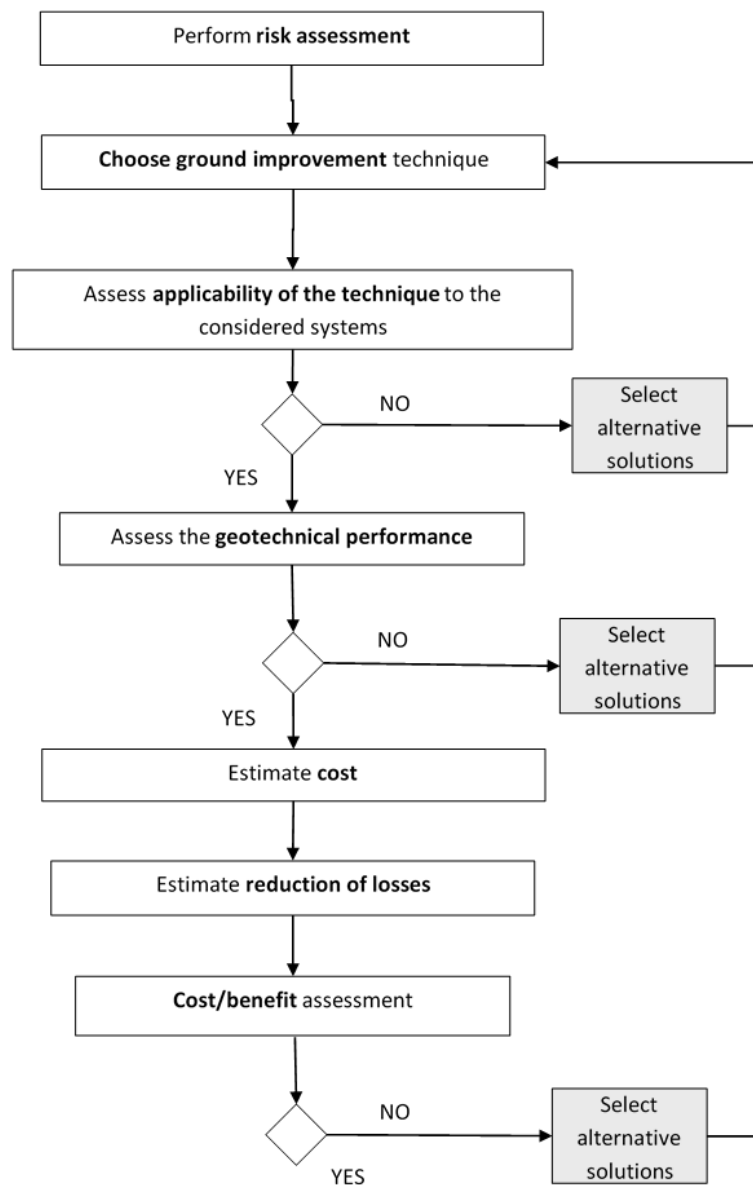


Figure 7-8: Flow chart describing mitigation analysis for risk assessment.

7.3.2 Reduction of structural vulnerability

For new residential buildings, both ground improvement solutions or surface foundation solutions may be applied. However, on some sites, practical constraints like soil conditions, site access, flooding, lateral spreading potential, dewatering requirements and building type/layout may limit to undertake ground improvement. Where any of these constraints apply, foundation reinforcement has generally to be chosen for a new residential building. This option involves constructing new residential buildings on land that is vulnerable to liquefaction and didn't underwent ground improvement.



This project has received funding from the European Union's Horizon 2020 research and innovation programme under grant agreement No. 700748

Manual for the assessment of liquefaction risk, defining the procedures to create the database, collect, define, symbolize and store information in the Georeferenced Information System and to perform and represent the risk analysis

As an example, in 2012, the Ministry of Business, Innovation and Employment of New Zealand has issued a set of Guidelines entitled “Repairing and rebuilding houses affected by the Canterbury Earthquakes”, organized in different parts. The logic of this document is to subdivide the area of Christchurch in three different zones assigning flats into three foundation technical categories based on the expected future liquefaction performance:

- TC1: Liquefaction damage is unlikely in future large earthquakes. Standard residential foundation assessment and construction is appropriate.
- TC2: Liquefaction damage is possible in future large earthquakes. Standard enhanced foundation repair and rebuild options in accordance with MBIE guidance are suitable to mitigate against this possibility.
- TC3: Liquefaction damage is possible in future large earthquakes. Individual engineering assessment is required to select the appropriate foundation repair or rebuild option.

As a general guiding principle, the code suggests building using light materials rather than heavy materials. Light construction (roof, walls and floors) significantly reduces the imposed loads on the subsoils and therefore the potential for liquefaction-induced settlement. For the buildings of TC3 category, the countermeasures listed in Figure 7-9 are suggested to reinforce foundations.

Type	Objectives	Dwelling Constraints	Land Constraints
Deep piles	Negligible settlement in both small and larger earthquakes	No height and/or material constraints likely	Not suitable where either <i>major or severe</i> global lateral movement likely or dense non-liquefiable bearing layer not present
Site ground improvement	Improving the ground to receive a TC2 foundation	Limits on some two storey/heavy wall types and plan configurations	Some ground improvements can be specified to accommodate <i>major</i> lateral stretch
Surface structures/ shallow foundations	Repairable damage in future moderate events	Only suitable for light and medium wall cladding combined with light roofs, regular in plan	In the absence of ground improvement, Type 1 & 2a options only suitable for minor to moderate vertical settlement and varying lateral stretch, Type 2b can accommodate up to 200 mm SLS settlement Type 3 (specific design) concepts can be designed for major lateral stretch and some for potentially significant vertical settlement

Figure 7-9: Proposed TC3 foundation types (MBIE, 2012).

Depending on the performance under Serviceability (SLS) and Ultimate Limit State (ULS) the different foundation types are proposed (Figure 7-10 and Figure 7-11).



This project has received funding from the European Union's Horizon 2020 research and innovation programme under grant agreement No. 700748

Manual for the assessment of liquefaction risk, defining the procedures to create the database, collect, define, symbolize and store information in the Georeferenced Information System and to perform and represent the risk analysis

	Vertical Land Settlement (SLS)		Lateral Stretch (ULS)	
	<100 mm (Moderate)	>100 mm (Potentially Significant)	<200 mm (Moderate)	<500 mm (Major)
Type 1 – light-weight platform (standard solution) Enhanced NZS 3604 subfloor	Yes	No ¹	Yes	No
Type 2 – underslab platform (standard solution) Type 2A – 150 mm underslab on gravel	Yes	No ¹	Yes	Yes
Type 2B – 300 mm underslab on gravel		Up to 200 mm ¹		
Type 3 – concepts for specific design Type 3A – Re-levellable platform Type 3B – Stiff platform	Yes	Subject to design	Yes	Yes

Figure 7-10: Summary of foundation types proposed for TC3 structures (MBIE, 2012).

Figure 15.16: Perimeter foundation details for Type 1 surface structure

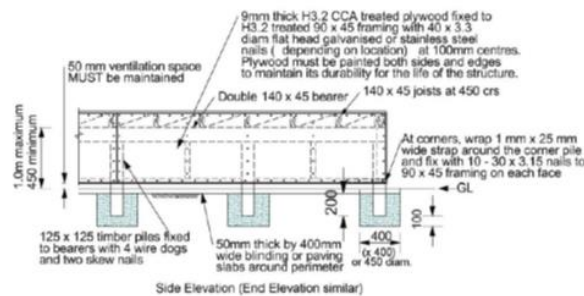


Figure 15.19: Detail of Type 2A surface structure at the timber piles (including gravel raft)

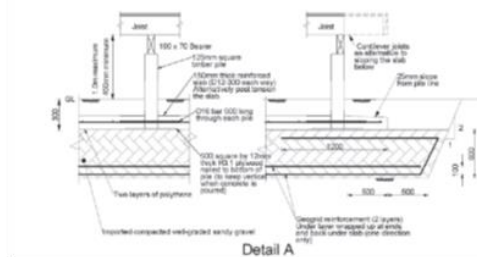


Figure 15.20: Section through Type 2B surface structure at the timber piles (including gravel raft)

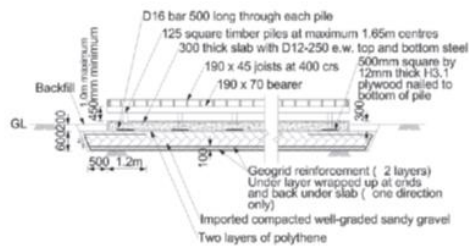


Figure 15.23: Type 3A surface structure - Detail at supporting blocks

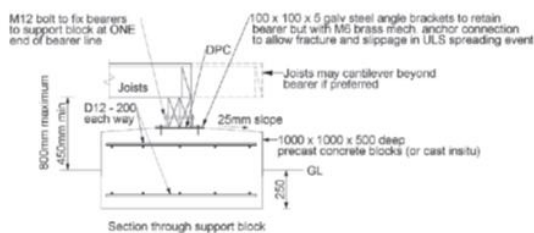


Figure 15.25: Type 3B surface structure - Section through pre-stressed concrete support beam and beam connection

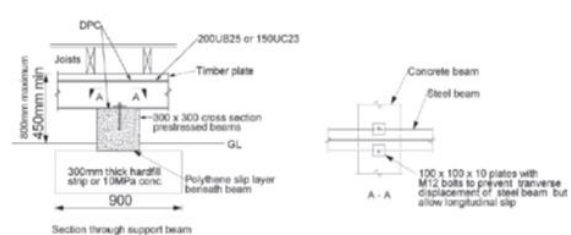


Figure 7-11: Schematic plots of the different foundation types (MBIE, 2012).



This project has received funding from the European Union's Horizon 2020 research and innovation programme under grant agreement No. 700748

8. REFERENCES

- Akkar, S., Sandikkaya, M.A., Şenyurt, M., Azari Sisi, A., Ay, B.O., Traversa, P., et al 2014. "Reference database for seismic ground-motion in Europe (RESORCE)". *Bull Earthquake Engineering* 12:311–39.
- Andrus, R. D., and Stokoe, K. H. 1997. "Liquefaction resistance based on shear wave velocity". NCEER Workshop on Evaluation of Liquefaction Resistance of Soils, Salt Lake City, UT, Technical Report NCEER-97-0022.
- Andrus, R. D., and Stokoe, K. H. 2000. "Liquefaction resistance of soils from shear wave velocity". *J. Geotech. Geoenviron. Eng., ASCE*, 126 (11), 1015 – 1025.
- Arias, A. 1970. "A measure of earthquake intensity". *Seismic design for nuclear power plants*, R. J. Hansen, ed., MIT Press, Cambridge, Mass.
- ASTM Committee D-18 on Soil and Rock, 2011. "Standard practice for classification of soils for engineering purposes (unified soil classification system)". West Conshohocken, PA: ASTM International.
- ASTM International (2011a). "Standard Test Method for Standard Penetration Test (SPT) and Split-Barrel Sampling of Soils". ASTM D1586-11. West Conshohocken, PA: ASTM International.
- ASTM International (2011b). "Standard Practice for Determining the Normalized Penetration Resistance of Sands for Evaluation of Liquefaction Potential". ASTM-D6066-11. West Conshohocken, PA: ASTM International.
- ASTM International (2014a). "Standard Test Methods for Downhole Seismic Testing". ASTM D7400-14. West Conshohocken, PA: ASTM International.
- Baecher, G. B., Christian, J. T. 2003. "Reliability and statistics in geotechnical engineering". Chichester, England: Wiley, 605 pp.
- Bagriacik, A., Davidson, R., Hughes, M., Bradley, B., & Cubrinovski, M. 2018. "Comparison of statistical and machine learning approaches to modeling earthquake damage to water pipelines". *Soil Dynamics and Earthquake Engineering*, 76-88.
- Baker, J.W. and Cornell, C.A. 2008. "Uncertainty propagation in probabilistic seismic loss estimation". *Structural Safety*, 30, 236–252.
- Bardet J. P., Lin, C. H. 2000. "EERA - A Computer Program for Equivalent-linear site Response Analyses of Layered Soil Deposits".
- Bardet, J. P., Tobita, T., Mace, N., Hu, J. 2002. "Regional modeling of liquefaction induced ground deformation". *Earthq Spectra* 2002; 18(1): 19–46.
- Bartha, G., and Kocsis, S. 2011. "Standardization of geographic data: the European Inspire Directive". *European Journal of Geography* 2 2: 79-89, 2011.



This project has received funding from the European Union's Horizon 2020 research and innovation programme under grant agreement No. 700748

Manual for the assessment of liquefaction risk, defining the procedures to create the database, collect, define, symbolize and store information in the Georeferenced Information System and to perform and represent the risk analysis

- Bird, J., Crowley, H., Pinho, R., Bommer, J. 2005. "Assessment of building response to liquefaction induced differential ground deformation". *Bulletin of the New Zealand Society for Earthquake Engineering*, 38-4, Dec. 2005, 215-234.
- Bird, J., Bommer, J., Crowley, H., Pinho, R. 2006. "Modelling liquefaction-induced building damage in earthquake loss estimation". *Soil Dynamics and Earthquake Engineering* 26 (2006) 15–30.
- Bommer, J.J., and Abrahamson, N.A. 2006. "Why do modern probabilistic seismic-hazard analyses often lead to increase hazard estimates?". *Bulletin of Seismological Society of America* 96:6, 1967–1977.
- Boulanger, R.W., Idriss, I.M., 2014. "CPT and SPT based liquefaction triggering procedures". Department of Civil and Environmental engineering, University of California at Davis.
- Boulanger, R.W., and Idriss, I.M. 2015. "CPT-based liquefaction triggering procedure". *Journal of Geotechnical and Geoenvironmental Engineering*, 142(2), p.04015065
- Boulanger, R., Ziotopoulou, K. 2012. "PM4Sand (Version 2): a sand plasticity model for earthquake engineering applications". Report no. UCD/CGM-12/01, center for Geotechnical Modeling.
- Boulanger, R.W., and Ziotopoulou, K. 2015. "PM4Sand (Version 3): A Sand Plasticity Model for Earthquake Engineering Applications". Center for Geotechnical Modeling, Department of Civil and Environmental Engineering, University of California, Davis, California, Report no. UCD/CGM-15/01, pp. 70-76.
- Boulanger, R.W. and Idriss, I.M. 2016. "CPT- Based Liquefaction Triggering Procedures". *Journal of Geotechnical and Geoenvironmental Engineering*, 142(2), 04015065.
- Bradley, B.A., Lee, D.S., Broughton, R., and Price, C. 2009. "Efficient evaluation of performance-based earthquake engineering equations". *Structural Safety*, 31, 65–74.
- Bradley, B., 2013. "Ground motion selection for seismic risk analysis of civil infrastructure". *Handbook of seismic risk analysis and management of civil infrastructure systems*, S. Tesfamariam and K. Goda editors, Woodhead Publishing Limited, pp. 79-112.
- Bray, J.D., Rathje, E.M., Augello, A.J., and Merry, S.M. 1998. "Simplified seismic design procedure for geosynthetic-lined, solid waste landfills". *Geosynthetics International*, 5(1-2): 203-235.
- Bray, J.D. and Macedo, J. (2017). 6th Ishihara lecture: Simplified procedure for estimating liquefaction induced building settlement. *Soil Dynamics and Earthquake Engineering*, 102: 215–231. <http://dx.doi.org/10.1016/j.soildyn.2017.08.026>
- Bruneau, M., Chang, S., Eguchi, R., Lee, G., O'Rourke, T., Reinhorn, A. M., Shinozuka, M., Tierney, K., Wallace, W., and Winterfeldt, D. V. 2003. "A Framework to Quantitatively Assess and Enhance the Seismic Resilience of Communities". *Earthquake Spectra*, 19(4), 733–752.
- Bullock, Z., Karimi, Z., Dashti, S., Porter, K., Liel, A. B., Franke, K. W. 2018. "A physics-informed semi-empirical probabilistic model for the settlement of shallow-founded structures on liquefiable ground". *Géotechnique* [<https://doi.org/10.1680/jgeot.17.P.174>]
- Caltrans (2008). "Quantifying the impacts of soil liquefaction and lateral spreading on project delivery". California Dept of Transportation, Memos to Designers 20-14, July 2008, 10 pp.
- Caltrans (2008), Soil liquefaction and lateral spreading analysis and guidelines, California Dept of Transportation, Memos to Designers 20-15, July 2008, 8 pp.



This project has received funding from the European Union's Horizon 2020 research and innovation programme under grant agreement No. 700748

Manual for the assessment of liquefaction risk, defining the procedures to create the database, collect, define, symbolize and store information in the Georeferenced Information System and to perform and represent the risk analysis

- CCS, 2018, La cobertura de los riesgos extraordinarios en Espana, Consorcio de Compensacion de Seguros, 18 pp.
- CEN (2004a). EN 1998-1, Eurocode 8—design of structures for earthquake resistance, part 1: general rules, seismic actions and rules for buildings. European Committee for Standardization, Brussels.
- CEN (2004b). EN 1998-5, Eurocode 8—design of structures for earthquake resistance, part 5: Foundations, retaining structures and geotechnical aspects. European Committee for Standardization, Brussels.
- Campbell, K. W., and Bozorgnia, Y. 2012. “A Comparison of Ground Motion Prediction Equations for Arias Intensity and Cumulative Absolute Velocity Developed Using a Consistent Database and Functional Form”. *Earthquake Spectra*, 28(3), 931-941.
- Cetin, K. O., Seed, R. B., Der Kiureghian, A., Tokimatsu, K., Harder, L. F., Kayen, R. E., and Moss, R.E. S. 2004. “Standard penetration test-based probabilistic and deterministic assessment of seismic soil liquefaction potential”. *J. Geotechnical and Geoenvironmental Eng., ASCE* 130(12), 1314–340.
- Chang, W, Rathje, E.M., Stokoe, K. H., and Cox, B.R. 2004. “Direct evaluation of effectiveness of prefabricated vertical drains in liquefiable sand.” *Soil Dynamics and Earthquake Engineering*, 24(9-10) 723-731.
- Chilès, J. P. and Delfiner, P. (2012) *Geostatistics: Modeling Spatial Uncertainty*, 2nd Edition – Wiley - ISBN: 978-0-470-18315-1, p. 726.
- Ching, J., Porter, K.A. and Beck, J.L. 2009. “Propagating uncertainties for loss estimation in performance-based earthquake engineering using moment matching”. *Structure and Infrastructure Engineering*, 5(3), 245–262.
- Chiou, B.S.J., Darragh, R.B., Gregor, N.J., Silva, W.J. 2008. “NGA project strong-motion database”. *Earthquake Spectra* 24:23–44.
- Cimellaro, G. P. 2013. “Resilience-based design (RBD) modelling of civil infrastructure to assess seismic hazards”. *Handbook of seismic risk analysis and management of civil infrastructure systems*, S. Tesfamariam and K. Goda editors, Woodhead Publishing Limited, pp.268-306.
- Comerio, M.C. (editor) 2005. “PEER testbed study on a laboratory building: exercising seismic performance assessment”. *PEER Report*. PEER 2005/12.
- Cornell, C.A., and Krawinkler, H. 2000. “Progress and Challenges in Seismic Performance Assessment”. *PEER Center News*, 3, 1-3.
- Croce P., Flora A., Modoni G., 2014, *Jet grouting: Technology, Design and Control*. Taylor & Francis Group.
- Crowley, H., Bommer, J.J., Pinho, R., and Bird, J. 2005. “The impact of epistemic uncertainty on an earthquake loss model”. *Earthquake Engineering Structural Dynamics*, 34(14), 1653–1685.
- Crowley, H., Colombi, M., Crempien, J., Erduran, E., Lopez, M., Liu, H., Mayfield, M., Milanese, M. 2010. “Seismic Risk Report”, *Gem* 2010,5.
- CREW. (2012). “Community Resilience to Extreme Weather - the CREW Project”. *Final Report*. CREW Project, 110.
- CTMS, (2016). “Manuale per l’analisi della Condizione limite per l’emergenza (CLE)”. *Commissione Tecnica per la Microzonazione Sismica, Dipartimento della Protezione Civile*, 281 pp. (in Italian).



This project has received funding from the European Union's Horizon 2020 research and innovation programme under grant agreement No. 700748

Manual for the assessment of liquefaction risk, defining the procedures to create the database, collect, define, symbolize and store information in the Georeferenced Information System and to perform and represent the risk analysis

- CTMS, (2017). "Microzonazione sismica - Linee guida per la gestione del territorio in aree interessate da liquefazione (LQ)". Commissione Tecnica per la Microzonazione Sismica, Dipartimento della Protezione Civile, 57 pp. (in Italian).
- Cubrinovski, M., Ishihara, K. 2002. "Maximum and minimum void ratio characteristics of sands". *Soil Found.* 42 (6), 65–78.
- Cubrinovski, M., Hughes, M., Bradley, B., Noonan, J., McNeill, S., English, G., & Hopkins, R. (March 2014). "Performance of Horizontal Infrastructure in Christchurch City through the 2010-2011 Canterbury Earthquake Sequence". Christchurch: Civil & Natural Resources Engineering, University of Canterbury.
- Cubrinovski, M., van Ballegooy, S. 2017. "System response of liquefiable deposits". 3rd Int. Conf. on Performance Based Design in Earthquake Geotechnical Engineering.
- Cutter, S. L., Barnes, L., Berry, M., Burton, C., Evans, E., Tate, E., & Webb, J. 2008. "A place-based model for understanding community resilience to natural disasters". *Global Environmental Change*, 18(4), 598–606. <http://doi.org/10.1016/j.gloenvcha.2008.07.013>
- Dafalias, Y.F., and Manzari, M.T. 2004. "Simple Plasticity Sand Model Accounting for Fabric Change Effects". *Journal of Engineering Mechanics*, 130 (6).
- D'Appolonia, E. 1954. Symposium on dynamic testing of soils. ASTM International.
- Dickenson, S. 2005. "Recommended guidelines for liquefaction evaluations using ground motions from probabilistic seismic hazard analyses". Report to the Oregon Department of Transportation, June 2005, 93 pp.
- EERI Endowment Subcommittee (2000). "Financial Management of Earthquake Risk". EERI Publication. ISBN 0-943198-21-6.
- Dipartimento della Protezione Civile, DPC (2008). "Indirizzi e criteri per la Microzonazione Sismica, part. 1 and 2". Roma 2008.
- Dipartimento della Protezione Civile, DPC (2017). "Linee guida per la gestione del territorio in aree interessate da liquefazioni (LQ). Versione 1.0". Roma 2017.
- Eguchi, R. T. 1991. "Seismic Hazard Input for Lifeline Systems". 10.
- Eidinger, J. 1998. "Water Distribution System".
- Ellingwood, B. 2001. "Earthquake risk assessment in building structures". *Reliability Engineering and System Safety*, 74, 251–262.
- El Mohtar C.S., Bobet, A., Santagata, M.C., Drnevich V.P., Johnston C.T., 2013, Liquefaction Mitigation Using Bentonite Suspensions, *Journal of Geotechnical and Geoenvironmental Engineering*, 139 (8).
- EN1998-5. "Design of structures for earthquake resistance – Part 5: Foundations, retaining structures and geotechnical aspects".
- EQC (2012). Canterbury-guidance-part-b_EQC Residential_liquefaction, 34 pp.
- ESRI (2001), ArcGIS 9 What is ArcGIS.



This project has received funding from the European Union's Horizon 2020 research and innovation programme under grant agreement No. 700748

Manual for the assessment of liquefaction risk, defining the procedures to create the database, collect, define, symbolize and store information in the Georeferenced Information System and to perform and represent the risk analysis

- Fardis, M.N., et al. 2005. "Designers' Guide to EN 1998-1 and EN 1998-5. Eurocode 8: Design of Structures for Earthquake Resistance. General rules, seismic actions, design rules for buildings, foundations and retaining structures". Eurocode Expert, ICE and Thomas Telford, UK.
- FEMA, Federal Emergency Management Agency, 1992. "FEMA 178 - NEHRP Handbook for the Seismic Evaluation of Existing Buildings", Washington, D. C., Developed by the Building Seismic Safety Council (BSSC) for the Federal Emergency Management Agency (FEMA).
- FEMA/NIBS, 1998. "HAZUS - Earthquake Loss Estimation Methodology". Vol. 1, 1998.
- FEMA & NIBS, 1999. "HAZUS99 user and technical manuals", Federal Emergency Management Agency Report: HAZUS 1999, Washington D.C., USA.
- FEMA/NIBS 2003. "HAZUS-Earthquake – Technical Manual". Federal Emergency
- Fioravante, V. et al. 2013. "Earthquake geotechnical engineering aspects: the 2012 Emilia Romagna earthquake (Italy)". Seventh international Conference on Case Histories in Geotechnical Engineering, April 29 th – May 4th, 2013. Chicago (US)
- Galli, P. and Meloni, F. 1993. "Liquefazione Storica. Un catalogo nazionale". Quat. Ital. J. Quat. Sci. 6. Pagg. 271–292.
- Galli, P. 2000. "New empirical relationships between magnitude and distance for liquefaction". Tectonophysics 324, 169-187.
- Gerace, A. 2018. "Equivalent simplified soil profiles for liquefaction assessment". MSc Thesis, University of Porto (FEUP).
- Goda, K., and Hong, H.P. 2008. "Estimation of seismic loss for spatially distributed buildings". Earthquake Spectra, 24(4), 889–910.
- Grant, R., Christian, J.T., and Vanmarcke, E.H. 1974. "Differential settlement of buildings". Journal of Geotechnical Engineering Division, ASCE, 100(9), pp. 973-991.
- Grunthal, G., Wahlstrom, R. 2012. "The European-Mediterranean earthquake catalogue (EMEC) for the last millennium". Journal of seismology 16: 535-570
- Grunthal, G., Wahlstro, R. 2013. "The SHARE European earthquake catalogue (SHEEC) for the time period 1900-2006 and its comparison to the European-Mediterranean earthquake catalogue (EMEC)". Journal of seismology 17: 1339-1344.
- Hall, W.J., and Wiggins, J.H. 2000. "Acceptable risk: a need for periodic review". Natural Hazard Review, 1(3), 180–187.
- Hayes, W.W. 1998. "Reduction of earthquake risk in the United States: bridging the gap between research and practice". IEEE Transaction on Engineering Management, 45(2), 176–180.
- Iai, Tobita, Ozutsumi, Ueda 2011. "Dilatancy of Granular Materials in Strain Space Multiple Mechanism Model". Int. J. Numel. Meth. Geomech. 35: 360-392.
- ICC, (2009). "International Building Code". International Code Council, 752 pp.



This project has received funding from the European Union's Horizon 2020 research and innovation programme under grant agreement No. 700748

Manual for the assessment of liquefaction risk, defining the procedures to create the database, collect, define, symbolize and store information in the Georeferenced Information System and to perform and represent the risk analysis

- ICMS, (2008). "Indirizzi e criteri per la microzonazione sismica". Dipartimento della Protezione Civile e Conferenza delle Regioni e delle Province Autonome, 515 pp. (in Italian).
- Idriss, I. M. 1999. "An update to the Seed-Idriss simplified procedure for evaluating liquefaction potential". Proceedings, TRB Workshop on New Approaches to Liquefaction, Publication No. FHWARD- 99-165, Federal Highway Administration, January.
- Idriss, I. M., and Boulanger, R. W. 2008. "Soil liquefaction during earthquakes". Monograph MNO-12, Earthquake Engineering Research Institute, Oakland, CA, 261 pp.
- Idriss, I.M., Boulanger, R.W. 2010. "SPT-based liquefaction triggering procedure". Report # UCD/CGM-10/02 of the Center for Geotechnical Modeling, 259 pp.
- Insurance Compensation Consortium of Spain, (2008). "Natural catastrophes insurance cover. A diversity of systems". Consorcio de Compensacion de Seguros, Madrid.
- Ishihara, K. 1985. "Stability of Natural Deposits During Earthquakes". Proceedings of the 11th International Conference on Soil Mechanics and Foundation Engineering, San Francisco, 1:321-376.
- Isoyama, R. E. I. 2000. "Seismic Damage Estimation Procedures for Water Supply Pipelines". 12WCEE.
- Itasca Consulting Group, Inc. 2016. "FLAC — Fast Lagrangian Analysis of Continua, Ver. 8.0". Minneapolis: Itasca.
- Itasca 2017. "FLAC, Fast Lagrangian Analysis of Continua". Itasca Consulting Group, Inc. Additional information available on: www.itascacg.com/flac.
- Iwasaki, T., Tatsuoka, F., Tokida, K., Yasuda, S. 1978. "A Practical method for assessing soil liquefaction potential based on case studies at various sites in Japan". [conference]: 2nd International conference on Microzonation. - 1978: 885-896.
- Jamiolkowski, M., Ladd, C. C., Germaine, J. T., and Lancellotta, R. 1985. "New developments in field and laboratory testing of soils" .Proc., 11th Int. Conf. on Soil Mechanics JGS, 1998, Remedial Measures against Soil Liquefaction, Japan Geotechnical Society, Balkema Rotterdam.
- JGS (1998). "Remedial against liquefaction from investigation and design to implementation". Japanese Geotechnical Society, Balkema eds., 433 p.
- JGS (2011). Geo hazard during earthquake and mitigation measures – Lessons and recommendations from the 2011 Great East Japan Earthquake, 91 p.
- Joyner, W.B., and D.M. Boore, 1988. "Measurement, Characterization, and Prediction of Strong Ground Motion", Proceedings of Earthquake Engineering & Soil Dynamics II, pp. 43- 102. Park City, Utah, 27 June 1988. New York: Geotechnical Division of the American Society of Civil Engineers.
- Juang, C. H., Yang, S. H. and Yuan, H. 2005. "Model uncertainty of shear wave velocity-based method for liquefaction potential evaluation". J. Geotech. Geoenviron., 131(10), 1274-1282.
- Juang C.H., Ching, J. Luo. (2013). Assessing SPT-based probabilistic models for liquefaction potential evaluation: a 10-year update. Georisk: Assessment and Management of Risk for Engineered Systems and Geohazards. 7. 10.1080.



This project has received funding from the European Union's Horizon 2020 research and innovation programme under grant agreement No. 700748

Manual for the assessment of liquefaction risk, defining the procedures to create the database, collect, define, symbolize and store information in the Georeferenced Information System and to perform and represent the risk analysis

- Kaplan, S. 1981. "On the method of discrete probability distributions in risk and reliability calculations – application to seismic risk assessment". *Risk Analysis*, 1(3), 189–196.
- Kayen, R., Moss, R. E. S., Thompson, E. M., Seed, R. B., Cetin, K. O., Der Kiureghian, A., Tanaka, Y., Tokimatsu, K. 2013. "Shear-Wave Velocity-Based Probabilistic and Deterministic Assessment of Seismic Soil Liquefaction Potential". *Journal of Geotechnical and Geoenvironmental Engineering*.
- Karamitros, D.K., Bouckovalas, G. D., Chaloulos, Y.K. 2013. "Seismic settlements of shallow foundations on liquefiable soil with a clay crust". *Soil Dynamics and Earthquake Engineering*. 46. 64-76.
- Karimi, Z. and Dashti, S. 2017. "Ground motion intensity measures to evaluate II: the performance of shallow-founded structures on liquefiable ground". *Earthquake Spectra*, 33(1), 277-298.
- Kirsch, K., and Kirsch, F. "Ground Improvement by Deep Vibratory Methods", Second Edition, CRC press, 234 pp.
- Kramer, S.L. 1996. "Geotechnical Earthquake Engineering". Prentice Hall Publishers, 653 p.
- Kramer, S. L. and Elgamal, A. W. 2001. "Modeling soil liquefaction hazards for performance-based earthquake engineering". PEER Report 2001/13.
- Kramer, S.L. and Wang, C. H. 2015. "Empirical Model for Estimation of the Residual Strength of Liquefied Soil". *Journal of Geotechnical and Geoenvironmental Engineering* 141(9), May 2015.
- Krawinkler, H. (editor) 2005. "Van Nuys Hotel building testbed report: exercising seismic performance assessment". PEER Report. PEER 2005/11.
- Kunreuther, H. 1996. "Mitigating disaster losses through insurance2. *Journal of Risk and Uncertainty*, 12(2–3), 171–187.
- Kwona, O.-S., and Elnashai, A. 2006. "The effect of material and ground motion uncertainty on the seismic vulnerability curves of RC structure". *Engineering Structures*, 28(2), 289–303.
- Lang, D.H., and Aldea, A., 2011. "Specifications of Inventory Data for Earthquake Risk Assessment". Report 1.0 for Project "Earthquake Risk in the Romanian–Bulgarian Border Region", April 2011.
- Lang, D. H. 2012. "Earthquake Damage and Loss Assessment - Predicting the Unpredictable", Dissertation for the degree of Dr. philos, University of Bergen Norway.
- Lawson, A., Biggeri, A., Böhning, D., Lesaffre, E., Viel, J.F. and Bertollini, R. 2001. "Disease Mapping and Risk Assessment for Public Health". *International Journal of Epidemiology*, 30, 405-406.
- Lee, T.-H., and Mosalam, K.M. 2006. "Probabilistic seismic evaluation of reinforced concrete structural components and systems". PEER Report. PEER 2006/04.
- Liao, S. C., and Whitman, R. V. 1986. "Overburden correction factors for SPT in sand". *J. Geotechnical Eng., ASCE* 112(3), 373–77.
- Luco, N., Mai, P. M., Cornell, C. A., & Beroza, G. C. 2002. "Probabilistic Seismic Demand Analysis at a Near-Fault Site using ground motion simulations based on a stochastic-kinematic earthquake source model". 7th U.S National Conference on Earthquake Engineering.



This project has received funding from the European Union's Horizon 2020 research and innovation programme under grant agreement No. 700748

Manual for the assessment of liquefaction risk, defining the procedures to create the database, collect, define, symbolize and store information in the Georeferenced Information System and to perform and represent the risk analysis

- Lyman, A. K. B. 1941. "Compaction of cohesionless foundation soils by explosives". *Proceedings of the American Society of Civil Engineers*, 67(5), pp. 769-780.
- Macaulay, T. 2009. "Critical Infrastructures". Taylor & Francis, 342 pp.
- Madiati, C., Vannucchi, G., Baglione, M., Martelli, L., Veronese, T. 2016. "Utilizzo di prove penetrometriche statiche a punta meccanica per la stima del potenziale di liquefazione". *Rivista Italiana di Geotecnica* 3/16, pp.14-24.
- Makdisi, F.I., & Seed, H.B. 1978. "Simplified procedure for estimating dam and embankment earthquake-induced deformations". *Journal of Geotechnical Engineering*, 104(7): 849-867.
- Martin, G. R., Finn, W.D.L., and Seed, H. B. 1975. "Fundamentals of liquefaction under cyclic loading". *Journal of Geotechnical Division*, 101 (5): 423-438.
- Matheron, G. 1965. "Les variables régionalisées et leur estimation: une application de la théorie des fonctions aléatoires aux sciences de la nature". Masson, Paris, France.
- Maurer, B. W., Green, R. A., Oliver, S., Taylor, O. S. 2015. "Moving Towards an Improved Index for Assessing Liquefaction Hazard: Lessons from Historical Data". *Soils and Foundations*, 55(4): 778-787.
- May, P.J. 2004a. "Making choices about earthquake performance". *Natural Hazards Review*, 5(2), 64–70.
- May, P.J. 2004b. "Societal perspective about earthquake performance: the fallacy of acceptable risk". *Earthquake Spectra*, 17(4), 725–737.
- Mayfield, R. (2007). The return period of soil liquefaction. *Journal of Geotechnical and Geoenvironmental Engineering*. 133. 7(802).
- Mayne, P. W., Jones Jr, J. S. & Dumas, J. C. 1984. "Ground response to dynamic compaction". *ASCE Journal of Geotechnical Engineering*, 110(6), pp. 757-774.
- Mayne, P.W. 2006. "Undisturbed sand strength from seismic cone tests". *Geomechanics and Geoengineering: An International Journal*, 1, 4, 239-257.
- McGuire, R.K. 2004. "Seismic Hazard and Risk Analysis". EERI Monograph Series MNO-10, Earthquake Engineering Research Institute, 221 p.
- Melchers, R.E. 2001. "On the ALARP approach to risk management". *Reliability Engineering and System Safety*, 71, 201–208.
- Mele, L., Tan Tian J., Lirer S., Flora A., Koseki J., 2018, Liquefaction resistance of unsaturated sands: experimental evidence and theoretical interpretation, *Géotechnique* in press.
- Meyerhof, G. G. 1956. "Penetration Test and Bearing Capacity of Cohesionless Soils". *Journal of the Soil Mechanics and Foundation Division, ASCE*, Vol. 82, No. SM1, pp 1-19.
- Mian, J. F., Kontoe, S., Free, M. 2013. "Assessing and managing risk of earthquake-induced liquefaction to civil infrastructure". *Handbook of seismic risk analysis and management of civil infrastructure systems*, S. Tesfamariam and K. Goda Editors, 2013, Woodhead Publishing Limited, 113-138.



This project has received funding from the European Union's Horizon 2020 research and innovation programme under grant agreement No. 700748

Manual for the assessment of liquefaction risk, defining the procedures to create the database, collect, define, symbolize and store information in the Georeferenced Information System and to perform and represent the risk analysis

- Millen, M., Ferreira, C., Quintero, J., Gerace, A. and Viana da Fonseca, A. 2019. "Simplified equivalent soil profiles based on liquefaction performance". 7th International Conference on Earthquake Geotechnical Engineering. Rome, Italy.
- Ministry of Business, Innovation & Development – NZGS (2016): "Recommendation after the Canterbury Earthquake sequence (2010-2011)".
- Mitrani-Reiser, J., Haselton, C.B., Goulet C., Porter, K.A., Beck, J., and Deierlein, G.G. 2006. "Evaluation of the seismic performance of a code-conforming reinforced-concrete frame building - part II: loss estimation". 8th NCEE, San Francisco, California, April 18-22, 10 pp.
- Moehle, J.P. 2003. "A framework for performance-based earthquake engineering". Proc. ATC-15-9 Workshop on the Improvement of Building Structural Design and Construction Practices, Maui, HI, June.
- Murray, A., Grubestic, T. 2007. "Critical Infrastructure: Reliability and Vulnerability". Springer eds. 313 pp.
- Nadim, F. 2007. "Tools and Strategies for Dealing with Uncertainty in Geotechnics". In Probabilistic Method in Geotechnical Engineering, CISM Course and Lectures, D.V Griffith & G.A Fenton Eds. Springer, pp.71-95.
- NASEM 2016. "State of the Art and Practice in the Assessment of Earthquake-Induced Soil Liquefaction and Its Consequences". National Academies of Sciences, Engineering, and Medicine. Washington, DC: The National Academies Press. doi: 1017226/23474.
- National Research Council 1985. "Liquefaction of Soils During Earthquakes", Committee on Earthquake Engineering, Commission on Engineering and Technical Systems, National Academy Press, Washington, DC.
- Nguyen, T.V., Rayamajhi, D., Boulanger, R.W., Ashford, S.A., Lu, J., Elgamal, A., and Shao, L. 2012. "Effects of DSM grids on shear stress distribution in liquefiable soil". GeoCongress 2012, State of the Art and Practice in Geotechnical Engineering, ASCE GSP 255, Oakland, CA, PP. 1948-1957.
- Nigbor, R.L., Imai, T. 1994. "The suspension P-S velocity logging method". Pp. 57-61 in Geophysical Characterization of Sites, edited by R.D. Woods. International Society for Soil Mechanics and Geotechnical Engineering Special Publication TC 10. New York: International Science Publisher.
- NZGS (2016). "Earthquake geotechnical engineering practice, Module 2: Geotechnical investigations for earthquake engineering". New Zealand Geotechnical Society and Ministry of Business Innovation & Employment (MBIE) Earthquake Geotechnical Engineering Practice in New Zealand, 44 pp.
- NZGS (2016). "New Zealand Geotechnical Society, Earthquake Geotechnical Engineering Practice, Module 3: identification, assessment and mitigation of liquefaction hazards". New Zealand Geotechnical Society and Ministry of Business Innovation & Employment (MBIE) Earthquake Geotechnical Engineering Practice in New Zealand,
- O'Rourke, T. S.-S. J. 2012. "Underground Lifelines System Performance during the Canterbury Earthquake Sequence". Lisbon: 15WCEE.
- O'Rourke, T. S.-S. J. 2014. "Earthquake Response of Underground Pipeline Networks in Christchurch, NZ". 30(1).
- Palm, R. 1995. "Earthquake Insurance – A longitudinal study of California homeowners". Westview Press Inc., Boulder, CO.



This project has received funding from the European Union's Horizon 2020 research and innovation programme under grant agreement No. 700748

Manual for the assessment of liquefaction risk, defining the procedures to create the database, collect, define, symbolize and store information in the Georeferenced Information System and to perform and represent the risk analysis

- Palmer, D.J., Stuart, J.G. 1957. "Some observations on the Standard Penetration Test and a correlation of the test with a new penetrometer". 4th Int. Conf. Soil Mech. Found. Eng., Londra.
- Paté-Cornell, M.E. 1994. Quantitative safety goals for risk management of industrial facilities". *Structural Safety*, 13, 145–157.
- Pitilakis, K. H. C. 2014. "SYNER-G: Typology Definition and Fragility Functions for Physical Elements at Seismic Risk". Springer.
- Pitilakis, K., & Argyroudis, S. 2014. "Seismic Vulnerability Assessment: Lifelines". *Encyclopedia of Earthquake Engineering*.
- Porter, K.A. 2003. "An overview of PEER's Performance-based earthquake engineering methodology". ICASP9, Civil Engineering Risk and Reliability Association (CERRA), San Francisco, CA, July 6-9.
- Poulos, H.G., Carter J.P., Small J.C. 2001. "Foundations and retaining structures: research and practice". *Proc. XV ICSMGE, Istanbul*, vol.4, pp.2527-2606.
- Power, M. S., Dawson, A.W., Streiff, D.W., Perman, R.G., and Haley, S. C. 1982. "Evaluation of Liquefaction Susceptibility in the San Diego, California Urban Area". *Proceedings 3rd International Conference on Microzonation, II*, pp. 957-968.
- Rauch, A.F., Martin, J.R. 2000. "EPOLLS model for predicting average displacements on lateral spreads". *ASCE J Geotech Geoenviron Eng* 2000;126(4):360–71.
- RER, 2012. "Primo rapporto sugli effetti della liquefazione osservati a S. Carlo, frazione di S. Agostino (Provincia di Ferrara)". Regione Emilia-Romagna Servizio Geologico e dei Suoli e Protezione Civile Ufficio Rischio Sismico e Vulcanico (in italian).
- Robertson, P. 1990. "Soil classification using the cone penetration test". *Canadian Geotechnical Journal*, 27(1):151–158.
- Robertson, P.K., and Fear, C.E. 1995. "Application of CPT to evaluate liquefaction potential". *CPT '95, Linköping, Swedish Geotechnical Society*, 3, 57-79.
- Robertson, P.K. and Wride, C.E. 1998. "Evaluating Cyclic Liquefaction Potential Using the Cone Penetration Test". *Canadian Geotechnical Journal* 35, 442 - 459.
- Robertson, P.K., and Cabal, K.L. 2015. "Guide to Cone Penetration Testing for Geotechnical Engineering". Gregg Drilling & Testing, Inc.
- Sadigh, K., Egan, J. A., and Youngs, R. R. 1986. "Specification of Ground Motion for Seismic Design of Long Period Structures". *Earthquake Notes*, vol. 57, no. 1, p. 13, relationships are tabulated in Joyner and Boore (1988) and Youngs and others (1987).
- Seed, H.B., and Idriss, I.M. 1971. "Simplified procedure for evaluating soil liquefaction potential". *Journal of the Soil Mechanics and Foundations Division, ASCE*, 97(SM9): 1249–1273.
- Seed, H. B., and Idriss, I. M. 1982. "Ground Motions and Soil Liquefaction During Earthquakes". *Earthquake Engineering Research Institute, Oakland, California, Monograph Series*, p. 13.



This project has received funding from the European Union's Horizon 2020 research and innovation programme under grant agreement No. 700748

Manual for the assessment of liquefaction risk, defining the procedures to create the database, collect, define, symbolize and store information in the Georeferenced Information System and to perform and represent the risk analysis

- Seed, H. B., Tokimatsu, K., Harder, L. F., and Chung, R. M. 1985. "Influence of SPT Procedures in Soil Liquefaction Resistance Evaluations". *Journal of Geotechnical Engineering*, American Society of Civil Engineers, vol. 111, no. 12, p. 1425-1445.
- Schmertmann, J. H. 1991. "The mechanical aging of soils". *J. Geotech. Engng*, ASCE 117, No. 9, 1288–1330.
- Shakib, H. V. J. 2016. "Intensity measures for the assessment of the seismic response of buried steel pipelines". 14(4).
- Stokoe, K.H., and Santamarina, J.C. 2000. "Seismic-wave-based testing in geotechnical engineering". International Society for Rock Mechanics. Document No. ISRM-IS-2000-38. In *Proceedings of the ISRM International Symposium*, 19–24 November, Melbourne, Australia. 47 pp.
- Spacagna, R.L., and Modoni, G. 2018. "GIS-Based Study of Land Subsidence in the City of Bologna". *Mechatronics for Cultural Heritage and Civil Engineering*, pp.235-256. DOI: 10.1007/978-3-319-68646-2_10
- SYNER-G Guidelines for deriving seismic fragility functions of elements at risk: Buildings, lifelines, transportation networks and critical facilities (2013). Kaynia AM (ed.) *Systemic Seismic Vulnerability and Risk Analysis for Buildings, Lifeline Networks and Infrastructures Safety Gain*. Project N°: 244061, Call N°: FP7-ENV-2009-1.
- Tatsuoka, F., Zhou, S., Sato, T., and Shibuya, S. 1990. "Method of evaluating liquefaction potential and its application." Rep. on Seismic hazards in the soil deposits in urban areas, Ministry of Education of Japan, 75–109 (in Japanese).
- TC4 - ISSMGE (1999). *Manual for zonation on seismic geotechnical hazard*. Prepared by Technical Committee TC 4 for Earthquake Geotechnical Engineering.
- Tesfamariam, S., Goda, K. 2013. "Seismic risk analysis and management of civil infrastructure systems: an overview". In *Handbook of seismic risk analysis and management of civil infrastructure systems*, S. Tesfamariam and K. Goda editors, Woodhead Publishing Limited, pp.141-174.
- Tokimatsu, K., Seed, H.B. "Evaluation of settlements in sands due to earthquake shaking". *ASCE J Geotech Geoenviron Eng* 1987;113(8): 861–78.
- Tonkin & Taylor, (2013). "Liquefaction Vulnerability Study". Christchurch: Tonkin & Taylor Ltd.
- Tonkin & Taylor, 2016. "Practical Implications of Increased Liquefaction Vulnerability". Technical Report (61 pp.).
- Toprak, S., Holzer, T. L., Bennett, M. J., Tinsley, J. C. 1999. "CPT- and SPT-based probabilistic assessment of liquefaction potential". *Proceedings of Seventh US Japan Workshop on Earthquake Resistant Design of Lifeline Facilities and Counter-measures Against Liquefaction*, T. D. O'Rourke, J. P. Bardet, and M. Hamada, eds., Report MCEER-99-0019, MCEER, NY.
- Toprak, S., E. N. 2017. "Pipeline Damage Predictions in Liquefaction Zones using LSN". Santiago, Chile : 16th World Conference on Earthquake, 16WCEE 2017 .
- UNDRO, Office of the United Nations Disaster Relief Co-ordinator 1979. "Natural Disasters and Vulnerability Analysis". Report of Expert Group Meeting, 9 – 12 July 1979.
- UNISDR. 2015. "Reading The SENDAI Framework for Disaster Risk Reduction". *Royal Society Meeting Note*, (June), 34. <http://doi.org/10.1007/s13753-015-0051-8>



This project has received funding from the European Union's Horizon 2020 research and innovation programme under grant agreement No. 700748

Manual for the assessment of liquefaction risk, defining the procedures to create the database, collect, define, symbolize and store information in the Georeferenced Information System and to perform and represent the risk analysis

- Università degli Studi di Ferrara, Dipartimento di Fisica e Scienze della Terra 2014. "Microzonazione sismica del Comune di Sant'Agostino".
- van Ballegooy, S., Malan, P., Lacrosse, V., Jacka, M.E., Cubrinovski, M., Bray, J.D., O'Rourke, T.D., Crawford, S.A., Cowan, H. 2014. "Assessment of Liquefaction-Induced Land Damage for Residential Christchurch". *Earthquake Spectra* (30) No. 1: pages 31–55, February 2014.
- Vick, S.G. 2002. "Degrees of Belief: Subjective Probability and Engineering Judgment". ASCE press, 472p.
- Viggiani, C., Mandolini, A., Russo, G. 2012. "Pile and piled foundations". Taylor & Francis, 278 pp.
- Yamauchi, T., Tezuka, H., and Tsukamoto, Y. 2017. "Development of Rational Soil Liquefaction Countermeasure Consisting of Lattice-Shaped Soil Improvement by Jet Grouting for Existing Housing Estates". In *Geotechnical Hazards from Large Earthquakes and Heavy Rainfalls* (pp. 49-59). Springer, Tokyo.
- Yasuda, S., Ishikawa, K. 2018. "Liquefaction-induced Damage to Wooden Houses in Hiroshima and Tokyo during Future Earthquakes". 16 ECEE, Thessaloniki, Greece, June 2018.
- Yasobant, S., Vora, K.S., Hughes, C., Upadhyay, A. and Mavalankar, D.V. 2015. "Geovisualization: A Newer GIS Technology for Implementation Research in Health". *Journal of Geographic Information System*, 7, 20-28.
- Yoshida, Y., Kokusho, T. 1988. "Empirical Formulas of SPT blow-counts for gravelly soils". Proc. ESOPT 1, Rotterdam.
- Youd, T.L., Hansen, C.M., Bartlett, S.F. 2002. "Revised multilinear regression equations for prediction of lateral spread displacement". *ASCE J Geotech Geoenvironmental Engineering*, 28(12), pp.1007–1017.
- Youd, T.L., Perkins, DM., "Mapping of liquefaction severity index". *ASCE J Geotech Eng* 1987;113(11):1374–92.
- Youd, T. L., and Perkins, D. M. 1978. "Mapping Liquefaction-induced Ground Failure Potential". *J. Geotech. Eng. Div., ASC E*, 104, 433–446pp.
- Youd, T. L., Idriss, I. M., Andrus, R. D., Arango, I., Castro, G., Christian, J. T. , Dobry, R. , Finn, L., Harder, L. F. J., Hynes, M. E. , Ishihara, K., Mitchell, J. K., Moriwaki, Y. , Power, M. S., Robertson, P. K., Seed, R. B., & Stokoe, K. H., 2001. "Liquefaction Resistance of Soils: Summary Report from the 1996 NCEER and 1998 NCEER/NSF Workshops on Evaluation of Liquefaction Resistance of Soils". *Journal of Geotechnical and Geoenvironmental Engineering*, 1–17.
- Youd, T.L., Carter, B.L., 2005. "Influence of soil softening and liquefaction on spectral acceleration". *Journal of Geotechnical and Geoenvironmental Engineering*, 131-7, July 2005, pp.811-825.
- Walley, P. 1991. "Statistical Reasoning with Imprecise Probabilities". Chapman and Hall, London.
- Wang, R., Zhang, J.M., and Wang, G. 2014. "A unified plasticity model for large post-liquefaction shear deformation of sand". *Computers and Geotechnics*, 59: 54-66.
- Wang, R., Liu, X., and Zhang, J.M. 2015. "Analysis of seismic pile response in liquefiable ground using a constitutive model for large post-liquefaction deformation". 6th International Conference on Earthquake Geotechnical Engineering, Christchurch, New Zealand, 1-4 November 2015; Paper No. 670.
- Wen, Y.K. 2001. "Reliability and performance-based design". *Structural Safety*, 23, 407–428.



This project has received funding from the European Union's Horizon 2020 research and innovation programme under grant agreement No. 700748

Manual for the assessment of liquefaction risk, defining the procedures to create the database, collect, define, symbolize and store information in the Georeferenced Information System and to perform and represent the risk analysis

- Zadeh, L.A. 1965. "Fuzzy sets". *Information and Control*, 8, 338–353.
- Zhang, G., Robertson, P.K., Brachman, R.W.I. 2002. "Estimating liquefaction-induced ground settlements from CPT for level ground". *Canadian Geotechnical Journal* 39: 1168–80.
- Zhang, G., Robertson, P.K., Brachman, R.W.I. 2004. "Estimating liquefaction-induced Lateral Displacements from CPT for level ground". *Journal of Geotechnical and Geoenvironmental Engineering*. AUGUST 2004.
- Zhang, J.M., and Wang, G. 2012. "Large post-liquefaction deformation of sand, part I: physical mechanism, constitutive description and numerical algorithm". *Acta Geotechnica*, 7: 69-113.
- Zhu, J., Daley, D., Baise, L. G., Thompson, E. M., Wald, D. J., and Knudsen, K. L. 2015. "A geospatial liquefaction model for rapid response and loss estimation". *Earthq. Spectra*, 31(3), 1813-1837.
- Ziotopoulou, K., and Boulanger, R. W. 2013. "Numerical modeling issues in predicting post-liquefaction reconsolidation strains and settlements". In *Proceedings of the 10th International Conference on Urban Earthquake Engineering*.
- Ziotopoulou, K., Maharjan, M., Boulanger, R.W., Beaty, M.H., Armstrong, R.J. and Takahashi, A. 2014. "Constitutive modeling of liquefaction effects in sloping ground". *Proceedings of the 10th National Conference in Earthquake Engineering*, Earthquake Engineering Research Institute, July 21-25, Anchorage, Alaska.
- Ziotopoulou, K., and Boulanger, W. 2015. "Validation protocols for constitutive modeling of liquefaction". *6th International Conference on Earthquake Geotechnical Engineering*, 1-4 November, Christchurch, New Zealand.